ENGINEERING RESEARCH INSTITUTE
UNIVERSITY OF MICHIGAN
ANN ARBOR

A VOLTAGE-TUNABLE MAGNETRON FOR OPERATION IN THE FREQUENCY RANGE 1500 TO 3000 MEGACYCLES

Technical Report No. 15
Electron Tube Laboratory
Department of Electrical Engineering

BY
J. A. BOYD

Approved by: W. G. DOW

Project 2009

CONTRACT NO. DA-36-039 sc-15450
SIGNAL CORPS, DEPARTMENT OF THE ARMY
DEPARTMENT OF ARMY PROJECT NO. 3-99-13-022
SIGNAL CORPS PROJECT NO. 27-112B-0

Submitted in partial fulfillment of the requirements for the Degree of Doctor of Philosophy in the University of Michigan

November 1953

ABSTRACT

This report describes the design and construction of a microwave generator which can be used in many of the applications where electronically-tunable power is needed. This generator consists of an external-cavity interdigital magnetron and its associated cavity structure. This magnetron operates in the frequency range of 1500 to 3000 mc with a power output of the order of 250 milliwatts.

In the design of this magnetron, emphasis was placed on maintaining the anode-to-anode capacitance at a minimum,and on shaping the anode bars in such a manner that higher-order space harmonics would be reduced. Several types of cathodes were tested, including oxide-coated, thoriated tungsten, and pure tungsten. Results indicate that a pure tungsten cathode is most satisfactory for use in this tube. The cavity structure consists of a ridge waveguide, tapered at each end to a 50-ohm coaxial output.

A number of tubes have been built and tested. Results of these experimental investigations indicate that this magnetron is useful as a local oscillator for use in spectrum analyzers, microwave receivers, and as a source of electronically-tunable microwave power for general microwave measurement and development work.

A universal voltage-tuning equation for a magnetron has been derived. The experimental data are interpreted in terms of this theoretical tuning curve and the properties of the rf circuit arrangement. The importance of the circuit impedance in determining the power output of a voltage-tunable magnetron is discussed. The sensitivity of the Model 11 voltage-tunable magnetron operation to the temperature of the cathode is related to the low impedance of the rf circuit.

ACKNOWLEDGEMENTS

The author wishes to express his appreciation to the several people who helped in the preparation of this work. Professors W. G. Dow, G. Hok, J. S. Needle and H. W. Welch, Jr. of the Department of Electrical Engineering offered many valuable suggestions and comments. The author wishes to thank the members of the University of Michigan Electron Tube Laboratory for their help and encouragement during the course of this investigation. The magnetrons and test equipment which was designed by the author were constructed, under the supervision of Mr. J. R. Black, by the members of the University of Michigan Electron Tube Laboratory.

TABLE OF CONTENTS

TABLE OF CONTENTS (Cont'd)

TABLE OF CONTENTS (Con't)

LIST OF ILLUSTRATIONS

LIST OF ILLUSTRATIONS (Cont'd)

LIST OF ILLUSTRATIONS (Cont'd)

LIST OF ILLUSTRATIONS (Cont'd)

LIST OF ILLUSTRATIONS (Cont'd)

A VOLTAGE-TUNABLE MAGNETRON

FOR OPERATION IN THE FREQUENCY RANGE 1500 TO 3000 MEGACYCLES

CHAPTER I

PRIOR ART AND PRELIMINARY EXPERIMENTS

1.1 Statement of the Problem

One of the most difficult problems in making measurements at microwave frequencies, and in developing microwave systems, is that of obtaining a satisfactory source of rf power. The first requirement is that the rf power source be capable of generating sufficient power for the desired application. Perhaps the next most important requirement is that the output frequency of the rf power source be easily tunable over a wide range. For many applications which require the use of a sweeping local oscillator it is desirable, if not absolutely necessary, to have a source of electronically tunable rf power.

For a simple standing-wave measurement, a few milliwatts of rf power in the transmission line of the standing-wave detector are sufficient (Ref. 1). However, in order to prevent the circuit under study from affecting the frequency or the amplitude of a self-excited oscillator used as a signal generator it is usually necessary to place at least 10 db of attenuation between the source and the point of measurement. This places the power output requirements for a satisfactory signal generator at an order of magnitude of 100 to 200 milliwatts. Since the power level requirements are very similar for local oscillator

applications in microwave receivers, the same signal generator source can ordinarily be used for either of these applications. In the measurement of such characteristics as attenuation and antenna patterns, the power requirements are increased by an order of magnitude, requiring a signal generator output of the order of 500 to 1,000 milliwatts.

This report describes the design and construction of a microwave generator which can be used in many of the applications where electronically tunable power is needed. This generator consists of an external-cavity interdigital magnetron and its associated cavity structure. This magnetron operates in the frequency range of 1500 to 3000 mc with power output in the order of 250 milliwatts.

In this chapter a brief review of the microwave tubes available for local oscillator application is presented, together with a summary of previous work on voltage-tunable magnetrons and a discussion of preliminary experiments which were performed in this investigation. In Chapter 2 the design of an interdigital magnetron and its associated cavity structure is presented. This tube has been designated the Model 11 magnetron. A number of tubes have been built and tested, and experimental data which were obtained from several models of the tube are presented in Chapter 3. A discussion of the experimental results is presented in Chapter 4. This discussion includes proposed explanations for certain phenomena which were observed and which have not been previously explained. In Chapter 5 a summary of conclusions arrived at through this investigation is presented.

This investigation is a continuation of the work of Dr. J. S. Needle on "The Insertion Magnetron" (Ref. 2). The objective of the present investigation was to develop a voltage-tunable magnetron which would produce

several milliwatts of coherent power output. It was desired that the characteristics of the output signal be such that the magnetron would be useful as a microwave local oscillator for use in spectrum analyzers, receivers, etc. Dr. Needle first suggested to the author the use of an interdigital structure in the development of a voltage-tunable mangetron.

1.2 Microwave Signal Generators

Brief discussions of the various microwave tubes available for measurement and local oscillator application are presented in the following section.

1.2.1 Space-Charge Control Tubes. The frequency limit of operation of conventional space-charge control tubes is fixed by one or more of the following factors (Ref. 3): (1) the inductance of the leads to the tube elements, (2) the transit time of the electrons in the space between electrodes, (3) the losses by radiation from the tube structure and connecting leads, and (4) the necessity of using small structures with limited capabilities for heat dissipation. To overcome the difficulties listed above, space-charge control tubes for use at high frequencies were developed in the form of disc-seal triodes. These tubes (known as "lighthouse tubes", because of their shape) have a planar electrode structure, in contrast to the cylindrical form common in low-frequency tubes. The leads to the electrodes are brought out of the vacuum envelope through metal-to-glass disc seals, and the tube is designed in such a manner that it can be inserted into an external cavity, usually of the coaxial type. In this type of tube the difficulties of high frequency operation are decreased but are not eliminated. The lead inductance is made very small by the use of disc-seal connections, and the transit time is reduced by using very close spacing (a cathode-to-grid spacing of 0.1 mm and a

grid-to-plate spacing of 0.3 mm for the type 2C40). The operating range of the lighthouse tube extends to an upper limit of approximately 3000 mc.

By adjustment of movable sections of an external cavity, tuning ranges in the order of 2 to 1 may be obtained. The type 2C40 is capable of delivering 125 mw of power at a frequency of 3000 mc with a plate voltage of 250 volts. The frequency of oscillator operation is, in general, insensitive to the plate voltage, which is an advantage in certain applications. The lighthouse tube has not come into general use as a signal source for measurements because of (1) the difficulty in tuning, (2) the difficulty of frequency modulation, and (3) the upper limit to the operating frequency.

1.2.2 Klystrons. In contrast to the lighthouse tubes, in which the transit time effect is minimized, klystrons make use of transit time in their basic mode of operation. In the lighthouse tube the density of the electron beam is controlled by varying the grid potential, thus controlling the potential of the virtual cathode (or potential minimum). The velocity of the electrons in the grid-plate interaction region are approximately equal. The klystron depends on velocity-modulation of the electrons for its operation. In the double-cavity klystron amplifier, a beam of electrons from a gun is first accelerated to a high velocity. The beam then passes through the gap of the input (buncher) cavity where each electron receives an additional acceleration (which may be either positive or negative, depending upon the phase and magnitude of the rf potential across the cavity gap at the instant the electron passes through). The electrons are then allowed to traverse a drift space where the variation in velocities will give rise to bunching of the electrons. The beam then passes through the gap of a second cavity

where the high frequency components of the beam current, which are produced by the bunching action, cause an rf voltage to be developed across this second cavity. The frequency of this voltage is the same as that of the rf voltage applied to the buncher cavity. Power may be coupled from the second cavity and the device used as an amplifier, or with the proper feedback arrangement, the device will operate as a self-excited oscillator.

For measurement and local-oscillator applications the most generally useful type of klystron is the reflex-klystron oscillator. The principle of operation is similar to that of the double-cavity klystron; however, the reflex klystron uses only one cavity and operates only as an oscillator. In the reflex klystron the beam passes once through the cavity, then, by means of a negative electrode (the reflector) it is made to return through this cavity on a second transit. By proper adjustment of the beam voltage, reflector voltage, and reflector spacing, the electrons will be bunched and in the proper phase on their return through the cavity and will produce sustained oscillations in the cavity.

Reflex klystrons have a maximum power output in the order of 0.5 watt in the 3000 mc frequency range, which is more than adequate for most measurement applications. There are two types of reflex klystrons in general use; the external-cavity type and the self-contained cavity type. In both types, oscillations may be obtained by adjusting accelerator and reflector voltage. A small amount of frequency tuning may be accomplished by varying only the reflector voltage; a variation in frequency of the order of 30 mc at 3000 mc may be obtained in this manner. The cavities may be tuned mechanically to obtain wider frequency coverage, however, this tuning range is limited in the case of the self-contained oscillator.

Even though the reflex klystron is the most common source of microwave power for measurement purposes, it has serious deficiencies. The range over which it can be easily tuned by electronic means is small. Perhaps the most serious difficulty for measurement purposes is that of obtaining sufficient power over a wide range of frequencies. Due to the narrow electronic modes of operation in the reflex klystron, it is very difficult to obtain sufficient power output to make satisfactory measurements over a wide range of frequencies. The modes referred to are not associated with the circuit, but are distinguished by different transit times in the drift space. Both power output and frequency are a function of the reflector voltage so considerable amplitude modulation is obtained when the reflector voltage is modulated to give frequency modulation.

1.2.3 Backward-Wave Traveling-Wave Tubes. There has recently been discovered a new type of traveling-wave tube, known as the backward-wave traveling-wave tube. This tube uses a slow-wave structure similar to that used in conventional traveling-wave tubes differing, however, in that the electrons interact with a space-harmonic wave which has a phase velocity in the same direction as the beam,although the group velocity is in the opposite direction to that of the beam. This tube, when operated under the proper conditions, functions as a self-excited oscillator. Papers describing the operation of these tubes have been presented at Institute of Radio Engineers conventions by personnel of the Bell Telephone Laboratories and Stanford University. In private conversations, Dr. Stanley Kaisel of Stanford University has described a backward-wave oscillator tube which can be electronically tuned over a 2 to 1 frequency range and delivers power output in the order of 1 watt. Dr. Kaisel indicates that power in the order of tens of watts

may eventually be obtained from this type of oscillator. It appears that this type of tube will find many applications in microwave work. For low power local oscillator and signal generator applications it seems that the tube will be expensive because of the slow-wave structure required. One disadvantage of this tube for local oscillator application is the non-linear relation between voltage and frequency; for example, a two-to-one change in frequency requires a six-to-one change in voltage.

1.2.4 Magnetrons. The magnetron has been developed as a high-power transmitter tube and is, in general, an inherently higher-power tube than is needed for measurement and local oscillator applications. A low power magnetron suitable for local oscillator applications at frequencies below 1000 mc has been developed (Ref. 4). However, until the present there has been no magnetron suitable for these applications at frequencies above 1000 mc.

1.2.4.1 Classification of Magnetrons. In rf magnetron devices a continuous transfer of energy between a dc electric field and an rf field takes place in the presence of a strong magnetic field which is at right angles to the dc field; thus, electron interaction with an rf field occurs in the presence of crossed electric and magnetic fields. Other electronic devices utilize a dc magnetic field to enhance their operation, but only magnetron devices are dependent upon the presence of crossed dc electric and magnetic fields for their fundamental mode of operation. The first analysis of the dc smooth anode magnetron was made by A. W. Hull in 1921 (Ref. 5); much of the work which has followed has been based on Hull's original analysis.

The present investigation is concerned with the cylindrical multisegment magnetron oscillator in which there exists an axial dc magnetic field and a radial dc electric field. The rf circuit may be thought of as a re-entrant filter type transmission line. The Carcinotron is a magnetron oscillator which utilizes an rf structure which is not re-entrant. In this device, the electrons interact with a space harmonic of an rf wave that has a group velocity in the opposite direction to that of the electrons. The feedback necessary for oscillation is present between adjacent segments in the rf structure.

For magnetron amplifiers (Ref. 6), a slow wave transmission structure is required to transmit the rf wave; the slow wave structure may serve as the anode. A criterion for an amplifier circuit is that the circuit not be re-entrant as in the cylindrical magnetron. The fundamental mode of operation is the same for the cylindrical magnetron oscillator, the Carcinotron and the magnetron amplifier.

There are three fundamental modes in which electrons can interact with the electric and magnetic fields of a cylindrical magnetron such that a net transfer of energy from the dc electric field to an rf field can occur. All of these modes of operation are capable of producing sustained oscillations under the proper operation conditions. The negative-resistance magnetron oscillator depends upon the existence of a static negative-resistance characteristic between the two halves of a split anode magnetron. The cyclotron frequency magnetron oscillator operates by reason of synchronism between the period of rf oscillation and the period of cycloidal motion of the electrons. The traveling-wave magnetron oscillator depends upon synchronism between the mean translational velocity of the electrons and the velocity of a traveling-wave component of the rf field.

1.2.4.2 The Negative-Resistance Magnetron Oscillator.

The basic idea of the negative resistance magnetron oscillator (Ref's 7, 8, 9) was reported by Habann in 1924 (Ref. 10). In its usual form it consists of a cylindrical anode and coaxial filament, the anode being split into two or more segments. The rf circuit is connected between the anode segments. The transit time of the electrons from cathode to anode does not enter into the basic mechanism of operation, but this transit time must be small relative to the period of the rf oscillation.

A qualitative picture of why this negative-resistance characteristic exists between the two anode segments can be given as follows: With both anode segments at the same potential and the magnetic field at a value above the critical or cutoff value, no electrons will reach either segment. The electron paths will be symmetrical curves terminating on the cathode. Now assume the potential of segment No. 1 has been increased and the potential of segment No. 2 has been lowered by an equal amount, ΔE. Consider an electron which starts toward segment No. 1 and, because of its curved path, crosses the slot plane between the two anode segments. This electron will have kinetic energy in excess of the potential energy corresponding to its position in this low potential field. It is this excess of energy which will allow the electrons to reach the segment of lowest potential. When the electron enters the low potential region, the radius of curvature of its motion will be decreased causing it to curve back somewhat short of the cathode. Thus, the electron may describe one or more loops finally arriving at the segment of lower potential in most cases.

On the other hand, electrons which start toward the segment of lower potential and cross the gap plane into a high potential will have their radius of curvature increased and may thus encircle the cathode. Kilgore constructed a special magnetron which made possible a visual study of electron paths by gas ionization (Ref. 9). The cathode was constructed with a small emitting spot and made rotatable so that electrons starting in any directions could be studied. His conclusions were that under certain conditions [i.e., where B = 1.5 to $2B_c$ (where B_c is the cutoff value of the magnetic field), and where the ratio of anode potentials is less than 4:1], most of the electrons arrive at the lower potential segment regardless of the direction in which they had started.

1.2.4.3 The Cyclotron Frequency Magnetron Oscillator.

The production of cyclotron frequency oscillations in a magnetron (Ref's. 7, 8) appears to have been first described by Zacek in 1924 (Ref. 11). This was the first electronic oscillation produced in a magnetron as defined by Megaw (Ref. 7), in which electronic oscillations are defined as, "oscillations produced in a circuit connected to a thermionic system, by virtue of electron inertia in the system". These oscillations were found to occur between anode and cathode in the cylindrical magnetron when the value of the magnetic field was near cut-off. The frequency of oscillation was found to be independent of any external circuit which may be connected between the anode and cathode but varied with magnetic field strength, anode voltage, and anode diameter. These oscillations were found to be strongest for wave lengths obeying a relation of the form:

$$\lambda = \frac{\text{constant}}{B} \qquad (1.1)$$

Yagi showed that the oscillation period is equal to the electron transit time from cathode to anode and back (Ref. 12). He gives the following expression for the wave length of oscillation:

$$\lambda = 2\,c\,t$$

where $c = 3\times10^{10}$ cm/sec (1.2)

t = time required for an electron to travel from cathode to anode

Using the equation for the cycloidal motion of the electron as derived by Hull, Okabe calculated the constant in Eq 1.1 to be 10,650, and found an experimental value of 13,000 (Ref. 13).

A brief explanation of this mode of operation can be given as follows: An electron which leaves the cathode in such phase as to gain energy from the rf field as it moves toward the anode will also gain energy on its return to the cathode. This electron will thus strike the cathode with more energy than it had when it left, and will be removed from further interaction with the rf field. On the other hand, electrons which leave the cathode in such phase as to lose energy to the rf field when moving toward the anode will also remain in the proper phase to lose energy on their return trip to the cathode. These electrons will thus have insufficient energy to reach the cathode again, and will start over on another loop of smaller amplitude continuing to lose energy. This process continues until all the energy of the rotational component of the electron's motion has been absorbed by the rf field (Ref. 8). If the electron is not removed at this stage, in its subsequent motion the rotational motion will build up,extracting energy from the rf field.

The difficulty in removing the electrons at the proper time has prevented the cyclotron-frequency oscillator from coming into general use.

1.2.4.4 The Traveling-Wave Magnetron Oscillator. In 1935, Posthumus correctly explained a third type of magnetron operation in which the electrons interact with the tangential component of a traveling rf wave whose velocity is approximately equal to the mean translational velocity of the electron (Ref. 14). It is the traveling-wave magnetron that is in general use today as a generator of microwave power.

The present investigation is concerned with the traveling-wave magnetron; therefore, the mechanism of operation will be considered in greater detail in a later section. In the following section some of the structures that have been used in traveling-wave magnetrons will be described.

1.2.4.4.1 Traveling-Wave Magnetron Structure. Fig. 1.1 shows schematic diagrams of the various types of resonator structures that have been used for traveling-wave magnetrons. These structures may be classified as follows:

(a) multicavity, multianode magnetrons;

(b) split-anode magnetrons; and

(c) interdigital multianode magnetrons.

The multicavity magnetrons may be further distinguished by the type of resonators used, such as vane, slot, and hole-and-slot, as indicated in Fig. 1.1. The multicavity structures are inherently high-Q resonators and cannot easily be adapted to voltage-tunable operation. The split-anode magnetron and the interdigital magnetron are suitable

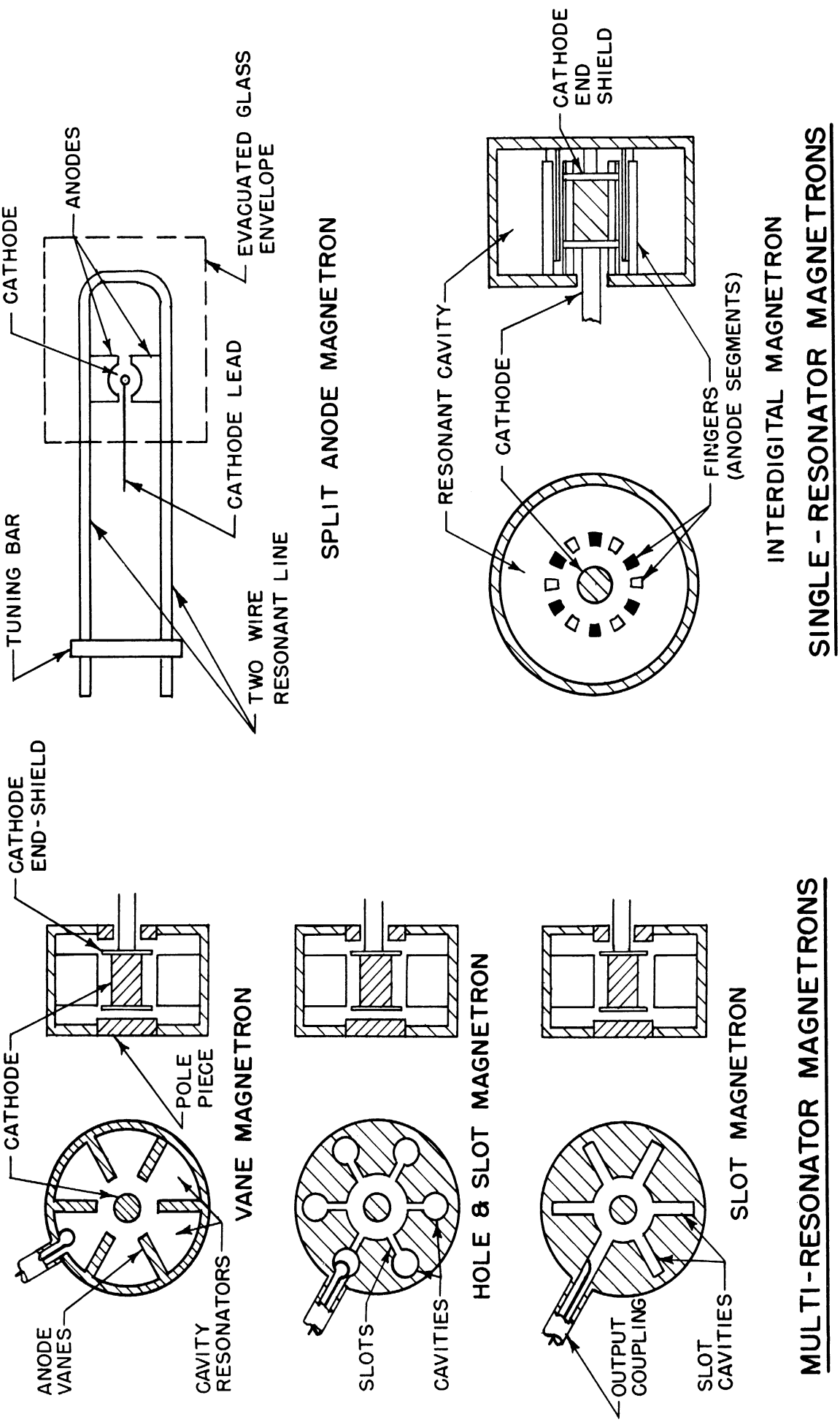

FIG. 1.1 TRAVELING WAVE MAGNETRONS

for voltage-tunable operation since they can be used with a single external cavity, which allows greater control over the frequency characteristics of the circuit. Also, the different modes of oscillation are in general spaced much farther apart in frequency for the split-anode and the interdigital magnetrons than for the multianode magnetrons. The split-anode magnetron is being used by a group at the General Electric Company to obtain voltage-tunable operation. Since the external circuit in this case consists of a parallel transmission line and, in some cases, lumped-constant circuits, the frequency of operation has been limited to the frequency range below 1000 mc. The interdigital structure is the one utilized in the present investigation and will be discussed in detail in a later section.

Figure 1.2 shows a schematic diagram of the bar-and-vane structure which was used by Needle (Ref. 2). This structure was used in such a manner that the magnetron oscillations excited a coaxial line. This is a variation of the vane type structure shown in Fig. 1.1; however, the bar-and-vane structure can be used with a single cavity. In addition to certain mechanical difficulties associated with this structure, the most important difficulty is that the impedance which the electrons "see" is limited to the order of 25 ohms.

1.2.4.4.2 Space-Charge Behavior in the Traveling-Wave Magnetron. In this section an approximate picture of the space-charge behavior in a traveling-wave magnetron will be presented. (For a more complete treatment of the magnetron space charge problem, see Ref. 16). In Appendix A the equations for the non-oscillating cylindrical magnetron are developed. Fig. 1.3 shows the basic space-charge configuration for a multisegment cylindrical magnetron under large

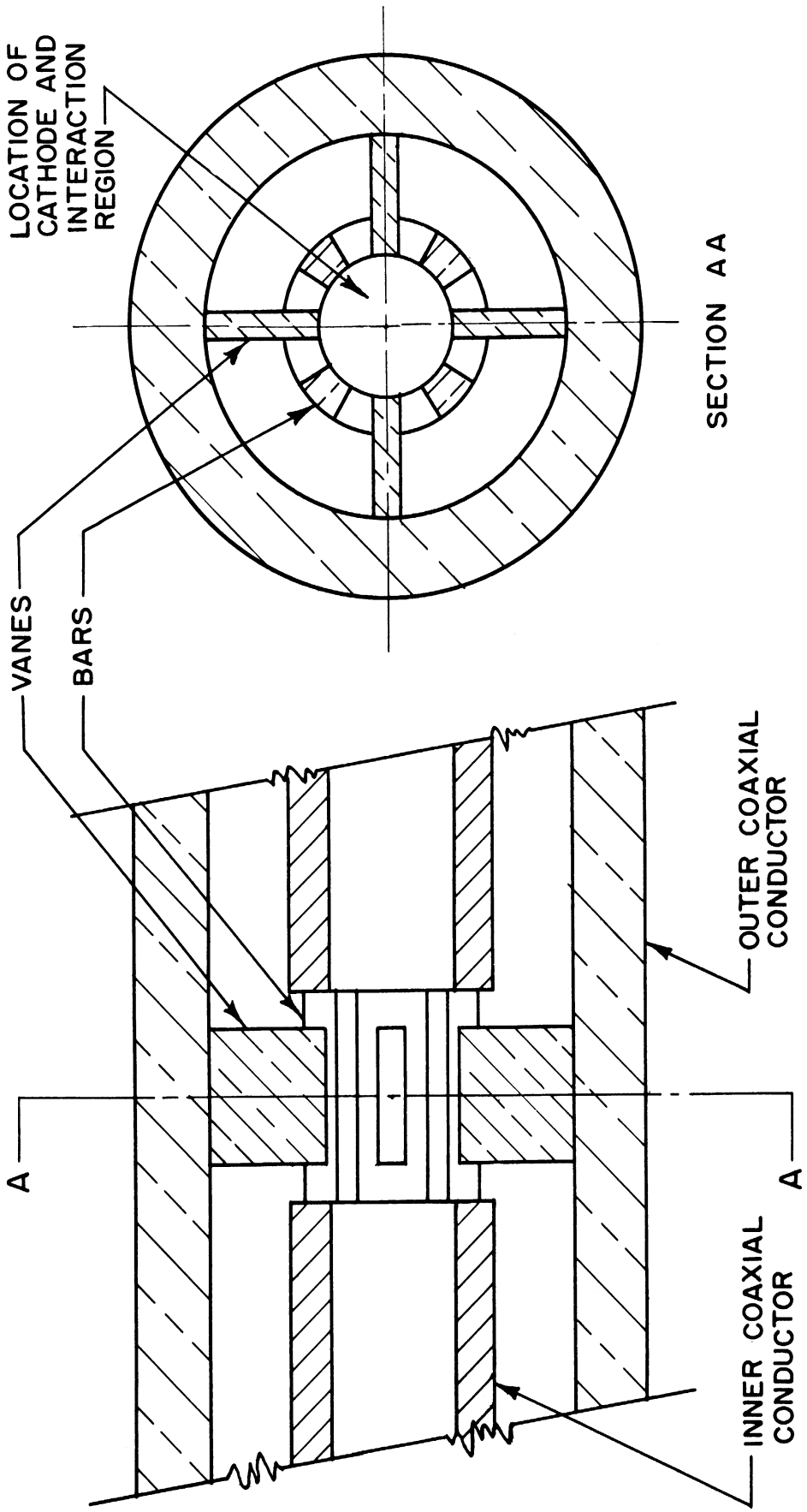

FIG. I.2
THE VANE-AND-BAR MAGNETRON GEOMETRY

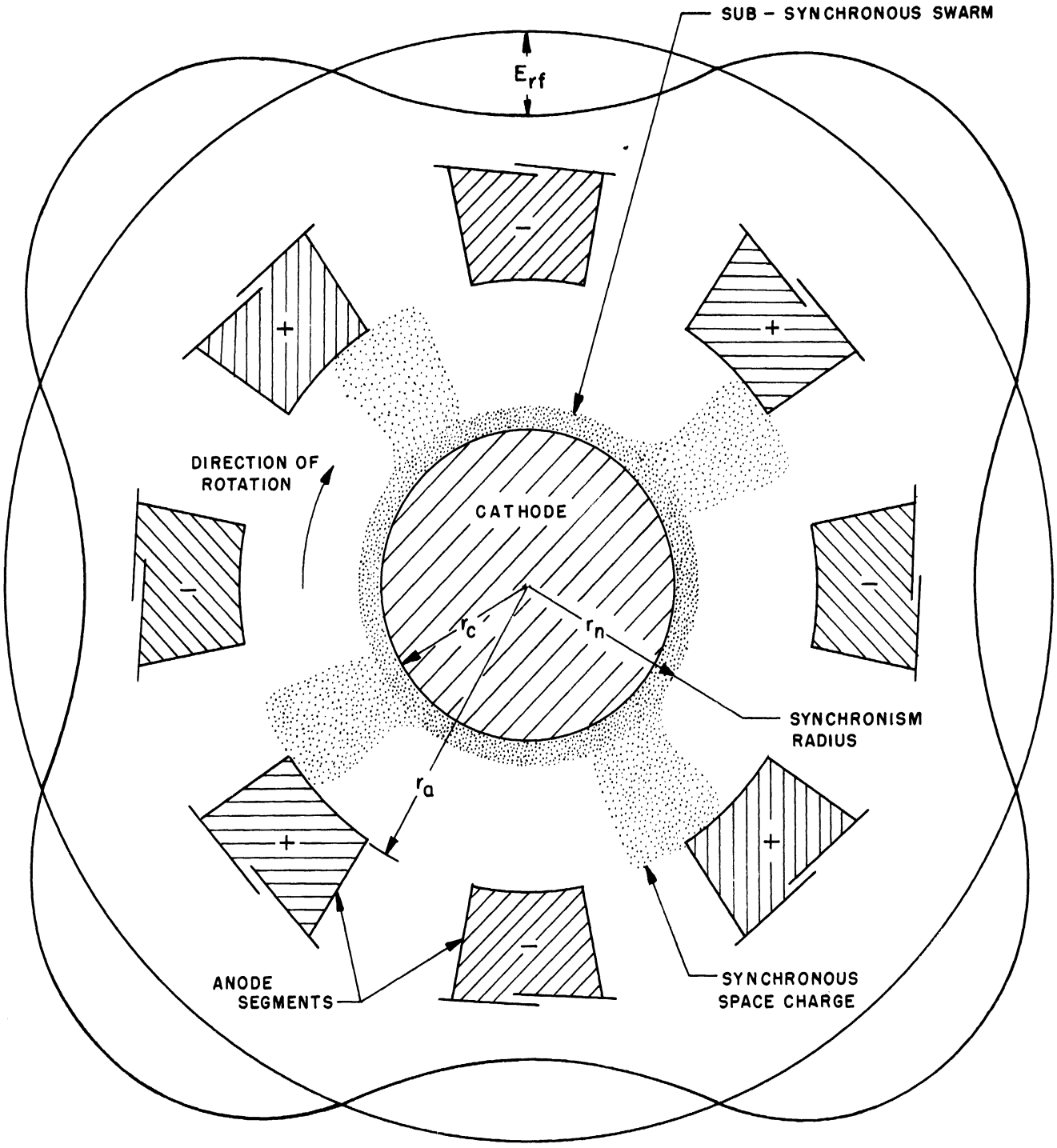

FIG. I.3

BASIC PHYSICAL PICTURE OF THE MAGNETRON SPACE CHARGE WITH LARGE SIGNAL R-F POTENTIAL ON THE ANODE (REF. 16)

signal conditions. That this picture is approximately correct has been established by using the self-consistent-field method for determining the orbits of individual electrons in an oscillating magnetron (Ref. 8). A complete quantitative solution of the oscillating magnetron problem does not exist. This is because of the complexity of the non-linear differential equations that are involved.

The anode segments shown in Fig. 1.3 are assumed attached to a suitable circuit (not shown). The circuit may assume many forms, some of which are shown in Fig. 1.1. In conventional magnetrons the circuit is operated near resonance; however, in the case of voltage-tunable magnetrons which will be discussed in this report, the circuit is non-resonant. In any case the type of circuit used does not affect the shape of the field distribution in the region between the cathode and anode. The dc field distribution is determined by the geometry of the anode-cathode combination. The rf field distribution, due to the rf potential which exists between adjacent anode segments in the oscillating magnetron, is determined almost entirely by the shape of the anode segments. In conventional magnetrons these anode segments have always been rectangular, however, in the present investigation it has been shown that for voltage-tunable operation considerable improvement is obtained by the use of round anode bars. The region in which there is mutual interaction between the electrons and the rf field is known as the interaction space.

The electrons in the interaction space are the agents which transfer energy from the dc field to the rf field. The electrons are supplied by the cathode and are caused to move into the interaction space by applying a dc voltage between cathode and anode, the cathode

being driven negative with respect to the anode. Since there is an axial magnetic field, the electrons follow approximately epicycloidal paths which progress around the cathode. The mean velocity of this progression depends upon the relative strengths of the dc electric and magnetic fields. By proper choice of the dc anode voltage, and of the strength of the magnetic field, it is possible to adjust the mean angular velocity of rotation of the electrons to any desired value.

The rf field (in the interaction space) with which the electrons interact is due to the rf potential which exists between the anode segments. The distribution shown in Fig. 1.3 is referred to as the π mode because there is a phase difference between the voltage on adjacent anode segments of 180 degrees, or π radians. This rf field distribution is stationary in space but varying in time and may be represented as the Fourier sum of a number of traveling waves which proceed in opposite directions around the interaction space. In the π-mode the electrons interact primarily with one fundamental component of these traveling waves which proceeds in the same direction as the electrons with a phase velocity equal to the velocity of the synchronous electrons (see Appendix A),

$$\omega n = \frac{2\pi f}{n}$$

Since the fundamental component of the rf wave and the electrons are assumed to be traveling at the same velocity, the mechanism of "phase-focusing" may be discussed by using a moving reference frame in which both the rf field distribution and the electrons are fixed. The mechanism of phase focusing depends upon the effect of the radial component of the rf field in determining

the mean drift velocity of the electrons in the interaction space. For example, in a region in which the radial component of the rf field aids the dc electric field, the mean rotational velocity of the electron is increased thus moving the electron forward relative to the rotating rf field distribution. Conversely, if the radial component of the rf field opposes the dc electric field, the mean rotational velocity of the electron is decreased thus moving the electron back relative to the rotating rf field distribution. The net effect of this action is to maintain the electrons in the position, relative to the rf field distribution, for maximum transfer of power.

Consider Fig. 1.4 in which the traveling wave is represented by a fixed wave in a traveling reference frame. Electrons in the region of cross-section "a" are able to deliver energy to the rf field. It should be remembered that the electrons give energy to the rf field as they gain energy from the dc field; therefore, for a transfer of energy from the dc field to the rf field to take place, the electrons must move toward the anode. Electrons in the region "b" are moved to the right due to the effect of the radial component of the rf field as explained above. Electrons in the region "c" are moved to the left. Thus, a spoke of space charge is maintained in the region "a" and transfers energy from the dc field to the rf field.

In the "phase-sorting" mechanism consider an electron which enters the interaction space at either "d" or "e" (Fig. 1.4). This electron will be accelerated by the tangential component of the rf field, and this increase in mean rotational velocity will result in an increase in the force normal to the direction of motion; that is, the force directed toward the cathode. This normal force is due to

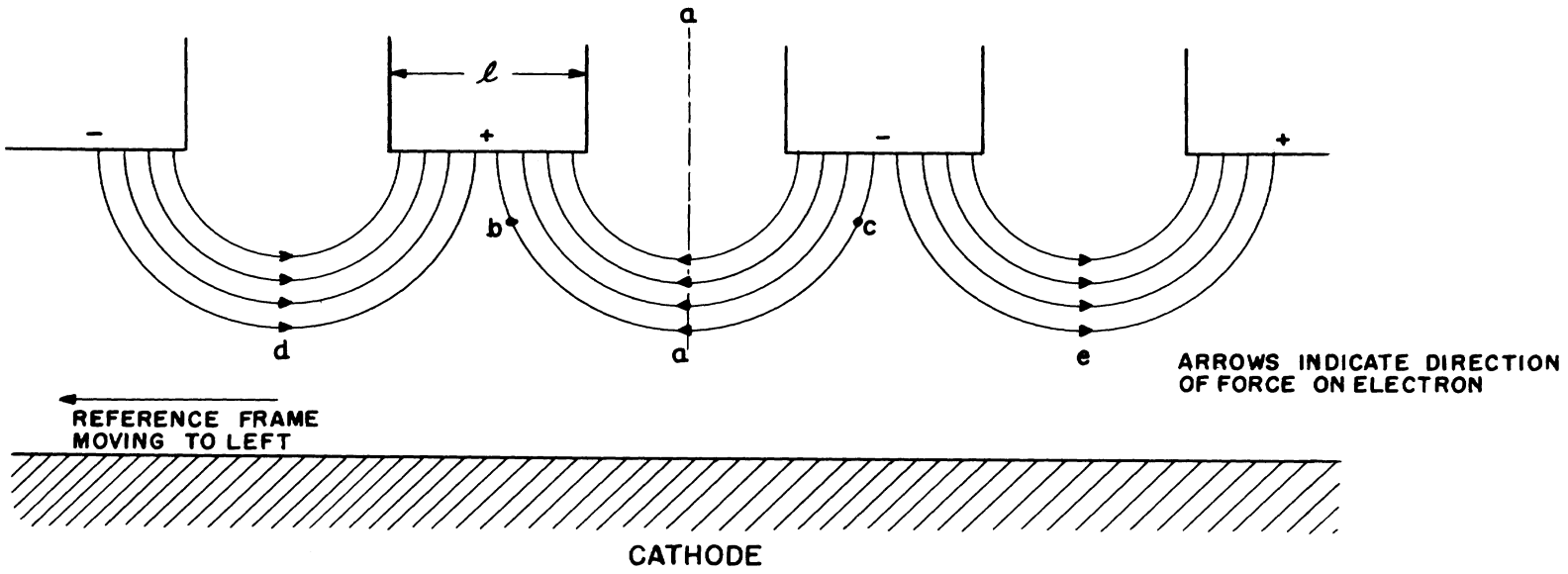

FIG. 1.4

SCHEMATIC DIAGRAM REPRESENTING TRAVELING WAVES
AND ROTATING ELECTRONS IN A MOVING REFERENCE FRAME

the axial magnetic field and, since the radial forces on these electrons are in equilibrium before interaction with the rf field, the electrons will be returned to the cathode. These electrons thus abstract energy from the rf field. This transfer of energy results in "back heating" of the cathode, since a large part of the energy obtained from the rf field in this manner is dissipated at the cathode. Now consider an electron which enters the interaction space at "a". The tangential component of the rf field acts to decelerate the electron, thus allowing it to move toward the anode, continually tranferring energy from the dc field to the rf field. Thus it has been shown qualitatively that electrons can only exist in the region "b" to "c" in Fig. 1.4, this region also being the optimum position for the transfer of energy from the dc field to the rf field.

The transfer of energy from the electrons to the circuit is best analyzed by using the theory of induced currents due to moving charges (Ref. 15). Assume that the spokes of the space charge extend out to the anode segments, or bars. Charge will be induced in the anode bars due to the presence of this space charge. As the space charge spokes rotate, an rf current will be caused to flow in the external circuit, a spoke of negative charge moving away from an anode bar will cause a positive current to flow away from the anode bar into the external circuit, and, when the spoke is moving toward an anode bar, a positive current will flow from the circuit into the anode bar. In the case of the π-mode there will be a space charge spoke between every other pair of anode bars; thus, the space charge will act as a current generator connected between the two sets of alternate anode bars. The maximum output of the current generator will occur when the spokes are

half way between the anode bars, a positive current flowing into the circuit from the anode bar from which the spoke is moving. If the anode bar which is delivering the positive current to the circuit is also at a maximum positive rf potential at this instant, then maximum energy will be delivered to the circuit by the space charge. This energy is obtained from the dc field. The mechanism by which the individual electrons transfer energy is not so easily explained using the induced current theory; however, the induced current method lends itself to quantitative analysis more readily than do other approaches. Since the space charge spoke is assumed to move in synchronism with the rf field, there will be a continuous transfer of energy from the dc field to the rf field.

It should be noted that there is an inherent relation between the position of the space charge spoke relative to the anode bars and the time phase of the rf current into the anode bars, while the phase relation between the rf current and rf voltage on the anode bars is determined by the external circuit. The phase relation between the rf current and voltage must be consistent with the requirements for phase focusing. The limits of this phase relation may be determined as follows (Fig. 1.4): Assume the spoke is symmetrically disposed about a positive maximum in the rf potential wave, then the maximum rf current will be delivered to the circuit from a given anode when the rf potential is zero, going from positive to negative. This would require that the external circuit be a pure inductive reactance; in this case the space charge can be considered as a passive capacitive reactance, since for oscillation to occur the sum of the conductances and the sum of susceptances must be zero in the complete circuit. By a similar

process of reasoning, it can be shown that the other extreme will be for the space charge to act as an inductive reactance delivering a leading current to a capacitive circuit.

Experimentally it has been found that conventional magnetron oscillators start oscillating below resonance; that is, when the external circuit is inductive (Ref. 16). As the anode voltage is increased the power output increases and the phase angle between rf voltage and current is decreased. Magnetrons do not seem to operate at frequencies very much above resonance; that is, most magnetrons operate best into a slightly inductive circuit.

1.3 Background of Voltage-Tunable Operation of a Magnetron

1.3.1 Summary of the Experimental Work Performed by the General Electric Company.

Frequency pushing is a well known phenomenon occurring in high-Q magnetron operation; it is the variation in frequency of the output signal associated with a change in anode current as the anode voltage is varied, the load being maintained constant. It is this characteristic of the magnetron that makes it impossible to obtain a purely amplitude modulated spectrum, since there is always frequency modulation present. Frequency pushing is characterized by a small change in frequency for a relatively large change in anode voltage. This frequency change is in the order of 5 mc for a 100 volt change in anode potential.

An entirely different mode of magnetron operation in which the generated frequency can be made dependent on the anode potential for certain operating conditions has been described in Reference 17. This mode of operation has been called "voltage tuning," and is here

defined as the variation in the frequency of the output signal from a magnetron as the anode potential is varied (when the dc anode current, magnetic field,and load impedance are maintained constant). To satisfy the condition of constant dc anode current requires that the cathode be operated under temperature-limited conditions; otherwise, the dc anode current will increase with an increase in the anode potential. Voltage tuning is characterized by a large change in the frequency of the oscillating magnetron for a relatively small change in the anode potential, in the order of 1 mc for a voltage change of 1 to 4 volts.

The initial General Electric Company experimental work was done with existing magnetron power tubes; split-anode, neutrode, and multi-vane tubes were used and found to operate as voltage-tunable magnetrons. Power outputs in the order of 10 to 200 watts, and a tuning range in the order of 2 to 1 were obtained. These tubes were operated in the 500 to 1000 mc range. The load conditions varied from low-Q resonant circuits (less than 10) to essentially non-resonant circuits. Figures 1.5 and 1.6 show typical results which were obtained using these power tubes. Figure 1.5 indicates the results obtained using a low-Q circuit and Fig. 1.6 shows the results for a non-resonant circuit. These figures are presented for comparison with figures showing results of the present investigation which are presented in Chapter 3.

Specially designed tubes were constructed by the General Electric Company which were operated at low power levels, in the order of a few milliwatts. These tubes were voltage-tuned from 50 to 1000 mc. Split-anode and interdigital-type tubes small enough to fit into a standard miniature tube envelope were constructed and tested (Ref. 4).

The results of the work on voltage-tunable operation performed by the General Electric Company may be summarized as follows:

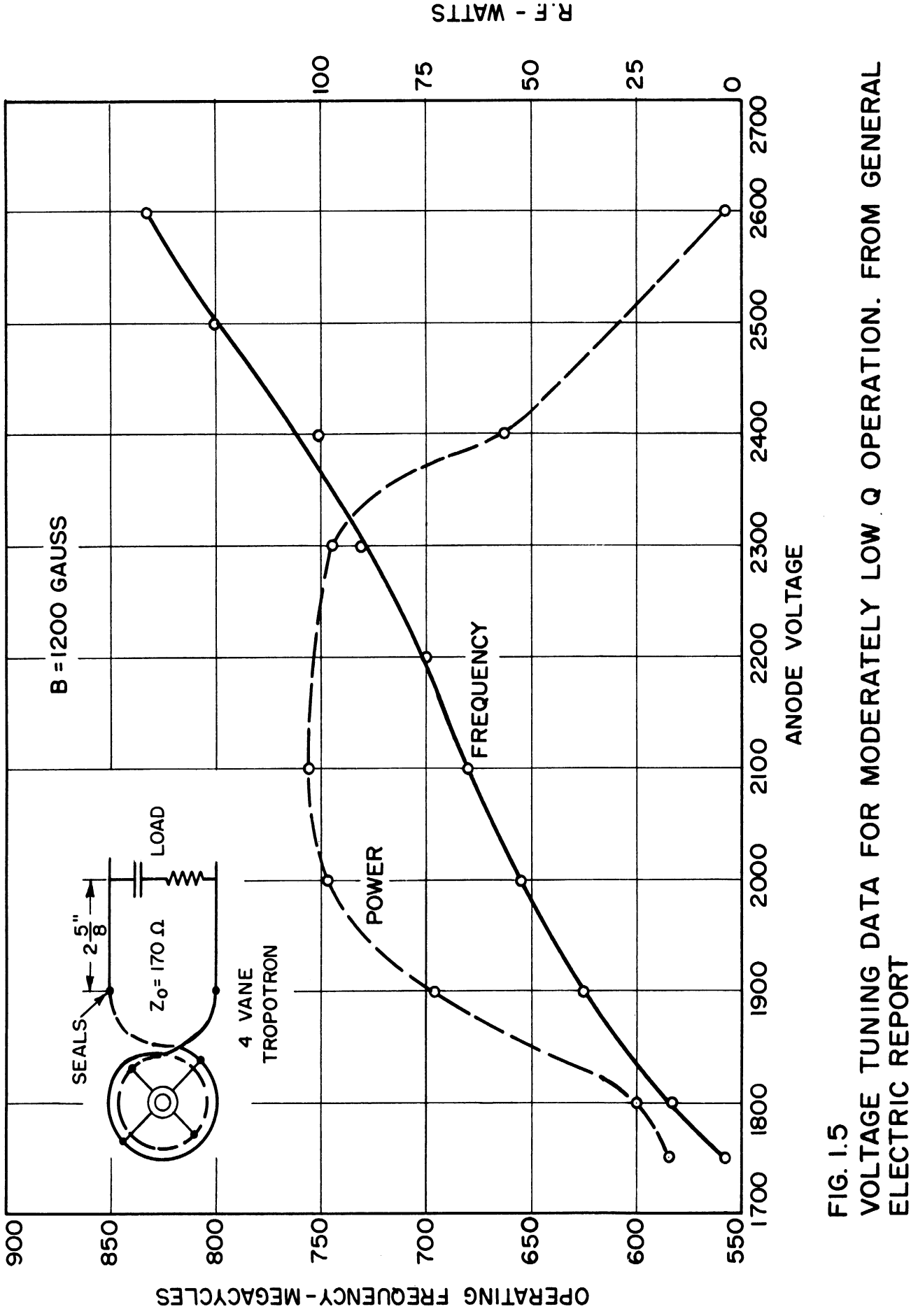

FIG. 1.5
VOLTAGE TUNING DATA FOR MODERATELY LOW Q OPERATION. FROM GENERAL ELECTRIC REPORT

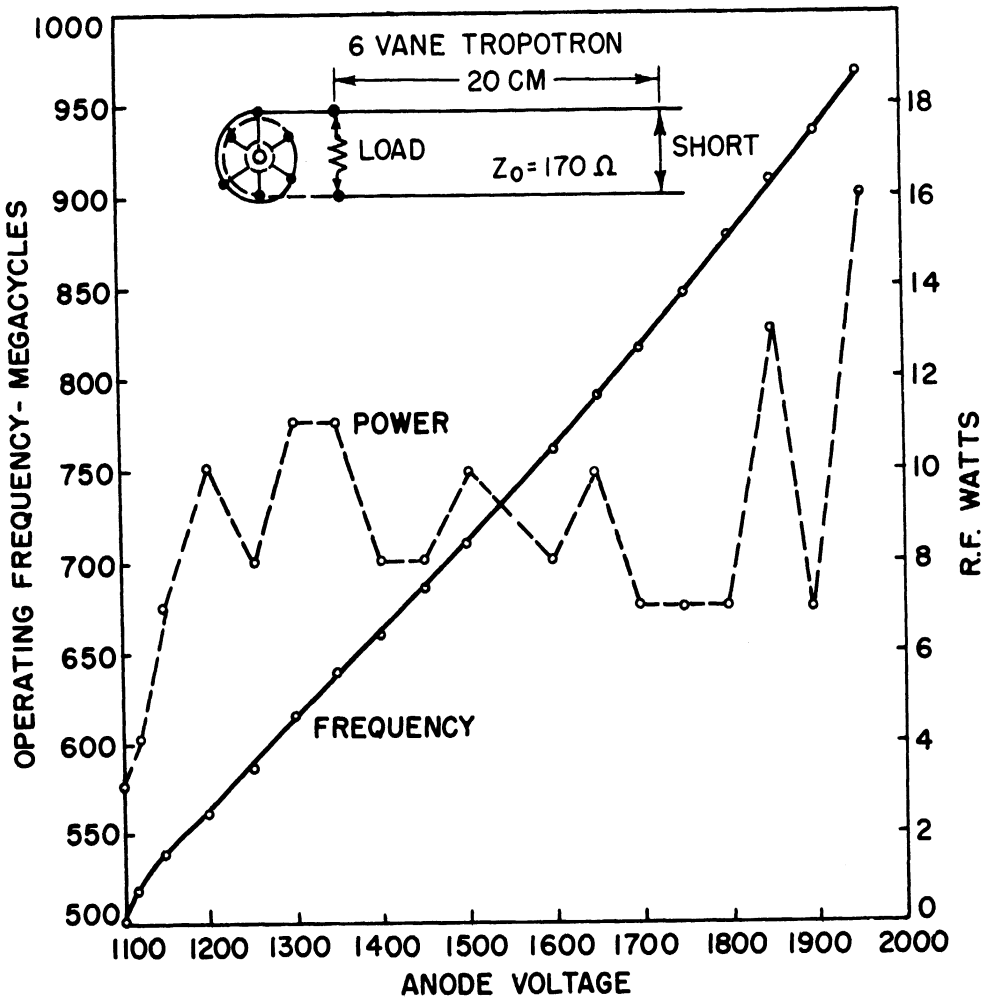

FIG. 1.6
VOLTAGE-TUNING DATA FOR OPERATION INTO NON-RESONANT CIRCUIT. FROM GENERAL ELECTRIC REPORT

a) It was necessary to limit the temperature of the cathode to obtain satisfactory voltage tuning. Stable operation could not be obtained with an oxide coated cathode; however, a thoriated tungsten helix gave satisfactory performance.

b) The signal frequency was sensitive to filament voltage, decreasing with increased emission.

c) The power outputs were less than would be expected under normal operating conditions.

d) The circuits used had a very low-Q,or were nonresonant.

e) The sensitivity was in the order of two to four volts per megacycle.

f) Under certain conditions a triangular cathode improved the operation over that obtained when circular types were used.

g) The relation between frequency and operating voltage was found to agree with the Hartree relation.

1.3.2 The University of Michigan Model 9 Magnetron.

Dr. J. S. Needle of the University of Michigan first obtained voltage-tunable operation of a magnetron in the frequency range of 2000 to 3000 mc. A bar-and-vane type anode structure was used in these experiments; Fig. 1.7 shows a drawing of the tube used. This tube was operated in an external coaxial cavity; Fig. 1.8 shows an assembly drawing of the cavity used for low-Q operation.

When the coaxial circuit is terminated in its characteristic impedance of 50 ohms, the external Q is very low, in the order of one or two. Using a Model 9 magnetron with a pure tungsten helical cathode,

DWG. NO. B - 10,009 B

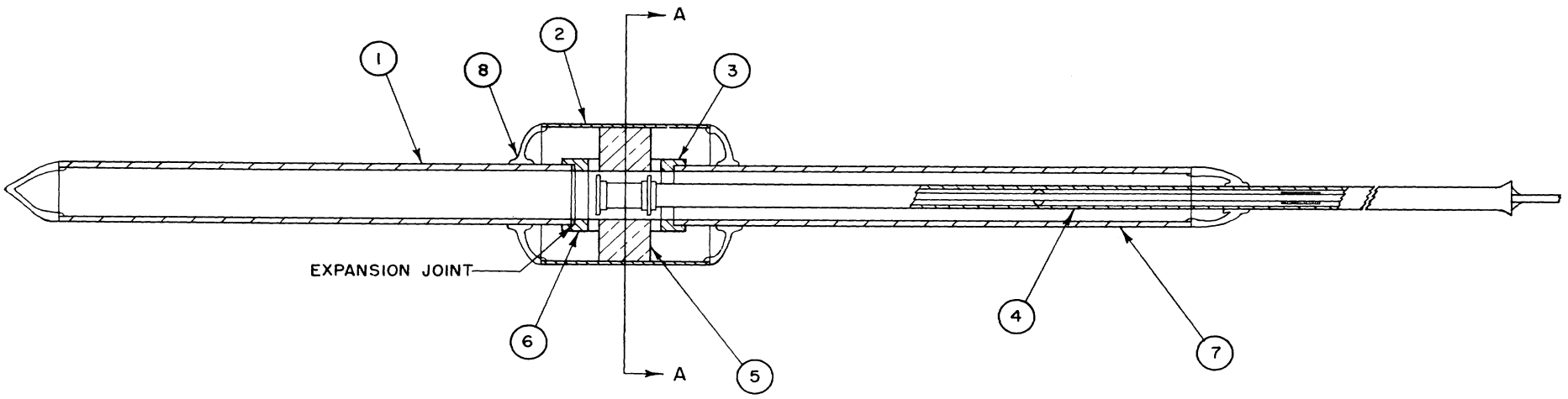

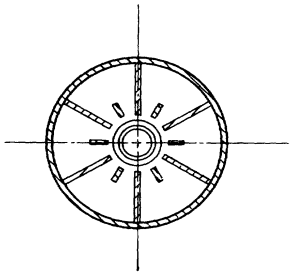

SECTION AA

1-INNER SLEEVE (KOVAR)
2-OUTER SLEEVE (KOVAR)
3-BAR-SUPPORT RING (CU)
4-CATHODE STEM (KOVAR)
5-VANE (CU)
6-BAR-SUPPORT RING (CU)
7-INNER SLEEVE (KOVAR)
8-GLASS SEAL

FIG. 1.7

1" / 2

ALL DIMENSIONS UNLESS OTHERWISE SPECIFIED MUST BE HELD TO A TOLERANCE - FRACTIONAL ± 1/64" DECIMAL ± .005" ANGULAR ± ½°

		ENGINEERING RESEARCH INSTITUTE UNIVERSITY OF MICHIGAN ANN ARBOR MICHIGAN	DESIGNED BY A.S.M.	APPROVED BY
			DRAWN BY MM	SCALE 2X
			CHECKED BY	DATE 1-22-51
		PROJECT M-921	TITLE LOW-POWER MAGNETRON MODEL 9B	
ISSUE	DATE	CLASSIFICATION	DWG. NO. B-10,009 B	

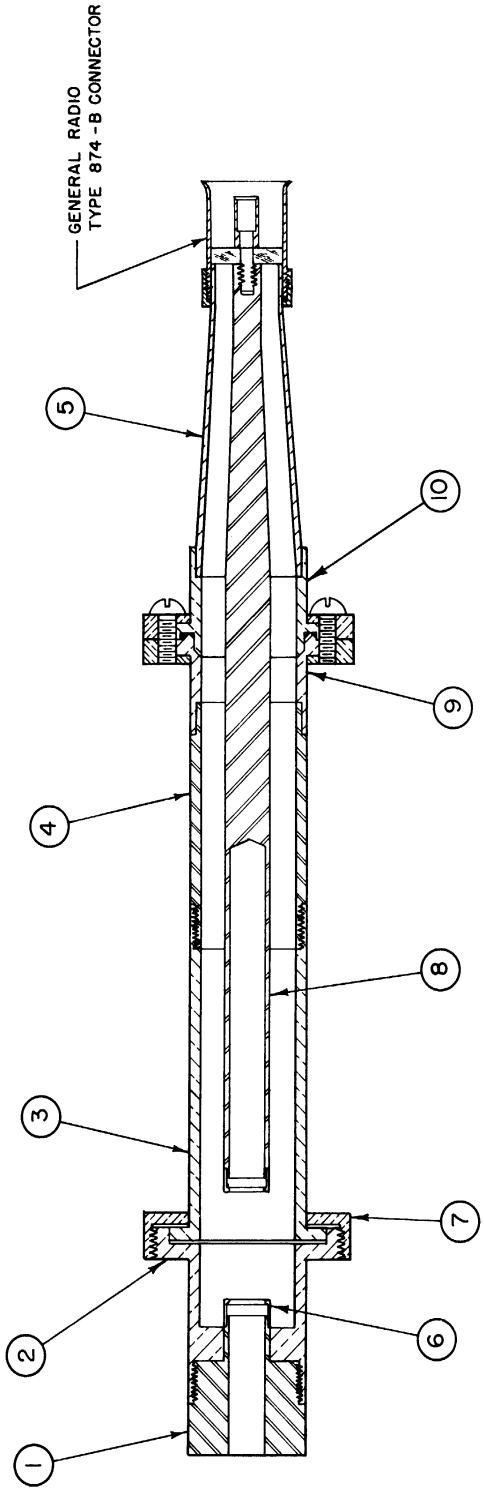

FIG. 1.8

1"

ALL DIMENSIONS UNLESS OTHERWISE SPECIFIED MUST BE HELD TO A TOLERANCE - FRACTIONAL ± 1/64" DECIMAL ± .005" ANGULAR ± ½°

ENGINEERING RESEARCH INSTITUTE
UNIVERSITY OF MICHIGAN
ANN ARBOR MICHIGAN

PROJECT M-921

CLASSIFICATION

ISSUE | DATE

DESIGNED BY U. S. N.
DRAWN BY [illegible]
CHECKED BY [illegible]
APPROVED BY
SCALE FULL
DATE 3-16-51

TITLE
CAVITY NO. 2, MOD. 9 MAG.

DWG. NO. B- 2052

DWG. NO. B

Needle was able to obtain voltage-tunable operation from 1650 to 2640 mc. The power output was very small, in the order of 10 to 30 microwatts of coherent signal.

To obtain coherent power output, it was necessary to limit the cathode temperature and,in this case, it was necessary to readjust the cathode input power for each new anode potential.

The results of the experimental work performed by Needle using the Model 9 magnetron may be summarized as follows:

a) In clean-signal voltage-tunable operation the frequency was proportional to the anode voltage and the relation is given approximately by the Hartree equation.

b) The frequency range of operation was of the order of two to one.

c) The external Q was low; therefore, the shunt susceptance varied slowly with frequency.

d) The interaction space appeared to have the properties of a constant-current generator when the load was frequency-sensitive.

e) The efficiency was low, in the order of 1 percent.

f) The temperature of the cathode was lower than for normal magnetron operation and was critical for clean-signal operation.

g) The frequency decreased with increasing cathode temperature.

h) When the conditions of operation results in a noise band the band width was roughly 5 percent of the average operating frequency and the noise band was voltage-tunable.

i) The constant-current-generator characteristics of the magnetron were modified when the cathode temperature was raised above a critical level.

j) Stable operation could not be maintained with an oxide-coated cathode.

k) Noise could be reduced by adjustment of the shape of the magnetic field.

1.3.3 Theoretical Analysis of a Voltage-Tunable Magnetron.

The following discussion of voltage-tunable operation of a magnetron is based on an analysis by Dr. H. W. Welch, Jr. of the University of Michigan (Ref. 16). Welch has shown that for certain assumed operating conditions the induced current in a magnetron circuit is given by the following expression:

$$I_g = \left[f_{\rho_s} \; 8Lr_c^2 \; (\sin \tfrac{N}{2} \beta) \; F \; (\alpha, N, R_a, R_n) \right] \qquad (1.3)$$

where

f = frequency of oscillation

ρ_s = space charge density in the spokes

L = axial length of the magnetron interaction space

r_c = magnetron cathode radius

β = one-half the spoke width in electrical degrees

N = number of anode segments

$F(\alpha, N, R_a, R_n)$ is a complex function depending upon the anode potential, magnetic field and the geometry of the magnetron interaction space. Thus, for a given anode voltage and magnetic field this factor is a constant.

In order to apply this equation it is necessary to assume that the rf potential is great enough to form well defined spokes. A quantitative analysis of the space-charge distribution in the spokes under temperature-limited operation has not been made; however, an estimate of the behavior of the density, ρ_s, as anode potential is raised and frequency is increased, can be made. When the cathode is operated under temperature-limited conditions the dc anode current cannot increase above a specified value as the anode potential is increased. It is assumed that once the dc anode current has reached this temperature-limiting value that the circuit conditions are such that phase focusing will be enhanced, then the spoke shape will be fixed. Under these conditions the induced current will be given by Eq 1.3.

The value of ρ_s is undetermined; however, it may be related to the dc anode current and anode potential in the following manner. Since the current density through the spoke to the anode is proportional to the dc anode current

$$(\rho_s v)_n = C_1 I_T \tag{1.4}$$

where

I_T = temperature-limited current

C_1 = a constant

$(\rho_s v)n$ = arrival current at the anode.

If the total amount of charge collected at the anode per second is limited to I_T, then an increase in anode potential must increase the arrival velocity of the electrons. Therefore,

$$v = C_2 E_2 \tag{1.5}$$

Combining this relation with Eq 1.4 we have

$$\rho_s = \frac{C_1 I_1}{C_2 E_a} \tag{1.6}$$

Also, we may assume

$$f = C_3 E_a \tag{1.7}$$

Substituting Eqs 1.6 and 1.7 into Eq 1.3, we have

$$I_g = \left[I_T \frac{C_3 C_1}{C_2} \quad 8Lr_c^2 \left(\sin \frac{N}{2} \beta\right) F\ (\alpha, N, R_a, R_n) \right] \tag{1.8}$$

This expression indiates that the induced current depends on frequency through the variation of R_n in the function $F\ (\alpha, N, R_a, R_n)$; however, F varies very slowly with frequency. Equation 1.8 shows that the induced current is directly proportional to the dc anode current I_T.

This implies that under temperature-limited operation the magnetron acts as a constant-current generator, with very slight variation in current with frequency. Combining the expression for the threshold potential (see Appendix A for derivation of this equation)

$$E_H = \frac{\pi B}{n} f(r_a^2 - r_c^2) - 2\pi^2 \frac{mf^2}{en^2} r_a^2 \tag{1.9}$$

with an expression relating anode potential to threshold potential

$$\frac{E_a - E_H}{2KV_{rf}} = \cos 2\theta \tag{1.10}$$

and

$$E_{rf} = \frac{I_g}{|Y_T|} \tag{1.11}$$

Welch obtains the following expression

$$E_a = \sqrt{2}\, K \cos 2\theta \frac{I_g}{(Y_T)} + \frac{\pi B}{n} r_c^2 f(R_a^2 - R_c^2) - 2\pi^2 \frac{m}{e} \frac{r_c^2}{n^2} R_a^2 f^2 \tag{1.12}$$

where

K = $\frac{\text{maximum value of rf potential difference between anode segments}}{\text{maximum value of fundamental traveling-wave component of anode rf potential}}$

θ = phase angle between center of spoke and zero of rf potential in electrical degrees

Y_T = admittance of circuit connected to magnetron anodes

This expression is general and represents an approximately linear relation between anode potential and frequency for the following conditions:

a) I_g, θ, $|Y_T|$ are not frequency dependent, and

b) the f^2 term is negligible; this requires that the magnetic field be relatively large.

The general expression for the power output is:

$$P = \frac{I_g^2}{|Y_T|} \cos \theta \qquad (1.13)$$

The first condition (a above) makes the power output constant. These ideal characteristics for voltage tuning are shown in Fig. 1.9.

Welch concludes that for good voltage tuning a circuit should have a constant admittance over a wide frequency range and be inductive, since a lagging phase angle of the order of -20° to -50° is necessary to produce good phase focusing.

The work of both Needle and Welch indicated that the circuit properties are some of the important parameters which limits the power output of a voltage-tunable magnetron at microwave frequencies. The electrons should "see" a low conductance and an inductive susceptance which varies slowly with frequency. One of the primary limitations on the operation of the Model 9 coaxial magnetron used by Needle in his work was the low impedance which the circuit presented to the electrons;

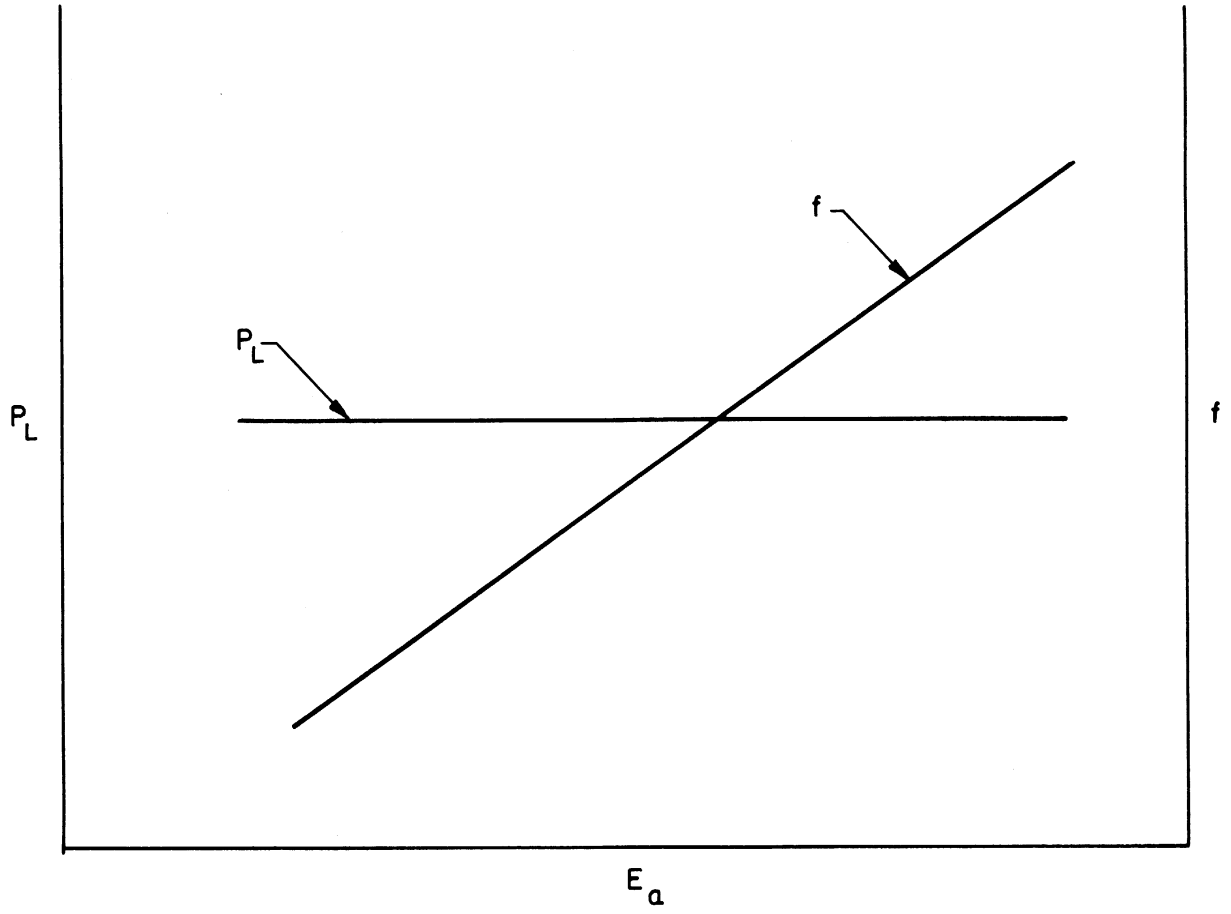

FIG. 1.9

IDEAL VOLTAGE TUNING CHARACTERISTICS

the maximum value of this impedance was of the order of 25 ohms. Since a circuit which possesses the characteristics discussed above is necessary if satisfactory voltage-tuning operation is to be obtained, consideration was given to the circuit problem before considering the design of a tube. Consideration of the above circuit requirements resulted in the conclusion that a waveguide structure offered a possibility for fulfilling these requirements.

1.4 Discussion of Preliminary Experimental Work Using a 3J22 Magnetron

In order to obtain as much information as possible before attempting to design a voltage-tunable magnetron a study was made of all devices which showed promise of yielding information useful in the design of a new tube. The Sylvania 3J22, an external-cavity interdigital magnetron designed for use in a mechanically-tunable resonator, appeared to possess some of the characteristics desired in a voltage-tunable magnetron. This tube was used in several preliminary experiments to obtain information which could be used in the design of a voltage-tunable magnetron. These experiments gave valuable information concerning the operation of a magnetron in various waveguide circuit arrangements. A brief discussion of the experiments performed is presented.

1.4.1 Experiment No. 1.

In the first experiment, a mechanically-tunable, rectangular cavity was used. The dimensions of the cavity were 2-1/2" by 5/16" by 7-1/2"; the length was varied by adjusting movable plungers in both ends. Since the interaction space of the magnetron was approximately equal to the height of the waveguide, the 3J22 tube could be mounted directly in the center of the cavity without any special matching arrangement. Data were obtained for various positions of the plungers and no voltage tuning was observed. The frequency was determined by the

position of the plungers. The tube was mechanically tunable from 1670 to 2500 mc, with a maximum cw power output of 60 milliwatts. Power was coupled out by using a coupling loop placed close to the tube. This type of circuit has a high Q and does not meet the requirements for voltage-tunable operation.

With the cavity filled with steel wool and with shorting plates beyond the steel wool, it was possible to voltage-tune the magnetron from 1870 to 2160 mc. This range of tuning required a change in anode potential of only 100 volts (from 700 to 800 volts). A maximum cw power output of 140 milliwatts was obtained. Lowering of the Q in this manner made voltage tuning possible; however, the circuit was not optimum since the power output varied over a wide range and the tuning range was rather limited.

1.4.2 Experiment No. 2. In the second experiment, a 3J22 was mounted in the center of a 23 inch section of the X-band waveguide. No special matching arrangement was required since the height of the waveguide was approximately the same as the length of the interaction space of the tube. A coupling loop was used, placed very near the tube. The tube operated at a frequency below the cutoff frequency of the waveguide; therefore, the waveguide presented an inductive susceptance to the tube. Even though this susceptance was not a slowly varying function of frequency, it was possible to voltage-tune the tube from 1730 to 2390 mc, with a change of 240 volts in anode potential (from 720 volts to 960 volts). A maximum cw power output of 1.6 watts was obtained. However, in the region of 2000 to 2150 mc the power output was too small to make quantitative measurements. The fact that the wave was attenuated very rapidly in the guide was demonstrated by using shorting plungers in the guide. As expected, for operating frequencies below cutoff frequency, it was found that

the plungers did not affect the operation of the tube until they were brought very near the tube.

1.4.3 Experiment No. 3. In the third experiment, a 3J22 was mounted in a section of S-band waveguide, and each end of the waveguide was connected to a tapered ridge waveguide-to-coaxial-line junction. A special tapered matching section was necessary for mounting the tube. A schematic diagram of the circuit arrangement used is shown in Fig. 1.10. One of the output terminals was connected through several feet of lossy line to a 50 ohm termination, and output power for measuring purposes was coupled out through the other coaxial terminal. On pulsed tests the tube was operated from 2160 to 5200 mc. Under cw operating conditions the tube was voltage-tuned from 2140 to 2950 mc, with a change of 200 volts in anode voltage (from 1300 volts to 1500 volts). The power output remained fairly constant at about 0.35 milliwatts over this range. Complete cw operating data were not obtained because of tube failure. Even though forced air cooling was used on the tube, the glass-to-copper seals used would not hold under these operating conditions. Another reason why cw operating data could not be obtained was that the cathode temperature was unstable due to back heating, and it was difficult to maintain the proper cathode power input. The voltage-tunable operation was sensitive to the cathode temperature, requiring that the temperature of the cathode be below that for normal operation of a magnetron. In some cases, the cathode input could be reduced to zero and the tube would continue to oscillate, the cathode heating being supplied entirely by back bombardment. This tube uses an oxide-coated cathode which was found to be less satisfactory for voltage-tunable operation than either a thoriated tungsten or a pure tungsten cathode.

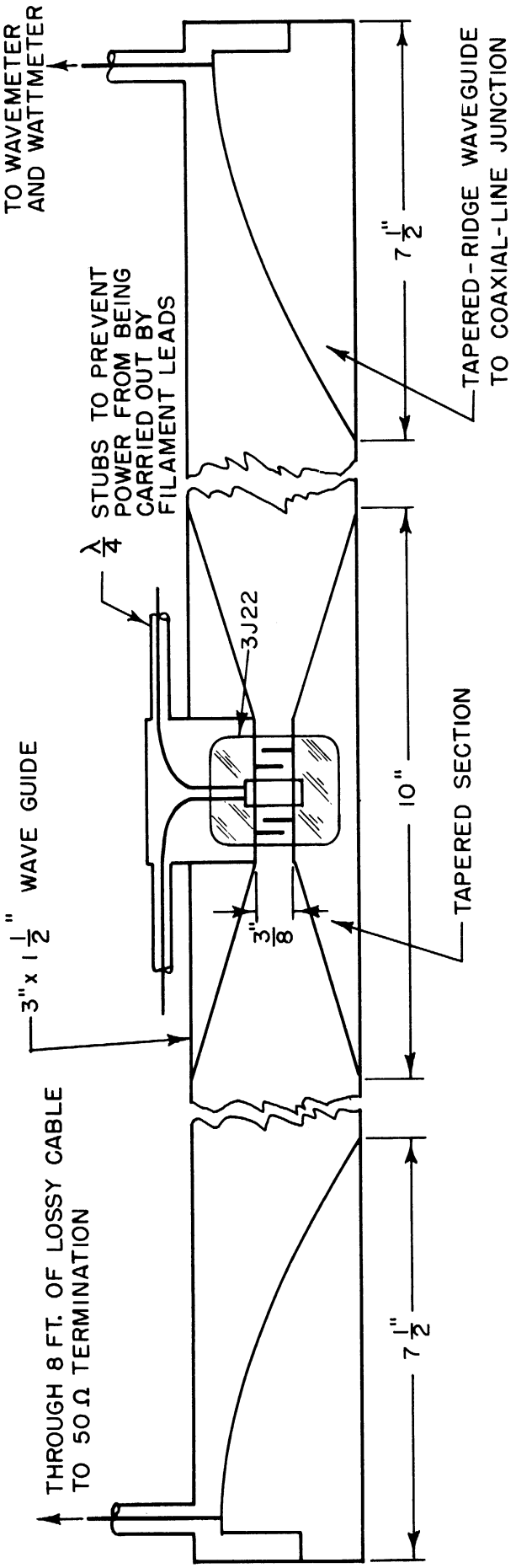

FIG. 1.10
SCHEMATIC DIAGRAM OF CIRCUIT ARRANGEMENT USED IN EXPERIMENT NO. 3

The results of this last experiment indicated that the circuit arrangement shown in Fig. 1.10 possessed the characteristics necessary for voltage-tunable operation. The tube could be voltage-tuned over a wide frequency range, and the power output did not display wide variation in amplitude as had been the case in all previous experiments. With both ends of the waveguide matched to a 50-ohm coaxial line by means of a tapered ridge waveguide-to-coaxial-line junction the admittance, as "seen" by the electrons in the interaction space, is determined by the type of termination used on the coaxial-line output terminals. The junctions used have a very large bandwidth. Therefore, when the coaxial line is terminated in its characteristic impedance, the conductance "looking" into the waveguide from the anode bars of the tube is approximately the characteristic conductance of the waveguide and the susceptance is a slowly varying function of frequency. In the arrangement used, the effective characteristic impedance of the waveguide is equal to that of a waveguide 3" by 3/8" since the tapered section used for mounting the tube extends the full width of the waveguide, but is only 3/8" deep at the tube end of the tapered section.

1.4.4 Conclusions Based on Preliminary Experimental Work Using 3J22 Magnetron. The experiments with the 3J22 magnetron indicated that an interdigital magnetron could be voltage-tuned when operated in the waveguide structure shown in Fig. 1.10. However, there are three important defects in the 3J22 which prevent satisfactory voltage-tunable operation:

a) The cathode temperature is unstable and cannot be maintained at the temperature necessary for good voltage-tunable operation.

b) The construction of the tube is such that it is impossible to satisfactorily decouple the cathode from the cavity when the tube is operated in the π-mode. This results in power being coupled out at the cathode support and prevents oscillation at high power levels.

c) The glass-to-copper seals fail when the power input is raised to a sufficiently high level to obtain significant voltage-tunable power output.

The interdigital structure appears to be especially well suited for voltage-tunable operation, since it is adapted to operation in a single external cavity. In voltage-tunable operation it is desirable to have a cavity which will operate over a wide range of frequencies in a single mode. Even though a single resonant structure may have several modes of operation, they will be much more widely spaced in frequency than the closely spaced resonant modes of a multicavity structure.

CHAPTER 2

DESIGN OF THE MODEL 11 MAGNETRON AND ASSOCIATED CAVITY STRUCTURE

2.1 Introduction

On the basis of the results from the experiments using the 3J22 magnetron, it was concluded that an interdigital magnetron could be designed which would give satisfactory voltage-tunable operation. The design of the tube would be such that the obvious defects found in the 3J22 for voltage-tunable operation would be eliminated. It was also concluded that a waveguide cavity somewhat similar to that shown in Fig. 1.8 would be satisfactory for voltage-tunable operation of a magnetron. In this chapter, the design of such a tube, (designated the Model 11 magnetron) together with its associated cavity, is presented.

2.2 The Interdigital Structure

The interdigital magnetron has received attention because of its wide range tuning possibilities and the simplicity of its mechanical structure. Most of the work on this type of magnetron has been directed toward obtaining a tunable high-Q magnetron. The 3J22 magnetron which was developed in the Research Laboratory of Sylvania by Benedict and Breeden, is a glass-enclosed, external-cavity magnetron which gives a peak pulse power output of 80 watts, at a frequency of 5000 mc (Ref. 18). Crawford and Hare developed an all-metal interdigital magnetron "The

Donutron" (Ref. 19), which gave approximately 50 watts output under cw operating conditions at about the same frequency as the 3J22. Attempts to operate these tubes in the π-mode met with little success. These tubes exhibit a tendency to oscillate in the first-order mode. The power output obtainable in the first-order mode is less than in the π-mode because the rf fields in the interaction space are smaller in the case of the first-order mode. Hull and Randalls (Ref. 20) have shown that the difficulty in operating the interdigital magnetron in the π-mode is due to the loading of the cavity as a result of power coupled out by the cathode. They obtained peak power outputs up to 1.4 kw, and cw outputs up to 500 watts at frequencies near 3000 mc with efficiencies of about 70 percent. These results were obtained by using a specially designed tube with a cathode decoupling choke and a cylindrical pill-box cavity. The cathode coupling problem will be discussed in a later section.

2.3 Design of Cavity for the Model 11 Magnetron

In the design of the Model 11 magnetron and its associated cavity, two factors were considered essential if a satisfactory voltage-tunable magnetron was to be developed. These factors were:

a) Low anode-to-anode capacitance;

b) A high-impedance external cavity, the impedance being a slowly varying function of frequency. By high impedance, we mean in the order of 150 ohms.

The low anode-to-anode capacitance is necessary because this capacitance is in parallel with the external circuit and must be driven by the magnetron. The high overall impedance is necessary if significant power output is to be obtained, since the induced current in the external

circuit is proportional to the total dc anode current, and the dc anode current is limited (for voltage-tunable operation) by the temperature conditions under which the cathode must be operated. Since significant rf fields are required to produce effective bunching, the small induced current obtainable in the external circuit requires that a high impedance be an essential design objective of the circuit.

From Section 1.3.3 the power output is given by the relation:

$$P_L = \frac{I_g^2}{|Y_T|} \cos \theta \qquad (2.1)$$

where

Y_T = the total admittance as "seen" by the electrons

θ = the phase angle of this complex admittance (this is also the angle between the center of the space-charge spoke and the zero of the rf potential wave)

I_g = rf induced current in the admittance Y_T

In the waveguide structure the properties of low anode-to-anode capacitance and high circuit impedance are mutually exclusive. For a low anode-to-anode capacitance it is desirable to have the anode bars as short as possible and still maintain the necessary length of interaction space. However, if the interdigital tube is to be mounted in a manner similar to that shown in Fig. 1.7, the circuit impedance will be reduced as the space between anode supports is reduced, since the characteristic impedance of a waveguide is directly proportional to its height.

The ridge waveguide (Ref. 21) offers a possibility for increasing the circuit impedance over that of a rectangular waveguide for a given spacing between anode supports. The ridge waveguide is characterized by its lowered cutoff frequency and lowered impedance (compared with a rectangular guide of equal dimensions), and by a wide bandwidth free from higher-mode interference. Ridge waveguide may

have either a single or double ridge; Fig. 2.1 shows a cross-section of the ridge waveguide, indicating the dimensions which determine the characteristics of the waveguide. For given dimensions a_1 and b_1, the characteristic impedance of the ridge waveguide decreases with an increase in a_2, or a decrease in b_2. Thus, for a high impedance it it necessary to have a_2 as small as possible and b_2 as large as possible. The value of b_2 is determined by the allowable spacing between the anode supports.

A section of standard S-band waveguide, which has inside dimensions of 1.34 x 2.84 inches, was used. A single-ridge waveguide was used because of its mechanical simplicity. A value of 0.5 inches for b_2 was used, thus giving

$$\frac{b_2}{b_1} = \frac{.5}{1.34} = .394$$

The other impedance-determining factor a_2, was limited by the minimum diameter of the glass envelope of the tube. This value was determined by a consideration of the heat-dissipating capacity of the glass envelope, and the maximum power expected to be radiated from cathode and anode. These considerations resulted in a minimum diameter of the glass envelope of one inch. This gives a ratio of

$$\frac{a_2}{a_1} = \frac{1}{2.84} = .352$$

Using these ratios we find from the design curves given by Cohn (Ref. 21) that the characteristic impedance of such a ridge waveguide at infinite frequency, (Z_∞), is 160 ohms. This value of impedance was considered feasible; however, an even higher value would be desirable. Also, from these curves we find that the cutoff frequency of the ridge waveguide is 1250 mc as compared to a cutoff frequency of 2100 mc for the waveguide without the ridge. The characteristic impedance as a

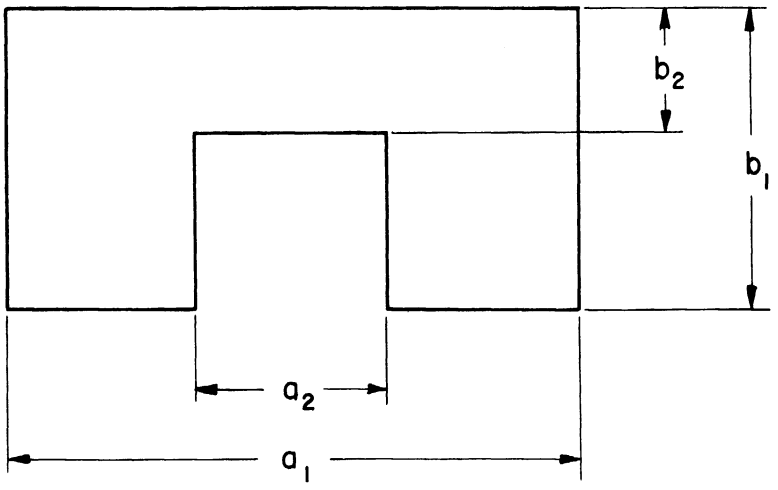

(a.) SINGLE-RIDGE WAVEGUIDE

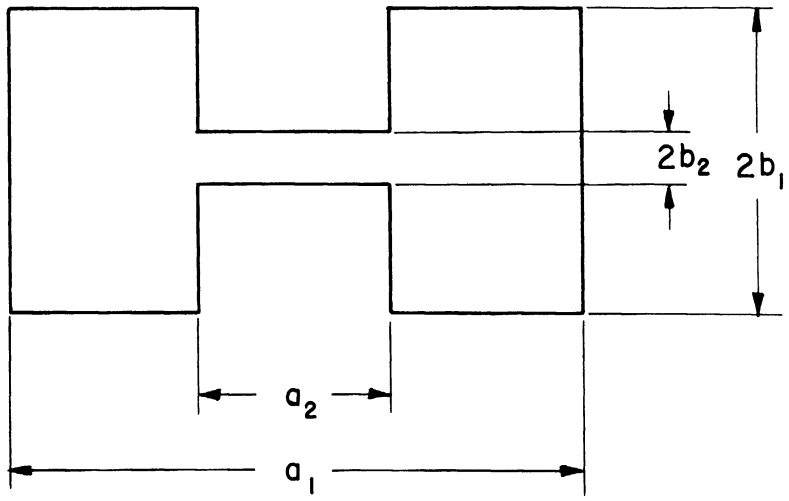

(b.) DOUBLE-RIDGE WAVEGUIDE

FIG. 2.1

CROSS SECTION SHAPE OF RIDGE WAVEGUIDES

function of frequency is given by the relation

$$Z_o = \frac{Z_\infty}{\sqrt{1 - \left(\frac{f_c^1}{f}\right)^2}} \qquad (2.2)$$

where

f_c^1 = cutoff frequency of ridge waveguide

f = operating frequency of ridge waveguide

Fig. 2.2 shows a plot of the characteristic impedance versus operating frequency.

Since it is desirable to have a coaxial output from the magnetron, a tapered-ridge waveguide-to-coaxial-line junction was used to terminate each end of the ridge waveguide. This arrangement is shown in Fig. 2.3. The junctions used are based on a design given by Cohn (Ref. 22). These junctions have an upper cutoff frequency of approximately 4800 mc, therefore, when used in conjunction with a ridge waveguide with a lower cutoff frequency of 1250 mc, give a very wideband structure. The impedance which this circuit presents to the magnetron is, to a very large extent, determined by the termination used on the coaxial output terminals. Theoretically, this impedance would be a pure resistance whose magnitude is given by Eq 2.2 when the coaxial output terminals are terminated in their characteristic impedances. This type of cavity has two outputs, which makes it necessary to dissipate 50 percent of the power in a line termination.

2.4 Design of Model 11 Magnetron

There are four principal factors that affect the operation of a magnetron and thus must be considered in design: the interaction space,

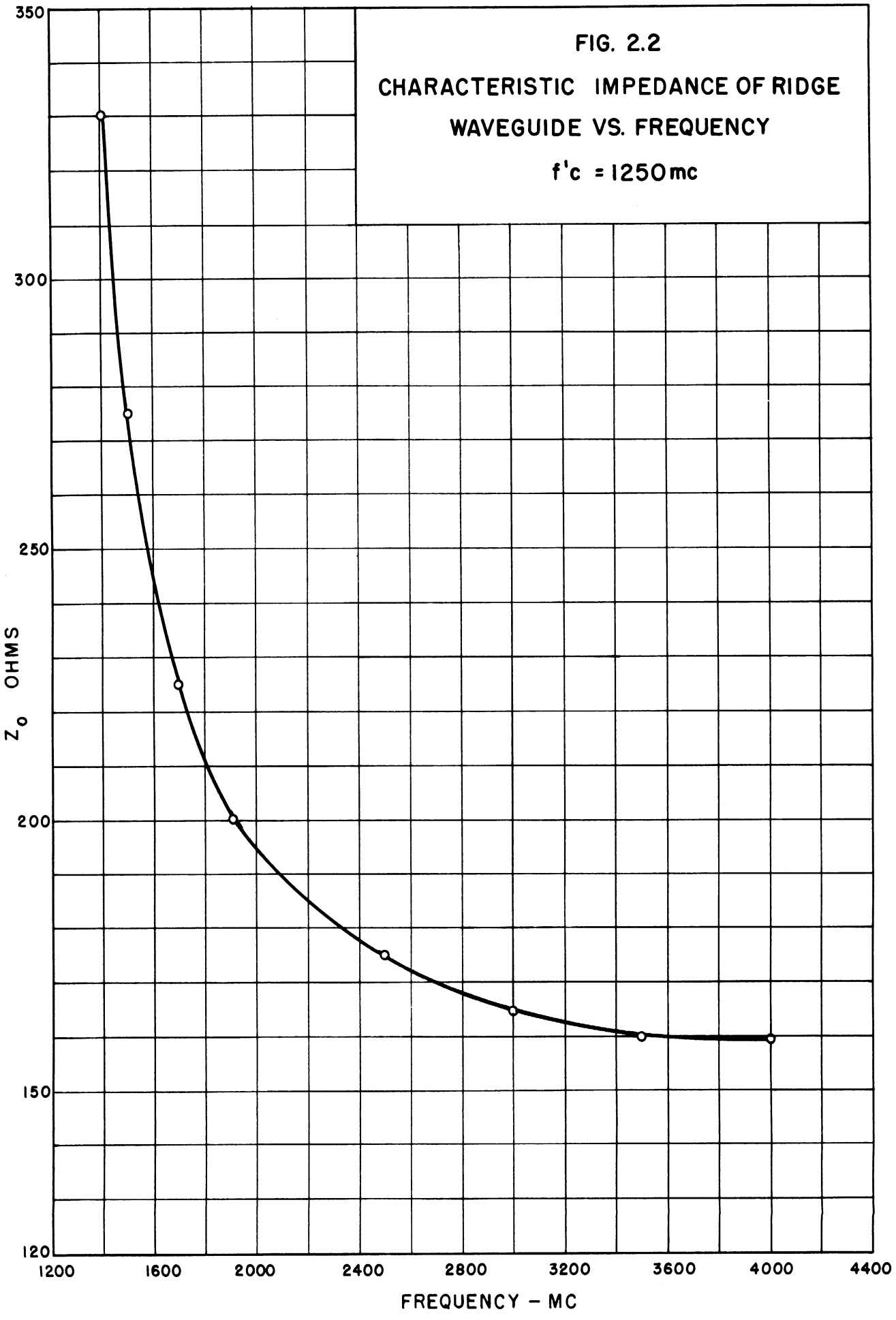
FIG. 2.2
CHARACTERISTIC IMPEDANCE OF RIDGE WAVEGUIDE VS. FREQUENCY
f'c = 1250mc
350
300
250
200
150
120
Z_o OHMS
1200
1600
2000
2400
2800
3200
3600
4000
4400
FREQUENCY - MC

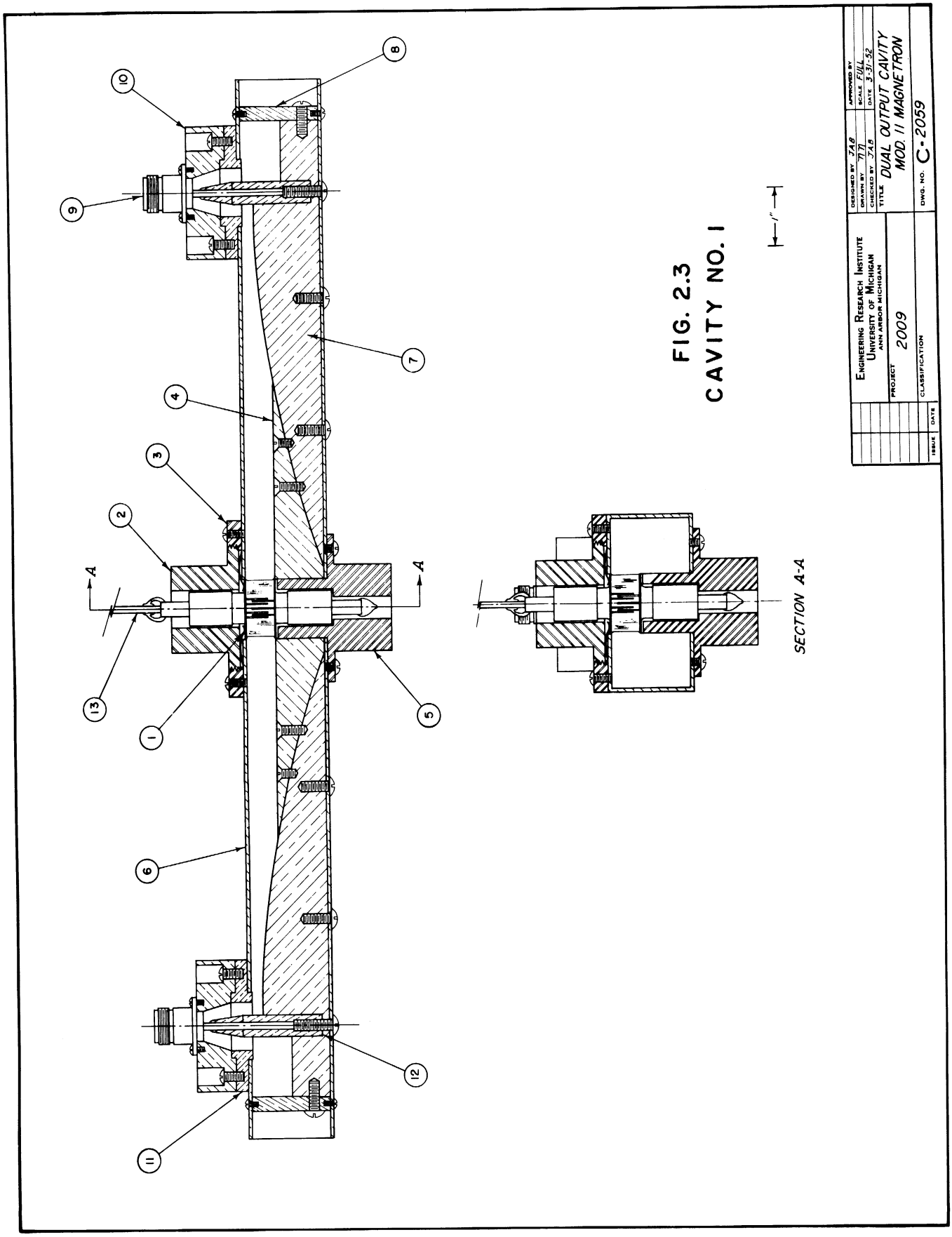

FIG. 2.3
CAVITY NO. 1

the magnetic circuit, the cathode, and the rf electric circuit. These factors are, in general, interdependent and cannot be considered separately. In addition, it is necessary that the overall design be consistent with good mechanical design with respect to such factors as heat dissipation, spacing, size of parts, and tolerances.

In general, there are two ways to design a magnetron. One method is to base the design on that of magnetrons which are known to operate satisfactorily and make the desired changes in tube parameters by using the "scaling relations" (Ref's 23, 24). The second method is to follow a more analytical procedure, making use of the theoretical expressions which describe the operation of a magnetron. The design of the Model 11 magnetron is based primarily on known operable magnetrons, with certain modifications which were considered necessary for the particular application intended for this tube. In the initial phase of design, tentative values were assigned to the various parameters involved in the design of the cavity and the tube. Since no one of the four factors (i.e., interaction space, magnetic circuit, cathode, and electric circuit) can be designed independently of the other three, the final values used are the result of a compromise in conflicting designs of separate components which we believe offers the greatest possibilities for satisfactory operation of the magnetron. The design of the cavity (the rf electric circuit), discussed in the previous section, was arrived at in this manner, and not through an independent process of design.

2.4.1 The Interaction Space. In the design of the interaction space for the Model 11 magnetron, there were two factors, the anode-to anode capacitance and the shape of the anode bars, which were considered to be critical to voltage-tunable operation. Thus, in addition to the

usual consideration of current, voltage, frequency, magnetic field and interaction space dimensions, special attention was given to these two parameters.

Hull (Ref. 25) has suggested that the operation of a typical magnetron can be improved by redesigning the interaction space to reduce the higher-order space (or Hartree) harmonics of the rf field. His analysis was made for the case of π-mode operation and for planar geometry. It appears that the greatest improvement is obtained for low values of operating voltage and magnetic field. If the anodes of a planar magnetron are shaped in accordance with the following equation, space-harmonics other than the π-mode components will not exist in the interaction space.

$$X = a + \frac{d}{\pi} \ell n \left| \sec \frac{\pi Z}{d} \right| \qquad (2.3)$$

Fig. 2.4 shows a plot of Eq 2.3, with the various parameters defined. This equation is for a planar structure; however, it is a good approximation for the cylindrical case when the number of anode bars is greater than 16 or when r_c/r_a is large. When the number of anode bars is small, a better approximation for the cylindrical case may be found by applying the conformal transformation $\omega = (X + i\pi/Nd)$ to the curve of Eq 2.3. The shape of that portion of the anode bars nearest the cathode determines the field configuration between the anode and cathode; therefore, it is necessary to consider only this portion of the anode bars. From a consideration of Fig. 2.4 it can be shown that a good approximation to the desired anode shape can be obtained by making the anode bars round with a diameter of 2/3d (where d is the center-to-center spacing of the anode bars).

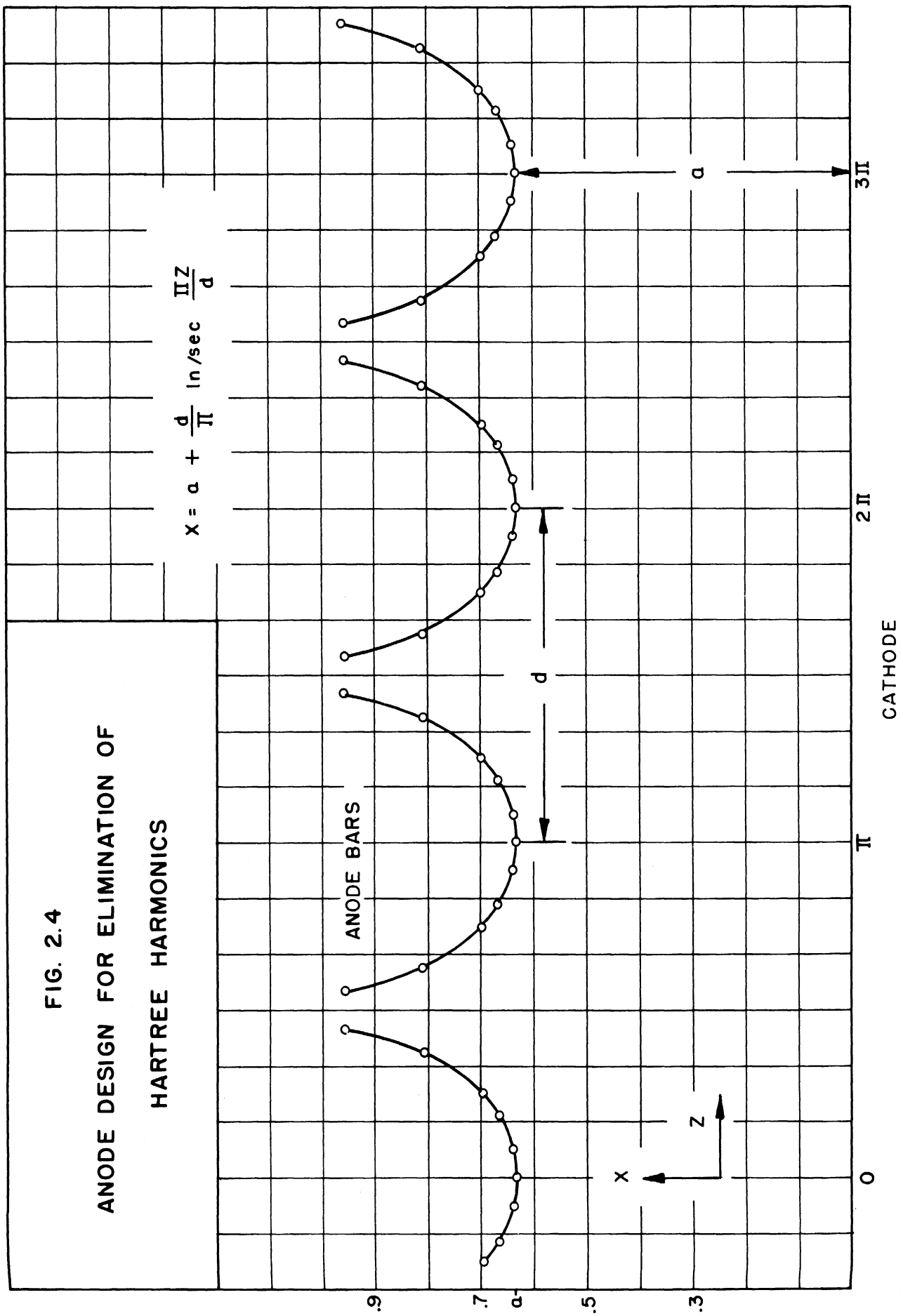

FIG. 2.4

ANODE DESIGN FOR ELIMINATION OF HARTREE HARMONICS

In a typical high-Q magnetron, the potential between adjacent anode bars is very nearly sinusoidal with time when the tube is oscillating in the π-mode. This is made possible through the filtering action of the magnetron cavity, since the rf field in the interaction space of most magnetrons contains considerable space harmonics. The induced current in a magnetron circuit due to the rotating space charge is determined by the space distribution and velocity of the charge in the interaction space. In the high-Q case, appreciable rf voltage can be developed only at the resonant frequency of the tank circuit; induced currents at harmonic frequencies may flow in the circuit but will contribute very little to output voltage because of the relatively low impedance at these harmonic frequencies. Therefore, under normal operating conditions (i.e., high voltage and magnetic field), the higher space harmonics of the rf field in the interaction space are of little concern in the case of the high-Q magnetron.

In the operation of a low-Q magnetron, the presence of the space harmonics other than the π-mode components can cause significant harmonic content to exist in the output voltage of the magnetron due to the fact that the impedance at the harmonic frequencies may be appreciable for a low-Q, wide-band circuit. In other words, the circuit will not serve as a filter to assure that only the fundamental frequency will occur in the output voltage.

On the basis of these considerations, it was decided to use round anode bars in the design of the Model 11 magnetron. However, the design suggested by Hull for the complete elimination of space harmonics called for an anode diameter of 2/3d (where d is the center-to-center spacing of adjacent anode bars), which is inconsistent with a design

for low anode-to-anode capacitance. Therefore, the spacing between adjacent anode bars was made equal to the diameter of the anode bars.

The decision to design the tube for operation in the frequency range of 2000 to 3000 mc was based primarily on the fact that test equipment was available in this range. The choice of 12 anode bars and the ratio of cathode to anode radii of .6 were chosen on the basis of known performance of operable tubes. From a mechanical viewpoint, it was desirable to use material which was commercially available for fabricating the anode bars; 0.035-inch molybdenum rod was chosen for this purpose. With the spacing between adjacent anode bars equal to 0.035 inch, this then fixed the center-to-center anode diameter at 0.268 inch, or an inside diameter of 0.233 inch. For an r_c/r_a ratio of 0.6 the diameter of the cathode is then 0.140 inch.

An efficiency of 10 percent and a power output of 5 watts was assumed for purposes of determining the length of active cathode required. Thus, a power input of 50 watts at an anode potential of 1000 volts requires 50 milliamperes of anode current. Allowing a factor of two, and designing the cathode to supply a space-charge-limited current of 100 milliamperes, requires an active length of cathode of 0.150 inch. The length of the overlap of the two sets of anode bars is determined by the length of the active portion of the cathode and the two end hats; this results in the anode bars being 0.395 inch long with an overlap of 0.280 inch. This leaves a length of 0.105 inch anode bar outside of the interaction space, and adds some inductance in series with the anode-to-anode capacitance. However, since this inductance is the equivalent inductance of the six anode bars in parallel it was considered that this inductance would have a less detrimental effect

on the operation of a voltage-tunable magnetron than would result from reducing the circuit impedance by decreasing the spacing of the anode supports.

Figures 2.5 and 2.6 give E_o versus r_a with $n\lambda$ as a parameter, and B_o versus r_c/r_a with $n\lambda$ as a parameter. Assuming an operating frequency of 3000 mc, which gives a value of $n\lambda$ of 60, we find E_o = 250 volts and B_o = 550 gauss. For good voltage-tunable operation (Ref. 16), it is desirable to operate at relatively high magnetic fields, perhaps $5B_o$, or in the order of 3000 gauss.

The anode-to-anode capacitance was determined by finding the capacitance from a single wire to two infinite planes placed d/2 from the wire, then taking 1/4 of this value to find the capacitance between adjacent anode bars. This method makes use of a conformal transformation and design equations given by Wholey and Eldred (Ref. 26). Fig. 2.7 shows a schematic diagram of the equivalent circuit used in making the calculations, with the various parameters defined. In this method, the single conductor and two infinite planes are transformed to a coaxial arrangement and the capacitance is then found by the standard formula:

$$C = 2\pi \frac{1}{\ell n \frac{r_1}{r_2}} \text{ farads per meter} \qquad (2.4)$$

The total anode-to-anode capacitance is 1.8$\mu\mu$f per centimeter, and since the anode overlap is approximately one half centimeter, this gives a capacitance of 0.9 $\mu\mu$f. This value will be increased somewhat by the presence of the cathode and cathode end hats.

Listed below are the values of the parameters which resulted from the design of the interaction space.

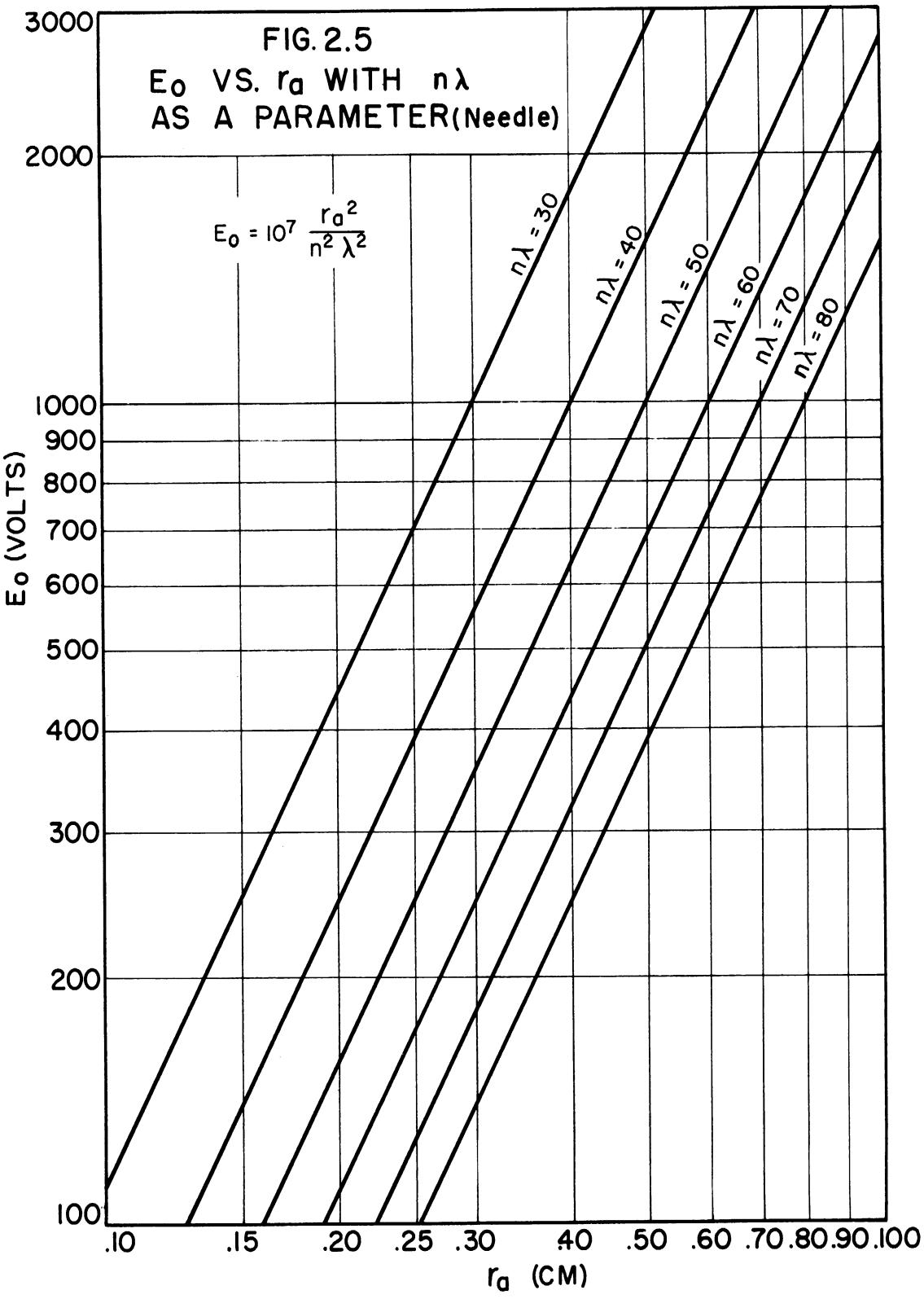
FIG. 2.5
E0 VS. ra WITH nλ
AS A PARAMETER(Needle)
E0 = 10^7 ra^2 / n^2 λ^2
nλ = 30
nλ = 40
nλ = 50
nλ = 60
nλ = 70
nλ = 80
E0 (VOLTS)
3000
2000
1000
900
800
700
600
500
400
300
200
100
.10
.15
.20
.25
.30
40
.50
.60
.70
.80
.90
.100
ra (CM)

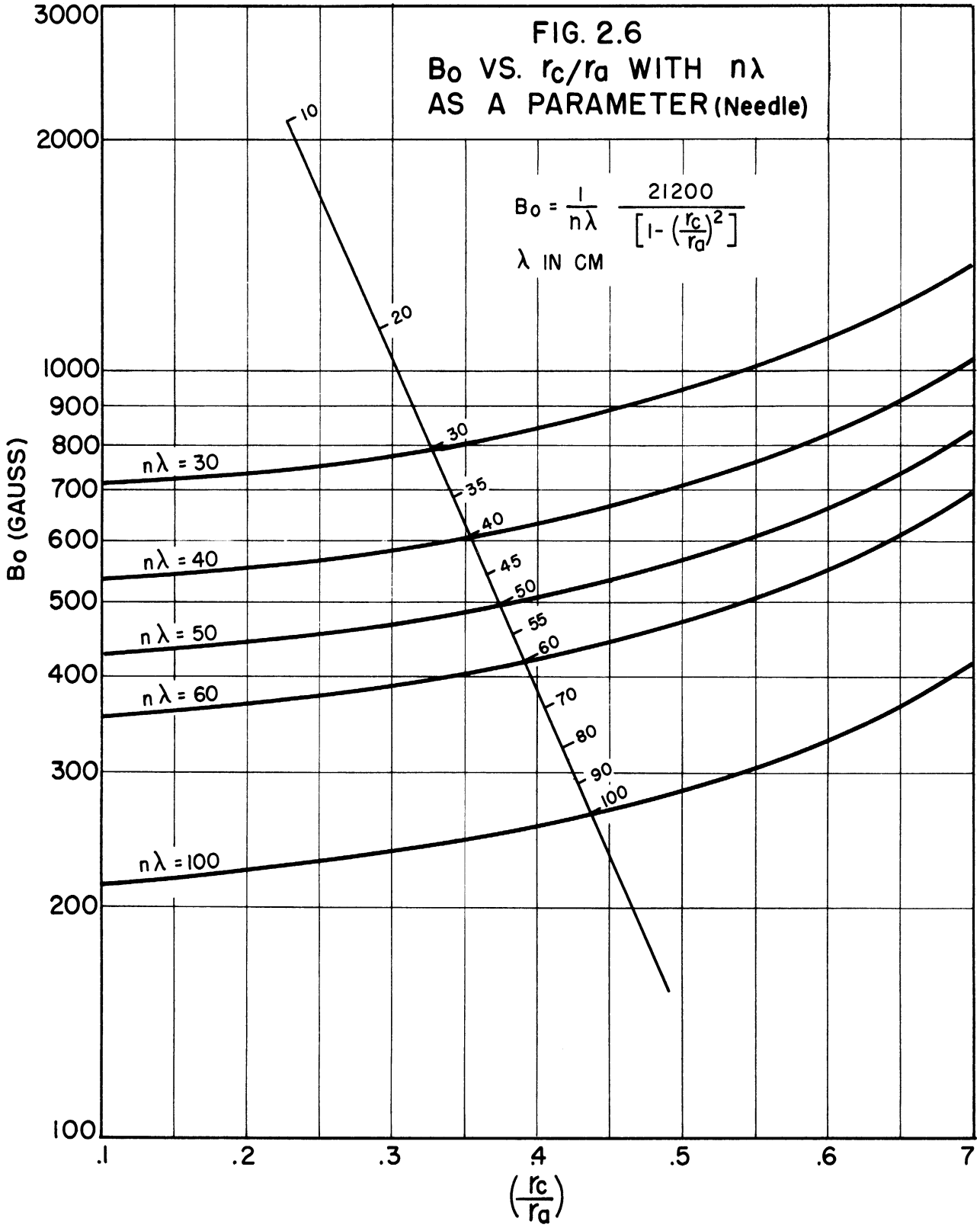
FIG. 2.6
Bo VS. rc/ra WITH nλ
AS A PARAMETER (Needle)
Bo = 1/nλ · 21200/[1-(rc/ra)²]
λ IN CM
Bo (GAUSS)
(rc/ra)
nλ = 30
nλ = 40
nλ = 50
nλ = 60
nλ = 100
10
20
30
35
40
45
50
55
60
70
80
90
100
3000
2000
1000
900
800
700
600
500
400
300
200
100
.1
.2
.3
.4
.5
.6
7

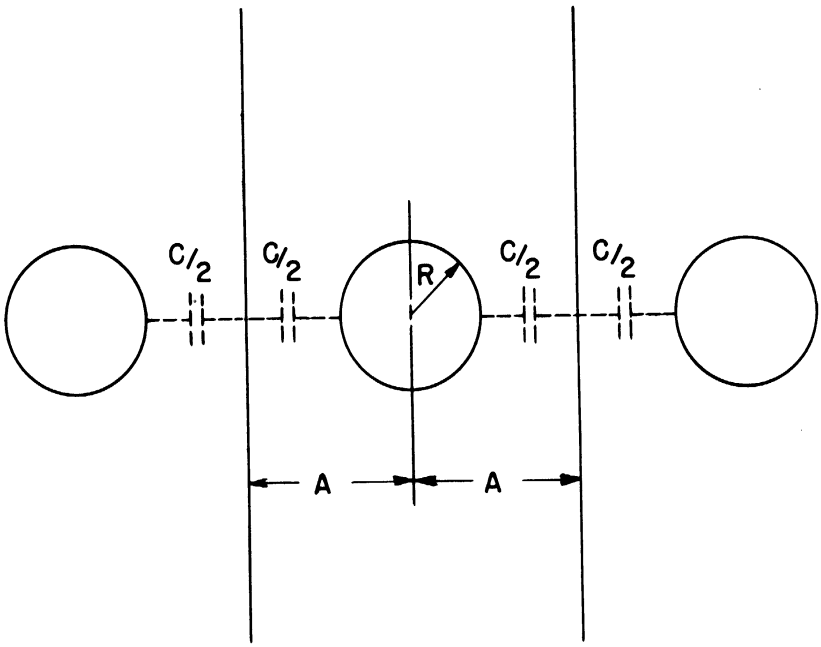

$\frac{R}{A} = 1/2$

C = CAPACITANCE BETWEEN BAR AND TWO INFINITE PLANES

FIG. 2.7

SCHEMATIC DIAGRAM OF ARRANGEMENT
USED TO DETERMINE CAPACITANCE
BETWEEN ADJACENT ANODE BARS

f = 3000 mc (chosen to suit available test equipment)

P_i = 50 watts

I_b = .050 amperes (required to satisfy the maximum power demand at an anode voltage of 1000 volts)

N = 12 (number of anode bars, based on existing magnetrons)

r_c/r_a = 0.6 (ratio of cathode to anode radii, based on existing magnetrons)

r_a = .233 inch (determined by size of molybdenum rod available, and anode radius of existing magnetrons)

L_c = .150 inch (length of emitting surface on cathode required to satisfy maximum power requirements with a safety factor of two)

ℓ_s = .290 inch (overlap length of anode bars; chosen to allow for length of emitting portion of cathode and end hats)

E_o = 250 volts

B_o = 550 gauss

C_p = .9$\mu\mu$f (anode-to-anode capacitance, no cathode present)

2.4.2 The Magnetic Circuit. In the design of the magnetic circuit there were two factors which were considered to be important to the successful operation of the tube: that the magnetic field be as nearly uniform as possible throughout the interaction space and that relatively high fields, in the order of 3000 gauss, be obtained without unreasonable requirements for an electromagnet. The uniform field is necessary if the tube is to operate satisfactorily over a wide range of anode voltages. A high magnetic field will improve voltage-tunable operation for two reasons: first, the power output will be more nearly constant (Ref. 16); and second, since the cathode is operated under temperature limited conditions, the dc anode current will be small, therefore it is desirable to have a high value of cutoff voltage so that the dc power input to the tube will be large enough to give

significant rf power output. The high dc input is necessary because of the very low efficiency of voltage-tunable magnetrons. Iron pole pieces were built into the tube; this arrangement satisfied the demand for a low-reluctance magnetic circuit which will produce a very nearly uniform magnetic field in the interaction space, and also satisfied the requirements of mechanical strength and feasibility. Figure 2.8 shows a drawing of the Model 11 magnetron with an oxide-coated cathode in place. As indicated, the iron pole pieces, part 1, serve as anode supports. The molybdenum rods are brazed onto the pole pieces. Parts 2 and 3 are made of Kovar to facilitate making the glass seals as indicated.

2.4.3 The Cathode. The cathode serves two useful functions: it serves as a source of electrons (which must be sufficient to satisfy the maximum power requirements), and the end hats on the cathode prevent leakage current; that is, they confine the electron flow to the region of the interaction space. It is implied that the cathode also has certain undesirable features; these will be discussed in a later section. As previously stated in the discussion of the interaction space, the diameter of the cathode was determined primarily from information on existing magnetrons; it was necessary to consider this in designing the interaction space, since the cathode serves as one boundary of the interaction space. The length was determined by the emission required to satisfy the assumed maximum input power. It was considered necessary to keep the leakage current to a minimum; therefore, the end hats were designed to give as complete shielding as possible while still maintaining reasonable mechanical and electrical tolerances. The construction and mounting techniques were based largely on previous experience with the Model 9 magnetrons. Figure 2.9 shows an assembly drawing of the

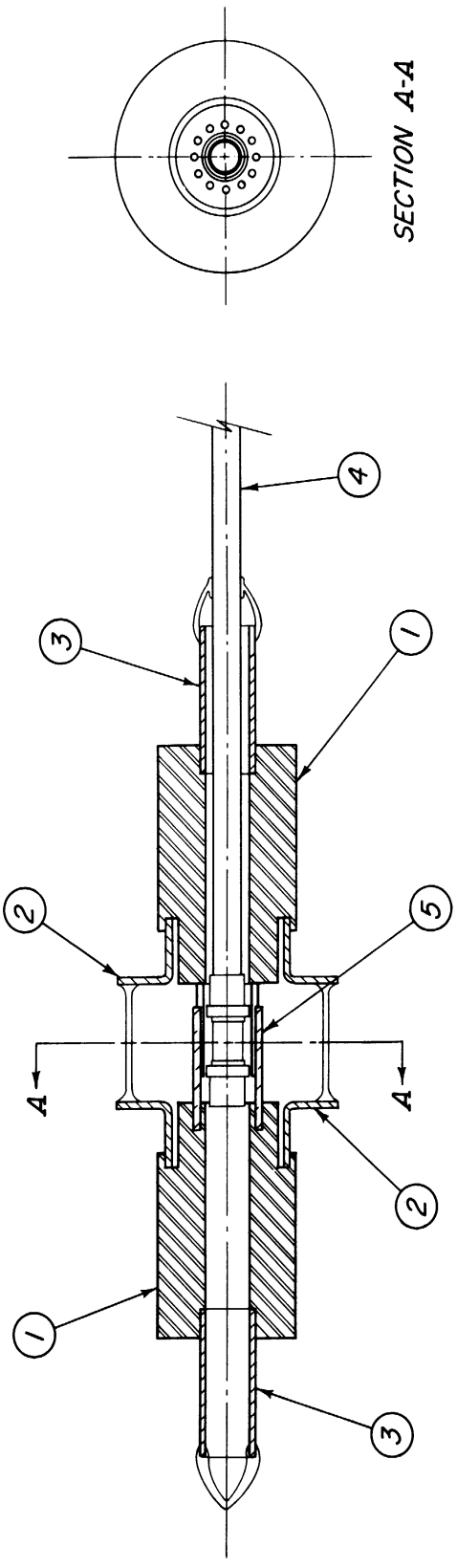

FIG. 2.8

1/2"

ALL DIMENSIONS UNLESS OTHERWISE SPECIFIED MUST BE HELD TO A TOLERANCE - FRACTIONAL ± 1/64" DECIMAL ± .005" ANGULAR ± 1/2°

ENGINEERING RESEARCH INSTITUTE
UNIVERSITY OF MICHIGAN
ANN ARBOR MICHIGAN

PROJECT 2009

CLASSIFICATION

ISSUE | DATE

DESIGNED BY JAB | APPROVED BY
DRAWN BY TTT | SCALE X2
CHECKED BY JAB | DATE 3-27-52

TITLE INTERDIGITAL EXTERNAL CAVITY MAGNETRON MOD II

DWG. NO. B- 10,011

DWG. NO. B

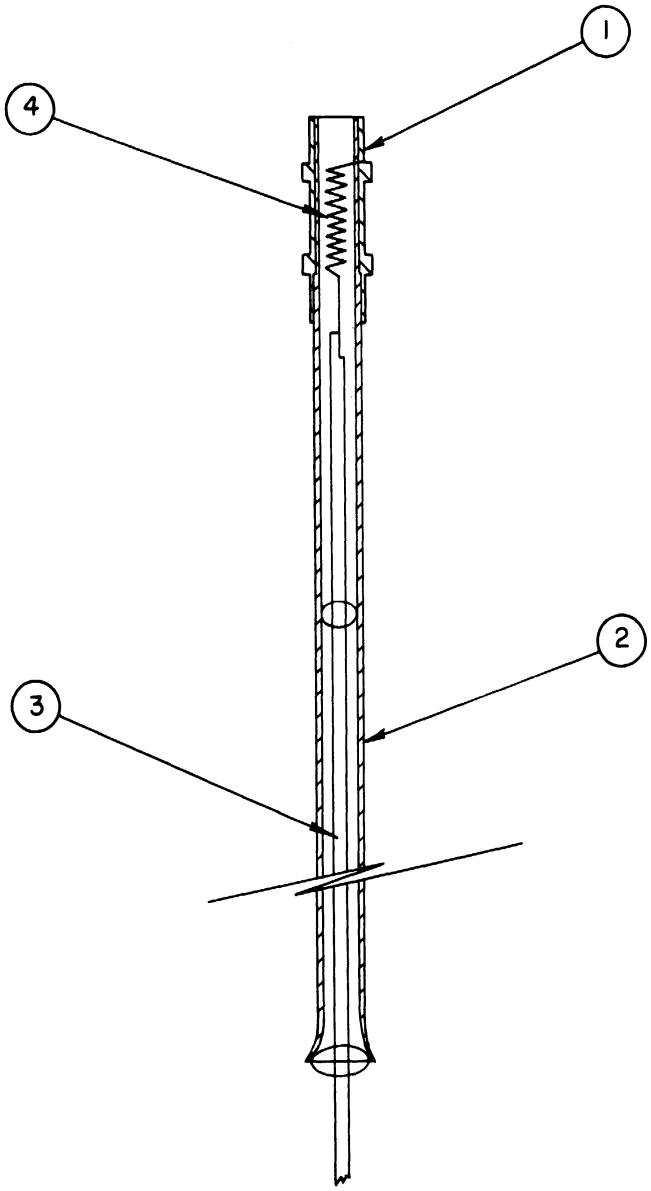

FIG. 2.9

ALL DIMENSIONS UNLESS OTHERWISE SPECIFIED MUST BE HELD TO A TOLERANCE - FRACTIONAL ± 1/64," DECIMAL ± .005," ANGULAR ± 1/2°

		ENGINEERING RESEARCH INSTITUTE UNIVERSITY OF MICHIGAN ANN ARBOR MICHIGAN	DESIGNED BY	APPROVED BY
			DRAWN BY MM	SCALE X 2
			CHECKED BY VRB	DATE 4-14-52
		PROJECT 2009	TITLE OXIDE CATHODE ASSEMBLY FOR MOD II	
ISSUE	DATE	CLASSIFICATION	DWG. NO. A- 8027	

oxide-coated cathode used in Model 11. Part 1 is the nickel base to which the oxide coating is applied; parts 2 and 3 were made of Kovar to make possible the necessary glass seals.

Figure 2.10 shows an assembly drawing for the thoriated-tungsten and pure-tungsten cathodes. In this design, additional material has been added to part 1 to increase the heat dissipating capacity of the cathode, since with the oxide-coated cathode backheating caused the temperature of the cathode to be unstable. The dimensions of this cathode are approximately the same as for the oxide-coated cathode. Parts 1, 3 and 5 are made of molybdenum to provide maximum heat-dissipating capacity. Parts 6 and 7 are made of Kovar to facilitate making the necessary glass seals. The diameter of this cathode was increased to 0.150 inch in order to make use of existing equipment for winding the helices.

One of the chief difficulties in the operation of voltage-tunable magnetrons is that the operation is very sensitive to the temperature of the cathode. Also, in the case of the interdigital magnetron (as will be shown in a later section), the cathode serves to couple power out of the cavity and may have a very serious effect on the operation of the tube unless some method of decoupling is used. The button cathode shown in Fig. 2.11 was designed to eliminate both of these difficulties. This cathode consists of an emitter and a repeller (or collector, depending on the mode of operation). The emitter consists of either a nickel or molybdenum base which is given an oxide coating, the emitter and repeller are designed so that they serve as end hats and are spaced so that the interaction space has the same length as when regular cathodes are used. This arrangement eliminates the cathode as a physical

DWG. NO. A

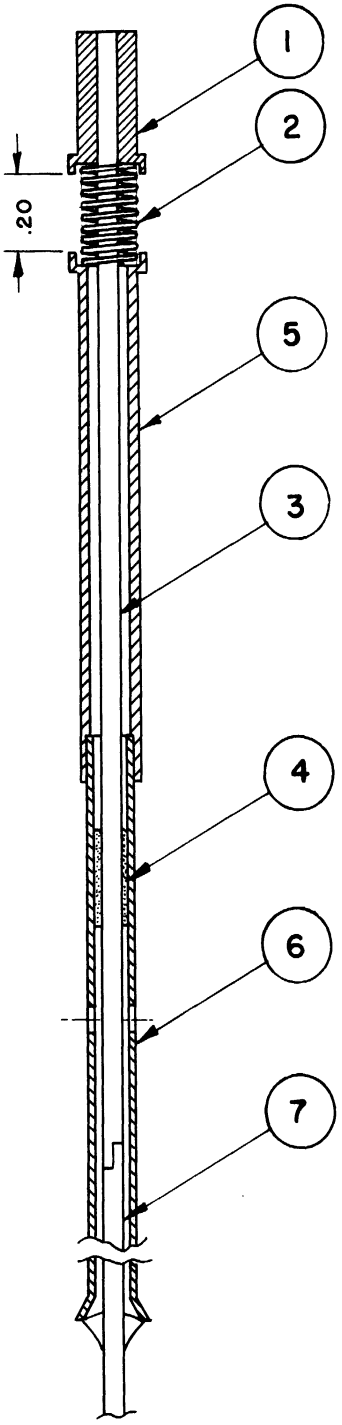

FIG. 2.10

ALL DIMENSIONS UNLESS OTHERWISE SPECIFIED MUST BE HELD TO A TOLERANCE - FRACTIONAL ± 1/64," DECIMAL ± .005," ANGULAR ± ½°

		ENGINEERING RESEARCH INSTITUTE UNIVERSITY OF MICHIGAN ANN ARBOR MICHIGAN	DESIGNED BY J.A.BOYD	APPROVED BY
			DRAWN BY P L W	SCALE 2X
			CHECKED BY	DATE 7-1-52
		PROJECT 2009	TITLE TUNGSTEN CATHODE FOR MODEL II MAGNETRON	
1	7-1-52	CLASSIFICATION	DWG. NO. A-8030	
ISSUE	DATE			

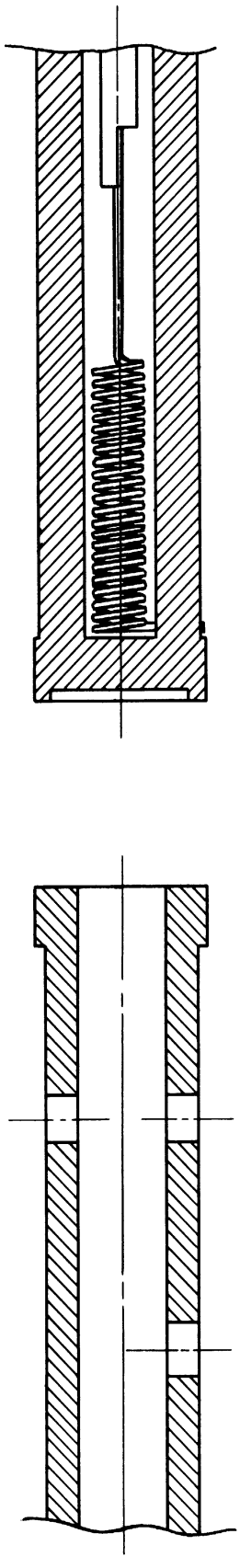

FIG. 2.11

BUTTON CATHODE, SECOND MODEL

boundary for the interaction space, and also prevents power from being coupled out by the cathode support.

2.5 Voltage-Tunable Magnetrons Models 11A and 11B

Two modifications were made in the design of the Model 11 magnetron:

a) Square anode bars are used with an inside anode diameter of .235 inch. The anode bars are .030 inch. The bars are formed by grinding .045 molybdenum rods to the desired dimension. This tube, which is otherwise identical to the Model 11, has been designated Model 11A.

b) The inside anode diameter was changed to 0.205 inch, and .030 inch molydenum rods were used as anode bars. With this arrangement, the spacing between adjacent anode bars is also .030 inch. This tube, which is otherwise identical with the Model 11, has been designated Model 11B.

The purpose of the Model 11A was to make possible a comparison of two similar tubes, one with round anode bars, and one with square anode bars.

The design of the Model 11B was based on a consideration of the operation of a voltage-tunable magnetron. The output of the Model 11 is in the order of 15 milliwatts, which indicates a very small rf voltage across the anode bars. For small rf voltages, it is reasonable to expect that bunching and interaction efficiency will be enhanced by increasing the ratio r_c/r_a so that the rf fields will penetrate farther into the interaction space. The Model 11B was designed for the purpose of determining the validity of this assumption. Tungsten cathodes

with a diameter of .150 inch were used in the Model 11B, giving an r_c/r_a ratio of .75, as compared to a nominal value of .6 for conventional high-Q magnetrons.

2.6 Analysis of Cathode Circuit

Hull and Randals (Ref. 20) have shown that the reason the interdigital magnetron will not operate in the π-mode in a high-Q cavity at high power level is that power is coupled out by the cathode support. The power coupled out by the cathode support reduces the unloaded Q of the circuit to such an extent that stable oscillations cannot be maintained at high power levels. These tubes operate satisfactorily in the first order mode because the currents induced in the cathode support (due to different portions of the circuit) cancel; therefore, there is no loading on the cavity. However, it is possible to obtain higher efficiencies when the tubes are operated in the π-mode.

Figure 2.12 shows a rolled-out view of the anode structure as seen from the cathode. Figure 2.12(a) shows the rf potential distribution around the anode support for the π-mode of operation. This mode is characterized by the fact that all of the anodes of a set are always at the same rf potential. Figure 2.12(b) shows the rf potential distribution around the anode support for the first-order mode of operation; this mode is characterized by the fact that the rf potential on a set of anodes varies sinusoidally around the anode support. There is one complete cycle of variation around the anode in the first-order mode of operation. Higher-order modes of operation are similar to the first order mode, there being n sinusoidal variations of the anode rf potential around the anode support for the n^{th} mode.

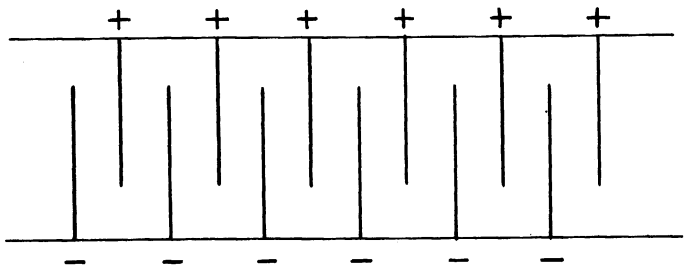

(a) Π MODE

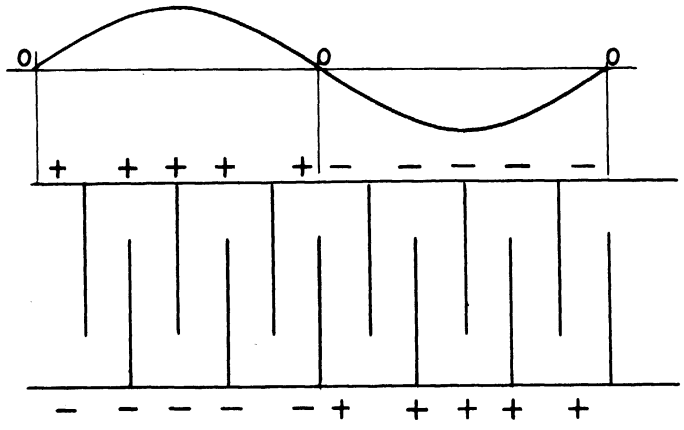

(b.) FIRST ORDER MODE

FIG. 2.12

POTENTIAL DISTRIBUTION ON ANODE
STRUCTURE OF INTERDIGITAL MAGNETRON

Figure 2.13 shows a cross-section of the Model 11 magnetron with an equivalent circuit to show how power is coupled out by the cathode support. Operation in the π-mode is assumed. C_1 is the capacitance between the lower end hat and the lower anode set, C_2 is the capacitance between the upper end hat and the upper anode set, and Z is the impedance between the cathode support and the pole piece looking out from the cathode. The voltage e_s is the rf voltage existing between the anode sets.

The power coupled out by the cathode may be expressed in terms of the power dissipated in the resistance R in the equivalent circuit. This expression is

$$P = \frac{e_s^2 R}{R^2 \left(1 + \frac{C_2}{C_1}\right)^2 + \left[X \left(1 + \frac{C_2}{C_1}\right) - \frac{1}{\omega C_1}\right]^2} \qquad (2.5)$$

For optimum operating conditions in the π-mode it is desirable to minimize the power coupled out by the anode support. This can be accomplished in two ways; (1) make R approach zero or, (2) make R approach infinity. These conditions can be approximated by placing a "choke" on the cathode support as shown in Fig. 2.13a. For the condition of R = 0 the choke must be slightly greater than an odd number of quarter wavelengths long. Figure 2.14 shows an adjustable choke which was used on the Model 11 magnetron.

2.7 Equivalent Circuit of Model 11 Magnetron and Associated Cavity

The essential properties of an operating magnetron may be shown by a simple circuit using lumped constant elements (Ref. 24). This approximate equivalent circuit is valid when the magnetron is operating in a single mode. A general solution of the equivalent-circuit problem would require the solution of Maxwell s equations with

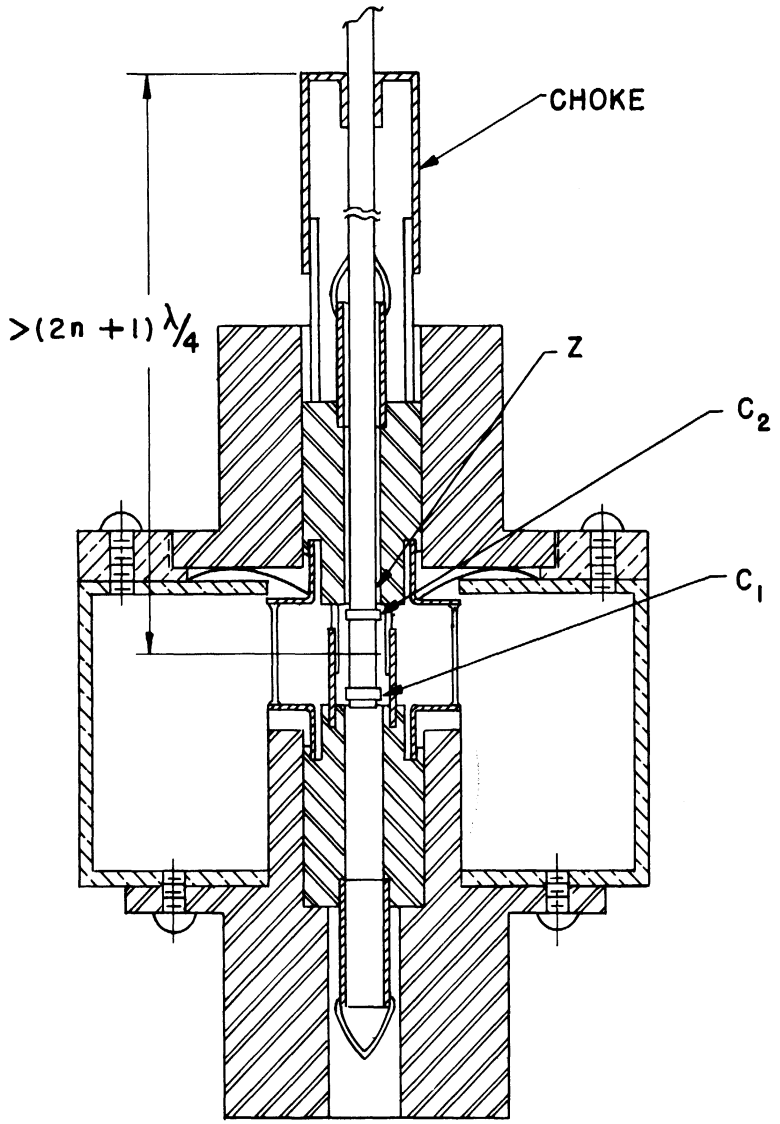

(a.)

CROSS SECTION OF MODEL II MAGNETRON
WITH OXIDE CATHODE IN AN S-BAND CAVITY

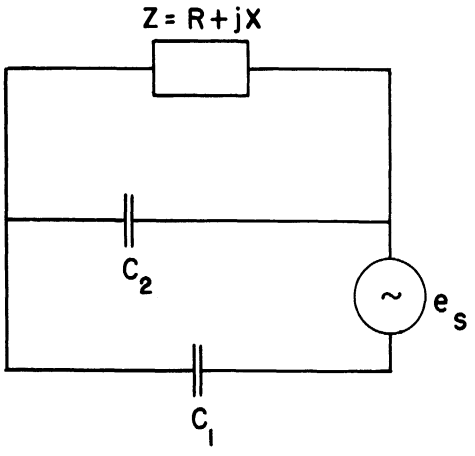

(b.)

EQUIVALENT CIRCUIT OF
CATHODE AND SUPPORT

FIG. 2.13

DWG. NO. A

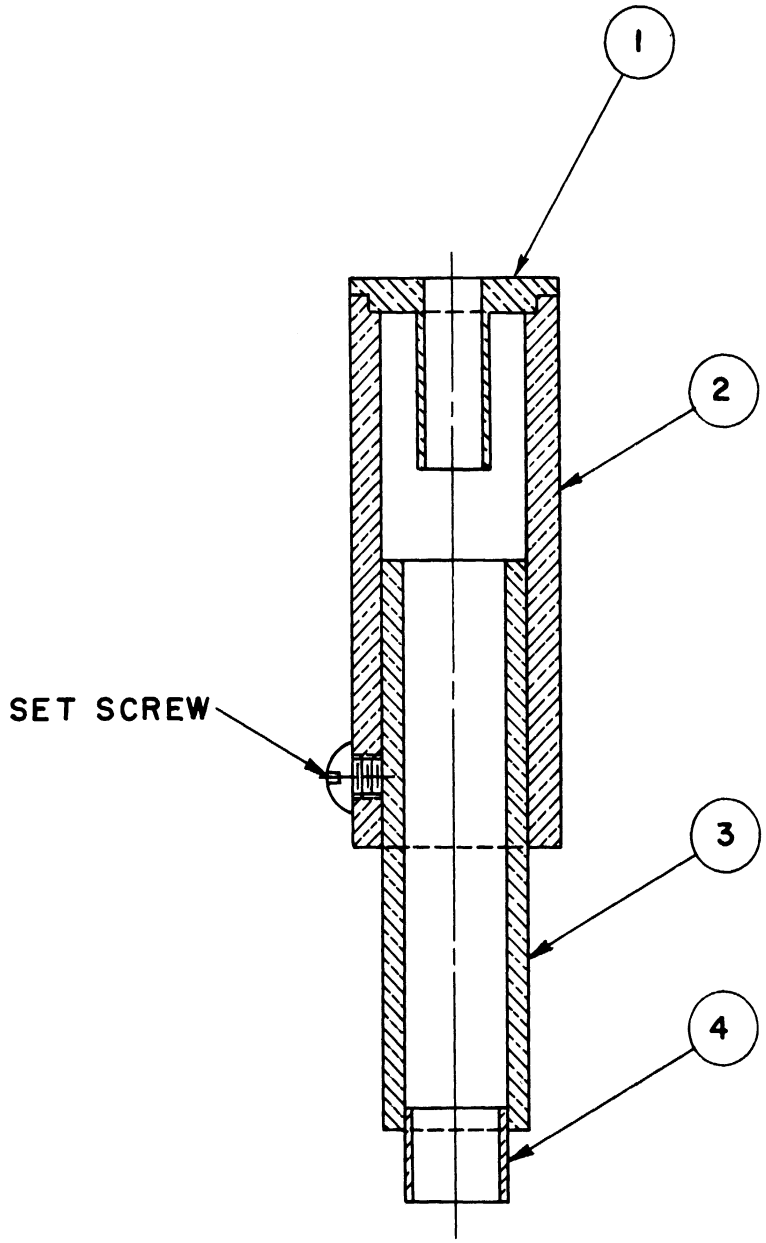

FIG. 2.14

ALL DIMENSIONS UNLESS OTHERWISE SPECIFIED MUST BE HELD TO A TOLERANCE - FRACTIONAL ± 1/64," DECIMAL ± .005," ANGULAR ± ½°

		ENGINEERING RESEARCH INSTITUTE UNIVERSITY OF MICHIGAN ANN ARBOR MICHIGAN	DESIGNED BY JAB	APPROVED BY
			DRAWN BY PLW	SCALE 2X
			CHECKED BY	DATE 8-1-52
		PROJECT 2009	TITLE ADJUSTABLE CHOKE	
1	8-1-52	CLASSIFICATION	DWG. NO. A-2070	
ISSUE	DATE			

the boundary conditions as determined by the cavity; however, suitable values may be obtained for the lumped constant circuit elements by an approximate solution of the problem. Figure 2.15 shows an approximate equivalent circuit for the Model 11 magnetron and its associated cavity. Figure 2.15(a) is a first approximation in which the various elements are defined as follows:

I_g is a current generator representing the rf current induced in the circuit by the space charge. θ is the phase angle between the rf voltage and rf current, the relation being

$$\left|Y_T\right| \angle \theta = \frac{I_g \angle \theta}{E_{rf}}$$

where I_g and E_{rf} are rms values, θ being defined so that it is negative for a lagging current.

C_p is the total capacitance between anode sets, equal to approximately $1 \mu\mu f$.

L_p is the equivalent inductance of the anode bars between the interaction space and the anode supports, equal to approximately $130 \mu\mu h$.

Z_c is the impedance of the coaxial line formed by the cathode support and the pole piece looking out from the cathode, its value is given approximately by

$$Z_c = - j Z_o \cot \frac{2\pi \ell}{\lambda} \qquad (2.6)$$

where

Z_o = 28.5 ohms (characteristic impedance of the line)

ℓ = length of the line

λ = wave length

This assumes that the losses in the line, and losses due to radiation from the extension of the center conductor, are negligible.

C_1 and C_2 are as defined in Fig. 2.13.

G_t is the equivalent conductance representing the losses in the waveguide portion of the structure.

T_1 and T_2 represent the waveguide-to-coaxial junctions, assumed to be ideal transformers.

$Z\ell_1$ and $Z\ell_2$ are the external loads connected to the coaxial output terminals.

Figure 2.15(b) represents a second approximation in which it has been assumed that the coaxial output terminals are terminated in their characteristic impedances and that the losses in the wave guide are negligible compared to the load. Since the reactance due to 2 L_p is never more than 10 percent of the reactance due to C_p, X_{L_p} is neglected. X_c is the equivalent reactance of the combination of C_1, C_2, and Z_c, where Z_c is assumed to be a pure reactance.

$$X_c = \left[\frac{Z_c' \omega (C_1 + C_2) - 1}{\omega C_1 (1 - Z_c' \omega C_2)} \right] \tag{2.7}$$

where Z_c is given by Eq 2.6, and $j Z_c' = Z_c$. Z_o is the characteristic impedance of the ridge waveguide assumed to be a pure resistance given by

$$Z_o = Z_\infty \frac{1}{\sqrt{1 + \left(\frac{f_c'}{f}\right)^2}} \tag{2.8}$$

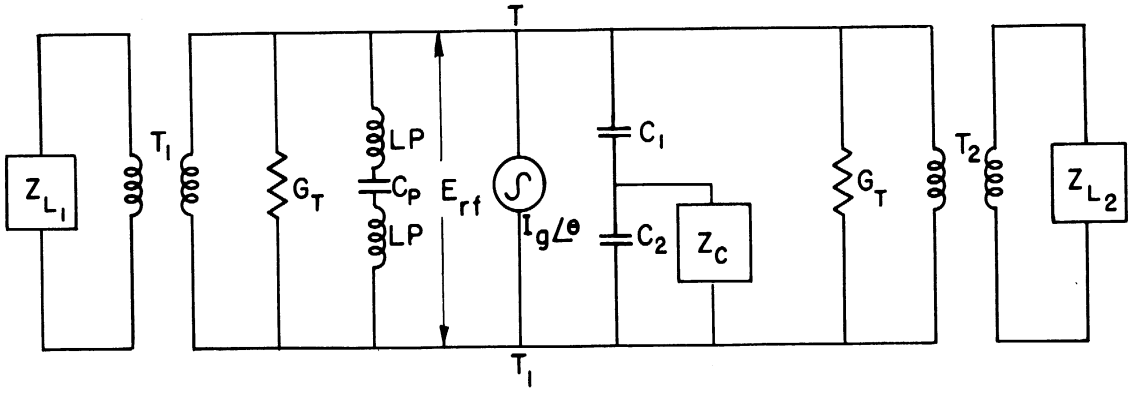

(a.)

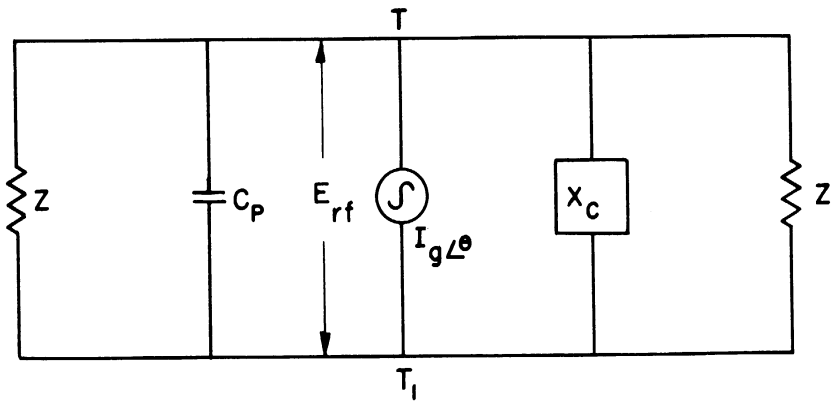

(b.)

FIG. 2.15

EQUIVALENT CIRCUIT OF MODEL II MAGNETRON

The admittance of the circuit shown in Fig. 2.15(b) may therefore be expressed as

$$Y_T = \frac{2}{Z_o} + j\omega c_p + \frac{1}{jX_c} \qquad (2.9)$$

where X_c may be either positive or negative.

In a study of the cathode circuit problem, it was discovered (Ref. 28) that when helical cathodes are used, rf power is coupled through the heater connections in addition to that coupled through the cathode support. In this study, both Model 9 and Model 11 magnetrons were used. In the previous discussion of the cathode circuit it was assumed that no appreciable rf voltage could exist across the emitting portion of the cathode. However, when an open helix is used, as shown in Fig. 2.10, a voltage can exist between the end hats, and the coaxial line formed by the filament leads will be excited. If the frequency of operation is such that the coaxial line formed by the filament leads is near an odd number of quarter wavelengths then rf power will be coupled out of the cavity by this arrangement. Figure 2.16 shows a schematic diagram of the equivalent circuit for the filament leads and cathode support when an open helix is used as the cathode emitter. C_1 and C_2 are the capacitances between end hats and respective anode sets, Z_1 is the impedance of the helix between end hats, and Z_2 is the impedance of the coaxial line formed by the filament leads.

Therefore, for the case of the open helix cathode, we must modify Eq 2.9 for the total admittance of the circuit. We define

$$Z_f = X_1 + X_2 + X_3 \qquad (2.10)$$

where

$$X_1 = \frac{1}{j\omega C_1}$$

$$X_2 = \frac{\frac{1}{j\omega C_2} Z_c}{Z_c + \frac{1}{j\omega C_2}}$$

$$Z_2 = -j Z_o \cot \frac{2\pi \ell}{\lambda}$$

$$Z_3 = \frac{Z_1 Z_2}{Z_1 + Z_2}$$

Z_o = 39.2 ohms (characteristic impedance of coaxial filament line)

Thus, Eq 2.9 becomes

$$Y_T' = \frac{2}{Z_o} + j\omega C_p + \frac{1}{Z_f} \qquad (2.11)$$

when an open helix cathode is used.

Further discussion of the equivalent circuit and Eq 2.11 for the admittance is given in Section 4.1 where experimental results are correlated with the above analysis.

The Q-parameters which are normally associated with magnetron circuits have little significance when used in connection with the circuit shown in Fig. 2.15. The loaded Q, defined as

$$Q_L = 2\pi \frac{\text{maximum energy stored in electric field}}{\text{energy dissipated in total conductance per cycle}}$$

is very low, probably less than five. Energy can be stored in the anode-to-anode capacitance, the cathode support line, and the waveguide cavity. The losses in the internal circuit are small compared to energy dissipated in the external load, and the unloaded Q, defined as

$$Q_o = 2\pi \frac{\text{maximum energy stored in electric field}}{\text{energy dissipated in internal circuit losses per cycle}}$$

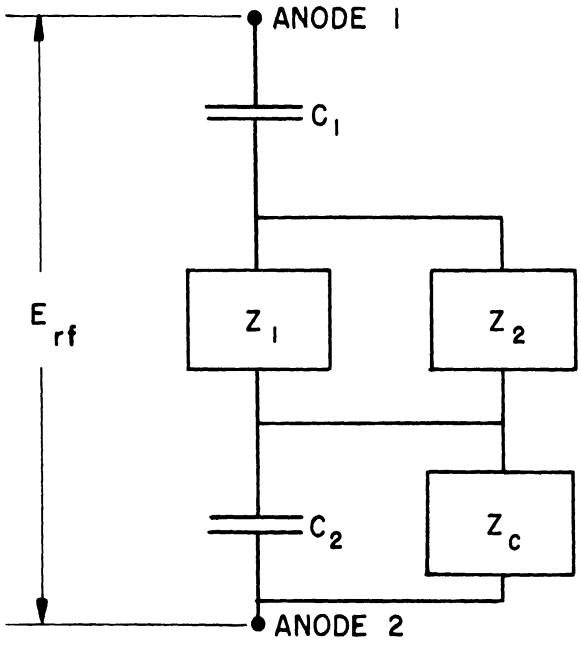

FIG. 2.16

EQUIVALENT CIRCUIT OF CATHODE LEADS
AND CATHODE SUPPORTS FOR OPEN HELIX CATHODE

is relatively high. Therefore, the external Q, defined as

$$Q_e = 2\pi \frac{\text{maximum energy stored in electric field}}{\text{energy dissipated in external load per cycle}}$$

is approximately equal to the loaded Q, Q_L. The relation between the various Q's being

$$\frac{1}{Q_e} = \frac{1}{Q_L} - \frac{1}{Q_o} \tag{2.12}$$

Since the operation of a voltage-tunable magnetron is very sensitive to the character of the load, a small mismatch in the terminations will produce a significant effect on the operation of the tube. The power output varies as the impedance of the circuit varies, the power decreases with a decrease in impedance. A large change in impedance may cause discontinuities in the oscillations as the frequency is varied. The mismatch of the load is important because of the so-called "long-line effect" (Ref's 16, 27). When an oscillator is connected to a load by a transmission line which is a few wavelengths long, if the load is not perfectly matched to the transmission line, the admittance and phase characteristics of the load, as seen by the oscillator, will vary periodically with frequency. For a lossless line this impedance may be expressed as

$$Z = Z_o \frac{Z_r + j\, Z_o \tan 2\pi\frac{\ell}{\lambda}}{Z_o + j\, Z_r \tan 2\pi\frac{\ell}{\lambda}} \tag{2.13}$$

where

Z_o = characteristic impedance of the line

Z_r = terminating impedance on the line

This impedance varies periodically with the electrical length of the line, the period being a half wavelength $\frac{2\pi\ell}{\lambda} = 180°$. Figure 2.17

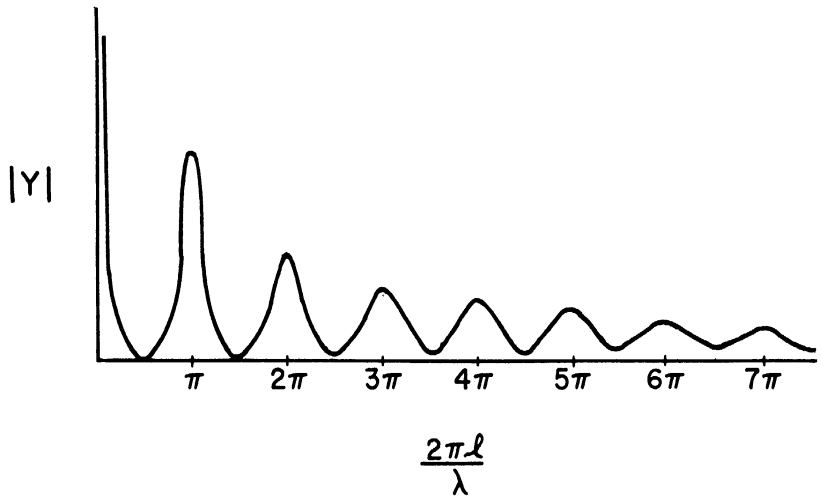

ABSOLUTE VALUE, ADMITTANCE OF SHORT CIRCUITED TRANSMISSION LINE

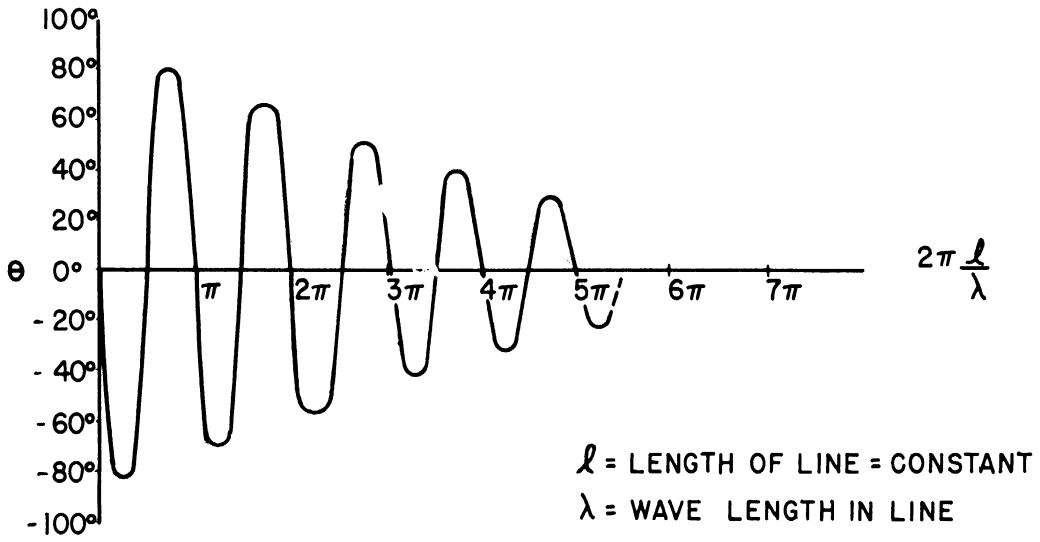

PHASE ANGLE OF ADMITTANCE OF SHORT CIRCUITED TRANSMISSION LINE

FIG. 2.17
TYPICAL PHASE AND ADMITTANCE CHARACTERISTICS
OF SHORT CIRCUITED TRANSMISSION LINE

shows typical phase and admittance characteristics of a shorted transmission line with attenuation. In the case of a lossy line, the limiting value of the admittance as the length of the line is increased is the characteristic admittance of the line. This suggests a possible method of eliminating the long-line effect, by the use of lossy line or attenuators. The use of attenuation in the transmission line is a widely used technique to isolate an oscillator from its load. For microwave oscillators used as signal generators, the long-line effect is a serious problem since it reduces the available power and results in insufficient power for many measurement applications. This effect can also be eliminated by making the line between oscillator and load very short; however, it is seldom feasible to depend on this technique alone. Making the line as short as possible is desirable, however, since this makes the variations in admittance farther apart in frequency and, in the case of high-Q magnetrons, results in a wider range of operating frequency between the "holes" caused by the unstable operation of the magnetron due to the long-line effect.

CHAPTER 3

EXPERIMENTAL RESULTS

3.1 Introduction

Considerable data on the operation of the various forms of the Model 11 tube, (Model 11, 11A and 11B) were obtained and in this chapter typical results are presented for each form. A total of thirty-one tubes were studied in this investigation, in this chapter data is presented from ten of these tubes. The data have been selected so that each tube reported on represents a significant step in the research program.

In this chapter the data are presented without comment. In Chapter 4 the data are discussed and the results of the experimental investigation are correlated with theory. The reader not interested in the mass of experimental data may proceed to Chapter 4 and obtain an evaluation of the significant results.

Several types of cathodes were used, namely; oxide-coated, thoriated tungsten, tungsten, and a button cathode. Results are presented which indicate effects of these various cathodes on the operation of the tube. Presentation of the data is arranged according to tube model rather than according to the types of measurements which were performed.

The results of experimental tests on the Model 11 tubes are presented first. This was the first model to be constructed and the results of the tests were in general quite satisfactory. Measurement techniques were designed and perfected during the testing of these Model 11 tubes. The Model 11B magnetron was designed in an attempt to improve the efficiency of the Model 11 tubes. Data are presented which indicate the improvement in operating characteristics of the Model 11B over the Model 11. Tungsten cathodes were used in all Model 11B tubes. The Model 11A tube was designed to allow comparison of the operating characteristics of two similar magnetrons, one having round anode bars and the other square anode bars. Sufficient data are presented on the Model 11A to allow comparison with the Model 11. Measurements were made on the cavity which show its bandwidth and relative impedance. Flux plots are presented which show the potential distribution in the interaction space of the Model 11B and Model 11A tubes. Diode characteristics for Model 11A and 11B tubes are presented. These data were obtained in an effort to determine the conditions at the cathode which were optimum for voltage-tunable operation.

Figures 3.1 and 3.2 show photographs of a tube and its various parts. Figure 3.2 shows a close-up of the anode structure before and after the Kovar flange has been brazed into place. In this investigation, the local oscillator application of the tube has been emphasized; therefore, most of the data presented below have resulted from measurements made under cw operating conditions.

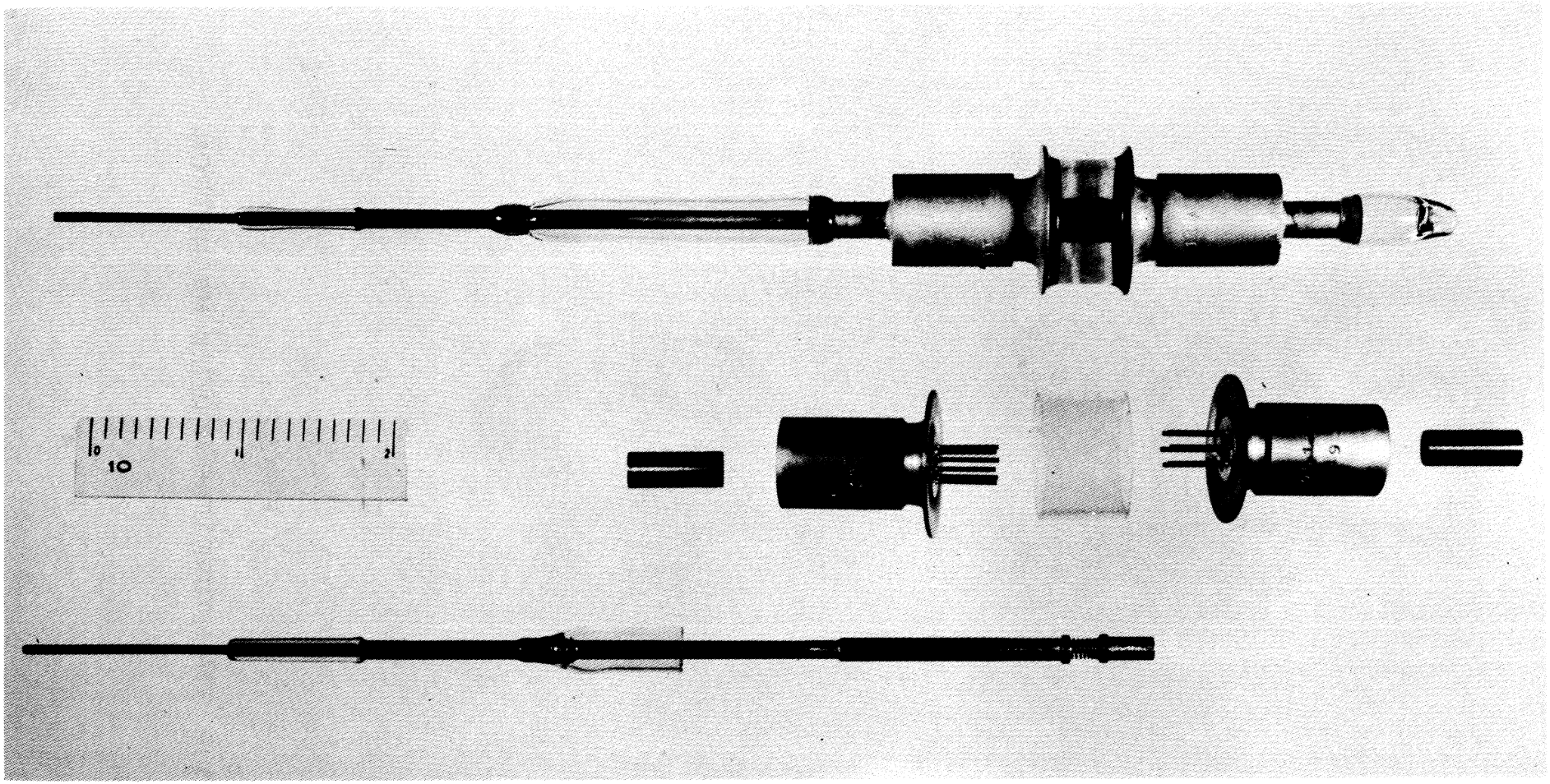

SCALE: INCHES

FIG. 3.1

PHOTOGRAPH OF MODEL II MAGNETRON

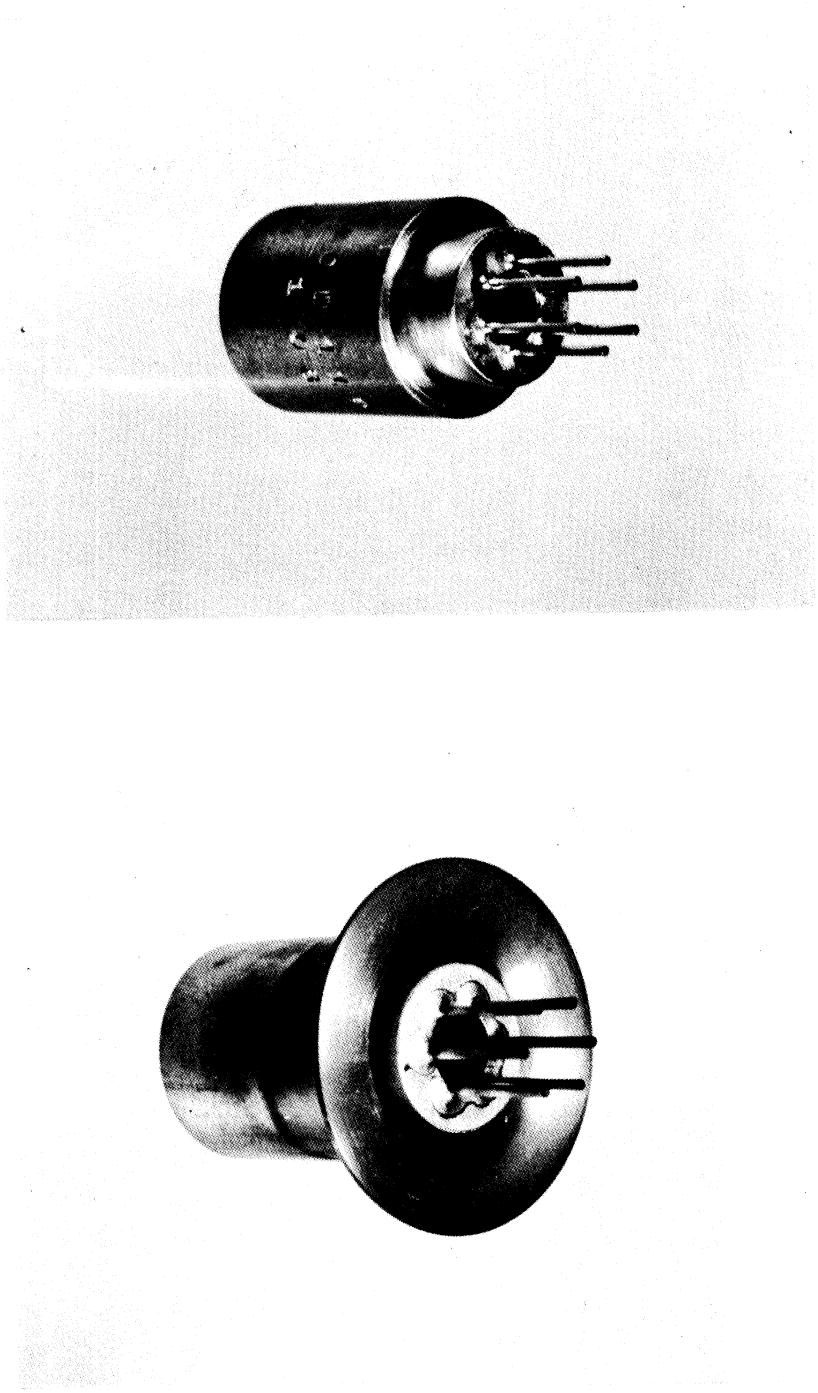

FIG. 3.2

ANODE STRUCTURE FOR MODEL II MAGNETRON

3.2 Model 11

3.2.1 Model 11, No. 74. The first tube completed was the Model 11, No. 74. This tube used an oxide-coated cathode. Under pulsed operation, the tube was voltage-tunable from 2060 to 2750 mc. A schematic diagram of the test equipment used in these tests is shown in Fig. 3.3. As indicated there it is possible to observe either the volt-ampere characteristic of the tube, or to observe the output of the wavemeter as a function of the anode voltage. Thus, by tuning the wavemeter and observing a continuous output over a wide voltage range, it was determined that the tube was operating over the frequency range of 2060 to 2750 mc. The cathode temperature was critical but could be adjusted for stable operation. The cathode temperature affects not only the stability of operation but also the frequency of oscillation. An increase in cathode temperature causes a decrease in the frequency of oscillation. The external choke was used on the cathode support while making these tests. It was impossible to test this tube under cw conditions due to the backheating of the cathode. Once the tube started to oscillate, the backheating was sufficient to prevent the adjustment of the cathode temperature for voltage-tunable operation. There was a very narrow cathode temperature range in which the tube produced a coherent signal. The tube was operated with a magnetic field of 2625 gauss and a filament current of 1.25 amperes. Figure 3.4 shows a photograph of the test setup used; one end of the cavity was terminated in a 50 ohm resistor, and power was taken out of the other end. Figure 3.5 shows a close-up of the Model 11 magnetron mounted in its cavity and its associated electromagnet.

3.2.2 Model 11, No. 80. Results of the tests on the Model 11, No. 74, indicated a need for a change in the design of the cathode if cw

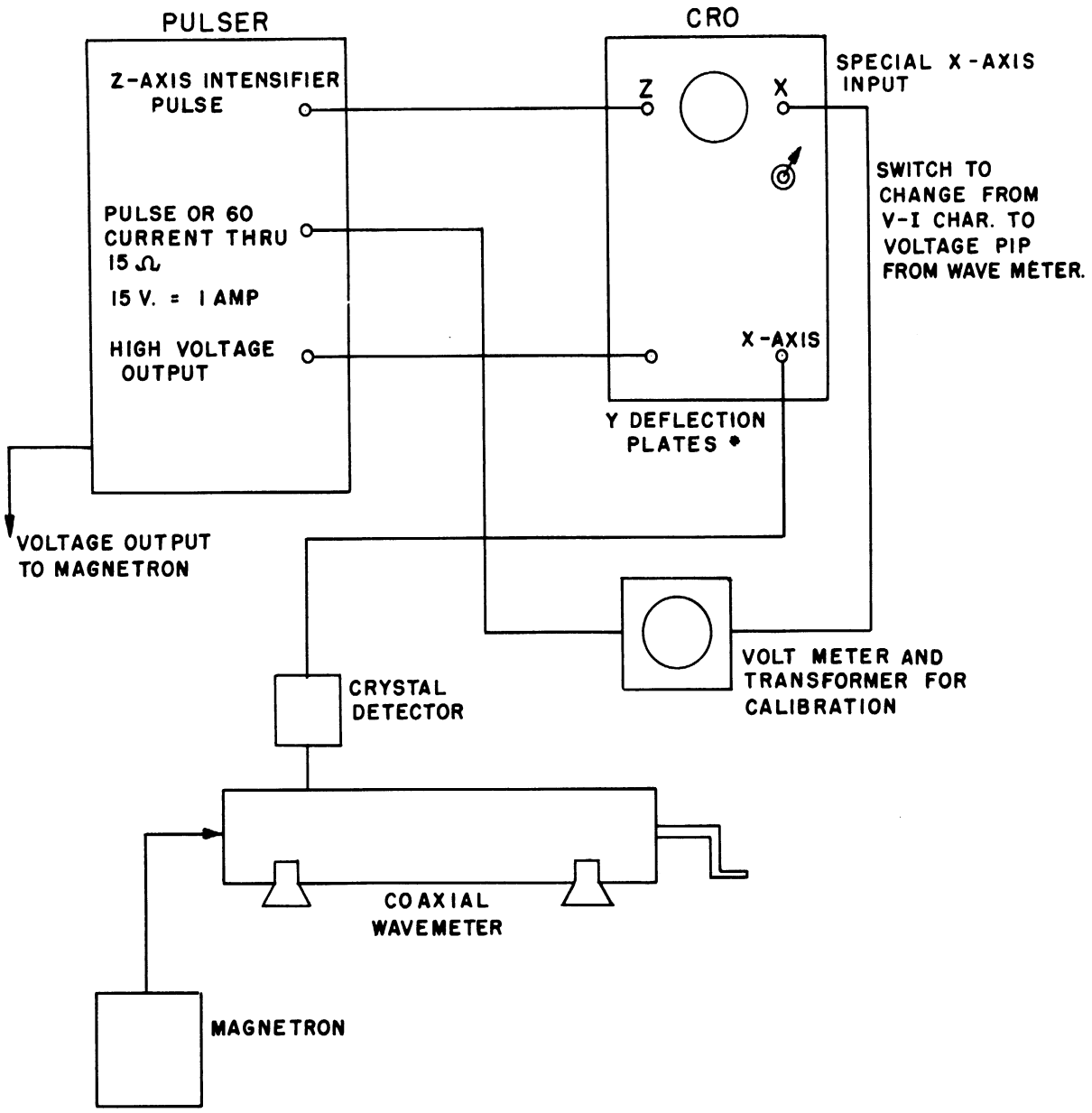

*VOLTAGE FROM PULSER IS APPLIED DIRECTLY TO THE VERTICAL DEFLECTOR PLATES OF THE SCOPE, THRU A VOLTAGE DIVIDER NETWORK WHICH IS USED FOR CALIBRATION.

FIG. 3.3

TEST EQUIPMENT FOR PULSED OPERATION OF MAGNETRON

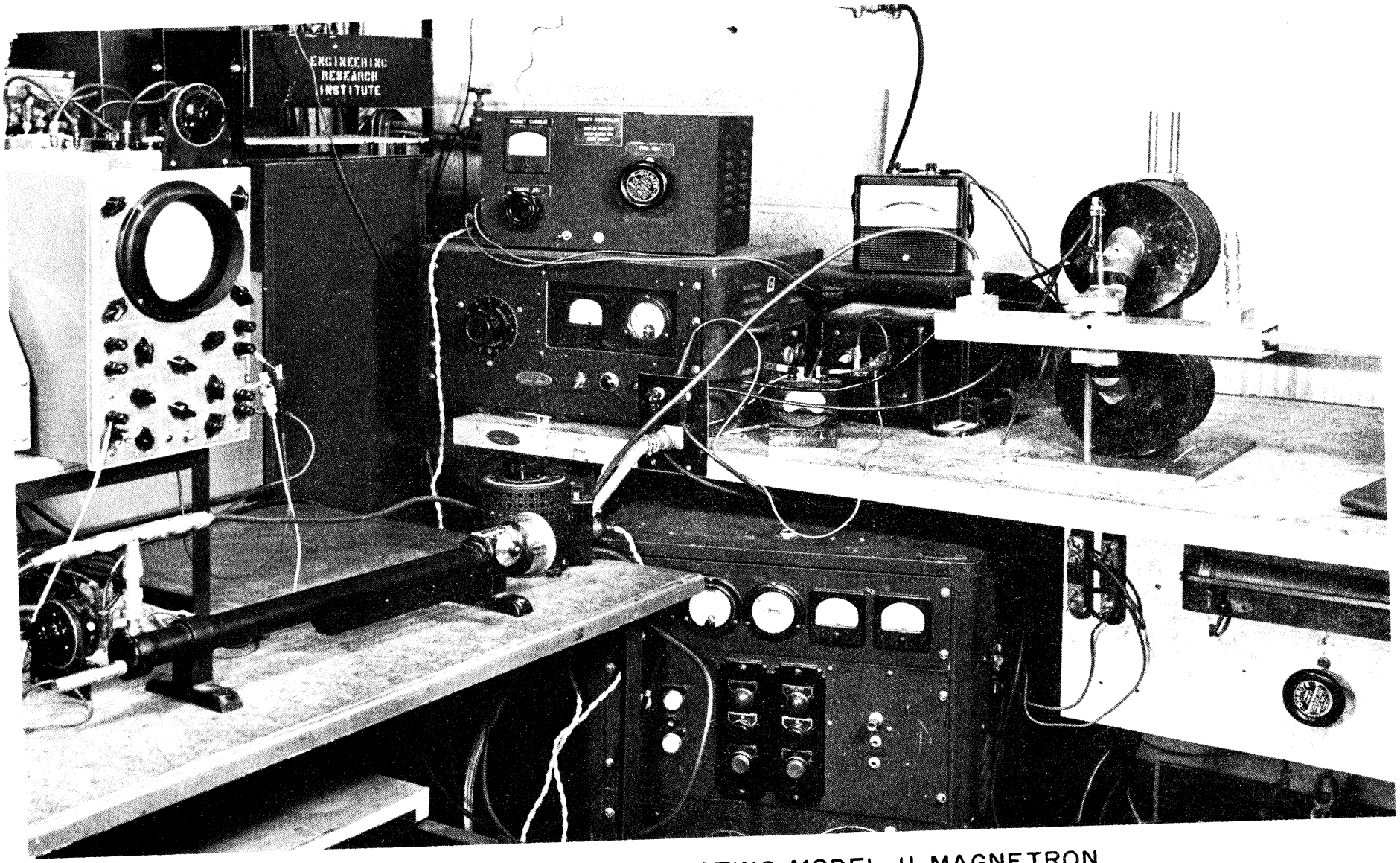

FIG. 3.4 PHOTOGRAPH OF EQUIPMENT USED IN TESTING MODEL II MAGNETRON

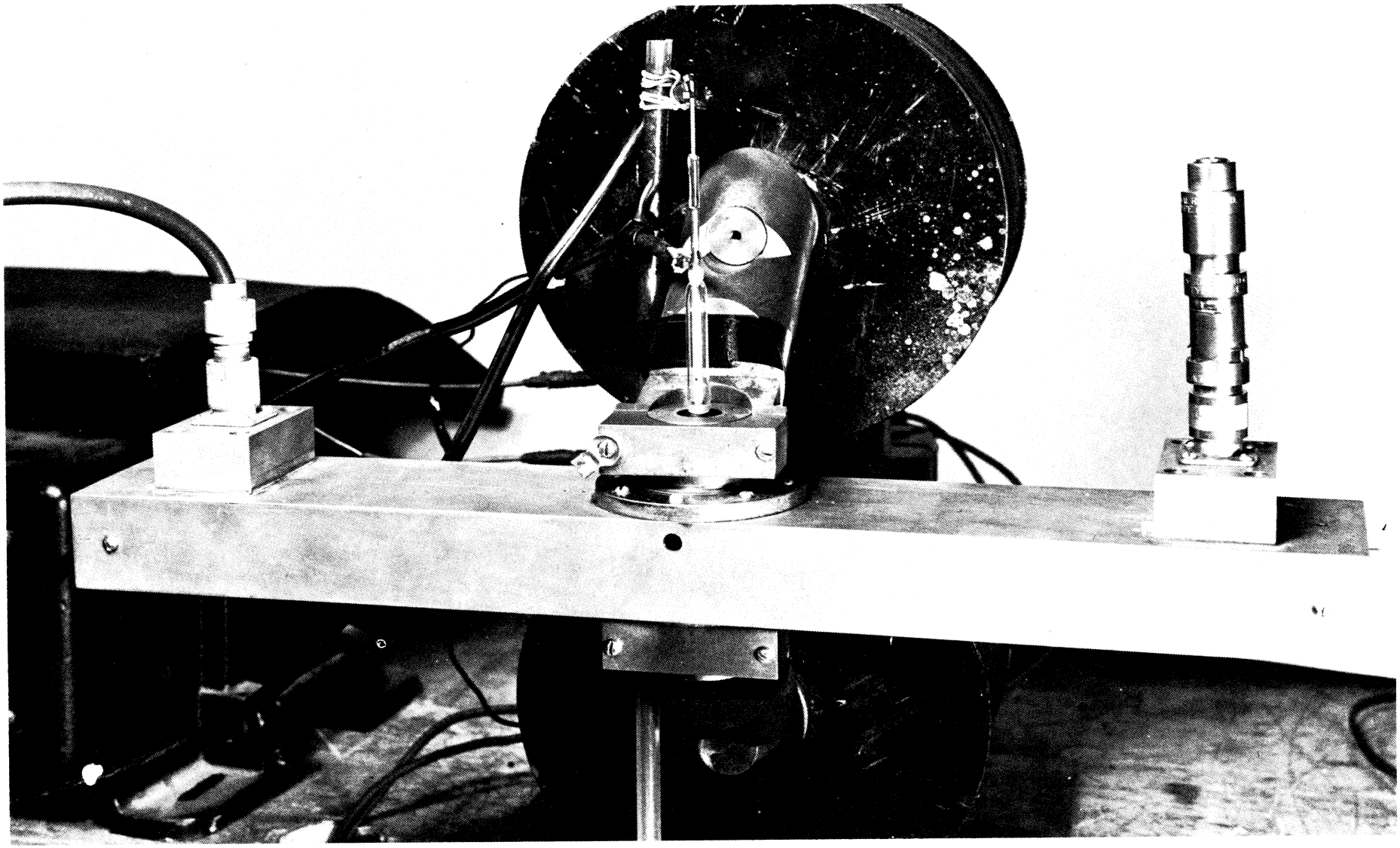

FIG. 3.5 PHOTOGRAPH OF MODEL II MAGNETRON MOUNTED IN CAVITY AND ELECTROMAGNET

operation was to be obtained. In an attempt to satisfy this need, the No. 80 tube was built, using a thoriated tungsten cathode which was not carburized. In order to determine the feasibility of using this tube as a local oscillator, it was employed as such in an S-band spectrum analyzer (as indicated in Fig. 3.6). The frequency was swept by superimposing an ac voltage on the magnetron dc anode supply.

The total range of the frequency sweep was determined by using the output of a klystron as the input to the spectrum analyzer and mechanically tuning this klystron over the range of frequencies covered by the magnetron local oscillator. The frequency of the klystron at the extreme points was determined by using a coaxial wavemeter. In this manner, it was determined that the magnetron frequency could be swept from 1760 to 2475 mc with continuous, and very nearly constant, power output. Initially, it was necessary to adjust the cathode temperature to a critical value, which once obtained, required no further adjustment over the frequency range. Figure 3.7 shows the results as presented on the oscilloscope. The voltage change corresponding to the frequency change of 715 mc was approximately 1000 volts. These tests indicated that the magnetron was quite satisfactory as a local oscillator in a spectrum analyzer.

Qualitative measurements on the noise content of the magnetron output were made by comparing its output signal with the output of a reflex klystron. This comparison was made by alternately feeding the two signals into an S-band spectrum analyzer, using a second reflex klystron as the local oscillator for the spectrum analyzer. When the magnetron was operated cw, the signal as observed on the spectrum analyzer appeared to be unstable in that there were random shifts in the frequency, and also,

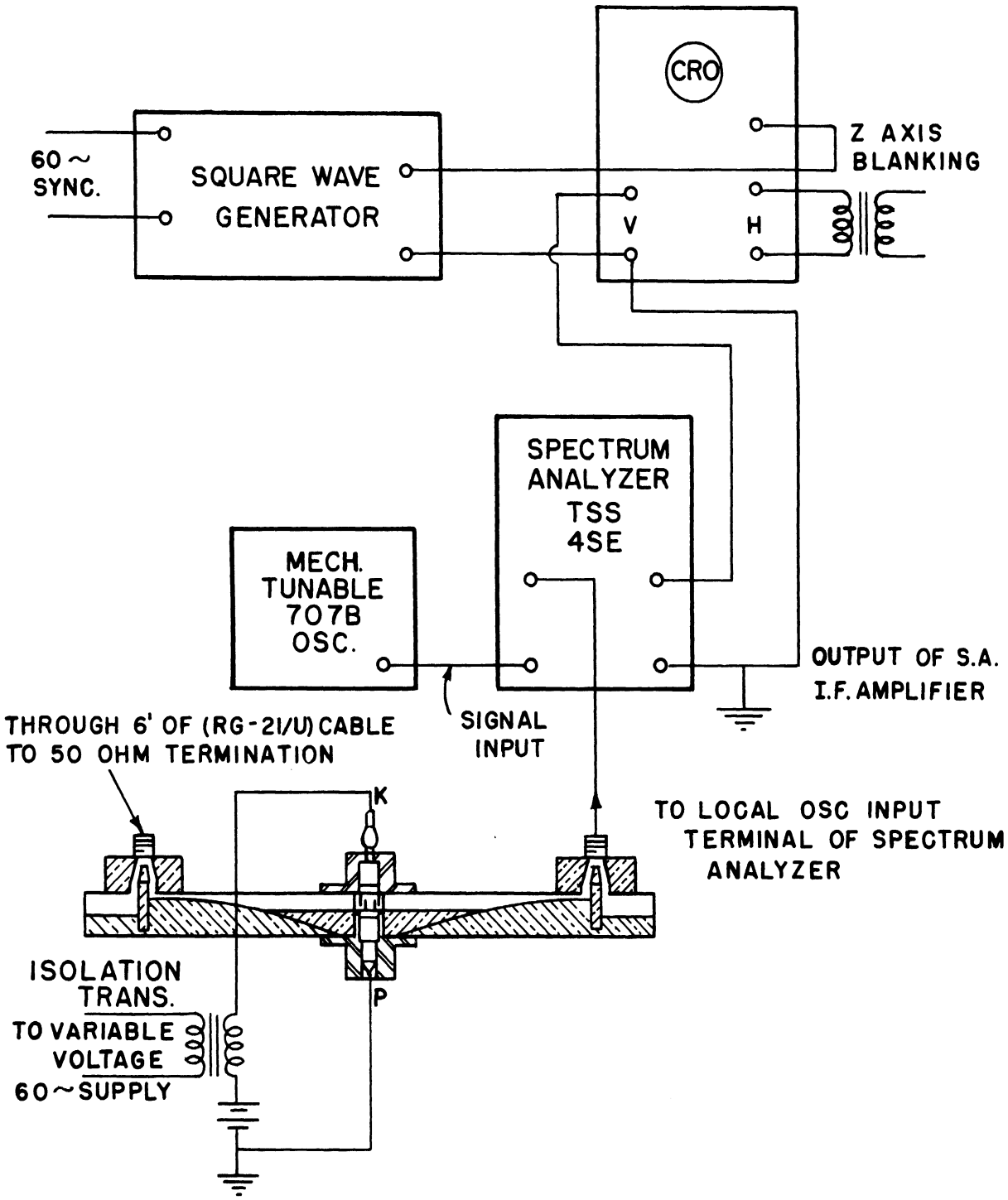

FIG. 3.6

EXPERIMENTAL SETUP USING MODEL II MAGNETRON AS LOCAL OSCILLATOR FOR SPECTRUM ANALYZER

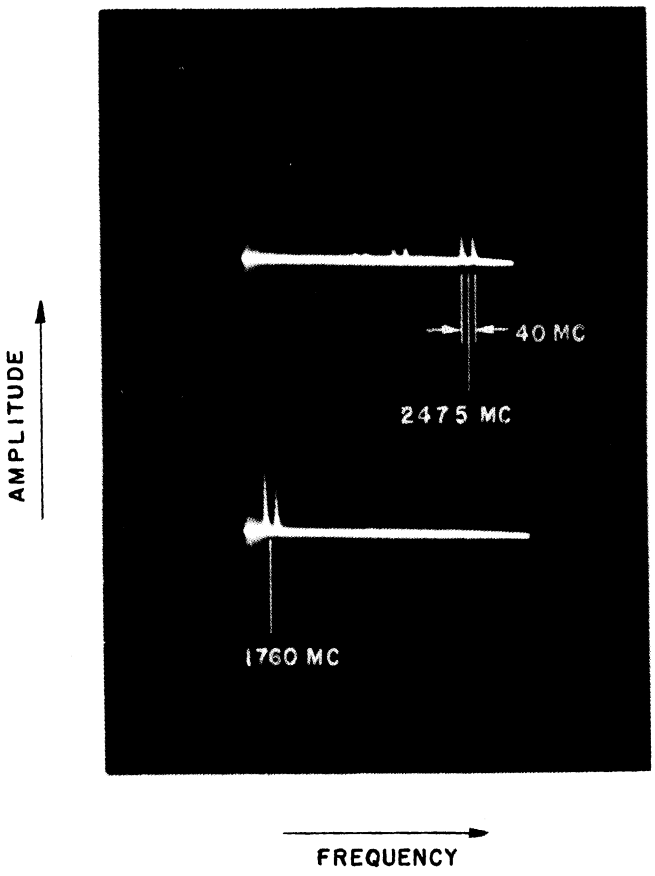

CONDITIONS OF OPERATION:

B = 3625 GAUSS

$I_{fil.}$ = 8.4 AMPS

E_{dc} = 2700 VOLTS

E_{ac} = 1250 VOLTS PEAK TO PEAK

CAMERA: DUMONT - OSCILLOGRAPH RECORD CAMERA, TYPE 297

f 2.8 B – 6 sec.

FIG. 3.7

OSCILLOGRAPH TRACES OBTAINED BY USING THE TEST FACILITY SHOWN IN FIG. 3.6

the signal was alternately noisy and clean. The cathode input power was a critical factor in this operation. When the anode voltage was modulated a very small amount at a 60 cycle rate the signal became steady and all visible noise disappeared. The magnetron output signal under these conditions compared favorably, in both magnitude and noise content, with a 707-B reflex klystron oscillator. Qualitative tests indicated a detectable magnetron signal on the spectrum analyzer screen at least 60 db above noise present. For the particular arrangement used, results were similar when the output from a reflex klystron was substituted for the magnetron.

An attempt was made to determine the effect of the cathode temperature on the operating characteristics of the tube. Since the cathode was visible through a small hole in the cavity, it was possible to measure cathode temperature optically. A Leeds and Northrup optical pyrometer was used; this allowed determination of the temperature to within 50 degrees out of approximately 1800 degrees centigrade. The cathode power input was changed very slightly but sufficiently to cause the output to change from a coherent signal to noise, and an attempt was made to measure the resulting cathode temperature change. It was found that this temperature change could not be optically detected with the instrument used.

The arrangement shown in Fig. 3.8 was used to monitor the output signal of the tube. This arrangement made it possible to observe the output as a function of voltage, and to determine the effects of changing various parameters. As indicated in Fig. 3.8, the x-axis sweeping voltage was obtained from the same source as the anode modulating voltage. Thus, with the proper phase shift adjustment, the horizontal sweep on the oscilloscope could be synchronized with anode sweep voltage. The z-axis input was used to blank the return trace from the screen. Since the frequency was

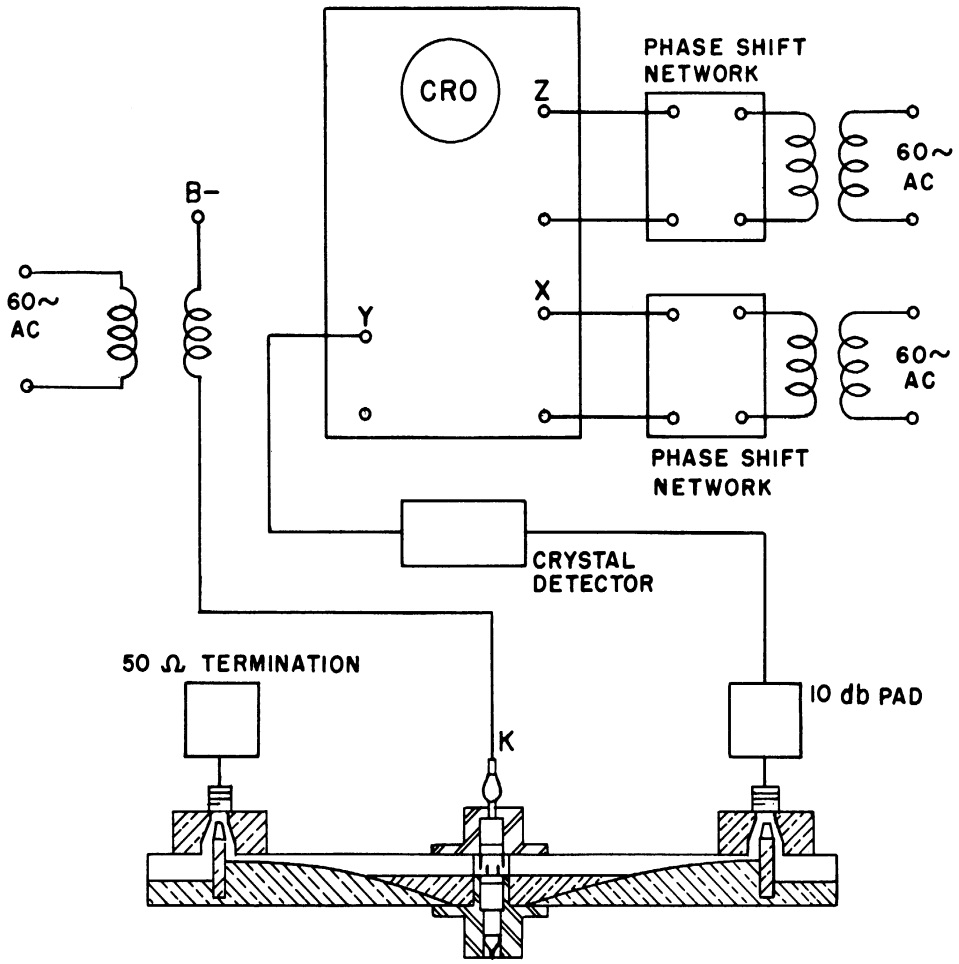

FIG. 3.8

CIRCUIT ARRANGEMENT USED TO OBSERVE OUTPUT SIGNAL vs ANODE VOLTAGE

linear with voltage it was possible to calibrate the oscilloscope to give power output as a function of frequency.

During the cw operation the voltage could be varied only over a quite limited range without readjustment of the cathode input power in order to maintain a clean signal. This was due to the change in the backheating which caused a corresponding change in the cathode temperature. However, when the anode voltage was varied at a 60-cycle rate, it was possible to adjust the cathode temperature so that the tube operated satisfactorily over a sweep range of 1250 volts. Thus, once the sweep range has been determined, giving an average backheating power, it is possible to adjust the cathode input power for optimum clean-signal operation of the tube.

Measurements of cw power output and frequency were made on this tube, and the results are shown in Fig. 3.9 and 3.10. Figure 3.9 shows the power output and frequency as a function of anode voltage. The power indicated here is the available power at one output terminal of the cavity; the other terminal was terminated in a 50-ohm resistance during these measurements. The actual power measurements were made at the end of 10 feet of RG-21/U cable. A Hewlett-Packard tunable bolometer (Model 475 B) and Power Meter (Model 430A) were used to measure power. Figure 3.11 shows a photograph of the test equipment used in the measurements. From these data it is seen that the power output varies between 4.5 and 16 mw over a frequency range of 1770 to 2930 mc. The discontinuities in the frequency vs. anode voltage curve are the result of readjusting the cathode input power at these points. The output signal was monitored, as shown in Fig. 3.8, to insure that power measurements of a coherent signal were being made. Since the frequency was sensitive to cathode temperature, a slight

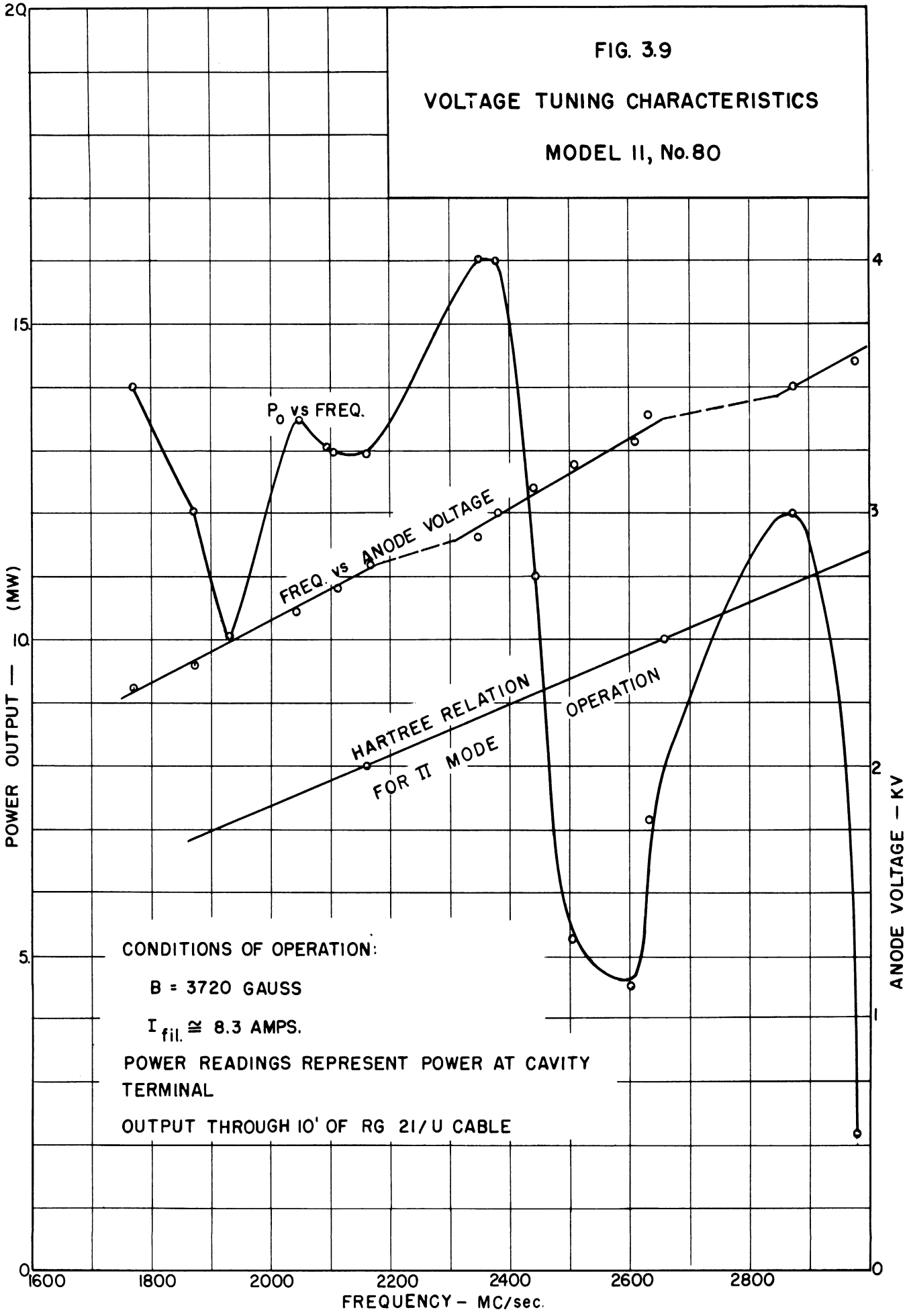
FIG. 3.9
VOLTAGE TUNING CHARACTERISTICS
MODEL 11, No. 80
P_0 vs FREQ.
FREQ. vs ANODE VOLTAGE
HARTREE RELATION FOR π MODE OPERATION
CONDITIONS OF OPERATION:
B = 3720 GAUSS
$I_{fil.} \cong$ 8.3 AMPS.
POWER READINGS REPRESENT POWER AT CAVITY TERMINAL
OUTPUT THROUGH 10' OF RG 21/U CABLE
POWER OUTPUT — (MW)
ANODE VOLTAGE — KV
FREQUENCY — MC/sec.
0
5
10
15
20
1
2
3
4
1600
1800
2000
2200
2400
2600
2800

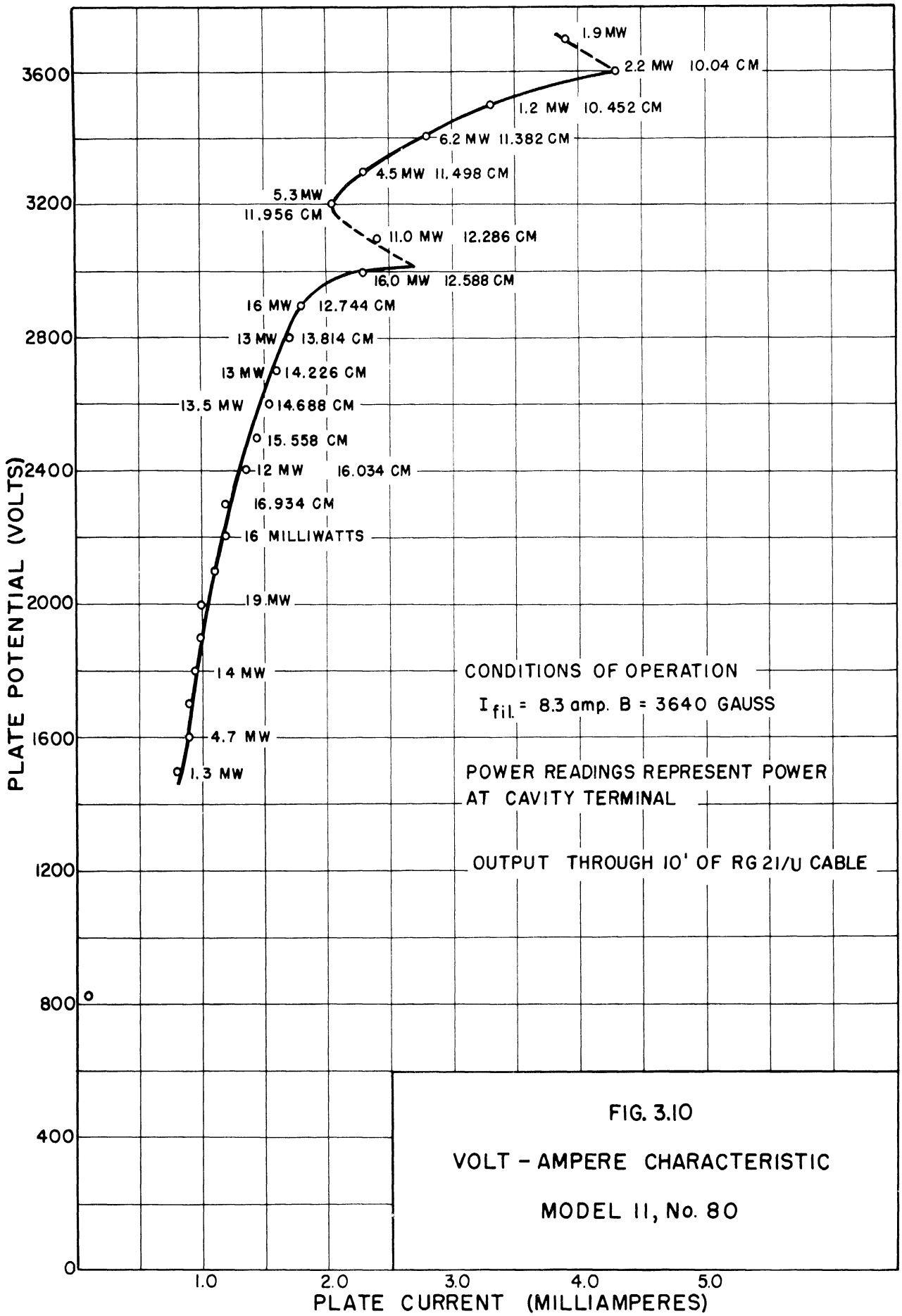

FIG. 3.10

VOLT - AMPERE CHARACTERISTIC

MODEL 11, No. 80

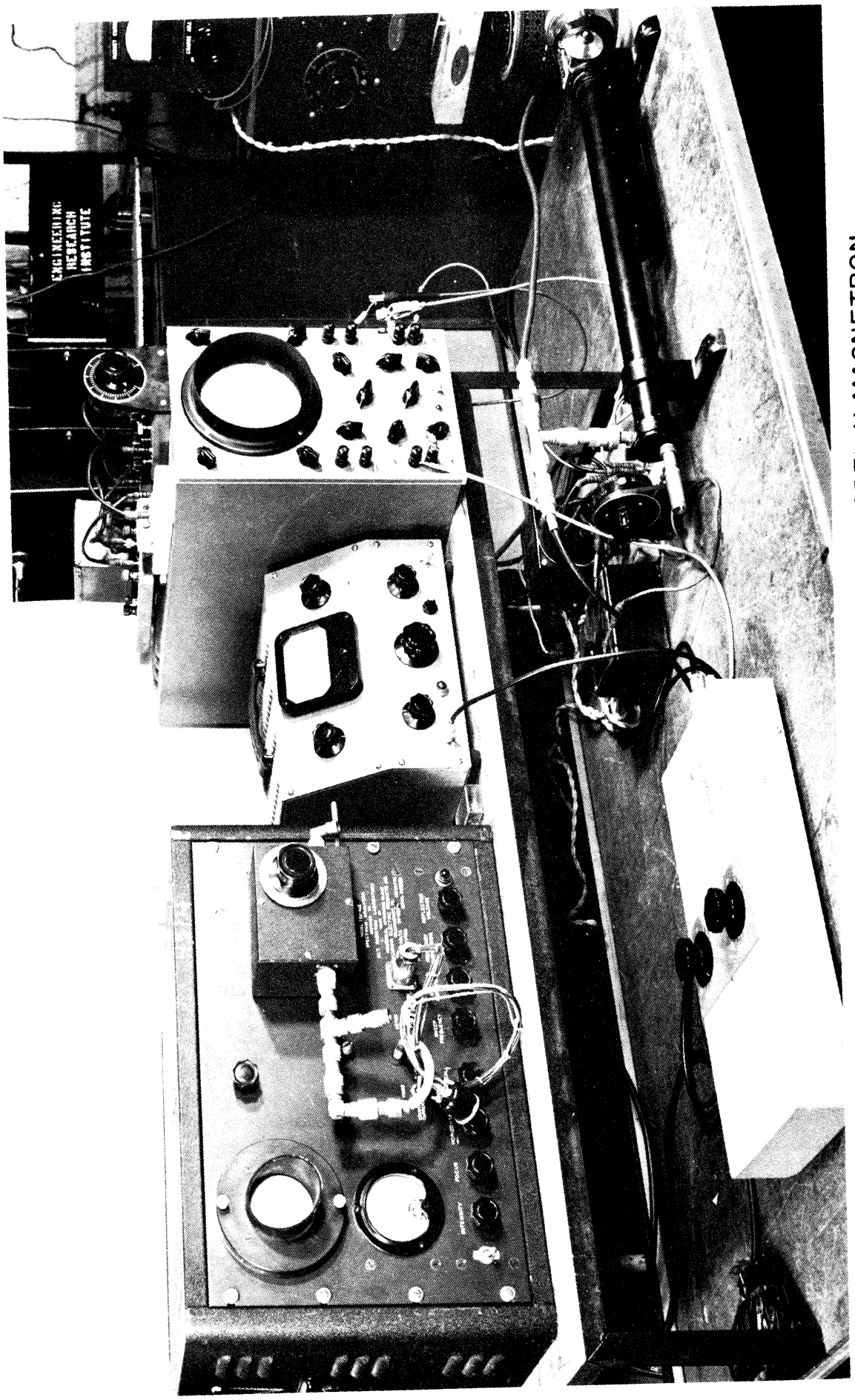

FIG. 3.11 PHOTOGRAPH OF TEST EQUIPMENT USED IN TESTING MODEL II MAGNETRON

discontinuity occurred in the frequency curve each time the cathode input power was adjusted. The adjustment required was very slight. The tube tuned at the rate of approximately 0.8 mc per volt change in anode potential. The frequency-voltage relation as obtained from the Hartree relation is also plotted in Fig. 3.9 for comparison with the experimental data (the π-mode of operation is assumed). The reasons for the difference between these two curves will be discussed in a later section.

The volt-ampere characteristic for the tube is shown in Fig. 3.10. This shows that the plate current varied from 1 to 4 ma over the voltage range used in these experiments.

3.2.3 Model 11, No. 81. Since the thoriated-tungsten cathode gave more stable operation than the oxide-coated cathode it was decided to go one step farther and use pure tungsten wire in the cathode helix. Except for the pure tungsten cathode, the Model 11, No. 81 was identical with the Model 11, No. 80.

As expected, the output signal from the Model 11, No. 81, was more stable and had fewer variations in output power than tube No. 80. The cathode temperature was still critical, but the operation of the tube was not as sensitive to changes in filament current as was the case for No. 80. More anode current and more power output was obtained from this tube than from No. 80. Figure 3.12 shows power output vs. anode voltage. The anode current varied from 3.4 ma at 2400 volts to 10.4 ma at 3500 volts. Complete frequency measurements were not taken, however, spot checks were made which indicated that the frequency range covered was from 2000 to 3000 mc.

During the construction of the cathode for this tube a small notch was burned in the cathode end hat while spot welding the filament

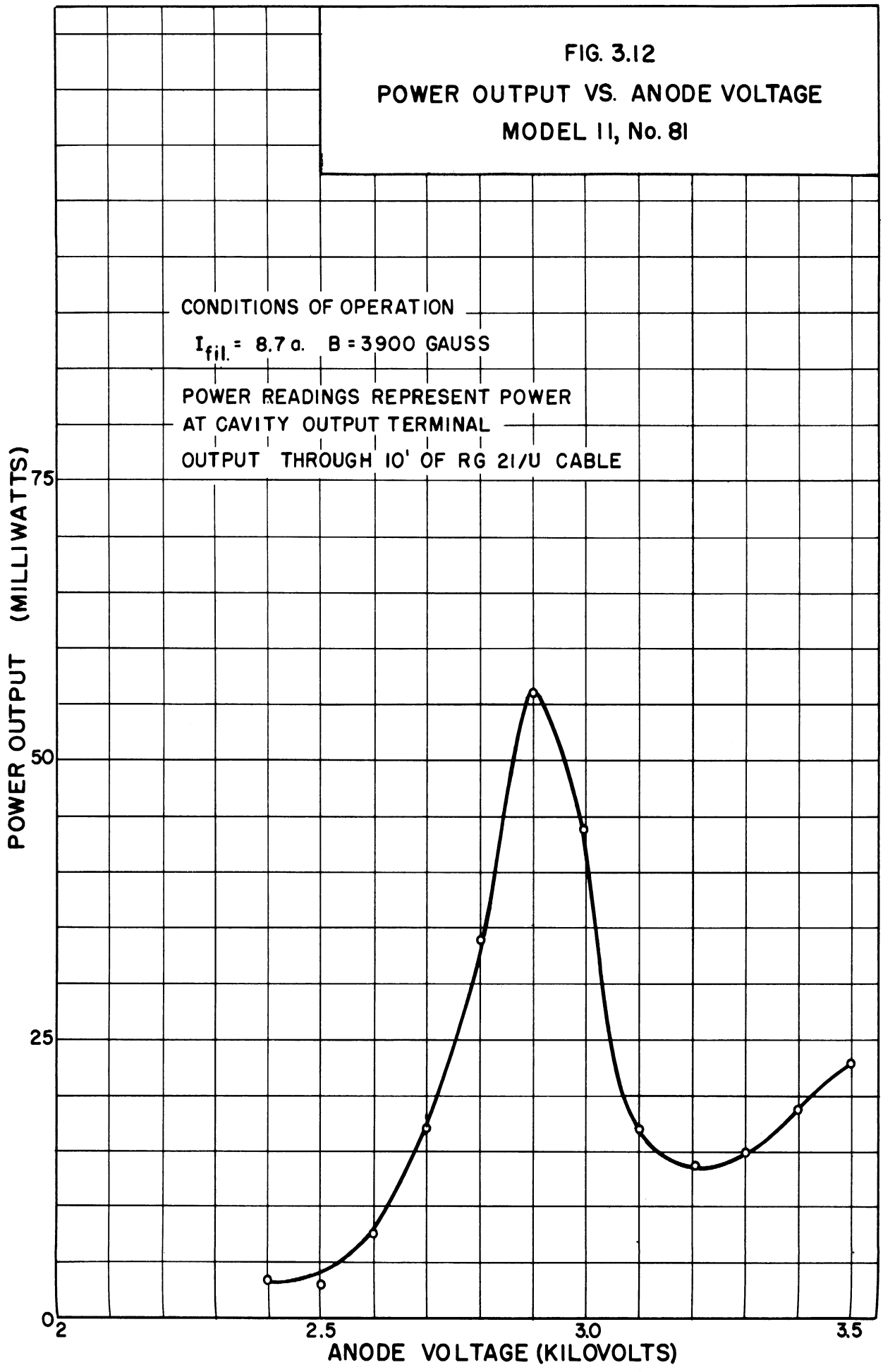
FIG. 3.12
POWER OUTPUT VS. ANODE VOLTAGE
MODEL 11, No. 81
CONDITIONS OF OPERATION
$I_{fil.}$ = 8.7 a. B = 3900 GAUSS
POWER READINGS REPRESENT POWER
AT CAVITY OUTPUT TERMINAL
OUTPUT THROUGH 10' OF RG 21/U CABLE
POWER OUTPUT (MILLIWATTS)
75
50
25
0
2
2.5
3.0
3.5
ANODE VOLTAGE (KILOVOLTS)

to the end hat. The uneven surface caused sufficient concentration of field strength at this point to cause the tube to break down at approximately 3600 volts. The resulting arc damaged one of the anode bars to the extent that it was not considered feasible to continue testing even though the tube could still be operated.

3.2.4 Model 11, No. 83. This tube was identical to No. 81, and results obtained were approximately the same; however, additional data were obtained from this tube. Figure 3.13 shows the voltage tuning characteristic of the tube as cw frequency measurements were made from 1780 to 2450 mc.

The break in the tuning curve (as indicated by the dotted section) is caused by readjustment of the cathode input power (which is necessary in order to maintain a coherent signal output). It is possible to operate the tube over a considerably wider frequency range when the anode voltage is swept.

When the tube was used as a local oscillator (as indicated in Fig. 3.6), it was possible to vary the frequency from 1840 to 2730 mc with a coherent signal output throughout the frequency range. Conditions for this test were as follows:

$B = 3940$ gauss $\qquad E_{dc} = 3350$ volts

$I_{fil} = 8.95$ amps $\qquad E_{ac} = 1200$ volts peak-to-peak

The power output of the Model 11 with a pure tungsten cathode was greater than 15 mw over a frequency range of several hundred megacycles (see Figs. 3.12 and 3.13). This is sufficient power to allow isolation of the oscillator (preventing the "long-line effect" from disturbing the oscillator), and still furnish sufficient signal power output for satisfactory use as a local oscillator.

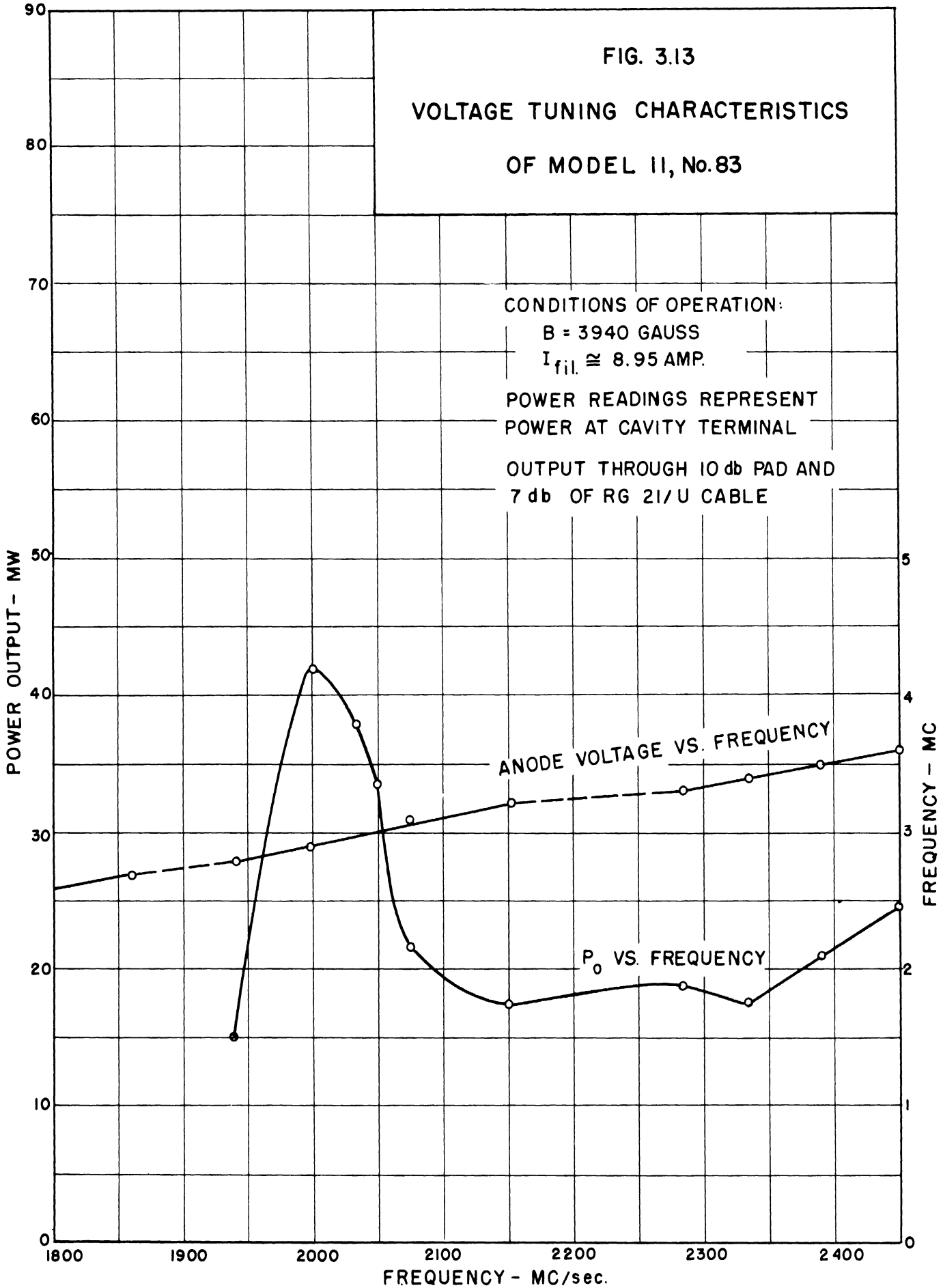
FIG. 3.13
VOLTAGE TUNING CHARACTERISTICS
OF MODEL 11, No. 83
CONDITIONS OF OPERATION:
B = 3940 GAUSS
$I_{fil.} \cong 8.95$ AMP.
POWER READINGS REPRESENT
POWER AT CAVITY TERMINAL
OUTPUT THROUGH 10 db PAD AND
7 db OF RG 21/U CABLE
ANODE VOLTAGE VS. FREQUENCY
P_0 VS. FREQUENCY
POWER OUTPUT - MW
FREQUENCY - MC
FREQUENCY - MC/sec.
0
10
20
30
40
50
60
70
80
90
1800
1900
2000
2100
2200
2300
2400
0
1
2
3
4
5

Figure 3.14 shows the spectra obtained when the anode voltage is modulated with a sine wave signal. There was some jitter in the spectrum since the power supply was not regulated. The cathode power was supplied by a storage battery during these tests.

3.3 Model 11B

Although the Model 11 magnetron operates satisfactorily as a local oscillator, the electronic efficiency is very poor. Since the impedance of the circuit is lower than for a high-Q magnetron, the rf fields in the interaction space are very weak. To compensate for this in the Model 11B, the anode diameter was decreased (from .233 inch in the Model 11) to .205 inch. This decrease in anode diameter increased the r_c/r_a ratio to .75 (from .6 in the Model 11), allowing greater penetration of the rf fields into the interaction space. Test results indicated a significant improvement in electronic efficiency as a consequence of these changes. The Model 11B is otherwise identical with the Model 11.

3.3.1 Model 11B, No. 88.

A pure tungsten cathode was used in this tube. Figure 3.15 shows the volt-ampere characteristic for this tube. These data were taken without any readjustment of the cathode input power. Figure 3.16 shows the voltage tuning characteristics for this tube. One terminal of the cavity was terminated in a 50-ohm resistor while these data were being taken. The frequency characteristic is approximately linear, having a slope of approximately 1.18 volts/mc. The sharp discontinuities which were present in the frequency characteristic curves of the other tubes are not present in this case. The frequency could be spot-tuned anywhere within the indicated frequency range without readjusting the cathode input power. When the anode voltage was modulated with a

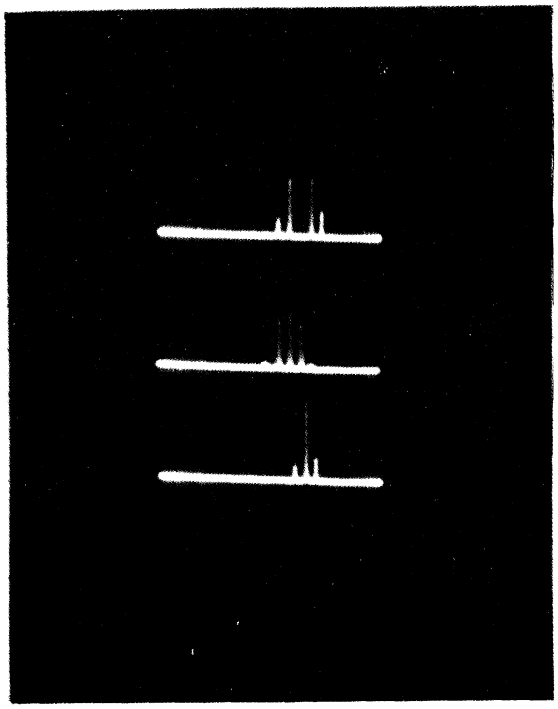

(a.)

INCREASING
MODULATION

fm = 2 MC

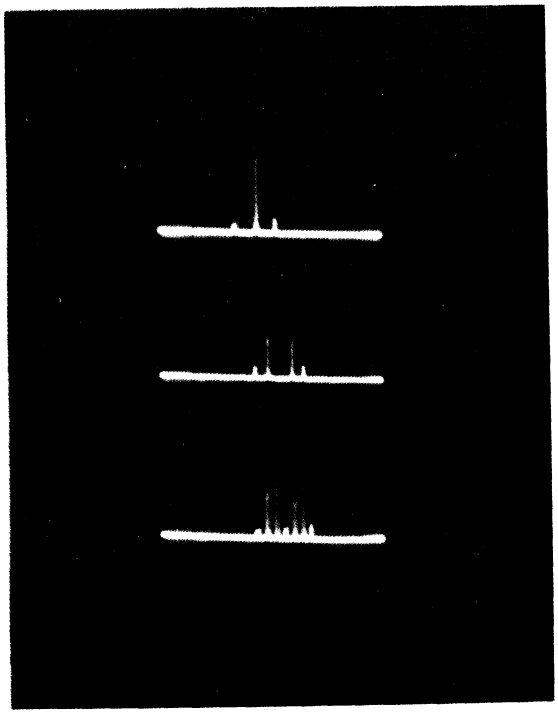

(b.)

fm = 3 MC

fm = 2.5 MC

fm = 1.5 MC

FIG. 3.14

SPECTRA OBTAINED BY MODULATING
MAGNETRON ANODE VOLTAGE

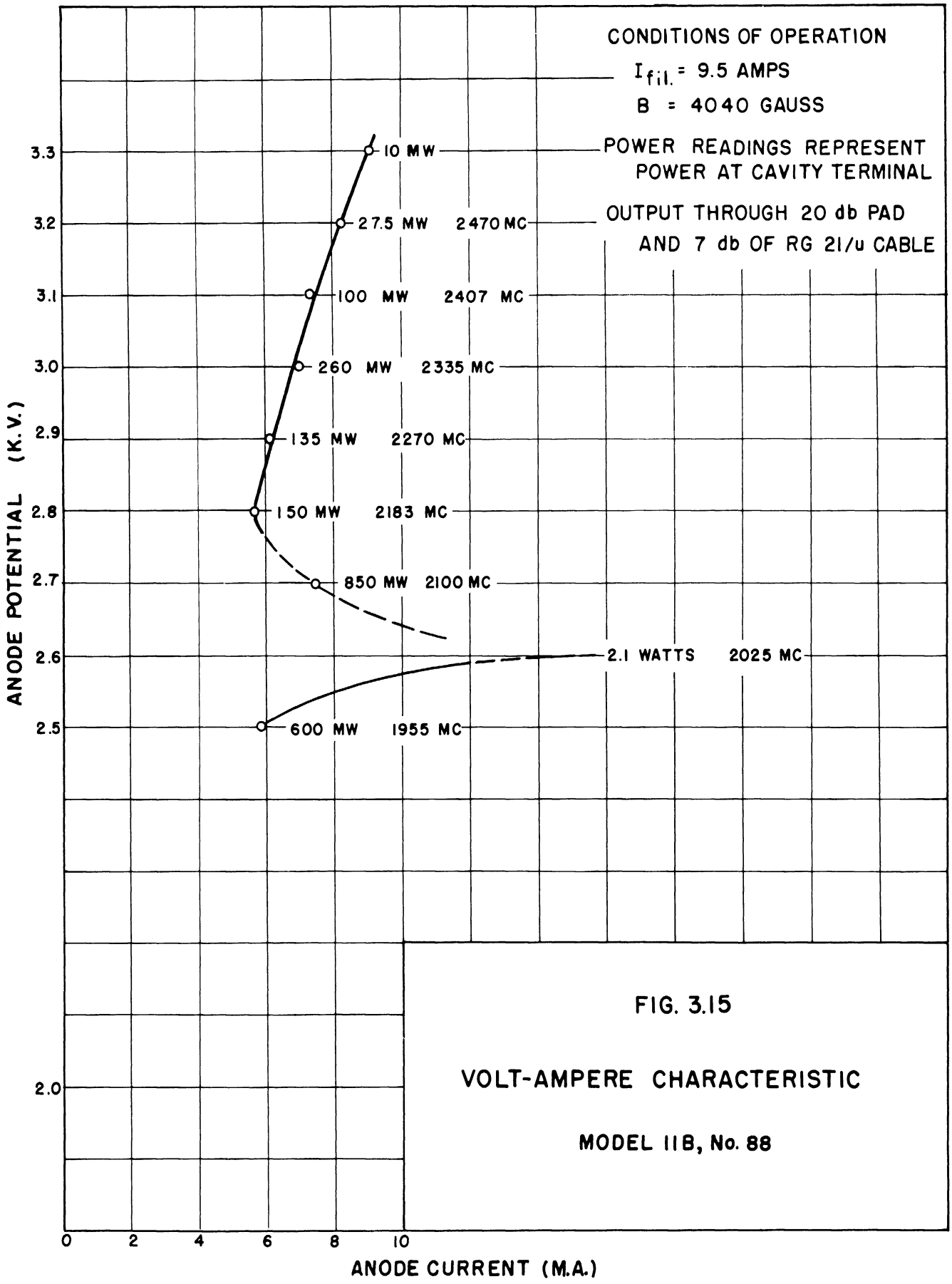

FIG. 3.15

VOLT-AMPERE CHARACTERISTIC

MODEL 11B, No. 88

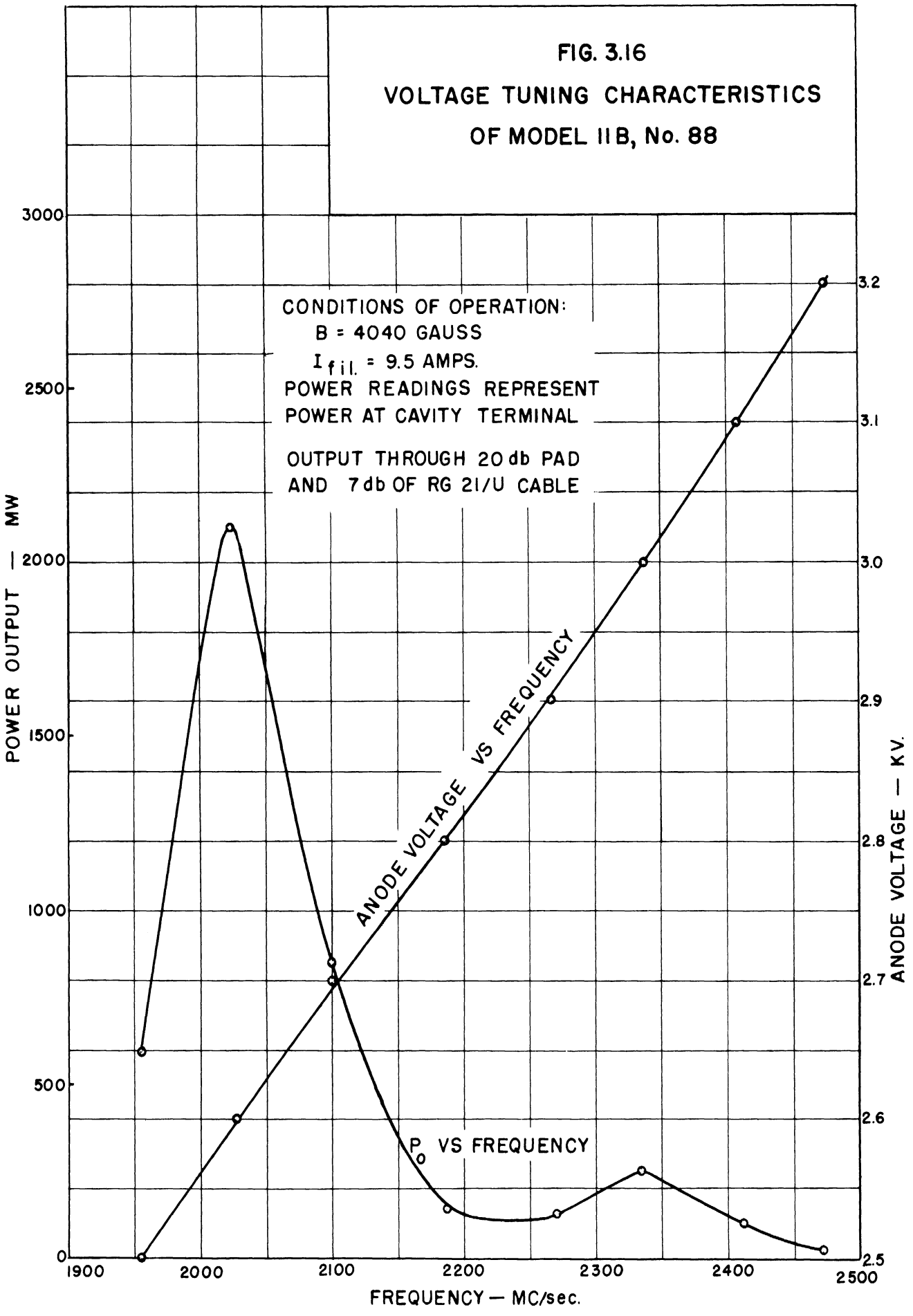
FIG. 3.16
VOLTAGE TUNING CHARACTERISTICS
OF MODEL 11B, No. 88
CONDITIONS OF OPERATION:
B = 4040 GAUSS
$I_{fil.}$ = 9.5 AMPS.
POWER READINGS REPRESENT
POWER AT CAVITY TERMINAL
OUTPUT THROUGH 20 db PAD
AND 7 db OF RG 21/U CABLE
ANODE VOLTAGE VS FREQUENCY
P_o VS FREQUENCY
POWER OUTPUT — MW
ANODE VOLTAGE — K.V.
FREQUENCY — MC/sec.
0
500
1000
1500
2000
2500
3000
1900
2000
2100
2200
2300
2400
2500
2.5
2.6
2.7
2.8
2.9
3.0
3.1
3.2

60-cycle sine-wave voltage, the tube could be tuned from 2000 to 2730 mc with a clean signal output over the entire range. The signal was monitored, using the circuit arrangement shown in Fig. 3.6. The frequency was measured in this case by using a coaxial-type wavemeter as an absorption meter in the circuit shown in Fig. 3.6.

As indicated in Fig. 3.6, the power output varied from 100 milliwatts to 2 watts over a frequency range of approximately 500 mc. This is considerably larger than the power output of the Model 11 tubes. Also, the operation of the tube was less sensitive to small changes in the cathode input power; once the adjustment of cathode input power was made, the operation of this tube was more stable than were the Model 11 tubes.

3.3.2 Model 11B, No. 92. This tube is identical with the Model 11B, No. 88. Figure 3.17 shows the volt-ampere characterisiic and Fig. 3.18 shows the voltage tuning characteristic of this tube. The frequency-vs.-anode-potential curve obtained by using the Hartree relation (assuming π-mode operation) is shown for comparison with the experimentally observed data. For a given frequency, the experimentally observed anode potential is approximately 50 percent higher than the value indicated by the Hartree relation. This discrepancy is discussed in a later section.

The output signal, as observed on the oscilloscope in the circuit arrangement shown in Fig. 3.6, appears to be free of noise. In obtaining the cw data the frequency could be varied from 1200 to 2350 mc without readjusting the cathode input power. When sweeping the anode voltage the frequency could be varied from approximately 2000 to 3000 mc with a change of 1200 volts in anode potential.

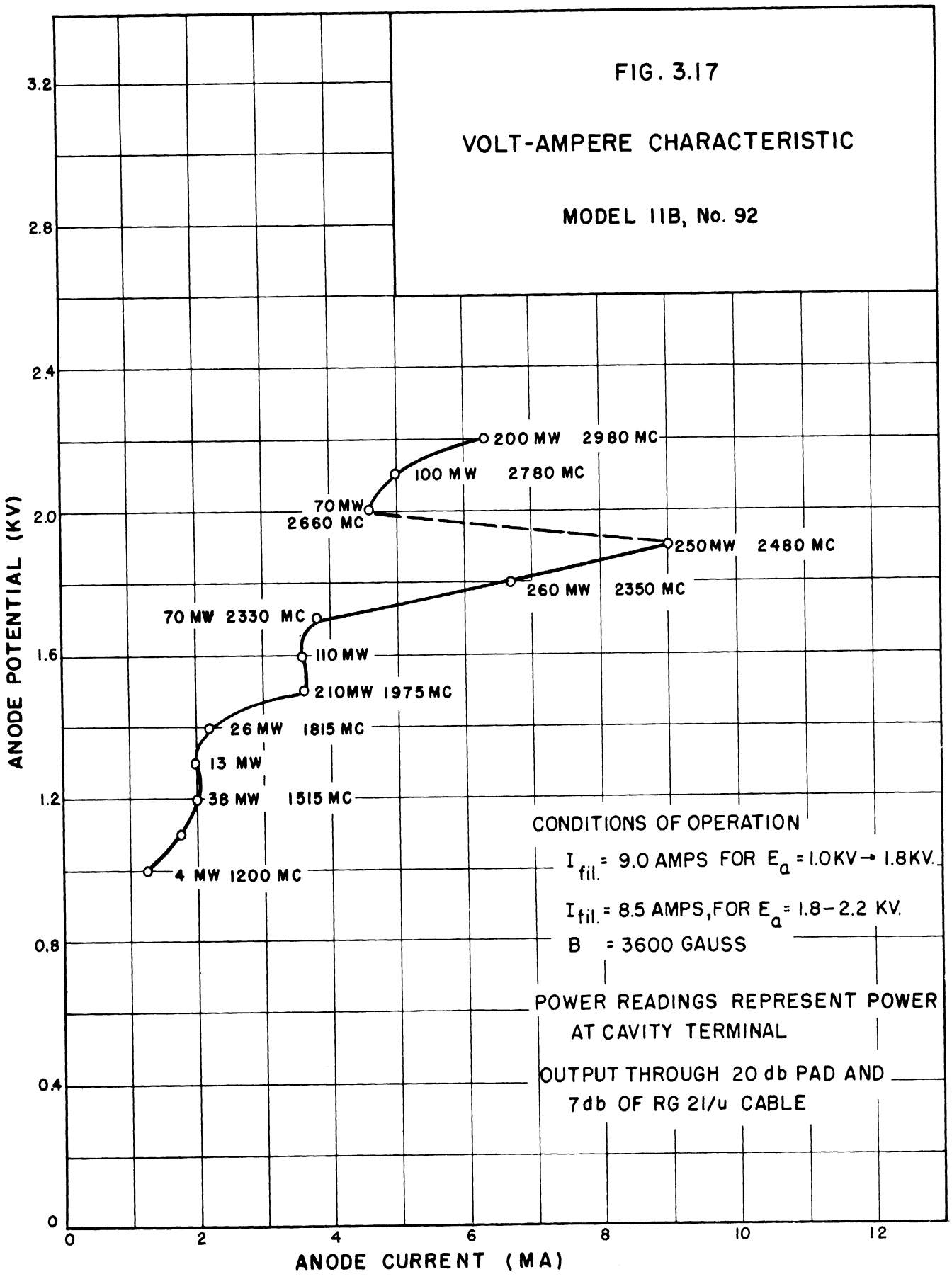
FIG. 3.17
VOLT-AMPERE CHARACTERISTIC
MODEL 11B, No. 92
ANODE POTENTIAL (KV)
ANODE CURRENT (MA)
3.2
2.8
2.4
2.0
1.6
1.2
0.8
0.4
0
0
2
4
6
8
10
12
200 MW 2980 MC
100 MW 2780 MC
70 MW
2660 MC
250 MW 2480 MC
260 MW 2350 MC
70 MW 2330 MC
110 MW
210 MW 1975 MC
26 MW 1815 MC
13 MW
38 MW 1515 MC
4 MW 1200 MC
CONDITIONS OF OPERATION
I fil. = 9.0 AMPS FOR Ea = 1.0KV → 1.8KV.
I fil. = 8.5 AMPS, FOR Ea = 1.8–2.2 KV.
B = 3600 GAUSS
POWER READINGS REPRESENT POWER AT CAVITY TERMINAL
OUTPUT THROUGH 20 db PAD AND 7db OF RG 21/u CABLE

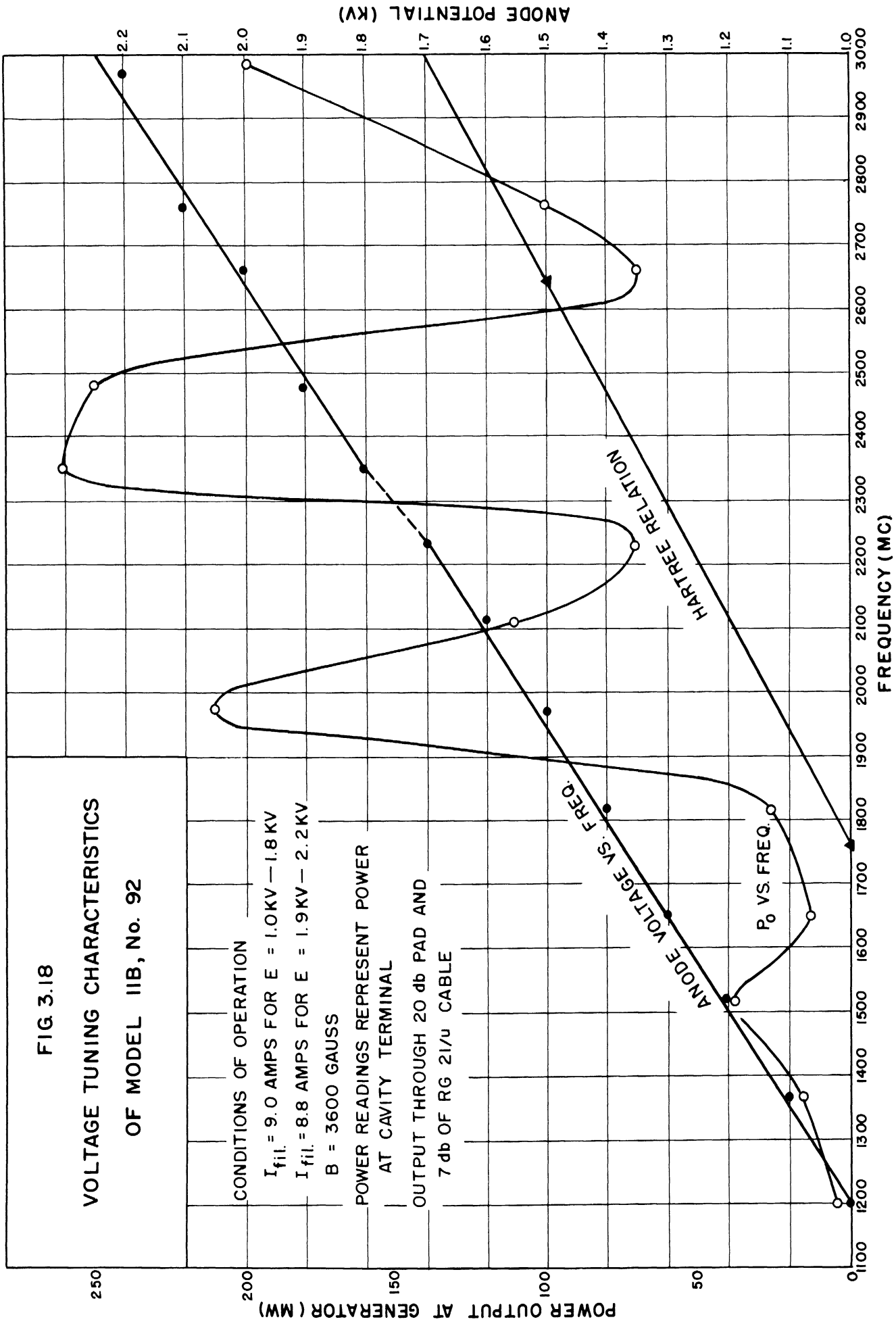
FIG 3.18
VOLTAGE TUNING CHARACTERISTICS
OF MODEL IIB, No. 92
CONDITIONS OF OPERATION
$I_{fil.}$ = 9.0 AMPS FOR E = 1.0KV—1.8 KV
$I_{fil.}$ = 8.8 AMPS FOR E = 1.9KV— 2.2 KV
B = 3600 GAUSS
POWER READINGS REPRESENT POWER AT CAVITY TERMINAL
OUTPUT THROUGH 20 db PAD AND 7 db OF RG 21/u CABLE
HARTREE RELATION
ANODE VOLTAGE VS. FREQ.
P_o VS. FREQ.
POWER OUTPUT AT GENERATOR (MW)
ANODE POTENTIAL (KV)
FREQUENCY (MC)

Figure 3.19 shows two pictures of power-output vs. anode-potential; the lower picture was taken with no choke on the cathode, and the upper picture was taken with the same conditions as in the lower one except that an external cathode choke was formed by using aluminum foil. This indicates that the large variations in power output (shown in Fig. 3.18) may be due to the loading effect of the cathode support at those frequencies.

3.3.3 Model 11B, No. 112. Tungsten rods were used as the anode bars in this tube. The heat dissipating capacity of the anode structure is increased over that of the tubes which use molybdenum anode bars. The processing technique was modified in the construction of this tube in that the cathode was vacuum-fired before mounting in the tube. This vacuum-firing of the cathode before mounting eliminated the coating of the glass envelope of the tube which had previously occurred in normal operation of the tubes. (This coating was due to molybdenum evaporated from the cathode.)

This tube was tested under dynamic operating conditions, and the results are as shown in Figs. 3.20 and 3.21. The conditions of operation are indicated on the figures. A 60-cycle voltage was superimposed upon the dc anode potential, giving an anode-voltage swing of 900 volts. Filament power was supplied from a battery to eliminate the frequency modulation caused by the variation of the magnetic field which is produced by an ac heater current.

Figure 3.20 shows the variation of the frequency with the anode voltage. To obtain these data the horizontal sweep on an oscilloscope was synchronized with the ac anode voltage, and therefore, could be calibrated in frequency. The output from the magnetron was fed through 22 db of attenuation into a coaxial-type wavemeter, and the output of the wavemeter

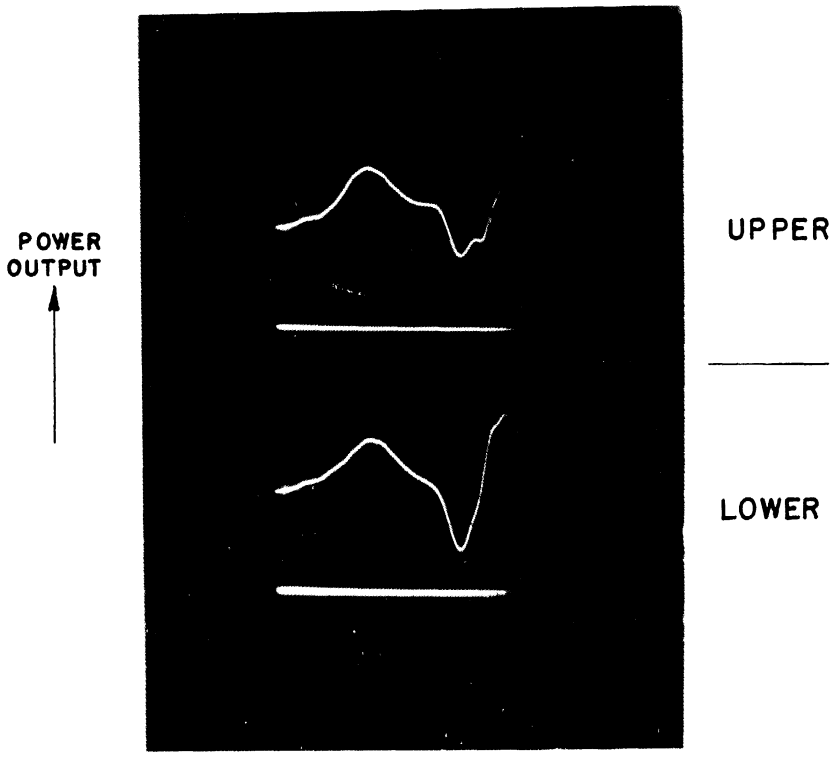

FIG. 3.19

POWER OUTPUT VS. ANODE POTENTIAL

MODEL 11B, No. 92

CONDITIONS OF OPERATION

$I_{fil.}$ = 8.7 AMPS B = 3500 GAUSS

E_{dc} = 2.0KV I_{dc} = 4 MA

E_{ac} = 600 VOLTS

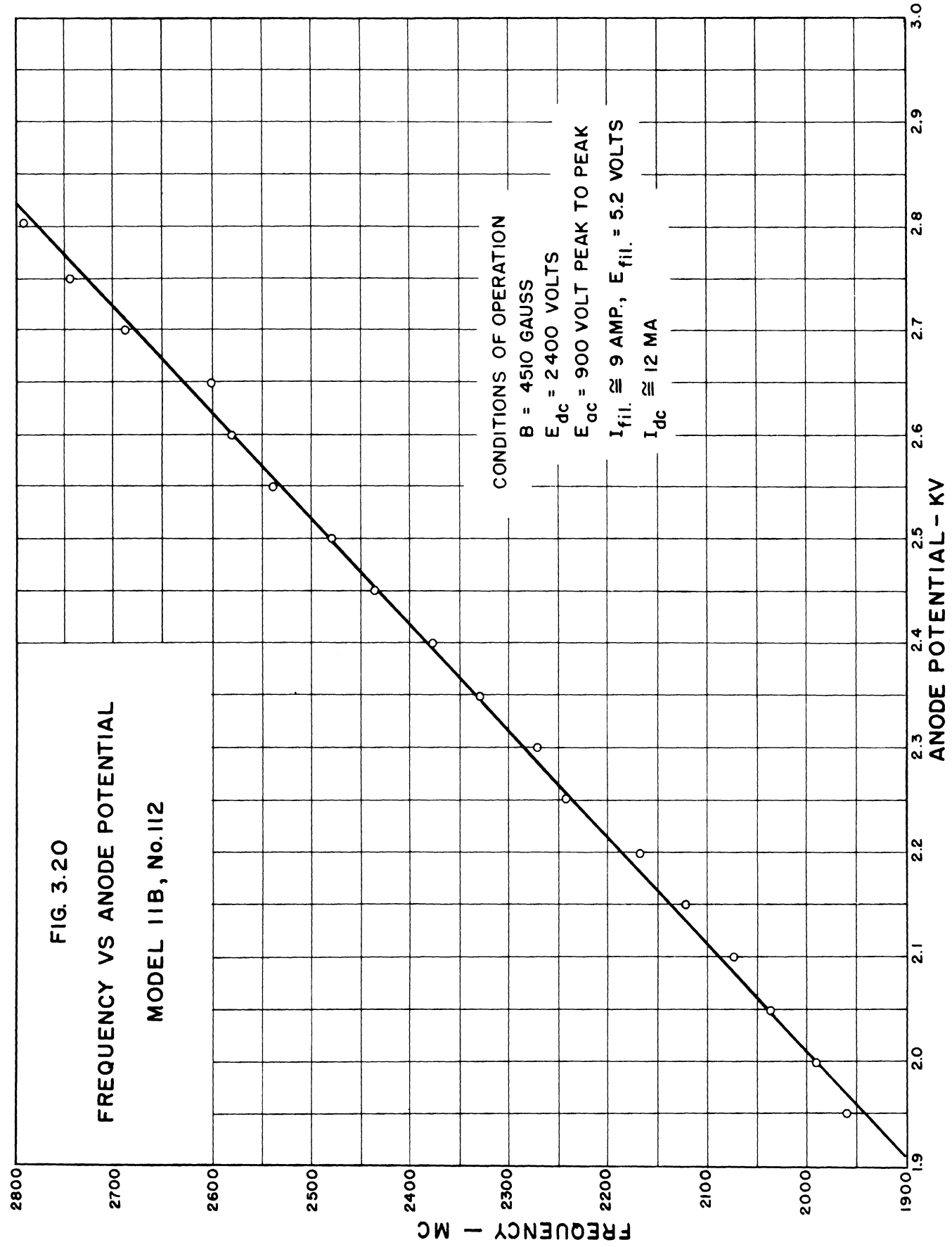
FIG. 3.20
FREQUENCY VS ANODE POTENTIAL
MODEL 11B, No.112
CONDITIONS OF OPERATION
B = 4510 GAUSS
E_{dc} = 2400 VOLTS
E_{ac} = 900 VOLT PEAK TO PEAK
$I_{fil.} \cong$ 9 AMP., $E_{fil.}$ = 5.2 VOLTS
$I_{dc} \cong$ 12 MA
FREQUENCY — MC
2800
2700
2600
2500
2400
2300
2200
2100
2000
1900
ANODE POTENTIAL — KV
1.9
2.0
2.1
2.2
2.3
2.4
2.5
2.6
2.7
2.8
2.9
3.0

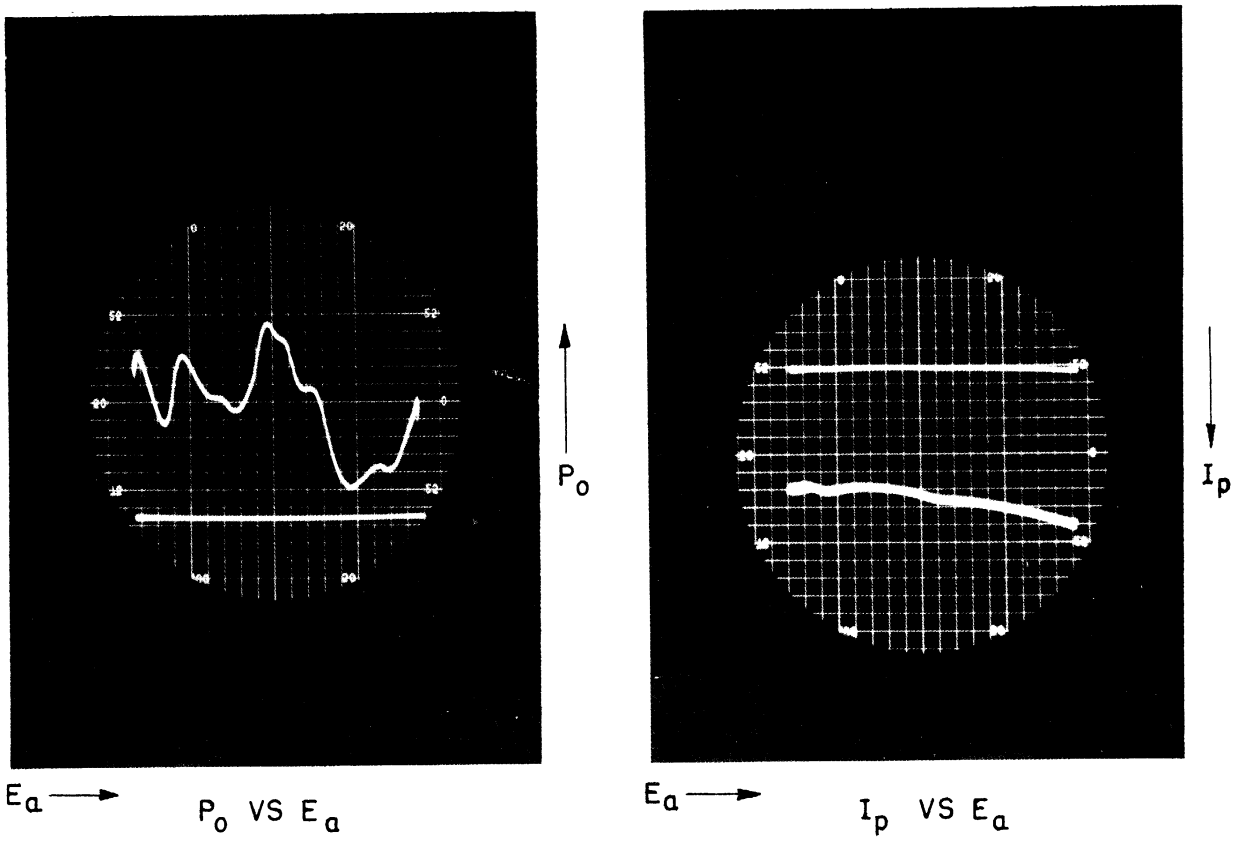

FIG. 3.21

POWER AND CURRENT CHARACTERISTICS
OF MODEL 11B, No. 112

B = 4510 GAUSS

E_{dc} = 2400 VOLTS

E_{ac} = 900 VOLTS PEAK TO PEAK

$I_{fil.} \cong$ 9 AMP

$I_{dc} \cong$ 15 AMP

$E_{fil.}$ = 5.2 VOLTS

passed through a crystal detector into the vertical input of the oscilloscope. (It was determined that 22 db was the minimum attenuation which would completely eliminate the effect of the wavemeter on the magnetron). In this manner, the frequency of operation could be measured at all voltages.

In addition to the voltage-tunable mode indicated in Fig. 3.20, there were two other modes which were very weak, but still detectable (by reducing the attenuation somewhat) over portions of the voltage range. One of these modes tuned from 2845 mc at 2100 volts to 3170 mc at 2300 volts; the second tuned from 4080 mc at 2050 volts to 4370 mc at 2200 volts. In the voltage range 2350 to 2850 only the main mode was present. Under certain conditions of operation, there are discontinuities in the operation of the main mode. These discontinuities in the operation are detectable in either the power output or anode current curves (shown in Fig. 3.21). Continuous operation can be obtained by proper adjustment of the various parameters. Frequency deviations of 400 to 600 mc can be obtained with no difficulty in maintaining continuous operation; for frequency deviations of the order of 800 to 1000 mc, the adjustment of the cathode temperature becomes more critical.

With the modulation voltage reduced to 450 volts peak-to-peak, the frequency of operation could be shifted as much as 50 mc by varying the filament heater current and still maintain coherent operation over the voltage range. An increase in cathode temperature decreases the frequency of oscillation. The tube seemed to operate best at, or near, the lower cathode temperature.

For cw operating conditions it was possible to vary the filament current from 8.9 amps to 9.3 amps, and still maintain a coherent

signal output. The power output varied from 52 mw at an anode current of 5 ma to 350 mw at an anode current of 18.75 ma. The corresponding frequency variation was from 2450 mc to 2320 mc.

Figure 3.21 shows the variation in power output and anode current with the anode voltage. The frequency range in Fig. 3.21 is approximately 900 mc (as shown in Fig. 3.20) and the peak power is of the order of 550 milliwatts. Figure 3.21(b) shows the variation of anode current with anode voltage, the average current being approximately 15 ma. It should be noted that there are no discontinuities in the operation and it was determined that the tube was oscillating coherently throughout the range. The decrease in the power output in the right (high frequency) side of Fig. 3.21(a) is due to the loading of the cathode circuit at that frequency.

This tube was operated with battery supplies for the filament and anode, and an electrically regulated power supply for the electromagnet. Under these conditions, the output signal (as observed on a spectrum analyzer) was stable; no jitter was present in cw operation. The output could be tuned over several hundred mcs without readjusting the cathode temperature. Qualitative measurements using the spectrum analyzer indicated that the coherent output signal was at least 65 db above the noise present in the output signal.

Satisfactory operation was obtained with anode voltages as low as 800 volts and frequencies in the order of 2000 mc.

Under these conditions the output power was reduced but the signal was stable and free of noise.

3.4 Model 11A

The Model 11A is similar to the Model 11 except that square anode bars are used. The anode bars are .030 inch square and are arranged such that the spacing between bars is approximately .030 inch. The inside anode diameter is .235 inch; this is approximately equal to the inside anode diameter in the Model 11. The original design of the Model 11 was based on the assumption that round anode bars would reduce the higher space harmonics in the interaction space and thus improve the operation of a low-Q voltage-tunable magnetron. The Model 11A was constructed for the purpose of comparing the operation of similar tubes with round and with square anode bars. The Model 11 and Model 11A are identical except for the shape, size, and spacing of anode bars. Since the Model 11 has more desirable characteristics as a voltage-tunable magnetron, it is concluded that a large portion of this improvement may be attributed to the use of round anode bars.

3.4.1 Model 11A, No. 90. The Model 11A, No. 90 has a thoriated tungsten cathode. Figure 3.22 shows the voltage-tuning characteristic, and Fig. 3.23 shows the volt-ampere characteristic for this tube. The frequency can be varied continuously from 1760 to 2510 mc; however, it is necessary to readjust the cathode input power at almost every point. The discontinuities in the anode potential vs. frequency curve are caused by this change in cathode temperature.

Figure 3.24 shows a photograph of power output vs. anode potential, using a 60 cycle, series modulating voltage. The circuit arrangement shown in Fig. 3.6 was used. This picture was taken under approximately the same conditions as indicated for Fig. 3.23. The blur at the left is due to noise at the low-voltage range of operation, and there is a discontinuity in the power output at the high voltage end.

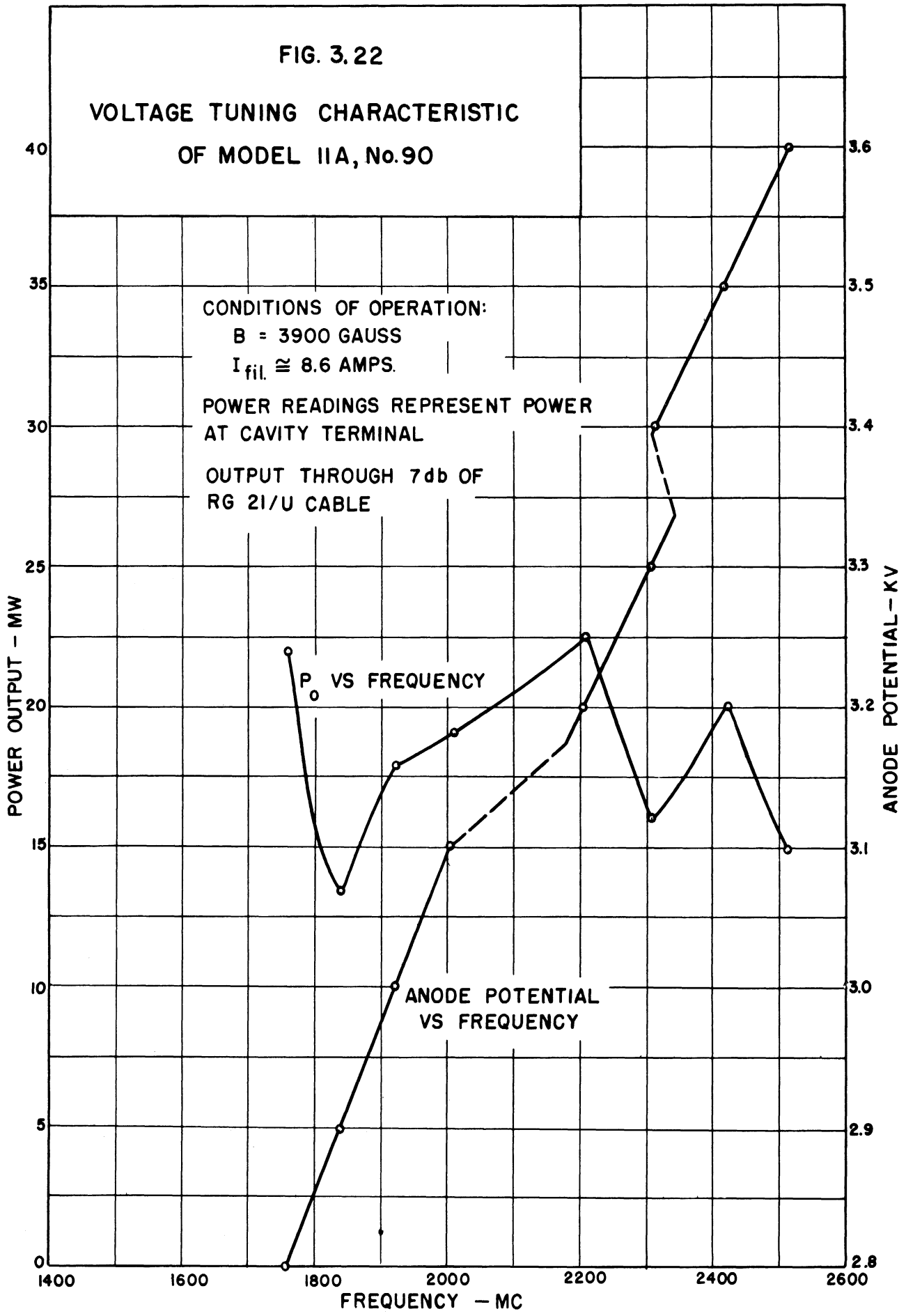
FIG. 3.22
VOLTAGE TUNING CHARACTERISTIC
OF MODEL 11A, No. 90
CONDITIONS OF OPERATION:
B = 3900 GAUSS
$I_{fil.} \cong$ 8.6 AMPS.
POWER READINGS REPRESENT POWER AT CAVITY TERMINAL
OUTPUT THROUGH 7db OF RG 21/U CABLE
P_o VS FREQUENCY
ANODE POTENTIAL VS FREQUENCY
POWER OUTPUT - MW
ANODE POTENTIAL - KV
FREQUENCY - MC
0
5
10
15
20
25
30
35
40
2.8
2.9
3.0
3.1
3.2
3.3
3.4
3.5
3.6
1400
1600
1800
2000
2200
2400
2600

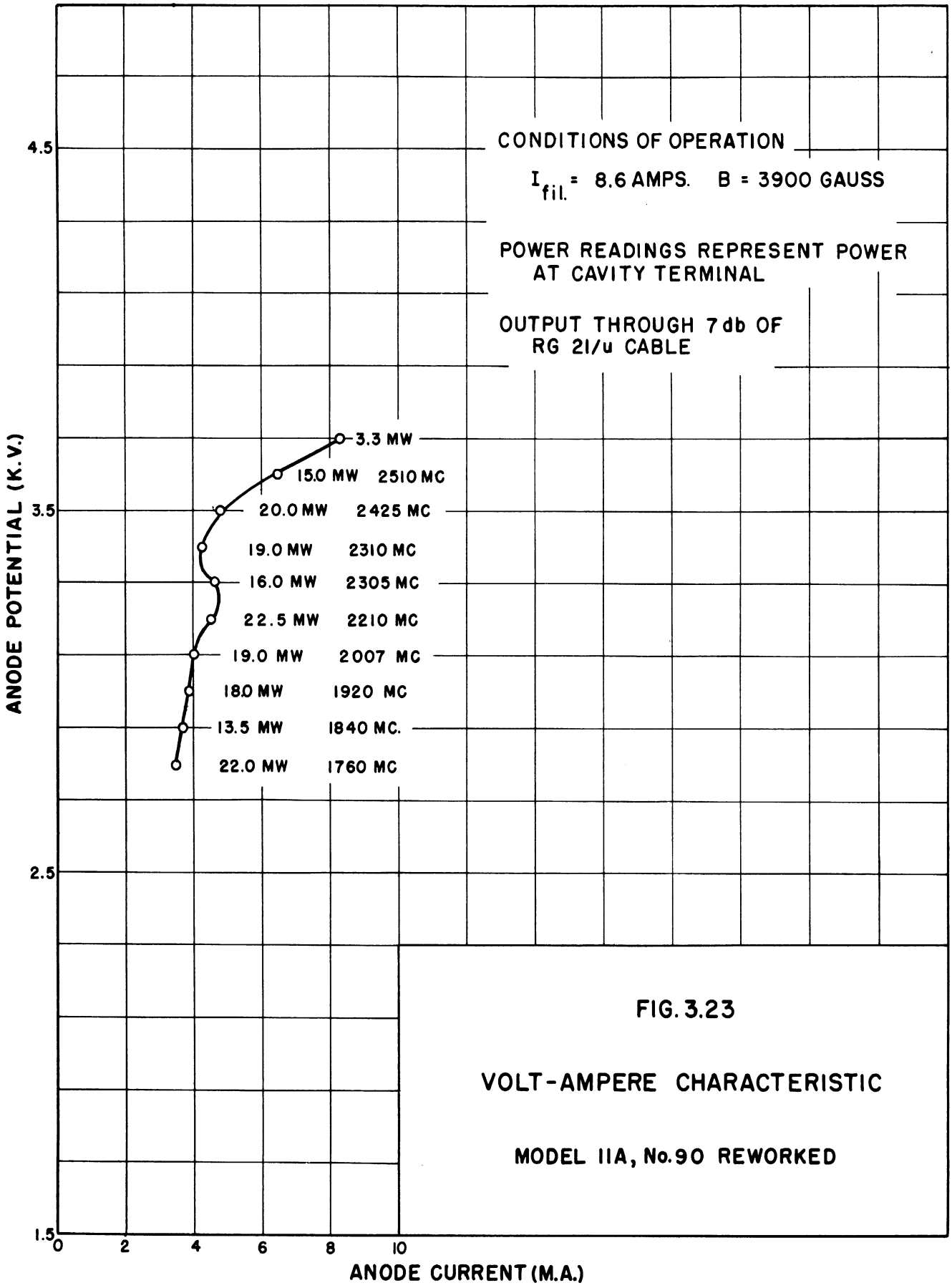

FIG. 3.23

VOLT-AMPERE CHARACTERISTIC

MODEL IIA, No. 90 REWORKED

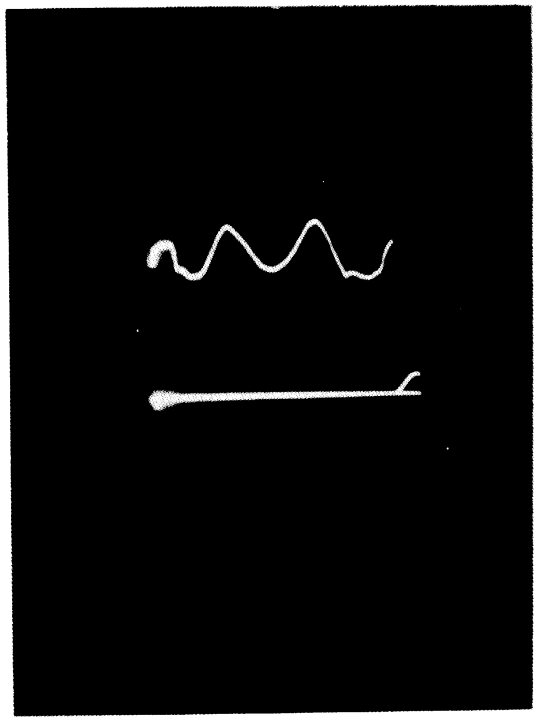

FIG. 3.24

POWER OUTPUT VS. ANODE VOLTAGE

MODEL IIA No. 90 REWORKED

CONDITIONS OF OPERATION

$I_{fil.}$ = 8.5 AMPS B = 3980 GAUSS

E_{dc} = 3.4 KV E_{ac} = 1000 VOLTS

CAVITY TERMINATED IN 50Ω LOAD

3.4.2 Model 11A, No. 89. The Model 11A, No. 89 is identical to the Model 11A, No. 90 except that No. 89 has a pure tungsten cathode. Figure 3.25 shows the volt-ampere characteristic for this tube. The operation is quite similar to the operation of the Model 11A, No. 90. It was necessary to readjust the cathode input power while taking the data. Figure 3.26 shows a photograph of power output vs. anode potential. The upper picture is for a sweep voltage of 550 volts peak-to-peak, and shows that there are no discontinuities in the output, however, there is noise present in the high voltage region. The lower picture is for a sweep of 1200 volts peak-to-peak, and shows the type of output which is obtained when one tries to sweep the tube over a wide frequency range. In addition to the discontinuities there is noise present over much of the frequency range.

The experimentally determined voltages are approximately 50 percent greater than indicated by the Hartree relation, assuming π-mode of operation. In general, the Model 11A is more sensitive to cathode temperature than either Model 11 or Model 11B, and cannot be tuned over as wide a frequency range. The output signal contains more noise than in either Model 11 or 11B. The power output is greater than for the Model 11, but less than for the Model 11B.

3.5 Button Cathode Model 11, No. 82

In Section 2.1 it was shown that the loading of the cavity by the cathode support is a result of the rf voltage which is coupled through the active portion of the cathode. As indicated in Section 2.4, the purpose of the button cathode is to eliminate this loading of the cavity by the cathode support (and the filament leads), when the tube is operating in the π-mode. A Model 11 tube, No. 82, was constructed using such

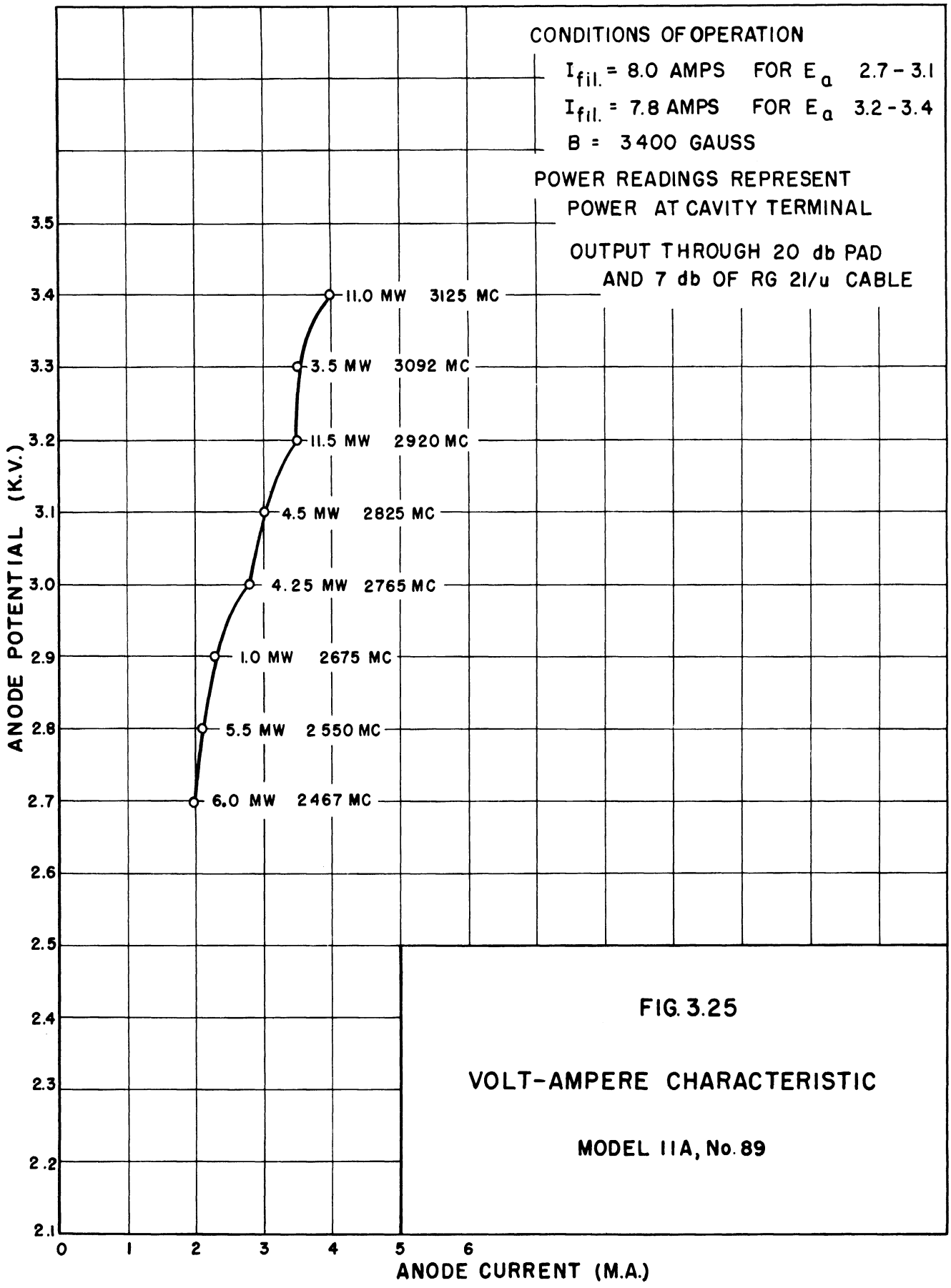

FIG. 3.25

VOLT-AMPERE CHARACTERISTIC

MODEL 11A, No. 89

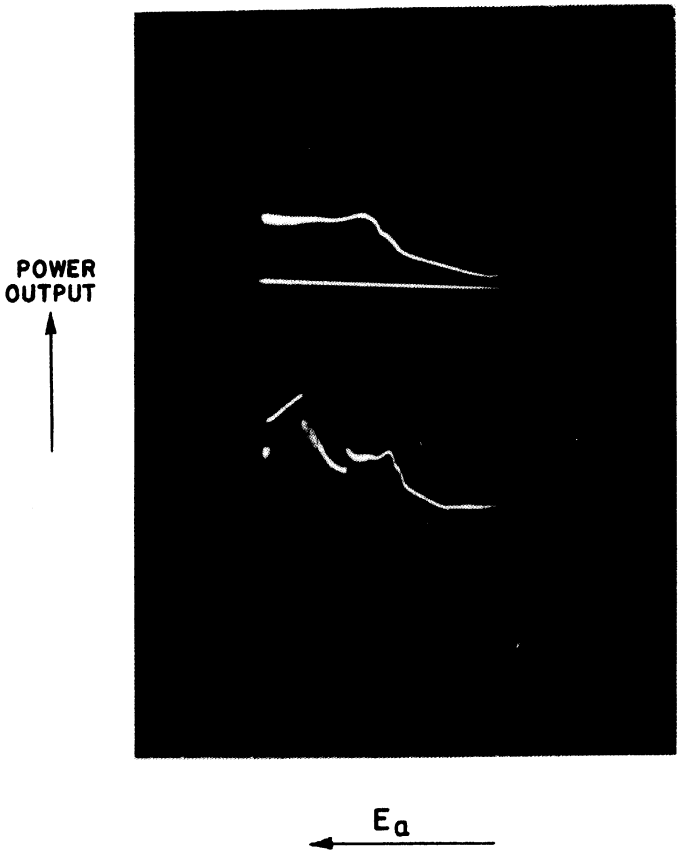

FIG. 3.26

POWER OUTPUT VS. ANODE VOLTAGE

MODEL II A, No. 89

CONDITIONS OF OPERATION

$I_{fil.}$ = 8.25 AMPS B = 4000 GAUSS

E_{dc} = 2.45 KV

TOP TRACE — E_{ac} = 550 VOLTS

LOWER TRACE — E_{ac} = 1200 VOLTS

a cathode. This arrangement is shown in Fig. 3.27. The upper end hat is oxide-coated and serves as the electron source for the tube. The lower end hat is pure nickel and contains no heater and no emitting surface. The lower end hat served to contain the electrons within the interaction space, serving as a repeller or as a collector, depending upon the mode of operation.

The tube was first tested with an anode voltage consisting of a 600 peak volt, 60-cycle sine wave superimposed upon the dc supply. For this test, the lower end hat (or collector) was connected directly to the cathode. A filament current of 1.8 amperes was required to start oscillation. However, once the tube started to oscillate, both the cathode and collector began to heat up. The filament current could be reduced to zero and the tube continued to oscillate; in fact, both the cathode and the collector were heated to a bright red by the back bombardment. Under these conditions there was a visible discharge between the cathode and collector, the discharge was light blue in color, and slightly smaller in diameter than the cathode emitting surface. This discharge appeared to terminate on the cathode and collector surfaces. The plate voltage could not be raised above 1500 volts because above this level the cathode temperature became unstable and tended to "run away", causing arc-over in the tube. The power output vs. anode voltage (as observed on an oscilloscope, using the circuit arrangement shown in Fig. 3.6), was stable and nearly uniform over a wide frequency range. It was impossible to make cw measurements due to the instability of the cathode temperature. Pulses tests indicated that the tube voltage-tuned from 1380 to 2380 mc with a magnetic field of 2900 gauss,and from 1200 to 1900 mc with a magnetic field of 3900 gauss. Thus, for similar values of B, the

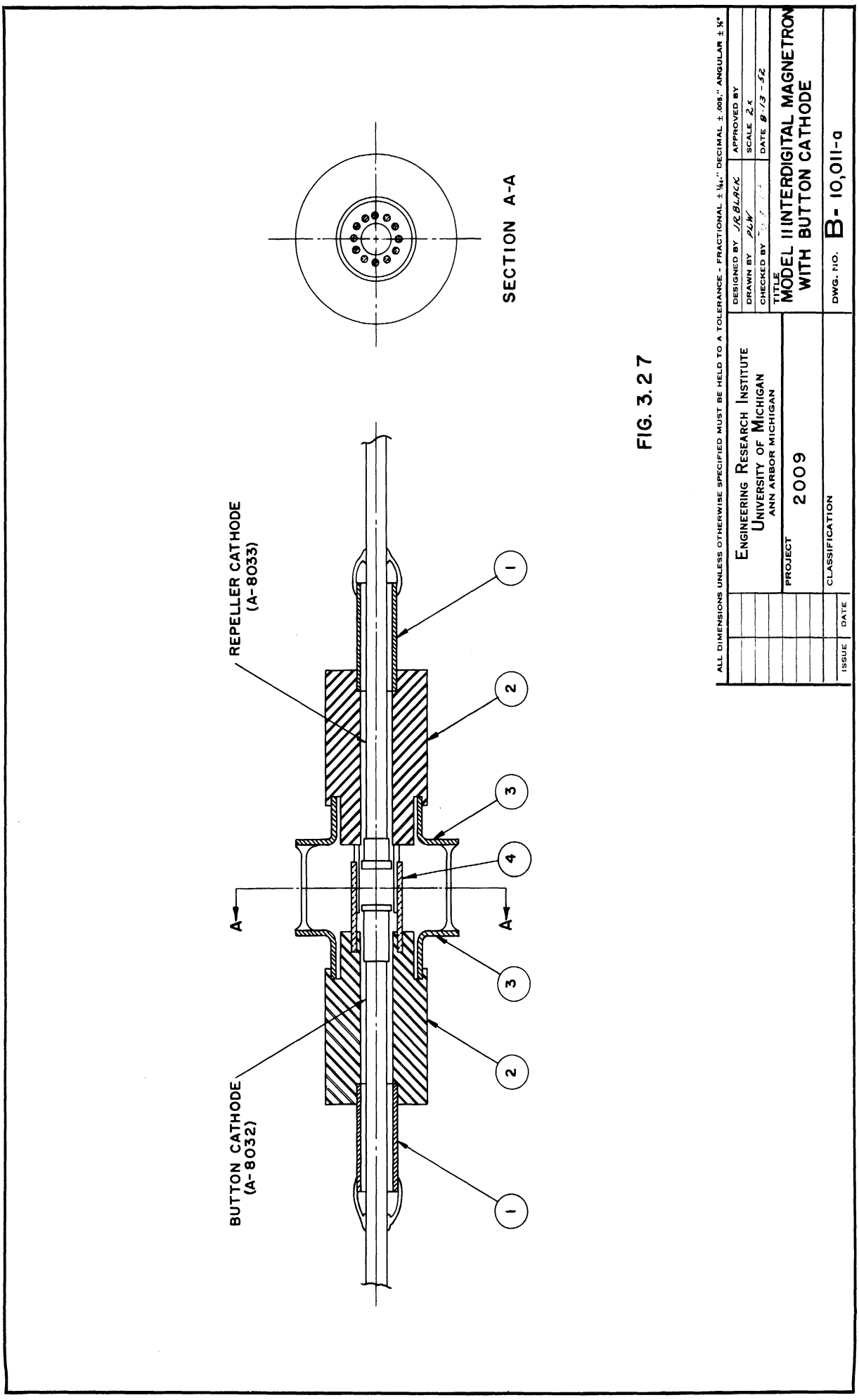
REPELLER CATHODE
(A-8033)
BUTTON CATHODE
(A-8032)
A
A
1
2
3
4
3
2
1
SECTION A-A
ALL DIMENSIONS UNLESS OTHERWISE SPECIFIED MUST BE HELD TO A TOLERANCE - FRACTIONAL ± 1/64" DECIMAL ± .005" ANGULAR ± 1/2°
ENGINEERING RESEARCH INSTITUTE
UNIVERSITY OF MICHIGAN
ANN ARBOR MICHIGAN
PROJECT 2009
CLASSIFICATION
ISSUE
DATE
DESIGNED BY J.R. BLACK
DRAWN BY P.W.
CHECKED BY
APPROVED BY
SCALE 2:1
DATE 8-13-52
TITLE
MODEL II INTERDIGITAL MAGNETRON
WITH BUTTON CATHODE
DWG. NO. B-10,011-a
DWG. NO. B

FIG. 3.27

frequency range of voltage-tunable operation for this tube is lower than for the tubes with regular cathodes.

The following experiments were performed to determine the nature and cause of the heating of the cathode and collector. First, a milliammeter was connected between the collector and cathode. This meter indicated that the collector was being bombarded by electrons. A variable voltage supply was then connected between the collector and cathode, the collector being negative with respect to the cathode. It was necessary to make the collector 100 volts negative, with respect to the cathode, before the collector current was reduced to zero. It was found that the condition for optimum voltage-tunable operation occurred when the collector current was at, or very near, zero. The tube was operated with the collector floating. Under these conditions the cathode heated up but the collector was not heated. However, the output did not appear to be as great, or the signal as clean, over a wide frequency range.

These experiments thus indicate that electrons exist in the interaction space which have energies sufficient to build up a space charge that it approximately 100 volts negative with respect to the cathode. These are the electrons which gain energy from the rf field in the sorting process and are returned to the cathode (in a magnetron with a physical cathode). In the normal magnetron structure, these high-energy electrons are collected on their return to the cathode and their energy is dissipated in the form of heat at the cathode, producing backheating. In the present case there is no physical cathode to collect these electrons, thus making possible the formation of a space-charge cloud which is 100 volts negative with respect to the emitter. Once

this space-charge cloud has been formed, both the collector and the button cathode will be bombarded by electrons producing the heating effects which were observed.

The collector was made 500 volts negative with respect to the cathode with no indication of ion current to the collector. A visible discharge would require that there be some ions present, and, of course, there will always be some gas molecules present in any vacuum envelope. The tube was vacuum processed a number of times in an attempt to obtain a vacuum in which the glow-type of discharge could not be maintained (pressures in the order of 10^{-7} mm of Hg were obtained); however, when the tubes were tested the discharge was always present. With this type of operation it was not possible to operate the tube at a high enough anode voltage to obtain a significant power output.

3.6 Measurements Using an Intermediate-Q Cavity

The Model 11B, No. 88 tube was tested in cavity No. 2 (shown in Fig. 3.28). This cavity consisted of a section of tapered-ridge waveguide in which the tube was mounted, a tapered-ridge waveguide-to-coaxial junction, and a section of waveguide with a shorting plunger. This tube was mounted in S-band ridge waveguide (the same as that used in cavity No. 1). The particular arrangement used was chosen as a matter of convenience since most of the components were available in the laboratory.

Voltage-standing-wave ratio measurements which were made on this cavity, with a dummy tube in place, indicated resonances at 2440 mc and at 3480 mc. These resonant points were dependent upon the position of the shorting plunger. Since there were frequency-sensitive elements in the cavity other than the shorted section of waveguide, there were

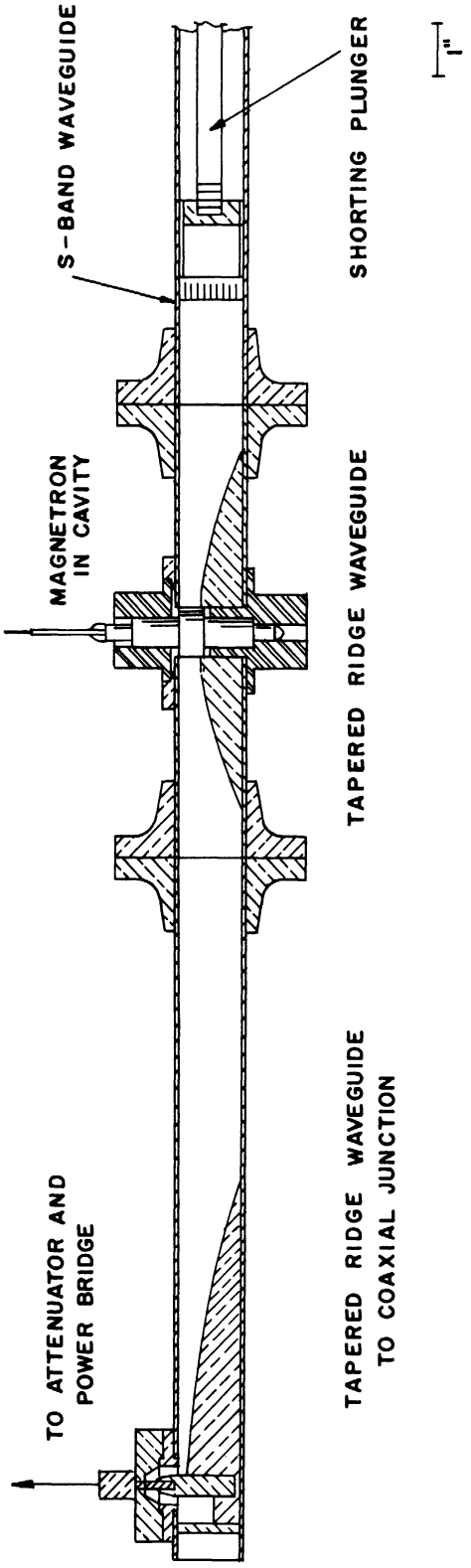

FIG. 3.28

SINGLE-ENDED CAVITY FOR MODEL II MAGNETRON
(CAVITY No. 2)

a number of variations in the VSWR over the frequency range of 2200 to 3500 mc. Since the cavity was terminated at one end in a nearly lossless short circuit, and at the other end in the characteristic impedance of the waveguide, the effective Q of the circuit was perhaps of the order of 10.

When the Model 11B, No. 88 tube was tested in this cavity it was found that the output was very sensitive to the position of the shorting plunger. For an anode voltage of 2500 volts dc, and a plate current of 10 ma, the anode voltage could be modulated by as much as plus or minus 800 volts and still maintain a uniform power output of 2500 milliwatts. The anode current was more unstable than when the tube was tested in cavity No, 1; the current tended to "run away" and level off at 30 to 40 ma. The signal output appeared to be free of noise.

CW power measurements were made with E_a = 2500 volts, $I_a \cong 40$ ma, and a power output up to 4 watts was observed. Several tests were made, allowing the tube to operate at this high-power level only long enough to obtain power readings.

The Model 11B, No. 112 tube was also tested in this cavity. Under cw operating conditions, 2 to 4 watts of coherent signal power was obtained. This tube could be operated continuously at this power level, since tungsten anode bars were used. The signal was voltage-tunable over a frequency range of approximately 200 mc, and the frequency limits of this voltage-tunable range depended upon the position of the shorting plunger.

3.7 Measurements on Cavity No. 1

The cavity impedance of interest is that which the electrons "see" when the tube is in operation. To obtain measurements of this quantity it is necessary to measure the impedance across the anode bars

with the tube in place. A factor of interest in high-Q magnetrons is the Q of the cavity. However, the cavity structure used with the Model 11 tubes is nonresonant so Q-measurements are useless in this case. Figure 3.29 shows an arrangement which makes possible the qualitative measurement of the impedance across the anode bars. This arrangement is equivalent to terminating the tapered coaxial line in the impedance across the anode bars, which is the quantity of interest. This tube, with the transducer mounted as shown in Fig. 3.29, was mounted in cavity No. 1. The output terminal of the transducer was then connected directly to a slotted line which was used to make the desired measurements of VSWR, position of minimum VSWR, and wavelength. The two output terminals of the cavity were terminated in 50-ohm resistors.

This arrangement allowed determination of the impedance at the output of the transducer. To determine the desired impedance across the anode terminals, it is necessary to know the transformation ratio of the transducer. With this type of transducer it is impractical to make the necessary measurements from which the transformation ratio can be determined. Measurements were made on the transducer to show that the transformation ratio is not frequency sensitive. These measurements consisted of shorting the transducer with a special inner conductor and making VSWR measurements to determine that there were no resonances in the frequency range in which the device was to be used. Thus, this device will allow measurements of the relative magnitude of the impedance across the anode bars.

Figure 3.30 shows the results of these measurements plotted on a circular impedance chart. The reference used for determining the

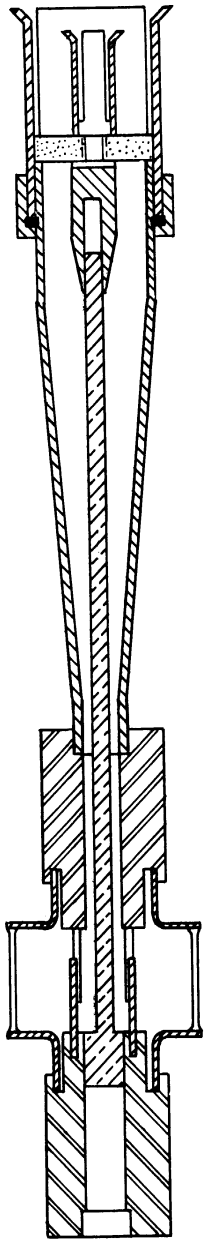

FIG. 3.29

COAXIAL OUTPUT AND DUMMY TUBE
USED IN COLD TESTING CAVITY No. 1

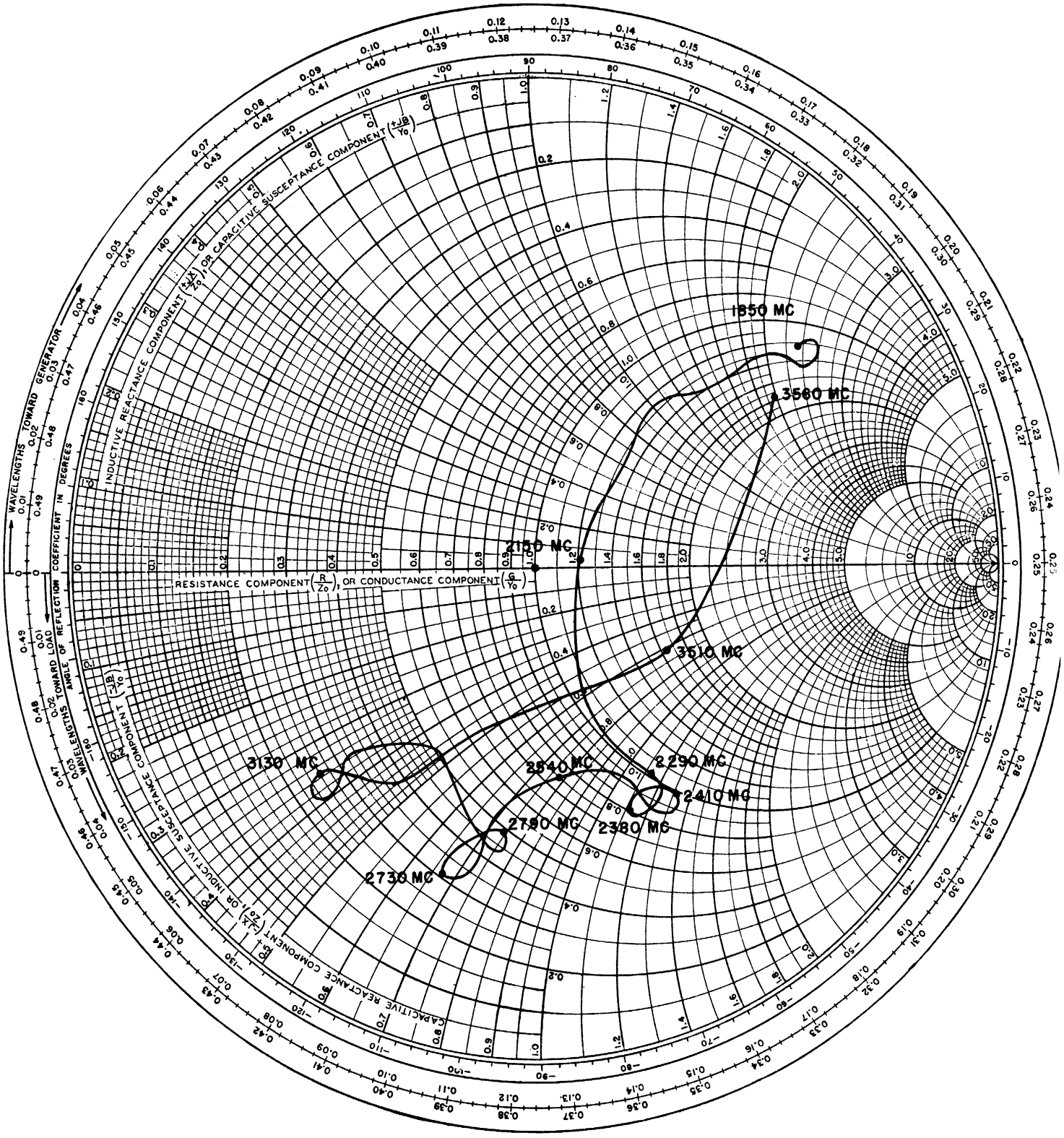

FIG. 3.30

IMPEDANCE VS FREQUENCY

CAVITY NO. 1

Z_0 = 39 OHMS

position of the voltage minimum was taken as the first discontinuity in the transducer shown in Fig. 3.29, which is the bottom of the top pole piece. If it is assumed that the transducer acts as an ideal transformer then the curve shown in Fig. 3.30 gives the impedance between the anode sets. The impedance as presented is normalized to the characteristic impedance of the coaxial line at the input of the transducer, (Z_o = 46 ohms).

3.8 Potential Distribution in Interaction Space

As an aid in studying the operation of the Model 11B and Model 11A tubes, a flux plot of the field distribution in the interaction space of each tube was made. These plots are shown in Figures 3.31 and 3.32.

One significant difference in the two flux plots is the variation in the field strength in the region "a" (Figs. 3.31, 3.32) for the two geometries, assuming equal rf voltages on each. Since a high rf field is necessary to produce effective bunching within this region, the square anode structure would seem to be more effective. However, since the anode-to-anode capacitance is greater for the square anode structure than for the round anode structure, it will require a greater induced current in the square anode structure to produce the same voltage. Thus, the development of a high rf field and the bunching of the electrons are interdependent phenomena and it is impossible to conclude from the flux plots alone which type of structure is better for voltage-tunable operation.

Figures 3.33 and 3.34 show potential distribution curves for the interaction spaces in the Model 11 and Model 11A tubes. These data were obtained by constructing models of the anode and cathode

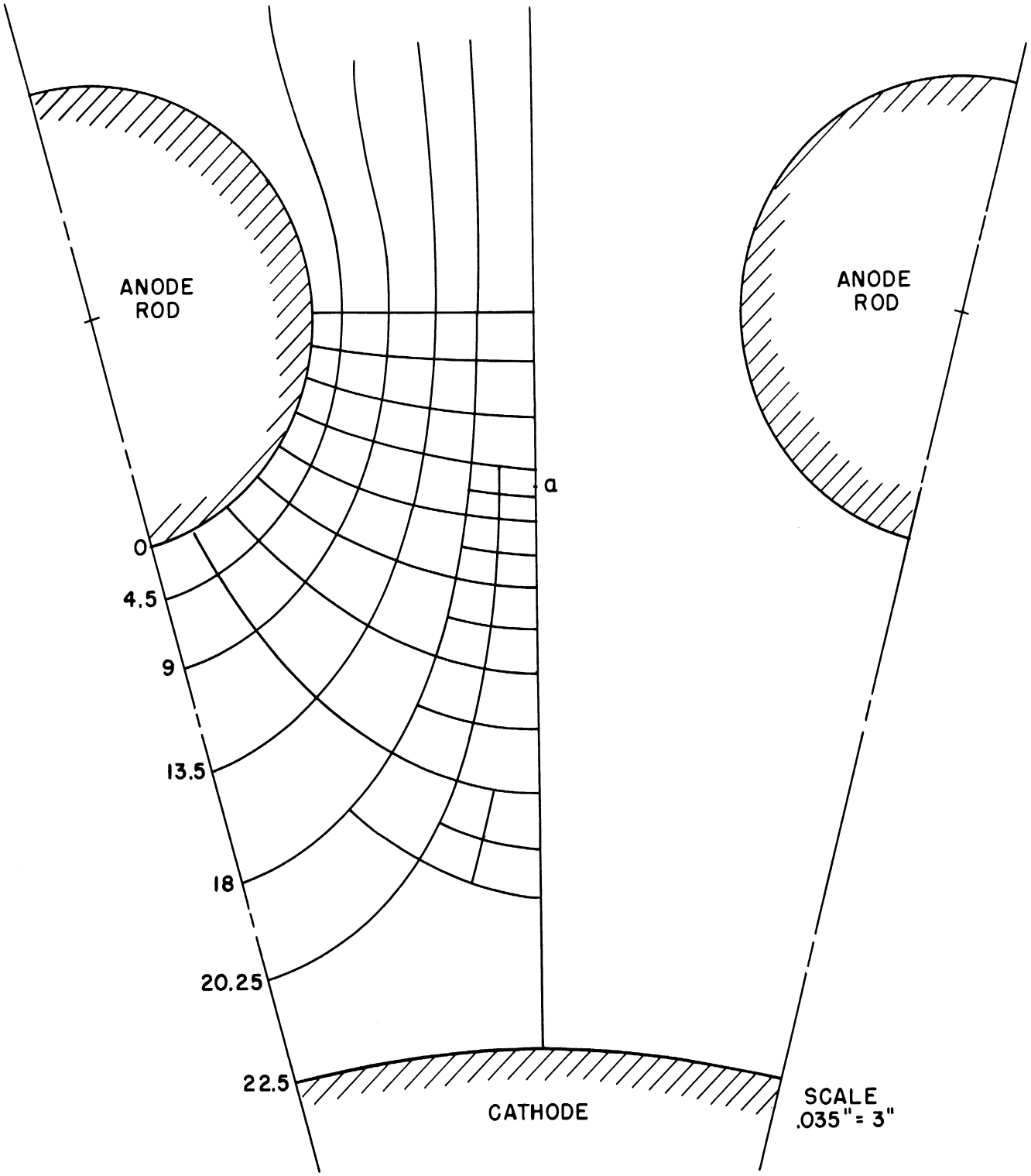

FIG. 3.31

FLUX PLOT FOR MODEL 11 B

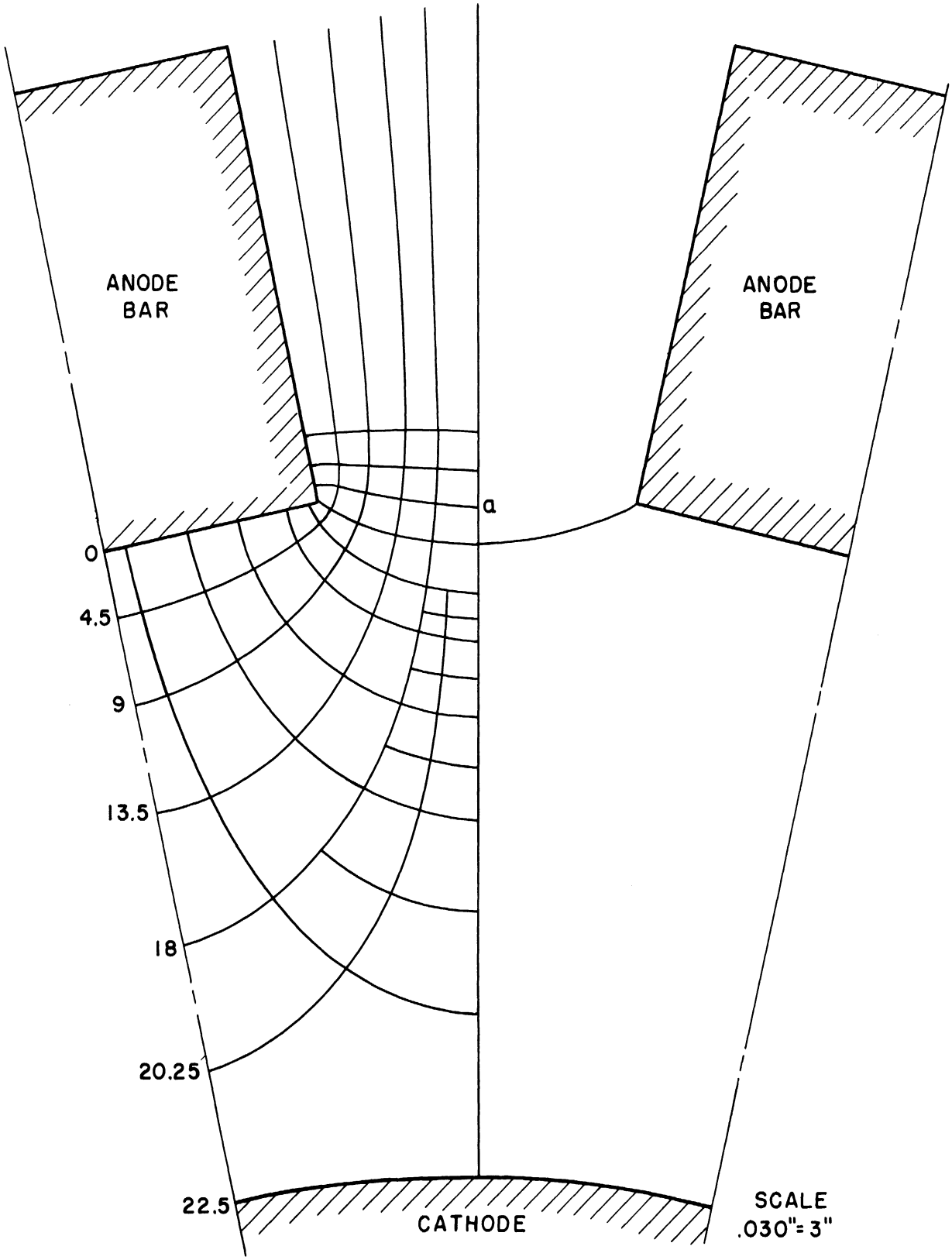

FIG. 3.32

FLUX PLOT FOR MODEL IIA

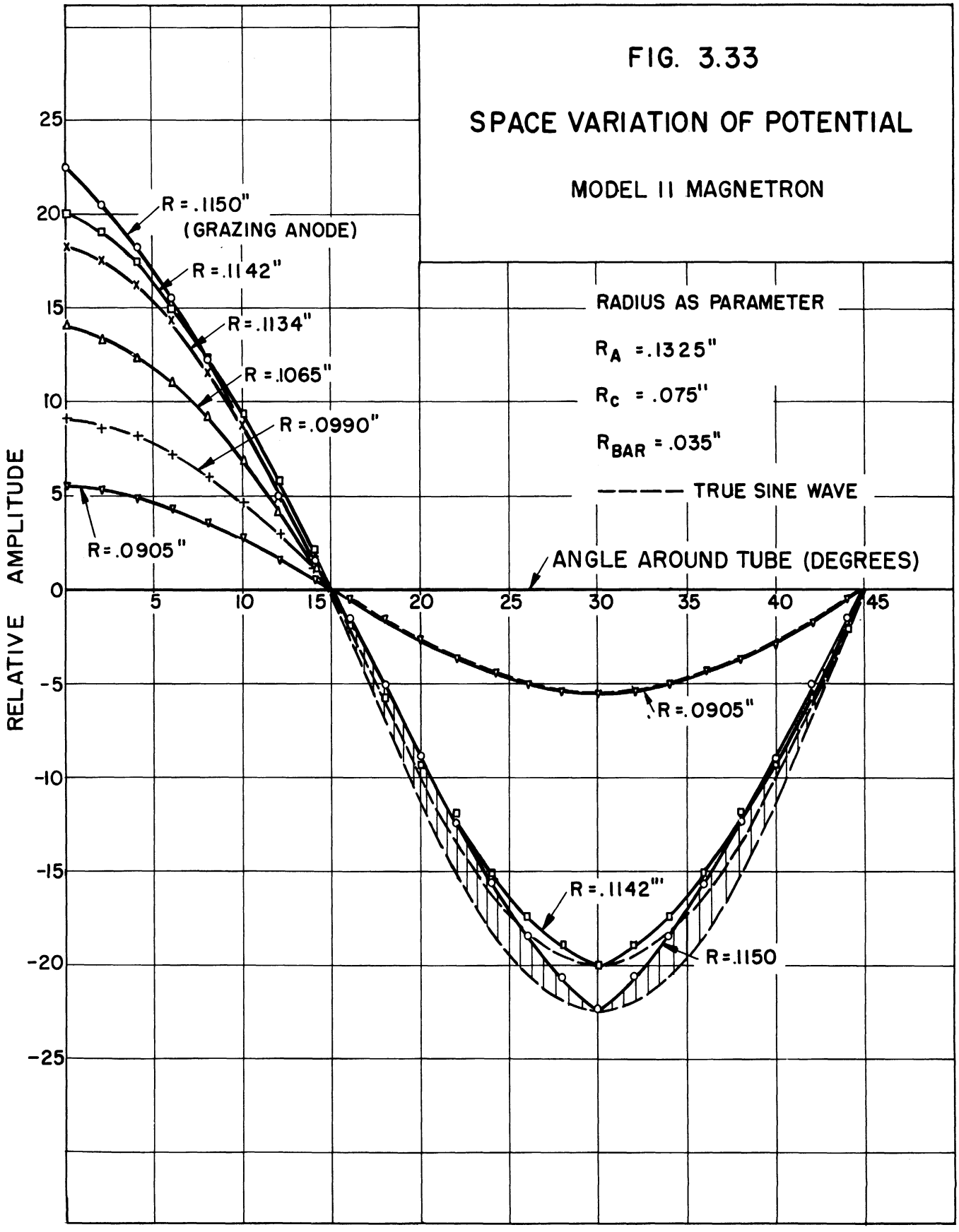
FIG. 3.33
SPACE VARIATION OF POTENTIAL
MODEL II MAGNETRON
RADIUS AS PARAMETER
R_A = .1325"
R_C = .075"
R_{BAR} = .035"
TRUE SINE WAVE
R = .1150" (GRAZING ANODE)
R = .1142"
R = .1134"
R = .1065"
R = .0990"
R = .0905"
ANGLE AROUND TUBE (DEGREES)
RELATIVE AMPLITUDE
25
20
15
10
5
0
-5
-10
-15
-20
-25
5
10
15
20
25
30
35
40
45
R = .0905"
R = .1142"
R = .1150

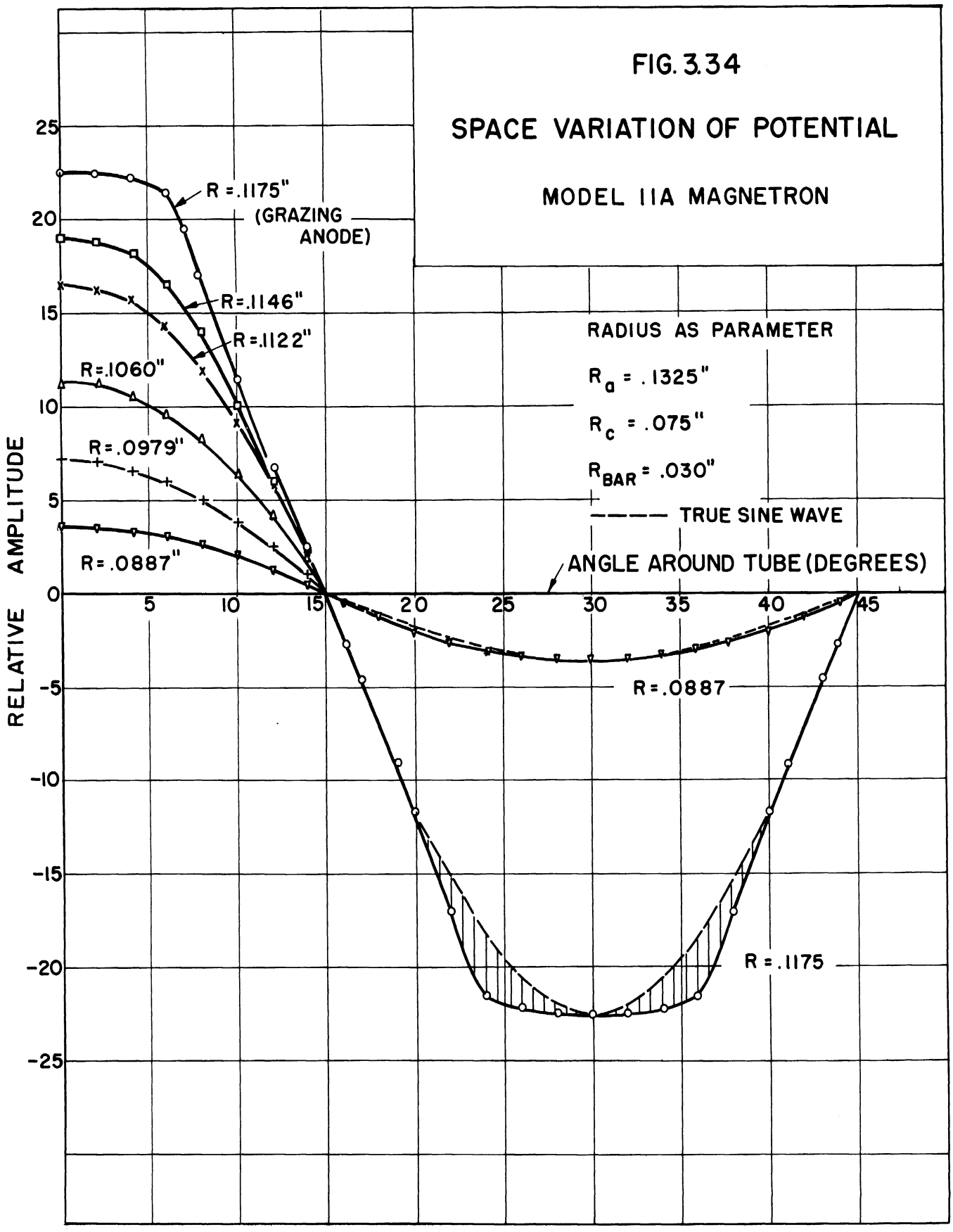
FIG. 3.34
SPACE VARIATION OF POTENTIAL
MODEL IIA MAGNETRON
RADIUS AS PARAMETER
R_a = .1325"
R_c = .075"
R_{BAR} = .030"
TRUE SINE WAVE
R = .1175" (GRAZING ANODE)
R = .1146"
R = .1122"
R = .1060"
R = .0979"
R = .0887"
ANGLE AROUND TUBE (DEGREES)
RELATIVE AMPLITUDE
25
20
15
10
5
0
-5
-10
-15
-20
-25
5
10
15
20
25
30
35
40
45
R = .0887
R = .1175

structures on resistive paper, and using metal foil for the tube elements. A dc voltage is applied between the anode segments and the cathode is maintained at a potential midway between the anode bars (representing a balanced cathode condition). Point-by-point readings are then made to determine the equipotential curves. These curves then represent the space distribution of potential in the tube, since the space distribution is not a function of time but only of the geometry of the tube structure. Fig. 3.33 shows the space potential distribution in the Model 11 with the radius as a parameter. Figure 3.34 shows similar data for the Model 11A.

The round anode structure has lower field intensity in the interaction region than the square anode structure. A lower electronic efficiency would therefore be expected for the round anode structure.

The significance of these data will be discussed in more detail in a later section.

3.9 Diode Characteristics

Unsuccessful attempts were made to measure the cathode temperature required to shift the mode of operation of the tube from a coherent signal to a noise signal output. Diode measurements were then made to obtain qualitative determination of the conditions at the cathode which were optimum for voltage-tunable operation. Figures 3.35 and 3.36 show the diode characteristics for Model 11A and Model 11B respectively.

Figure 3.23 shows that the maximum anode current for the Model 11A, No. 90 tube was approximately 8 ma. Figure 3.35 shows that when this tube is operated as a diode, its thoriated tungsten cathode is capable of supplying up to approximately 25 ma at a filament current of 8.6 amperes before temperature limitation sets in. Figure 3.15 indicates that the

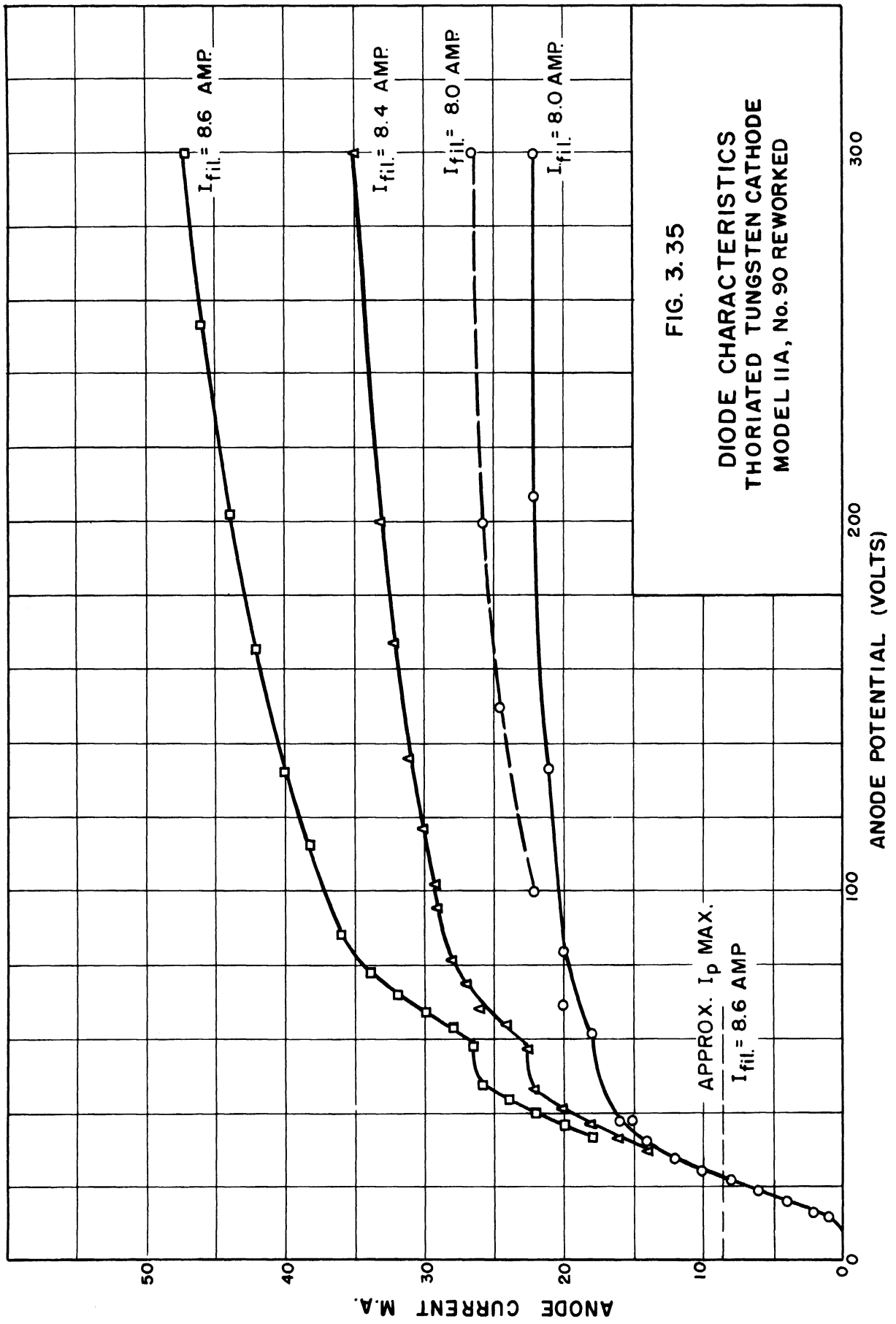
FIG. 3.35
DIODE CHARACTERISTICS
THORIATED TUNGSTEN CATHODE
MODEL IIA, No. 90 REWORKED
$I_{fil.}$ = 8.6 AMP.
$I_{fil.}$ = 8.4 AMP.
$I_{fil.}$ = 8.0 AMP.
$I_{fil.}$ = 8.0 AMP.
APPROX. I_p MAX.
$I_{fil.}$ = 8.6 AMP
ANODE CURRENT M.A.
ANODE POTENTIAL (VOLTS)
0
10
20
30
40
50
100
200
300

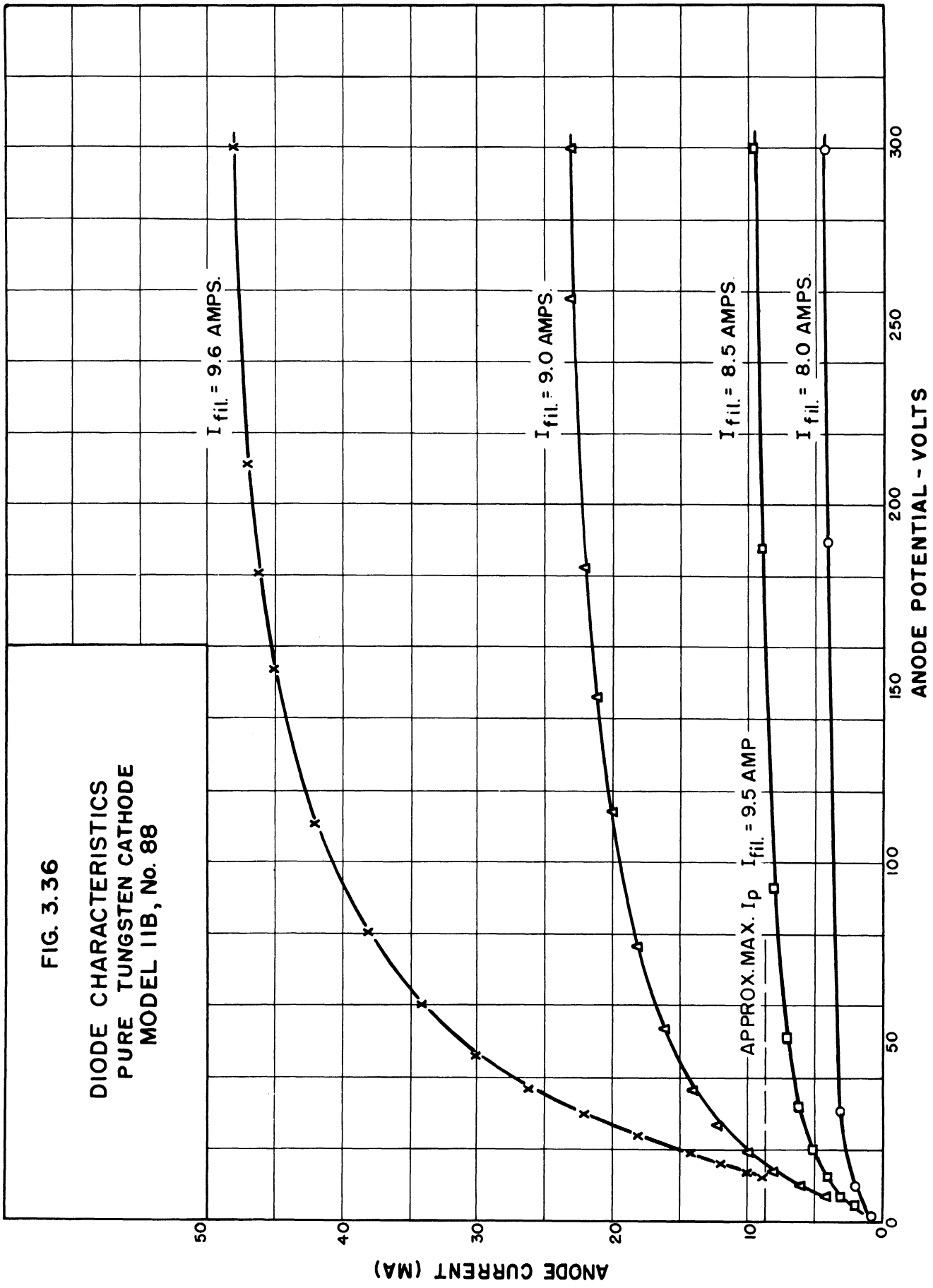
FIG. 3.36
DIODE CHARACTERISTICS
PURE TUNGSTEN CATHODE
MODEL 11B, No. 88
$I_{fil.}$ = 9.6 AMPS.
$I_{fil.}$ = 9.0 AMPS.
$I_{fil.}$ = 8.5 AMPS
$I_{fil.}$ = 8.0 AMPS.
APPROX. MAX. I_p $I_{fil.}$ = 9.5 AMP
ANODE CURRENT (MA)
ANODE POTENTIAL - VOLTS
0
10
20
30
40
50
0
50
100
150
200
250
300

anode current of the Model 11B, No. 88 was less than 9 ma over most of the operating range. Figure 3.36 shows that when No. 88 is operated as a diode, its pure tungsten filament can supply up to approximately 25 ma with a filament current of 9.6 amperes before temperature limitation occurs. From these data it is seen that for best voltage-tunable operation the cathode must operate at a temperature which could be expected to produce approximately three times the actual tube current if the tube were to be operated as a diode. This 3 to 1 ratio for voltage-tunable operation is in contrast to a ratio of from 5 or 10 to 1 for the diode current over the actual tube current in high-Q magnetron operation (Ref. 16).

These results would seem to indicate that there should be considerable space charge in the sub-synchronous swarm since there are apparently more electrons emitted than ever reach the anode, and would also indicate that it may not be necessary for the field to be zero at the cathode for voltage-tunable operation. However, when it is considered that the current at the anode is limited by the width of the space charge spokes, it becomes apparent that the diode current would be considerably greater than the tube current when operating as an oscillator. It is thus conceivable that the portion of the cathode which emits electrons in the proper phase for transmission to the anode may be operating under temperature limited conditions.

3.10 Summary of Experimental Results

The results of the experimental work performed during this investigation may be summarized as follows:

1. A voltage-tunable magnetron which operates in the frequency range 2000 to 3000 mc and delivers 100 mw or more of usable power has been built and tested. A voltage-tunable power output of 2 to 4 watts was obtained over a limited frequency range.
2. This tube has been used as a local oscillator in an S-band spectrum analyzer, and found to be quite satisfactory for this application. The noise content in the signal output under optimum conditions compares favorably with that of a klystron.
3. The operation of this tube as a voltage-tunable magnetron is quite sensitive to the cathode temperature (cathode temperature was found to affect the stability of operation, and an increase in cathode temperature was found to cause a decrease in magnetron frequency). Stable operation may be obtained at a single frequency with very little difficulty. However, for spot cw tuning, readjustment of the cathode input power may be necessary. When the anode voltage is modulated, the frequency may be varied as much as 800 mc with a signal output which is free of noise. The operation is more stable when the anode voltage is being modulated.
4. It has been shown that the external circuit characteristics are critical if a wide range of voltage tuning is to be achieved. A circuit which possesses the necessary characteristics for voltage-tunable operation has been developed and tested with this tube.

5. Voltage-tunable operation is improved if the anode bars are shaped in such a manner that the space harmonics in the interaction space are decreased. In this case, round anode bars were used and results show these to be more effective than square anode bars for coherent voltage-tunable operation.

6. A ratio of r_c/r_a greater than the value normally used in conventional high-Q magnetrons was found to produce a significant increase in the electronic efficiency of a voltage-tunable magnetron. The ratio of r_c/r_a for the Model 11 is .6; this value was increased to .75 for the Model 11B by decreasing the anode diameter.

CHAPTER 4

DISCUSSION OF EXPERIMENTAL RESULTS

4.1 Introduction

In this chapter a qualitative analysis of the mode of operation of the voltage-tunable magnetron is given. Experimental data are correlated with existing theory wherever possible, and additional theory is proposed in an attempt to explain phenomena which have not been previously observed or adequately explained.

The character of the rf circuit impedance, including cathode support and filament leads is discussed. The decrease in the power output at certain frequencies is correlated with resonances in the cathode support and filament lead structures. These resonances reduce the total shunt impedance of the rf circuit. The power output of the magnetron is shown to be very closely related to this shunt impedance, the power being a minimum when the shunt impedance is a minimum.

The results of the experimental investigation using several types of cathodes are discussed. The operation of the Model 11 magnetrons is sensitive to the temperature of the cathode in all cases. An oxide-coated cathode was found unsatisfactory for use in the Model 11 voltage-tunable magnetrons. A cathode consisting of a pure tungsten helix gave

most satisfactory operation. Diode characteristics for a thoriated tungsten and a pure tungsten cathode are discussed.

The design of the interaction space in the Model 11, Model 11A and Model 11B magnetrons is discussed. The improvement in the voltage-tunable operating characteristics of the Model 11B magnetron over that of the Model 11A are discussed. This improvement is attributed to a smaller value of anode-to-anode capacitance and the use of round anode bars in the Model 11B. The importance of the anode-to-anode capacitance in determining the operating characteristics of a voltage-tunable magnetron is discussed.

The space charge behavior in the Model 11 voltage-tunable magnetrons is discussed. A theoretical voltage-tuning equation for a magnetron is derived and the experimental data are compared with this theoretical equation. It is proposed that the very low electron interaction efficiencies obtained in the Model 11 magnetrons may be due to the electrons arriving at the anode with considerable radial energy. It is also proposed that the sensitivity of the Model 11 magnetron operation to cathode temperature may be attributed primarily to the low impedance which the anode and cavity structure presents to the electron stream.

4.2 Characteristics of Circuit Impedance

The various circuit components which affect the operation of the magnetron were discussed in Section 2.7. An examination of Eq 2.11.

$$Y_T' = \frac{2}{Z_\omega} + j\omega C_p + \frac{1}{Z_f} \qquad (2.11)$$

shows that all of the components considered are more or less frequency

sensitive. The first term on the right side of Eq 2.11 represents the admittance due to the ridge-waveguide structure and is assumed to be a pure conductance. The magnitude of this conductance is a function of frequency (Fig. 2.2). The second term on the right is the susceptance due to the anode-to-anode capacitance. Results of measurements on the cavity and a dummy tube verify the assumption that the total admittance, due to these first two terms, varies slowly over the frequency range in which the tube is operated. A plot of the impedance for the cavity and dummy tube is shown in Fig. 3.30.

The third term on the right in Eq 2.11 is the admittance due to the arrangement of the cathode circuit as described in Section 2.7. The lumped-constant equivalent circuit for the cathode is shown in Fig. 2.16. The exact expression for Z_f is complex since Z_1, Z_2, and Z_c are complex quantities. Z_2 and Z_c probably can be approximated very closely by assuming them to be pure reactances. The values of C_1, C_2, and Z_1 can be determined approximately. The operation of the magnetron will be adversely affected when Z_f is a minimum, corresponding to a series resonance of the circuit shown in Fig. 2.16. Since Z_f is a complex quantity its value will not reach zero but will pass through a minimum. It is to be expected that a decrease in the power output of the magnetron will occur at the frequency at which Z_f is a minimum. An examination of the power output vs frequency curves for all tubes tested shows that a minimum in the power output occurs at approximately 2600 mc. Figure 3.19 shows power output vs. frequency for the Model 11B No. 92. The lower curve was obtained with no choke on the cathode support. A choke was improvised from a piece of aluminum foil and placed on the cathode support producing the result shown in the top

picture. These results indicate that the sharp decrease in power output is due to the loading of the cathode circuit. The frequency of the power minimum shown in Fig. 3.19 is in the order of 2600 mc. Since the effect on magnetron operation is due to a combination of the cathode support and the filament leads, changing either Z_2 or Z_c will affect the value of Z_f and, therefore, the power output of the tube.

Figure 4.1 shows the value of the input reactance vs frequency for the open sections of transmission line formed by the cathode support and pole pieces, and by the filament leads. The length of the coaxial line formed by the cathode support and pole piece is 3.8 cm. From Fig. 4.1 we see that Z_c will have a positive reactance of approximately 16 ohms at 2600 mc (Z_o = 39 ohms). The approximate range of operation of the magnetron is indicated in Fig. 4.1. Recent studies of the cathode circuit problem (Ref. 28) show that a wide band coaxial filter can be built into the cathode support structure to eliminate the resonance effects of this line over a wide range of frequencies.

The length of the coaxial line formed by the filament leads is approximately 12 cm. The variation of the impedance of this line over the range of operation is indicated in Fig. 4.1. Theoretically, broad-band filters could be built into the coaxial filament lead to eliminate the loading due to this line; practically, this is difficult because of the very small spacings involved. If the emitting surface between end hats on the cathode consists of a solid cylinder, then the filament line will have no effect on the operation of the tube. The most common type of cathode of this form is the oxide-coated cathode; however, experience has shown that this type of cathode is unsatisfactory for good voltage-tunable operation. A possible solution would

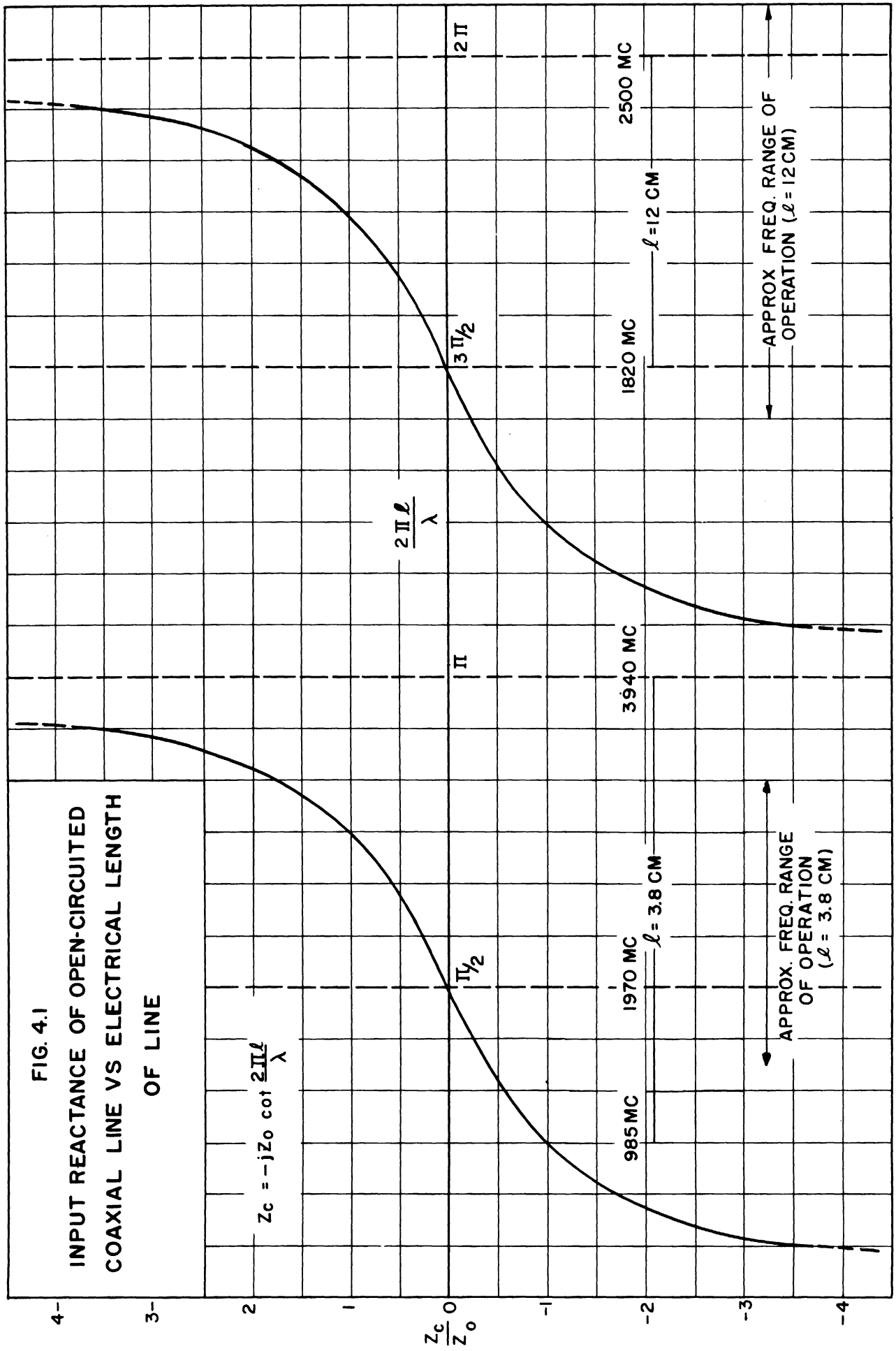
FIG. 4.1
INPUT REACTANCE OF OPEN-CIRCUITED COAXIAL LINE VS ELECTRICAL LENGTH OF LINE
$Z_c = -jZ_o \cot \frac{2\pi\ell}{\lambda}$
$\frac{Z_c}{Z_o}$
$\frac{2\pi\ell}{\lambda}$
$\pi/2$
π
$3\pi/2$
2π
985 MC
1970 MC
3940 MC
1820 MC
2500 MC
ℓ = 3.8 CM
ℓ = 12 CM
APPROX. FREQ. RANGE OF OPERATION (ℓ = 3.8 CM)
APPROX FREQ. RANGE OF OPERATION (ℓ = 12 CM)

be to use a pure tungsten cylinder. This cylinder might be heated indirectly by an internal helix; this, however, would require a high-current, high-temperature helix and, consequently, short cathode life. Another possibility would be to heat the tungsten cylinder by bombardment from a coaxial oxide-coated cathode. This would require the existence of a d-c potential between the tungsten cylinder cathode and the inner oxide-coated cathode. This arrangement would seem to satisfy the conditions for good voltage-tunable operation; however, the cathode would be more complicated to construct and would require an additional power supply to operate the tube.

Further work is needed on the cathode circuit to improve the uniformity of the power output of the Model 11 tubes.

4.3 The Cathode

Experience has shown that an oxide-coated cathode is unsatisfactory for coherent voltage-tunable operation of the Model 11 magnetrons. It has been possible to obtain coherent voltage-tunable operation using oxide cathodes; however, the mode of operation was very sensitive to the cathode temperature. The operation of the tube was unstable due to the backheating of the cathode. This backheating caused the mode of operation to shift to such an extent that the output signal changed from a coherent signal to a noise signal output. The noise signal could be voltage-tuned over approximately the same frequency range as the coherent signal. It was impossible to test the tubes which used oxide cathodes under cw operating conditions as the backheating was sufficient to cause the cathode temperature to "run away" even with no external filament power being supplied.

In order to overcome this difficulty in controlling the cathode temperature, a cathode using a thoriated tungsten helix as the emitter was designed. This cathode operates at a much higher temperature than the oxide cathode, 1750 degrees centigrade as compared to 850 degrees for the oxide cathode. It consequently requires greater heater power, considerably in excess of the backheating power, and thus allows control of the cathode temperature during cw operation of the tube. Good voltage-tunable operation was obtained with both the Model 11 and Model 11B magnetrons using thoriated tungsten cathodes. The operation was still sensitive to the cathode temperature; however, stable conditions could be obtained under which a coherent signal output was produced. The operation was more stable when the anode voltage was being modulated than when the anode voltage was operated at a fixed value.

A pure tungsten cathode which operates at approximately 2200 degrees centigrade was found to be most suitable for voltage-tunable operation if coherent signal output is desired. The operation of the magnetron is sensitive to the temperature of the cathode; however, the filament input power can be adjusted to give stable coherent operation.

The improvement in voltage-tunable operation of the magnetron with the use of a pure tungsten cathode is attributed to the fact that more filament power is required for the pure tungsten cathode than either the thoriated tungsten or oxide cathodes. This increase in filament power makes the operation of the tube relatively insensitive to backheating of the cathode. Therefore, once the cathode

temperature has been adjusted to the optimum value for voltage-tunable operation, a change in the backheating power does not seriously affect the operation of the tube.

Figures 3.35 and 3.36 show the diode characteristics for a thoriated tungsten and a pure tungsten cathode. The approximate maximum magnetron anode current is indicated in each case. It was suggested in Section 1.3 that the spokes of space charge will be in the order of 90 degrees wide, but may be as wide as 180 degrees. Thus, if only one-third of the cathode is effective in supplying the magnetron anode current, the anode current indicated in Figs. 3.35 and 3.36 corresponds to an operating point at approximately the knee of the diode characteristic curve. Even though for the small-signal case there may not be well-defined spokes, anode current can only be collected in the oscillating magnetron over a small portion of the rf cycle. Thus, it is impossible to determine from presently available data the exact operating conditions at the cathode for voltage-tunable operation. It has been determined experimentally that the mode of operation is sensitive to the cathode temperature and that the magnetron anode current varies with the temperature of the cathode. This change in the amplitude of the magnetron anode current could be due to a change in the mode of operation or to temperature-limited emission at the cathode. The experimental data do not definitely prove that the emission at the cathode is temperature-limited; however, they do agree with the results which would be predicted from the above argument, assuming temperature-limited emission.

4.4 The Design of the Interaction Space

The design of the interaction space of the Model 11 magnetron was based on the assumption that a small anode-to-anode capacitance was necessary for good voltage-tunable operation. It was also assumed that voltage-tunable operation would be improved if the anode bars were shaped in such a manner that the space, or Hartree, harmonics in the interaction space were reduced. The ratio of r_c/r_a was determined by the empirical formula

$$\frac{r_c}{r_a} = \frac{N - 4}{N + 4}$$

and from knowledge of known workable magnetrons. It has been pointed out in Section 2.4 that the design of the cavity and the design of the interaction space were interdependent, and it was assumed that for the electrode design chosen a circuit impedance of the order of 100 to 200 ohms would be necessary if satisfactory voltage-tunable operation was to be achieved. It has been shown experimentally that the cavity shown in Fig. 2.3 satisfies this requirement over a wide range of frequencies.

The Model 11 magnetron was designed using round anode bars and a ratio of r_c/r_a of 0.6. When a pure tungsten cathode was used, this tube operated quite satisfactorily as a voltage-tunable tube with power outputs in the order of 20 milliwatts. A tuning range in the order of 1000 mc was achieved. With the Model 11B magnetron, which is identical to the Model 11 except for differing r_c/r_a ratios (r_c/r_a ratio is .6 in the Model 11 and is .75 in the Model 11B), power outputs in the order of 250 milliwatts was obtained. The tuning range and stability of operation remained unchanged.

The Model 11A magnetron is approximately the same as the Model 11 except that square, rather than round, anode bars are used. This tube gave power outputs in the same order of magnitude as the Model 11; i.e., about 20 milliwatts. However, the voltage-tuning range was limited, and the output signal was more noisy than for the Model 11 or Model 11B. The operation of the tube was more sensitive to the temperature of the cathode.

From this data it is concluded that the shape of the anode bars has a pronounced effect on the operation of a low Q voltage-tunable magnetron. The operation of the Model 11 voltage-tunable magnetrons is much more satisfactory when round, rather than square, anode bars are used. Also, the operation of the voltage-tunable magnetron is improved if the r_c/r_a ratio is increased over the value which is normally used in conventional magnetrons. In this case, a value of 0.75 was used, where standard practice indicates a value of 0.6. There is no conclusive evidence that 0.75 is the optimum value; however, it is doubtful if much can be gained by increasing this ratio further. The present improvement in operation may be attributed to the deeper penetration of the rf field into the interaction space near the cathode. This would improve the phase focussing and thus increase electron interaction efficiency. Since only two values of r_c/r_a have been tried, it will require further experimental work to determine the optimum r_c/r_a value for low-Q voltage-tunable magnetrons.

The value of the impedance presented by the cavity shown in Fig. 2.3 is of the order of 80 ohms. Good voltage-tunable operation is obtained with this cavity; however, the efficiency of operation is low, less than 5 per cent. It is believed that a low-Q circuit with

an impedance of 400 to 600 ohms would allow voltage-tunable operation at a much higher efficiency. The impedance level of a non-resonant circuit is limited by the reactance of the anode-to-anode capacitance. For the Model 11 magnetrons this reactance is approximately 60 ohms at 2500 mc. Thus the anode-to-anode capacitance causes the impedance which the electrons "see" to be reduced considerably from the characteristic impedance of the waveguide. This capacitance causes the impedance to decrease with frequency. The upper limit in frequency of operation is determined by the value of this capacitance. Any reduction in this capacitance should improve the electronic efficiency of the Model 11 magnetrons.

It should be pointed out that although the nominal dimensions of the interaction space in the Model 11A and 11B tubes are similar, the values of the anode-to-anode capacitance is different for the two tubes, being less for the Model 11B. Thus some of the improvement in operating characteristics of the Model 11B over the Model 11A may be due to the smaller value of anode-to-anode capacitance and not all due to a reduction in the higher space harmonics resulting from use of round anode bars. However, the use of round anode bars also results in a lower value of anode-to-anode capacitance.

Further experimental work is necessary to determine which of the factors, reduction in capacitance or reduction in space harmonics, is the most significant in improving the operation of the Model 11B magnetrons.

4.5 Space-Charge Behavior

4.5.1 Theoretical Voltage-Tuning Equation for a Magnetron.

The characteristics of the magnetron which are related to the space-charge behavior are discussed in this section. In order to compare the voltage-tuning characteristics of all tubes, an equation describing the frequency-anode voltage characteristic for voltage-tunable magnetrons is derived. This equation is arranged in nondimensional form so that all experimental data can be compared with the theoretical expression by using a graphical presentation. This derivation is based on the equations for the high-Q magnetron; however, the results obtained should approximately describe the behavior of the low-Q voltage-tunable magnetron.

From Appendix A we have the following expressions:

$$E_H = B\frac{\omega_n}{2} r_a^2 \left(1 - \frac{r_c^2}{r_a^2}\right) - \frac{1}{2}\left(\frac{m}{e}\right) r_a^2 \omega_n^2 \quad \text{(Hartree equation)} \qquad \text{(A-31)}$$

$$E_U = \frac{B^2 e}{8m} r^2 \left(1 - \frac{r_c^2}{r_a^2}\right)^2 \quad \text{(Hull cutoff potential)} \qquad \text{(A-10)}$$

$$B_o = \frac{2\frac{m}{e}\omega_n}{\left(1 - \frac{r_c^2}{r_a^2}\right)} \qquad \text{(A-21)}$$

$$E_o = \frac{m}{2e} r_a^2 \omega_n^2 \quad \text{(synchronous energy equation)} \qquad \text{(A-18}$$

$$\frac{E_H}{E_o} = \frac{2B}{B_o} - 1 \quad \text{(normalized Hartree equation)} \qquad \text{(A-32)}$$

Solving Eq A-32 for B we obtain,

$$B = \frac{1}{2} B_o \left(1 + \frac{E_H}{E_o} \right) \tag{4.2}$$

Substituting Eq A-21 and A-18 for B_o and E_o in Eq 4.2 there results

$$B = \frac{\frac{m}{2e} r_a^2 \omega_n^2 + E_H}{\frac{1}{2} r_a^2 \omega_n \left(1 - \frac{r_c^2}{r_a^2} \right)} \tag{4.3}$$

If we now substitute Eq 4.3 for B in Eq A-31 and A-10, and divide Eq A-10 into A-31 then, after rearranging terms, we obtain

$$\frac{E_H}{E_u} = \frac{E_H r_a^4 \omega_n^2}{\frac{m}{8e} r_a^2 r_a^4 \omega_n^4 \frac{r^2 r_a^2 \omega_n^2 E_H}{2} + \frac{E_H^2 er^2}{2m}} \tag{4.4}$$

or

$$\omega_n^4 = \left(\frac{m}{8e} r^2 r_a^4 \right) + \left(\frac{r^2 r_a^2 E_H}{2} - E_u r_a^4 \right) \omega_n^2 + \frac{E_H^2 er^2}{2m} \tag{4.5}$$

Solving for ω_n^2, we obtain

$$\omega_n^2 = \frac{-\left(\frac{r^2 r_a^2 E_H}{2} - E_u r_a^4 \right) \pm \left[\left(- \frac{r^4 r_a^4 E_H^2}{4} \right) + \left(\frac{r^2 r_a^2 E_H}{2} - E_u r_a^4 \right)^2 \right]^{1/2}}{\frac{m}{4e} r^2 r_a^4} \tag{4.6}$$

If we assume $r = r_a$, after rearranging terms we obtain,

$$\omega_n^2 = \frac{E_u \left(1 - \frac{E_H}{2E_o} \right) \pm E_u \left(1 - \frac{E_H}{E_u} \right)^{1/2}}{\frac{m}{4e} r_a^2} \tag{4.7}$$

We now define f_o by the following equation,

$$E_u = \frac{m}{2e}\left(r_a^2\right)\frac{4\pi f_o^2}{n^2} \tag{4.8}$$

That is, frequency f_o will be generated by an electron at the anode with a tangential energy of E_u. If we now substitute Eq 4.8 into Eq 4.7 for E_u, and substitute $2\pi f/n$ for ω_n, there results,

$$\frac{f^2}{f_o^2} = 2\left(1 - \frac{E_H}{2E_u}\right) \pm 2\left(1 - \frac{E_H}{E_u}\right)^{1/2} \tag{4.9}$$

In all cases of interest,

$$f \ll f_o \qquad \text{and}$$

$$E_H \ll E_u$$

therefore we need consider only the negative sign in Eq 4.9. We now have for Eq 4.9

$$\frac{f^2}{f_o^2} = 1 - 2\sqrt{1 - \frac{E_H}{E_u}} + \left(1 - \frac{E_H}{E_u}\right) \tag{4.9a}$$

and therefore

$$\frac{f}{f_o} = \left[1 - \sqrt{1 - \frac{E_H}{E_u}}\right] \tag{4.10}$$

4.5.2 Comparison of Experimental Results with Theoretical Curves. Figure 4.2 shows a plot of Eq 4.10. This can be described as a universal voltage-tuning curve for a magnetron. Equation 4.10 expresses the relation between f/f_o and E_H/E_u for all mode numbers n. f_o is a characteristic frequency defined by Eq 4.8. Both E_H and f_o

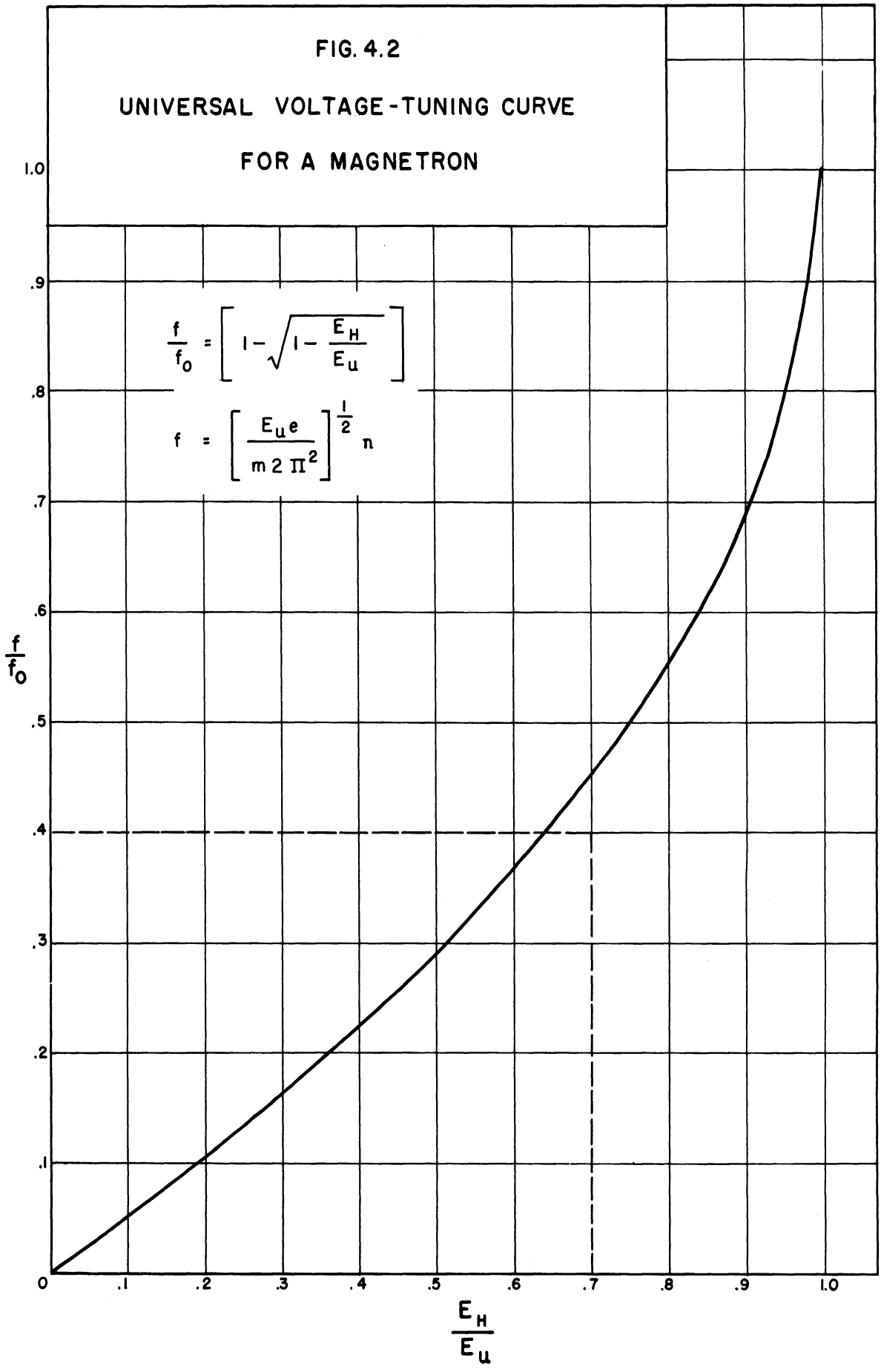
FIG. 4.2
UNIVERSAL VOLTAGE-TUNING CURVE
FOR A MAGNETRON
$\frac{f}{f_0} = \left[1 - \sqrt{1 - \frac{E_H}{E_u}}\right]$
$f = \left[\frac{E_u e}{m 2 \pi^2}\right]^{\frac{1}{2}} n$
$\frac{f}{f_0}$
$\frac{E_H}{E_u}$
0
.1
.2
.3
.4
.5
.6
.7
.8
.9
1.0

are functions of the mode number n; therefore, for quantitative comparison of experimental data, the correct value of n must be used.

In Fig. 4.3 typical data for the Model 11, 11A, and 11B magnetrons are plotted for comparison with the theoretical curve of Fig. 4.2. The experimental data for f/f_o has been plotted vs E_a/E_u, where f is the operating frequency and E_a the anode potential. The π-mode of operation has been assumed in presenting the experimental data in Fig. 4.3. It should be noted that the portion of the theoretical voltage-tuning curve shown in Fig. 4.3 is that portion within the area enclosed by the dashed lines in Fig. 4.2. This shows that all tubes tested operated in a region where the theoretical tuning curves were essentially linear. As shown in Fig. 4.3, all experimental voltage-tuning curves were linear with anode voltage. It can be seen from Fig. 4.3 that when the π-mode of operation was assumed, the operating anode voltage was greater than the Hartree voltage corresponding to the operating frequency for all models of the tube. The greatest deviation from the theoretical voltage-tuning curve was shown by the Model 11B tubes.

The voltage-tuning characteristics of the Model 11B No. 112 are shown in Fig. 4.4. The experimental results are discussed in Section 3.3. The data for the main mode of operation are plotted for three different assumed values of n; 3, 4, and 6. The data for the two spurious modes referred to in Section 3.3.3 are plotted with the value of n which agrees most closely with the theoretical curve. From Fig. 4.4 it can be seen that for n = 6 there is a constant relative discrepancy between the theoretical and experimental data; E_a is approximately 1.63 as large as the corresponding value of E_H.

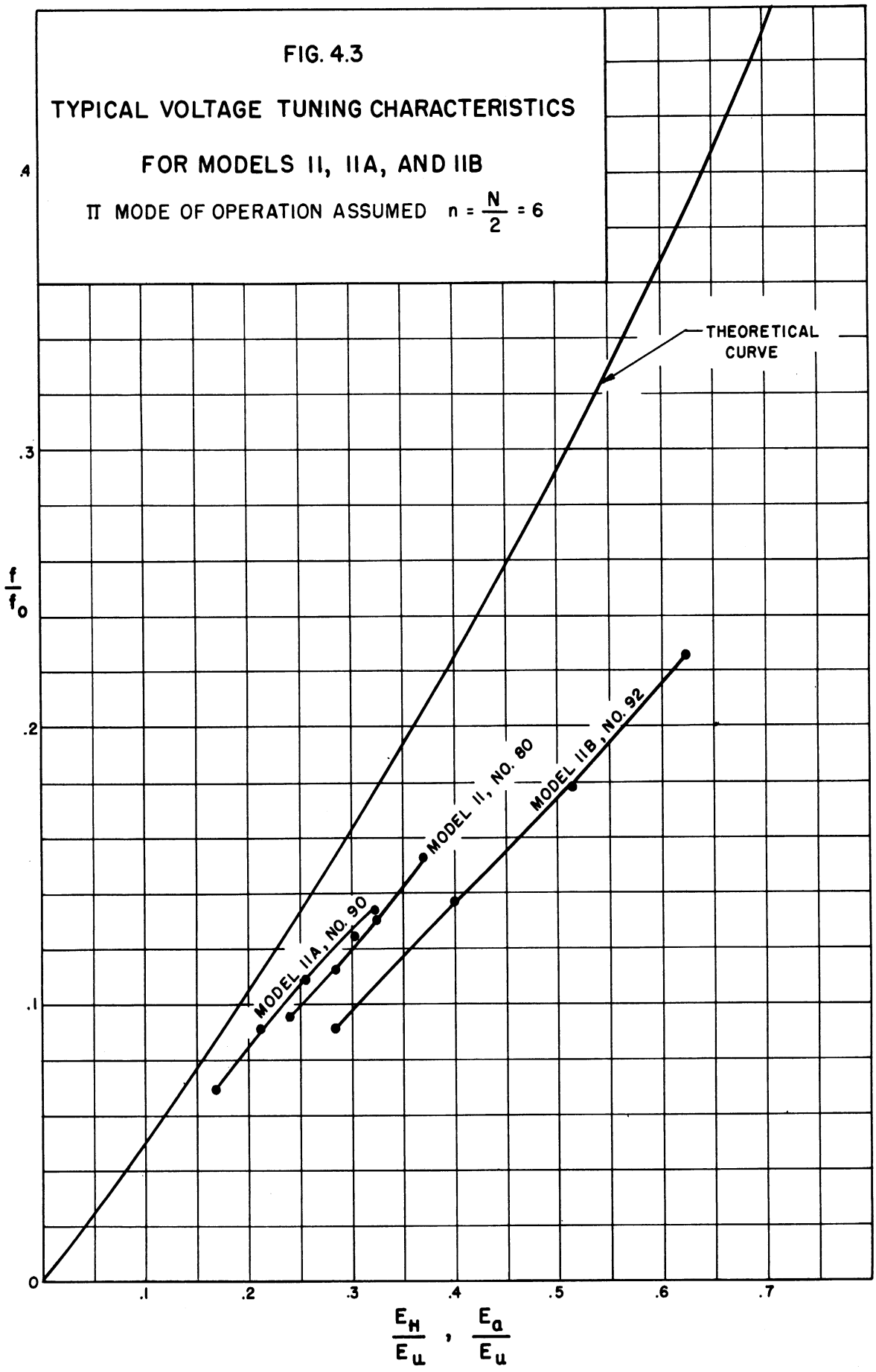
FIG. 4.3
TYPICAL VOLTAGE TUNING CHARACTERISTICS
FOR MODELS II, IIA, AND IIB
π MODE OF OPERATION ASSUMED n = N/2 = 6
THEORETICAL CURVE
MODEL IIA, NO. 90
MODEL II, NO. 80
MODEL IIB, NO. 92
f/f0
.4
.3
.2
.1
0
.1
.2
.3
.4
.5
.6
.7
EH/Eu , Ea/Eu

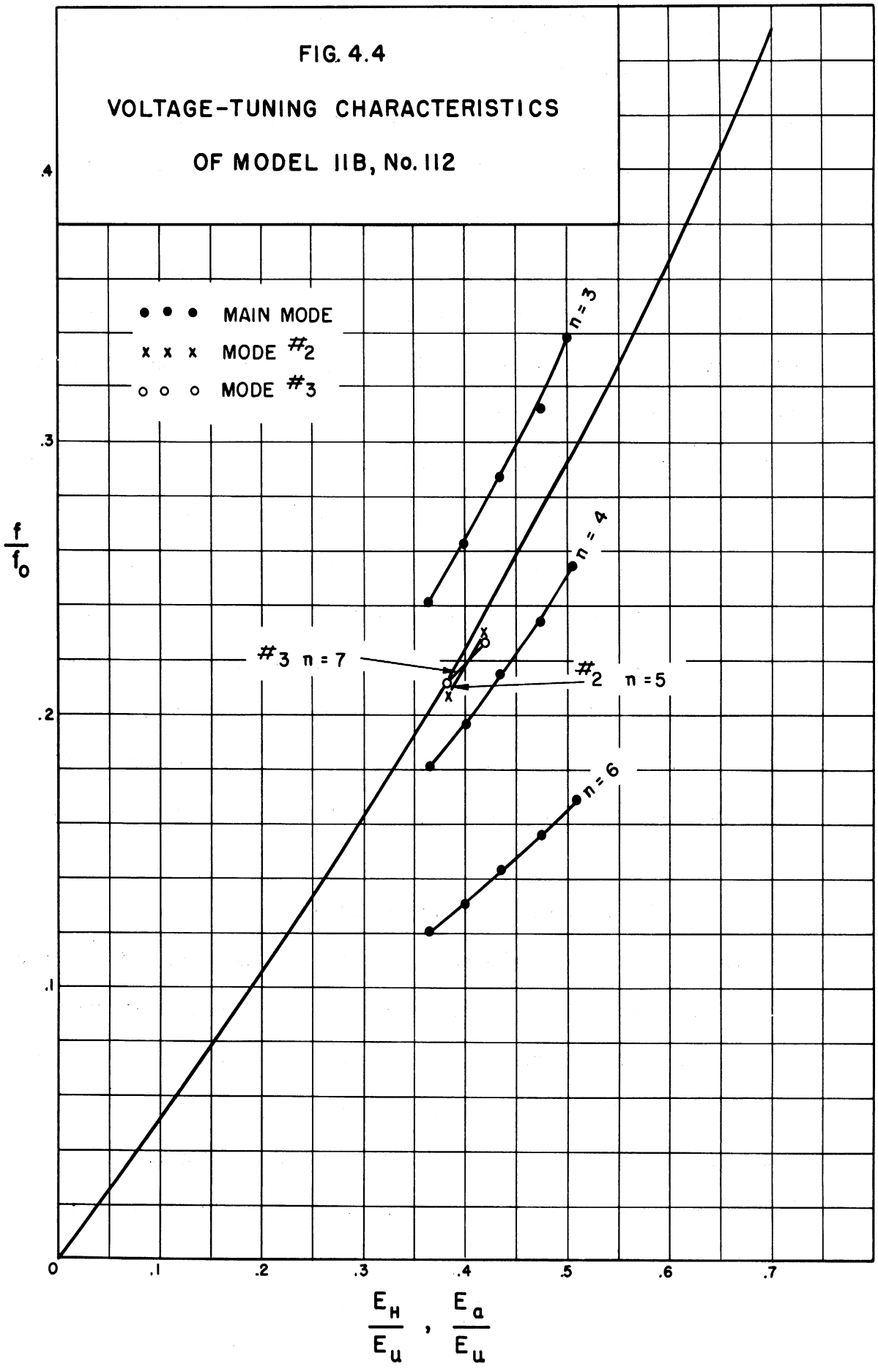
FIG. 4.4
VOLTAGE-TUNING CHARACTERISTICS
OF MODEL IIB, No. 112
MAIN MODE
MODE #2
MODE #3
n=3
n=4
n=5
n=6
#3 n=7
#2
f/f0
EH/Eu , Ea/Eu
0
.1
.2
.3
.4
.5
.6
.7

4.5.3 Radial Energy of the Electron. It was assumed that the Model 11 magnetron would operate in the π-mode. Rotating-probe measurements on this tube and its associated cavity structure show that with an rf voltage applied to one of the output terminals of the cavity, a π-mode voltage distribution does exist on the anode bars. The following explanation for the discrepancy between the experimental and theoretical voltage-tuning characteristics is proposed. This explanation is based on the assumption that, (1) the electrons arrive at the magnetron anode with considerable radial energy, and (2) the cathode is temperature-limited. These assumptions are consistent with the experimentally observed facts; (1) the efficiency is very low (order of 3 per cent), (2) the anode voltage is always greater than the Hartree voltage would predict (assuming π-mode of operation), (3) the operation is sensitive to cathode temperature, and (4) anode current varies with filament current. There was also experimental evidence that heating of the glass envelope was due to electrons with high radial velocities passing between the anode bars and striking the glass.

Consider Fig. 4.5 which shows the energy relations in a planar magnetron. Planar geometry is assumed in this discussion because the equations expressing the energy relations are simpler than those for the cylindrical magnetron and thus much easier to work with. Any conclusions arrived at by this analysis may be applied to the cylindrical magnetron with very little error, particularly for magnetrons with large values of r_c/r_a. The cutoff energy parabola for the planar magnetron is given by the following equation

$$E_{co} = \frac{B^2 e}{2m} y^2 \qquad (4.11)$$

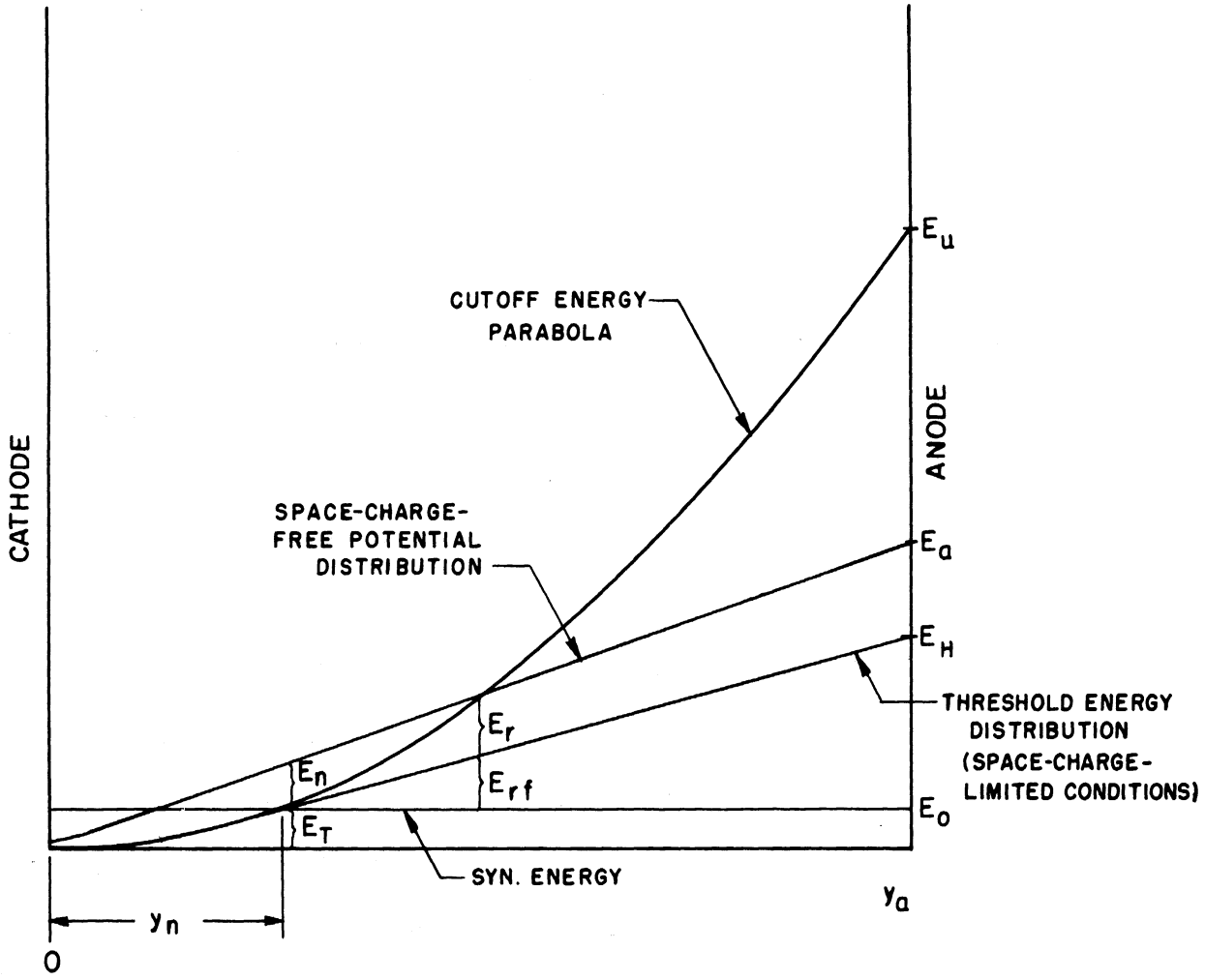

FIG. 4.5

ENERGY RELATIONS IN A PLANAR MAGNETRON

where y is the distance from the cathode. For $y = y_a$, the corresponding value of cutoff voltage has been labeled E_u in Fig. 4.5, corresponding to the Hull cutoff voltage in the cylindrical magnetron. Equation 4.11 is shown in Fig. 4.5, labeled cutoff energy parabola. The synchronous energy level is a constant, being proportional to the synchronous velocity (v_n) of the rf voltage wave. This value has been indicated in Fig. 4.5. If we assume that the electrons have no radial energy at the boundary of the synchronous swarm where synchronous velocity (v_n) is reached, then the boundary of this synchronous swarm is determined by the intersection of the cutoff energy parabola and the synchronous energy line as shown in Fig. 4.5. If the cathode is operated under space-charge-limited conditions the charge will build up within the synchronous swarm until the gradient at the cathode is zero.

It has been shown (Ref. 29) that for the case of zero potential gradient at the cathode, the actual potential distribution curve is tangent to the cutoff parabola at the swarm boundary. The anode potential required for establishing a swarm within the synchronous boundary y_n is determined by drawing a straight line tangent to the cutoff energy parabola at the intersection with the synchronous energy level. The straight line gives the potential distribution in the space-charge free region from y_n to the anode. The anode potential obtained by this method is shown in Fig. 4.5 as E_H, corresponding to the Hartree potential for the cylindrical magnetron. This voltage is given by the following expression (Ref. 16)

$$E_H = Bv_n y_a - \frac{1}{2}\frac{m}{e} v_n^2 \qquad (4.12)$$

This voltage must be exceeded before any electrons which are moving fast enough to deliver energy to the traveling wave exist in the interaction space. Since it is assumed that electrons arrive at the anode with zero radial velocity and synchronous energy equal to E_o, the energy transferred from the dc electric field to the rf field is the difference between E_H and E_o, indicated as E_{rf} in Fig. 4.5.

Now if we assume that the cathode is operating under temperature-limited conditions, the potential distribution may be as indicated by the curve OE_a in Fig. 4.5; this indicates that the potential gradient is no longer zero at the cathode. Since the electric field has been increased, ρ_c (the radius of the rolling circle which is used to depict the generation of the cycloidal motion of an electron in crossed electric and magnetic fields) has also been increased since

$$\rho_c = \frac{mE}{eB^2} \tag{4.13}$$

However, since v_x, the tangential velocity of the electron is a function of only B and y, in the absence of rf fields

$$v_x = \frac{e}{m}By \tag{4.14}$$

$$\text{for} \quad 0 < y < 2\rho_c$$

electrons will reach synchronous velocity at the same distance from the cathode as for the space charge limited case, $y = y_n$. In this case the electrons will possess considerable radial energy. Once synchronous velocity has been reached it will be possible for the electrons to interact with an rf field and transfer energy from the dc electric field to the rf field. In this manner the electrons may transfer some energy to the rf field and still reach the anode with considerable

radial energy. This would result in very low electron interaction efficiencies. This mode of operation would also result in higher operating voltages than are predicted by the Hartree relation.

4.5.4 Requirement for Temperature-Limited Operation of the Cathode. It has been shown in Section 1.3.3 that in order to obtain constant power in voltage-tunable operation it is necessary to operate the cathode under temperature-limited conditions. This is a very desirable characteristic for a voltage-tunable magnetron; however, this is not the compelling reason for operating the Model 11 magnetron cathode under temperature-limited conditions, this is necessary to obtain coherent signal output.

The sensitivity of the Model 11 magnetron operation to cathode temperature may be attributed primarily to the low impedance which the anode and cavity structure presents to the electron stream. Relatively large rf fields are required to produce effective bunching, and it is difficult to produce a sufficiently large voltage across an impedance of the order of 50 ohms (the approximate value of impedance presented to the electron stream by anode and cavity structure) to produce bunching. Since the bunching and production of the rf voltage are interdependent, the whole mechanism of phase focusing breaks down and a non-coherent signal is produced (for space-charge-limited conditions). For temperature-limited operation of the cathode, there will be less space-charge present in the interaction space. Therefore, smaller rf fields may produce effective bunching, and thus allow coherent signal output to be obtained. Now it might seem that if decreasing the space-charge improved the bunching, the tube should operate with very small values of current. However, it must be

remembered that the bunching and generation of an rf voltage are interdependent and a very small current would decrease the induced rf current, and thus cause a breakdown in the mechanism of phase focusing. It would be expected, therefore, that there would be some range of anode current which would satisfy the combined requirements for coherent operation of the magnetron. In the Model 11 magnetrons there is a range of anode current for which a coherent signal is produced, for values of anode current above and below this range non-coherent signals are produced.

There is also the possibility that the frequency stability of voltage-tunable operation may depend in some manner on the cathode operating under temperature-limited conditions. No experimental evidence has been obtained to indicate that this is the case. Since the tubes are always operated well below cutoff it appears that the frequency of operation will be determined by the tangential velocity of the edge of the electron swarm corresponding to dc operation of the tube. The electrons nearest the anode will interact with the anode structure and produce an rf voltage between anode bars; the configuration of the rf field in the interaction space will be determined by the anode and cavity structure. Since the electrons cannot reach the anode except by interacting with an rf field they must interact with a field whose frequency is determined by the electrons at the edge of the sub-synchronous swarm.

Experimental data obtained from Model 9 and Model 11 magnetrons indicate that one of the most important parameters in obtaining voltage-tunable operation is the impedance presented to the electron stream by the anode and cavity structure. Coherent operation

was obtained in the Model 9 with anode currents in the order of 100 micro-amperes. The operation was very sensitive to cathode temperature and coherent operation was obtained over a very narrow range of anode current. Coherent operation of Model 11 tubes has been obtained with anode currents in the order of 5 to 20 ma. The interaction space in the two models is quite similar. The most significant differences are in the anode-to-anode capacitance and cavity impedance. The anode-to-anode capacitance in the Model 9 is approximately 2 $\mu\mu$f and in the Model 11 approximately 1 $\mu\mu$f; the cavity impedance in the Model 9 is 25 ohms and in the Model 11 it is 80 ohms.

It is believed that voltage-tunable operation of a magnetron can be obtained under space-charge-limited operation of the cathode if the impedance of the cavity and anode structure can be made sufsufficiently large.

CHAPTER 5

SUMMARY OF CONCLUSIONS

A voltage-tunable magnetron has been developed with operating characteristics that make the tube useful as a source of microwave power. It has been shown that the tube is satisfactory as the local oscillator of a spectrum analyzer and as an rf power source for most rf measurement applications. Work is in progress to determine the feasibility of using the tube as the local oscillator in microwave receivers.

A pure tungsten cathode was found to give better voltage-tunable operation than either an oxide-coated or a thoriated-tungsten cathode. The cathode support and the filament leads were found to cause variations in the power output of the tube. Further work is required to eliminate these effects (possible solutions are indicated in Section 4.2).

It was shown that round anode bars improve the operation of the Model 11 magnetrons over that obtained with square anode bars. It was also shown that an increase in the r_c/r_a ratio over the value used in conventional magnetrons improves voltage-tunable operation. Further research is necessary to determine the optimum value for this ratio. With the present circuit arrangement, the anode-to-anode capacitance appears to be the limiting factor in obtaining higher power from the

tubes. A reduction in the value of this capacitance is necessary if significantly higher powers are to be obtained. Some improvement in efficiency and power output may be obtained by increasing the external circuit impedance; however, the improvement to be obtained in this way is limited.

A theoretical voltage-tuning curve for a magnetron is derived and experimental data are compared to the theoretical results. The operating anode voltage was found to be higher than predicted by the Hartree equation, assuming π-mode of operation. This increase in operating voltage is attributed primarily to the electrons reaching the anode with considerable radially directed velocity. It is proposed that the sensitivity of voltage-tunable operation to cathode temperature is due primarily to the low impedance which is presented to the electrons by the anode and cavity structure.

APPENDIX A

The Magnetron Equations[1]

In this section the basic equations, which approximately describe the operation of high-Q traveling-wave magnetrons, will be derived. These equations will provide a quantitative description of some of the various parameters which have previously been discussed in this report.

A.1 The Non-Oscillating Smooth-Bore Magnetron

It is necessary to derive certain equations for the non-oscillating smooth-bore magnetron which will be used later in the development of the equations for the multi-anode magnetron with applied rf field. Cylindrical geometry is assumed with an axial magnetic field, B. One equation of motion for this case is obtained by equating the time rate of change of the angular momentum of the electron and the torque on the electron. The angular momentum is the product of the moment of inertia mr^2 and the angular velocity $d\phi/dt$. The torque is the product of the tangential force on the electron and the radial distance from the axis. From this we have,

$$\frac{d}{dt}\left(mr^2 \frac{d\phi}{dt}\right) = rBe \frac{dr}{dt} \qquad (A.1)$$

[1]This derivation is based on material presented by Professor W. G. Dow in his course in Microwave Electron Tubes at the University of Michigan.

where

m = mass of electron

e = charge on electron

ϕ = azimuthal angle through which the electron travels

r = radial distance from center of cathode

This equation may be written as

$$\frac{d}{dt}\left(mr^2 \frac{d\phi}{dt}\right) = \frac{Be}{2} \frac{dr^2}{dt} \tag{A.2}$$

or

$$\int d\left(mr^2 \frac{d\phi}{dt}\right) = \frac{Be}{2} \int dr^2 \tag{A.3}$$

then

$$mr^2 \omega = \frac{Be}{2} r^2 + C \quad \text{where } \frac{d\phi}{dt} = \omega \tag{A.4}$$

We assume the electrons leave the cathode with zero velocity; therefore, when

$$r = r_c$$

$$\omega = 0$$

and

$$0 = \frac{Be}{2} r_c^2 + C$$

therefore

$$C = -\frac{Be}{2} r_c^2 \tag{A.5}$$

Therefore, we have

$$\omega = \omega_L \left[1 - \frac{r_c^2}{r^2}\right] \tag{A.6}$$

where

$$\omega_L = \frac{Be}{2m} \tag{A.7}$$

The energy of an electron at any radius r may be expressed as

$$E_{\phi}\, e = \frac{1}{2} mr^2 \omega^2 \qquad (A.8)$$

and substituting Eq A.6 for ω in the above equation and solving for $E\phi$, we have

$$E\phi = \frac{B^2 e}{8m} r^2 \left(1 - \frac{r_c^2}{r^2}\right)^2 \qquad (A.9)$$

Thus $E\phi$ is the tangential kinetic energy, in electron volts, of an electron at any radius r in a smooth-bore magnetron. This is true regardless of the radial potential distribution but assumes no tangential electric field and zero electron velocity at the cathode. If we assume that all the electrons travel in circular orbits around the cathode, then Eq A.9 gives the potential distribution in the smooth-bore magnetron. The potential distribution given by this equation is sketched in Fig. A.1, labeled tangential energy curve. The one other significant voltage associated with a smooth bore magnetron is the Hull cutoff potential for which electrons just graze the anode. This is obtained by setting $r = r_a$ in Eq A.9, giving

$$E_u = \frac{B\omega_L}{4} r_a^2 \left[1 - \frac{r_c^2}{r_a^2}\right]^2 \qquad (A.10)$$

A.2 The Non-Oscillating Magnetron with an Applied RF Field

We now assume a multi-anode magnetron structure to which an external rf potential has been applied. In order to find the potential distribution for this case, it is necessary to include a term in the original equation (A.1) which accounts for the energy per radian due to the interaction of the electron with the tangential rf field.

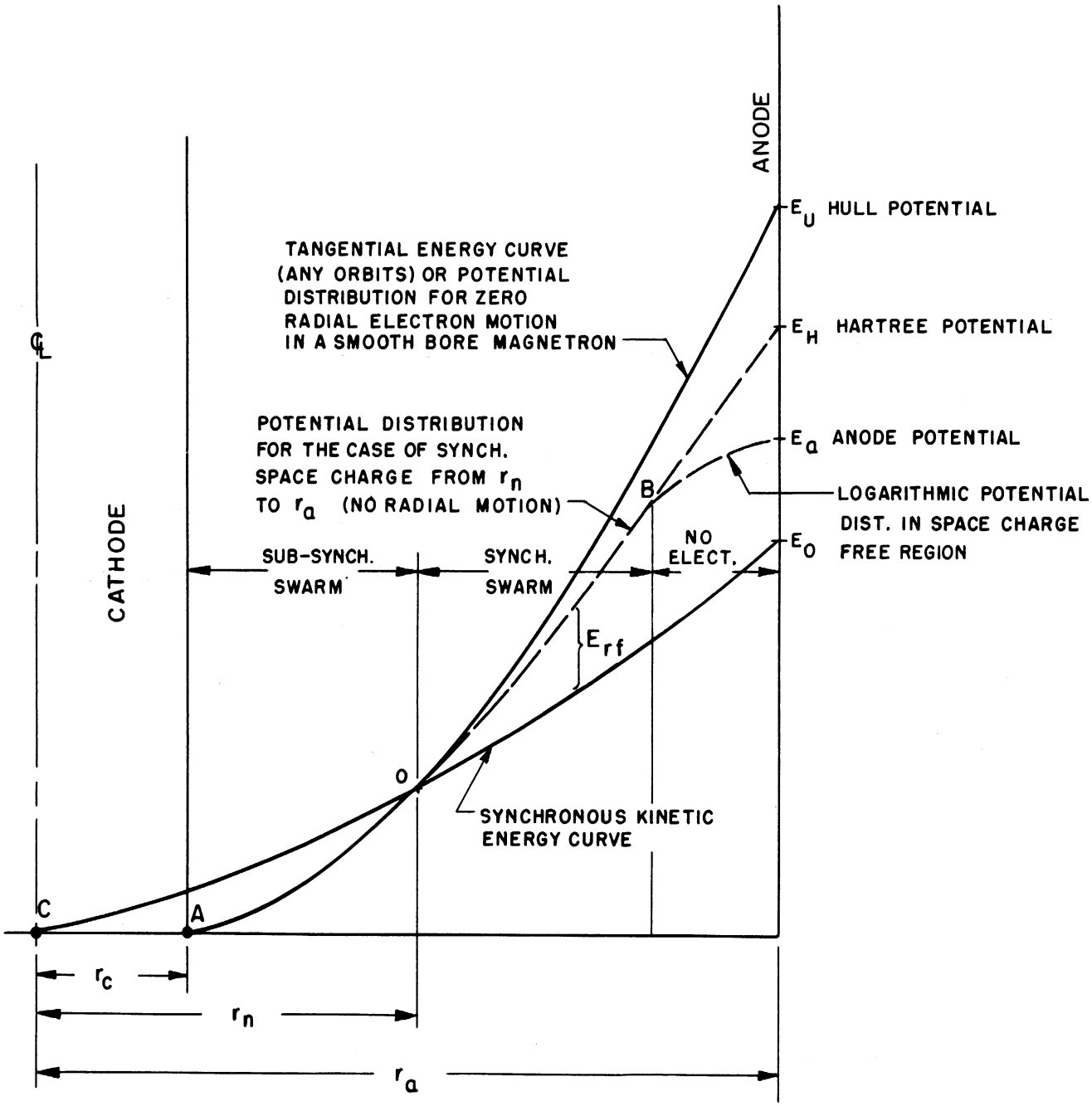

FIG. A-1

SKETCH SHOWING THE ENERGY CURVES AND POTENTIAL DISTRIBUTIONS DISCUSSED IN THE TEXT

We now define the following parameters:

E_{rf} = the energy in electron volts that has been given to the rf field by an electron since it passed radius r_n.

$e\ dE_{rf}$ = the work interchange between the electron and the rf field in proceeding through an angle $d\phi$.

r_n = the radius at which the electrons reach a synchronous velocity corresponding to the frequency of the applied rf voltage.

The corresponding torque on the electron due to the tangential rf field may be expressed as:

$$\text{torque} = \text{radius x force} = e \frac{d\ E_{rf}}{d\phi} \tag{A.11}$$

We now rewrite Eq A.1 using Eq A.11, and we have

$$B\ er \frac{dr}{dt} - e \frac{d\ E_{rf}}{d\phi} - \frac{d}{dt}\left(mr^2 \frac{d\phi}{dt} \right) = 0 \tag{A.12}$$

This becomes

$$\frac{1}{2} B\ e \frac{dr^2}{dt} - e \frac{d\ E_{rf}}{d\phi} - mr^2 \frac{d^2\phi}{dt^2} - \frac{m\ d\phi}{dt} \frac{dr^2}{dt} = 0 \tag{A.13}$$

Since all the electrons outside of r_n are assumed to be rotating at a constant angular velocity, $d^2\phi/dt^2 = 0$, and we have

$$\frac{1}{2} B\ e \frac{dr^2}{dt} d\phi - e\ dE_{rf} - m \frac{dr^2}{dt} \frac{d\phi^2}{dt} = 0 \tag{A.14}$$

Rearranging terms, we have

$$dE_{rf} = \left[\frac{1}{2} B \frac{d\phi}{dt} - \frac{m}{e} \left(\frac{d\phi}{dt} \right)^2 \right] dr^2 \tag{A.15}$$

and since $d\phi/dt$ is assumed constant and equal to ω_n for values of r greater than r_n and less than r_a, we have

$$E_{rf} = \int_{r_n}^{r} \left[\frac{1}{2} B \frac{d\phi}{dt} - \frac{m}{e} \left(\frac{d\phi}{dt} \right)^2 \right] dr^2 \qquad (A.16)$$

or

$$E_{rf} = \left[\frac{1}{2} B\omega_n - \frac{m}{e}\omega_n^2 \right] \left(r^2 - r_n^2 \right) \qquad (A.17)$$

We define E_o as follows:

E_o = the kinetic energy in electron volts of an electron pursuing a circular path at a radius r_a in synchronism with the rf field.

Therefore

$$E_o = \frac{m}{2e} r_a^2 \omega_n^2 \qquad (A.18)$$

Where

N = number of anode segments

n = number of positive nodes on rf wave (mode number)

and

$$\omega_n = \frac{2\pi f}{n} \qquad (A.19)$$

For the π-mode of operation

$$n = \frac{N}{2}$$

We can also express E_o in terms of Eq A.9 as follows,

$$E_o = \frac{B_o^2 e}{8m} r_a^2 \left(1 - \frac{r_c^2}{r_a^2} \right)^2 \qquad (A.20)$$

where B_o is the magnetic field which produces the cutoff condition when $E_a = E_o$. Thus, no interaction with the rf field is assumed in writing Eq A.20 since this is simply an expression of electron energy under specified conditions. B_o can be found from Eq A.6 by setting r equal

to r_a and solving for B_o. We have therefore

$$B_o = \frac{2\frac{m}{e}\omega_n}{\left(1 - \frac{r_c^2}{r_a^2}\right)} \tag{A.21}$$

The potential at the edge of the sub-synchronous space-charge swarm may be found by the use of Eq A.9 which gives

$$E_n = \frac{B^2 e}{8m} r_n^2 \left(1 - \frac{r_c^2}{r_n^2}\right)^2 \tag{A.22}$$

This corresponds to the synchronous kinetic energy of the electron at $r = r_n$; the synchronous kinetic energy is given by the following equation

$$e\,E_{syn} = \frac{1}{2} m r^2 \omega_n^2 \tag{A.23}$$

or

$$E_{syn} = \frac{1}{2}\frac{m}{e} r^2 \omega_n^2 \tag{A.23a}$$

The synchronous energy curve is shown in Fig. A.1 as C-O-E_o. For values of r less than r_n the synchronous energy is greater than the potential energy given by the potential distribution curve A-O-E_H. Therefore, all the electrons inside of r_n are rotating at less than synchronous velocity, and this region is described as the sub-synchronous swarm. It is assumed here that in the region outside of r_n all electrons rotate at synchronous velocity, therefore the difference between the two curves O-E_o and O-E_H must represent the energy given to the rf field by the electron. The curve O-E_H represents

the potential distribution in a non-oscillating magnetron in which the electrons are delivering energy to a tangential field.

$$E = E_{syn} + E_{rf} \tag{A.24}$$

for

$$r_a > r > r_n$$

The potential distribution for r less than r_n is given by Eq A.9 and is shown in Fig. A.1, Section A-0. The potential distribution curve must be tangent to A-0-E_u at r_n since no discontinuities in potential can exist. The potential distribution for the region r greater than r_n is indicated by the curve 0-B-E_a in Fig. A.1.

Equation A.24 may be written as follows,

$$E = \left[\frac{1}{2}\frac{m}{e} r^2 \omega_n^2\right] + \left[\frac{1}{2} B \omega_n - \frac{m\omega_n^2}{e}\right]\left[r^2 - r_n^2\right] \tag{A.24a}$$

From Eqs A.20 and A.22

$$\frac{E_n}{E_o} = \frac{\frac{B^2 e}{8m} r_n^2 \left(1 - \frac{r_c^2}{r_n^2}\right)^2}{\frac{B_o^2 e}{8m} r_a^2 \left(1 - \frac{r_c^2}{r_a^2}\right)^2} \tag{A.25}$$

From Eqs A.18 and A.23a we obtain

$$\frac{E_n}{E_o} = \frac{r_n^2}{r_a^2} \tag{A.26}$$

Combining Eqs A.25 and A.26 we obtain

$$\frac{B}{B_o} = \frac{\left(1 - \frac{r_c^2}{r_a^2}\right)}{\left(1 - \frac{r_c^2}{r_n^2}\right)} \tag{A.27}$$

From Eq A.21 we can write

$$\frac{B}{B_o} = \frac{Be}{2m}\frac{1}{\omega_n}\left[1 - \frac{r_c^2}{r_a^2}\right] \tag{A.28}$$

Combining Eqs A.27 and A.28 we obtain

$$\frac{\omega_L}{\omega_n}\left[1 - \frac{r_c^2}{r_a^2}\right] = \frac{\left[1 - \frac{r_c^2}{r_a^2}\right]}{\left[1 - \frac{r_c^2}{r_n^2}\right]} \tag{A.29}$$

or

$$r_n^2 = \frac{r_c^2}{1 - \frac{\omega_n}{\omega_L}} \tag{A.29a}$$

Substituting Eq A.29a into Eq A.24a and rearranging terms, we obtain

$$E = \frac{m}{e}\omega_L\,\omega_n\,(r^2 - r_c^2) - \frac{1}{2}\frac{m}{e}r^2\omega_n^2 \tag{A.30}$$

Thus Eq A.30 describes the potential distribution in the synchronous swarm of a non-oscillating magnetron in which the electrons are delivering energy to a tangential electric field. Equation A.30 is plotted in Fig. A.1 as O-B-E_H. Radial energy of the electrons is assumed to be negligible. The limiting value given by Eq A.30 by

letting $r = r_a$ is known as the Hartree voltage and is the theoretical voltage at which a magnetron can start oscillating.

$$E_H = \frac{m}{e} \omega_L \omega_n (r_a^2 - r_c^2) - \frac{1}{2} \frac{m}{e} r_a^2 \omega_n^2 \quad (A.31)$$

If Eq A.21 is solved for ω_n and this value is substituted in Eq A.31 then Eq A.31 may be normalized to Eq A.20 giving

$$\frac{E_H}{E_o} = 2 \frac{B}{B_o} - 1 \quad (A.32)$$

Eqs A.31 or A.32 may be used to predict very closely the starting or threshold potential of high-Q magnetron oscillators.

There are in general three regions to be considered in the non-oscillating magnetron interaction space: the inner or sub-synchronous swarm, the synchronous swarm, and the space-charge-free region. The boundary of the sub-synchronous swarm is determined by the intersection of the synchronous energy curve and the actual potential energy curve indicated as point 0 in Fig. A.1. For values of r less than r_n the synchronous energy is greater than the space potential given by Eq A.9; therefore, the electrons cannot reach synchronous energy in this region. In the region outside of $r = r_n$, it is assumed that the electrons give up energy to the rf field so that they remain at the synchronous energy level. This transfer of energy is continuous, energy being taken from the dc field and transferred to the rf field through the medium of the space charge. This is one of the distinguishing characteristics of the magnetron. The electrons can maintain synchronism to the limit that the potential distribution in the

interaction space satisfies Eq A.30. Outside of this limit there will be no electrons and a space-charge-free region will exist. The potential distribution in the region outside the synchronous swarm will be logarithmic.

Since the electrons reach the anode with an energy of at least E_o volts, the maximum electron interaction efficiency for a magnetron may be expressed as

$$\eta = \frac{E_a - E_o}{E_a} \tag{A.33}$$

The important relations for a conventional non-oscillating high-Q magnetron thus become:

$$E_U = \frac{B^2 e}{8m} r^2 \left(1 - \frac{r_c^2}{r_a^2}\right)^2 \tag{A.10}$$

This is the Hull cutoff potential for a magnetic cylindrical diode, no rf fields present.

$$E_o = \frac{B_o^2 e}{8m} r_a^2 \left(1 - \frac{r_c^2}{r_a^2}\right)^2 \tag{A.20}$$

$$E_o = \frac{1}{2}\frac{m}{e}\omega_n^2 r_a^2 \tag{A.18}$$

$$B_o = \frac{2\frac{m}{e}\omega_n}{\left(1 - \frac{r_c^2}{r_a^2}\right)} \tag{A.21}$$

$$E_H = \frac{m}{e}\omega_L \omega_n (r_a^2 - r_c^2) - \frac{1}{2}\frac{m}{e} r_a^2 \omega_n^2 \tag{A.31}$$

(Hartree relation)

$$\frac{E_H}{E_o} = 2\frac{B}{B_o} - 1 \qquad (A.32)$$

$$I_o = \frac{2\pi\, a_1}{\left[1 - \left(\frac{r_c}{r_a}\right)^2\right]\left[\frac{r_a}{r_c} + 1\right]} \frac{m}{e}\left(\frac{2\pi c}{n\lambda}\right)^3 r_a^{\,2}\, \epsilon_o L \qquad (A.34)$$

$\epsilon_o = \frac{10^{-9}}{36\pi}$ farads/meter

$c = 3 \times 10^8$ meters/sec.

$a_1 = 1$ for ordinary values of r_c/r_a

L = length of cathode emitting surface (meters)

I_o = the current that just begins to flow when the magnetic field is B_o and the anode voltage reaches E_o with no rf field applied (Ref. 24).

The ratios:

$$\frac{E_a}{E_o}, \frac{B}{B_o}, \frac{I_a}{I_o}$$

are, in general, sufficient to allow scaling of a magnetron. That is, in the design of a magnetron, one can first select values for f, E_a, B, and I_a, then design the interaction space so that the above ratios are the same as for a known operable magnetron and the performance of the new magnetron will be the same as in the original magnetron.

APPENDIX B

ASSEMBLY AND DETAIL DRAWINGS OF CATHODES FOR MODEL 11B MAGNETRON

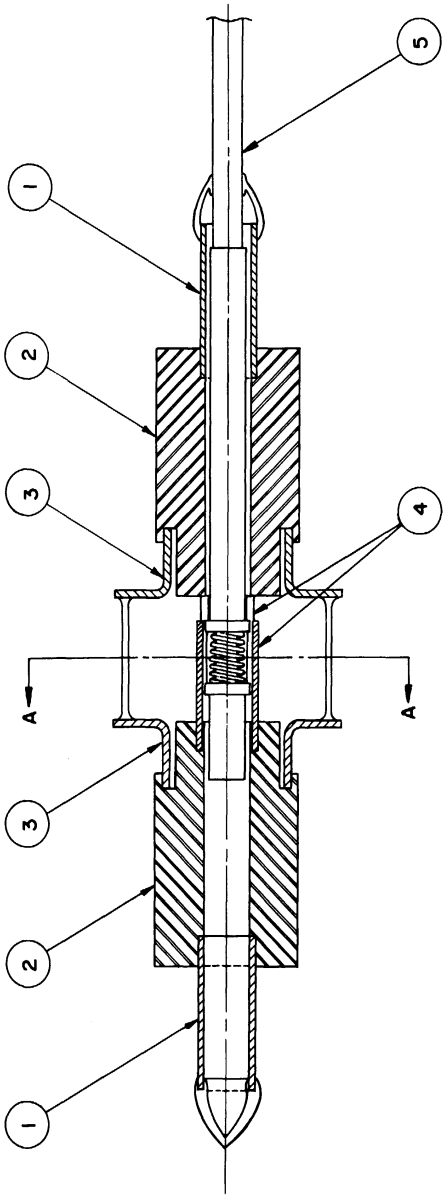

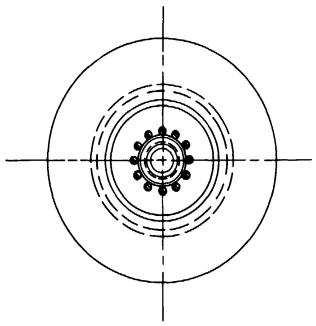

SECTION A-A

FIG. B - 1

ALL DIMENSIONS UNLESS OTHERWISE SPECIFIED MUST BE HELD TO A TOLERANCE - FRACTIONAL ± 1/64," DECIMAL ± .005," ANGULAR ± 1/2°

				DESIGNED BY J.A. BOYD	APPROVED BY
				DRAWN BY P.M.	SCALE 2:1
				CHECKED BY	DATE 9-12-52
ISSUE	DATE	PROJECT 2009		TITLE INTERDIGITAL EXTERNAL CAVITY MAGNETRON MODEL 11B	
		CLASSIFICATION		DWG. NO. B-10,011 B	

ENGINEERING RESEARCH INSTITUTE
UNIVERSITY OF MICHIGAN
ANN ARBOR MICHIGAN

DWG. NO. B

DWG. NO. A

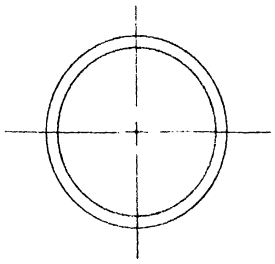

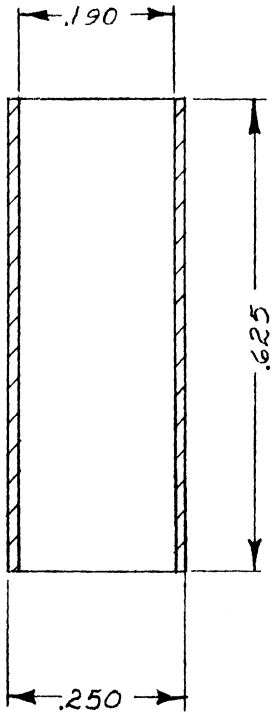

FIT TO DETAIL 1 DWG. 9096

FIG. B-2

KOVAR TUBING (STUPAKOFF # 90250018) 2 REQ'D

ALL DIMENSIONS UNLESS OTHERWISE SPECIFIED MUST BE HELD TO A TOLERANCE - FRACTIONAL ± 1/64," DECIMAL ± .005," ANGULAR ± ½°

		ENGINEERING RESEARCH INSTITUTE UNIVERSITY OF MICHIGAN ANN ARBOR MICHIGAN	DESIGNED BY JGB	APPROVED BY
			DRAWN BY	SCALE X4
			CHECKED BY	DATE 4-10-52
		PROJECT 2009	TITLE KOVAR SLEEVE	
		CLASSIFICATION	DWG. NO. A- 9097	
ISSUE	DATE			

LET	DATE	APPR.	CHANGE
A	5-1-53	VRB	.050 WAS .125

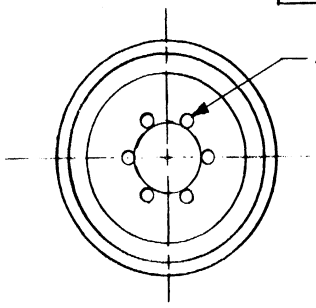

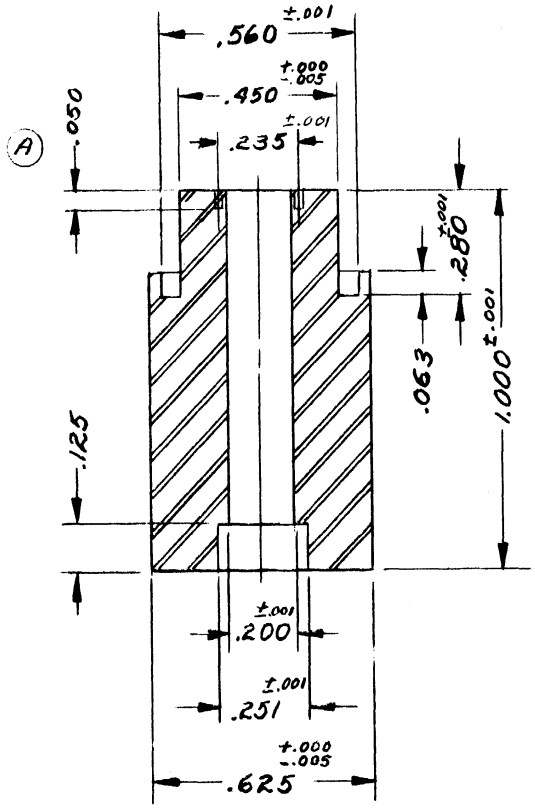

FIG. B – 3

H. R. STEEL - 2 REQ'D

ALL DIMENSIONS UNLESS OTHERWISE SPECIFIED MUST BE HELD TO A TOLERANCE - FRACTIONAL ± 1/64," DECIMAL ± .005," ANGULAR ± ½°

		ENGINEERING RESEARCH INSTITUTE UNIVERSITY OF MICHIGAN ANN ARBOR MICHIGAN	DESIGNED BY J.A.B.	APPROVED BY
			DRAWN BY PLW	SCALE 2 X
			CHECKED BY [illegible]	DATE 9-11-52
		PROJECT 2009	TITLE POLE PIECE - MODEL 11B MAGNETRON	
2	9-11-52	CLASSIFICATION	DWG. NO. A- 9104	
ISSUE	DATE			

DWG. NO. A

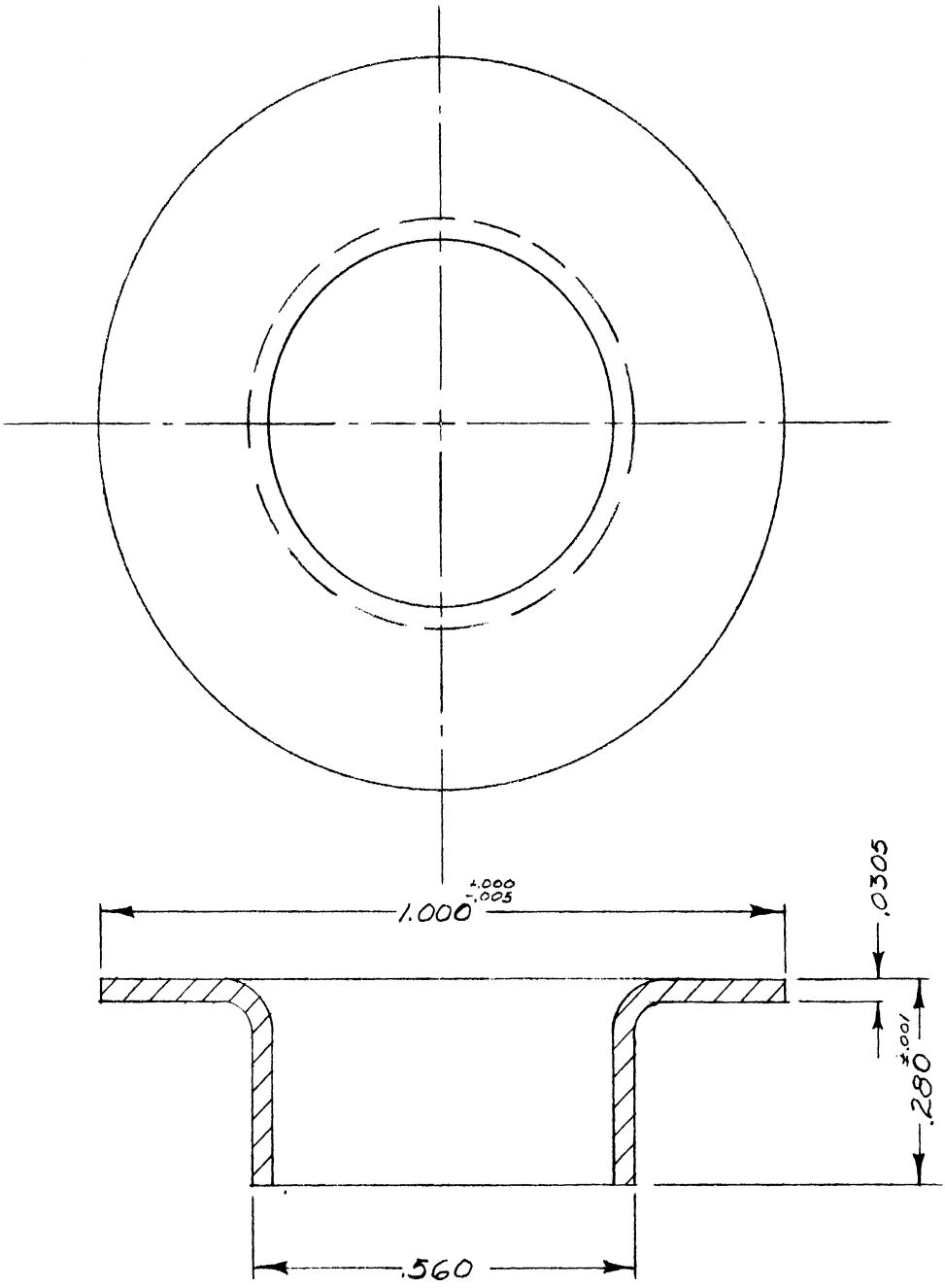

FIG. B-4

KOVAR (STUPAKOFF # 941002) 2 REQ'D

ALL DIMENSIONS UNLESS OTHERWISE SPECIFIED MUST BE HELD TO A TOLERANCE - FRACTIONAL ± 1/64" DECIMAL ± .005" ANGULAR ± ½°

		ENGINEERING RESEARCH INSTITUTE UNIVERSITY OF MICHIGAN ANN ARBOR MICHIGAN	DESIGNED BY JAB	APPROVED BY
			DRAWN BY MN	SCALE X4
			CHECKED BY VRS	DATE 4-9-52
		PROJECT 2009	TITLE KOVAR FLANGED FLAT-BOTTOM CUP	
		CLASSIFICATION	DWG. NO. A-9018	
ISSUE	DATE			

LET	DATE	APPR	CHANGE
A	5-19-53	PRB	.445 WAS .520
B	"	PRB	TUNGSTEN WAS MOLY

DWG. NO. A-5039

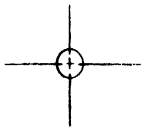

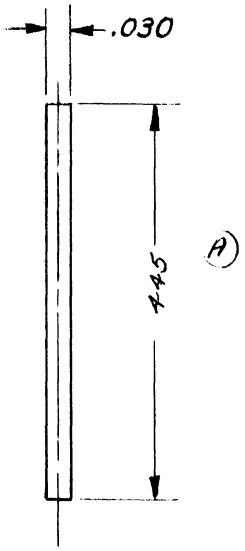

FIG. B-5

(B)

TUNGSTEN WIRE - 12 REQ'D.

ALL DIMENSIONS UNLESS OTHERWISE SPECIFIED MUST BE HELD TO A TOLERANCE - FRACTIONAL ± 1/64," DECIMAL ± .005," ANGULAR ± ½°

		ENGINEERING RESEARCH INSTITUTE UNIVERSITY OF MICHIGAN ANN ARBOR MICHIGAN	DESIGNED BY PLW / APPROVED BY
			DRAWN BY PLW / SCALE 4 X
			CHECKED BY / DATE 9-11-52
		PROJECT 2009	TITLE ANODE FINGERS MODEL IIB MAGNETRON
12	9-11-52	CLASSIFICATION	DWG. NO. A-5039
ISSUE	DATE		

APPENDIX C

ASSEMBLY AND DETAIL DRAWINGS OF CATHODES FOR MODEL 11 MAGNETRONS

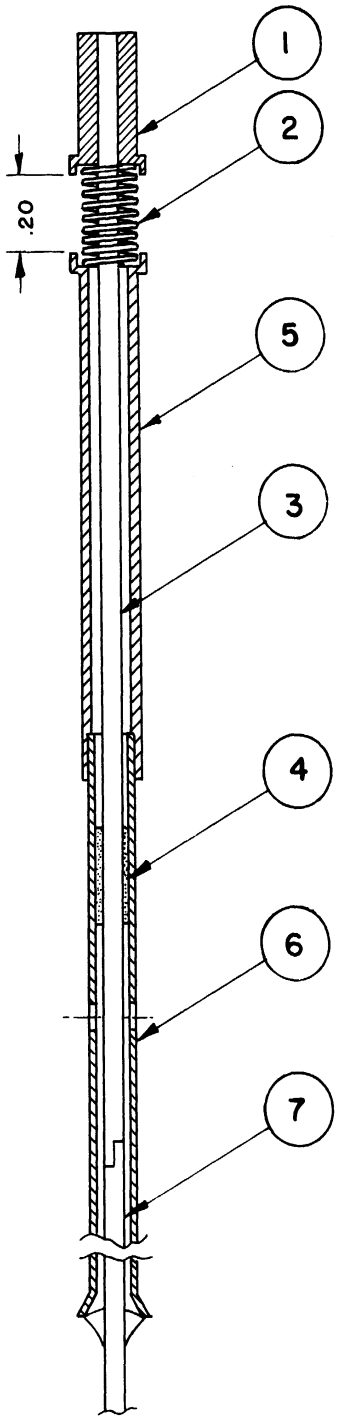

FIG. C-1

ALL DIMENSIONS UNLESS OTHERWISE SPECIFIED MUST BE HELD TO A TOLERANCE - FRACTIONAL ± 1/64," DECIMAL ± .005," ANGULAR ± ½°

		ENGINEERING RESEARCH INSTITUTE UNIVERSITY OF MICHIGAN ANN ARBOR MICHIGAN	DESIGNED BY J.A.BOYD	APPROVED BY
			DRAWN BY P L W	SCALE 2X
			CHECKED BY	DATE 7-1-52
		PROJECT 2009	TITLE TUNGSTEN CATHODE FOR MODEL II MAGNETRON	
1	7-1-52	CLASSIFICATION	DWG. NO. A-8030	
ISSUE	DATE			

	CHANGES	DATE	APPR.
A	.350 WAS .175 ADDED DRILL HOLE	9-15-52	JRB

DWG. NO. A

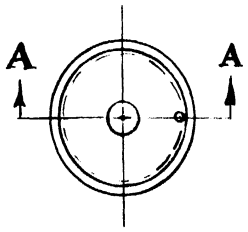

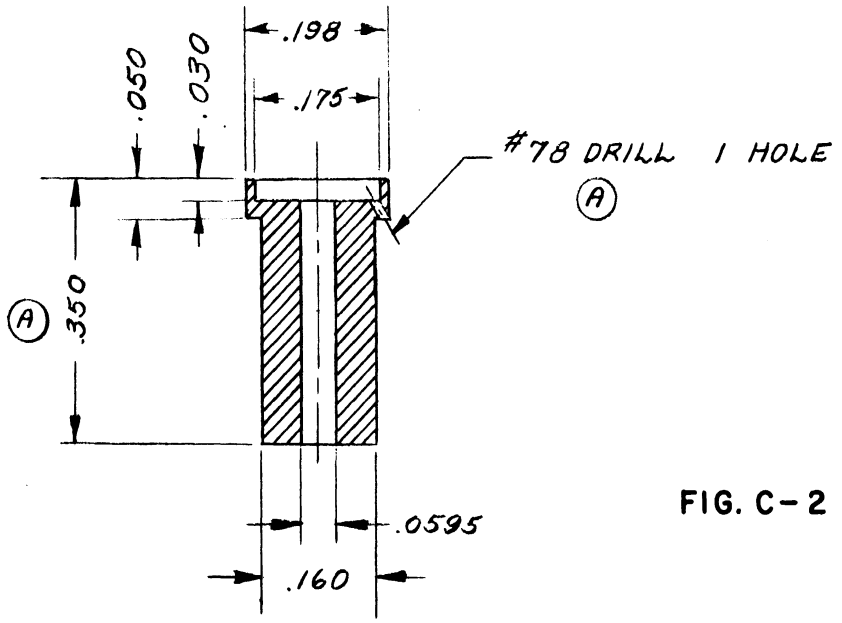

FIG. C-2

SECTION A-A

MOLY 1 REQ'D

ALL DIMENSIONS UNLESS OTHERWISE SPECIFIED MUST BE HELD TO A TOLERANCE - FRACTIONAL ± 1/64," DECIMAL ± .005," ANGULAR ± ½°

		ENGINEERING RESEARCH INSTITUTE UNIVERSITY OF MICHIGAN ANN ARBOR MICHIGAN	DESIGNED BY JAB	APPROVED BY
			DRAWN BY PLW	SCALE 4X
			CHECKED BY J-R-B	DATE 7-1-52
		PROJECT 2009	TITLE UPPER END HAT	
1	7/1/52	CLASSIFICATION	DWG. NO. A-8030-1	
ISSUE	DATE			

	CHANGES	DATE	APPR.
A	ADDED DIMS. .125	9-15-52	JRB

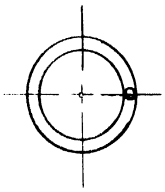

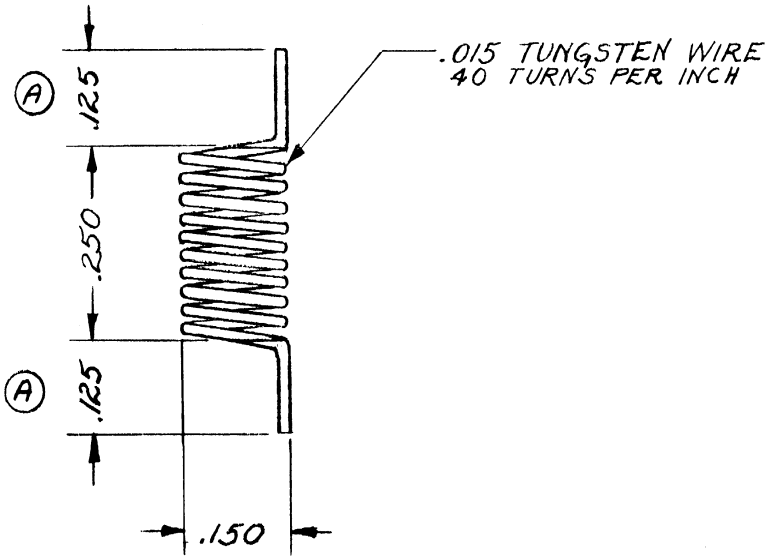

FIG. C-3

1 REQD.

ALL DIMENSIONS UNLESS OTHERWISE SPECIFIED MUST BE HELD TO A TOLERANCE - FRACTIONAL ± 1/64," DECIMAL ± .005," ANGULAR ± ½°

ENGINEERING RESEARCH INSTITUTE UNIVERSITY OF MICHIGAN ANN ARBOR MICHIGAN		DESIGNED BY JAB	APPROVED BY
		DRAWN BY PLW	SCALE 4X
		CHECKED BY JAB	DATE 7-1-52
PROJECT 2009		TITLE TUNGSTEN FILAMENT	
CLASSIFICATION	1 / 7-1-52 (ISSUE / DATE)	DWG. NO. A-8030-2	

DWG. NO. A

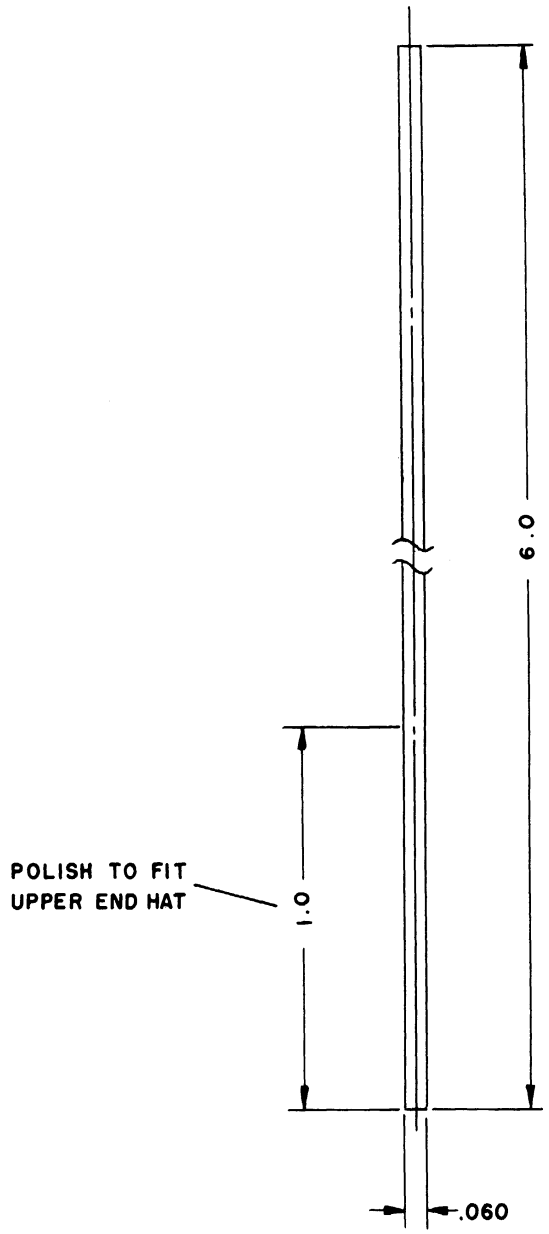

FIG. C– 4

MOLYBDENUM — 1 REQ'D.

ALL DIMENSIONS UNLESS OTHERWISE SPECIFIED MUST BE HELD TO A TOLERANCE - FRACTIONAL ± 1/64," DECIMAL ± .005," ANGULAR ± ½°

		ENGINEERING RESEARCH INSTITUTE UNIVERSITY OF MICHIGAN ANN ARBOR MICHIGAN	DESIGNED BY GED	APPROVED BY
			DRAWN BY PLW	SCALE 2 X
			CHECKED BY [illegible]	DATE 2 - 11-53
		PROJECT 2009	TITLE CENTER CONDUCTOR	
1	2·11·53	CLASSIFICATION	DWG. NO. A-8043-3	
ISSUE	DATE			

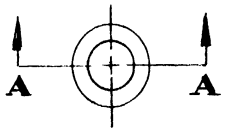

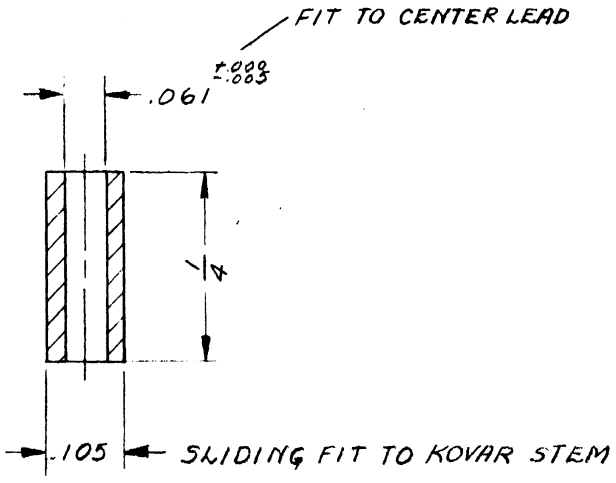

SECTION A-A

FIG. C-5

ALSIMAG 222 - 1 REQ'D.

ALL DIMENSIONS UNLESS OTHERWISE SPECIFIED MUST BE HELD TO A TOLERANCE - FRACTIONAL ± 1/64," DECIMAL ± .005," ANGULAR ± ½°

		ENGINEERING RESEARCH INSTITUTE UNIVERSITY OF MICHIGAN ANN ARBOR MICHIGAN	DESIGNED BY VAN NATTER	APPROVED BY
			DRAWN BY PLW	SCALE 4X
			CHECKED BY VRH	DATE 1-26-53
		PROJECT 2009	TITLE INSULATOR	
1		CLASSIFICATION	DWG. NO. A-8044-4	
ISSUE	DATE			

	CHANGES	DATE	APPR.
A	ADDED DRILL HOLE NOTE	9-15-52	JRB
B	REMOVED NOTE "#55 DRILL THRU 'E' DIM 3/4"	11-25-52	JRB

DWG. NO. A 8030-5

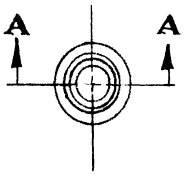

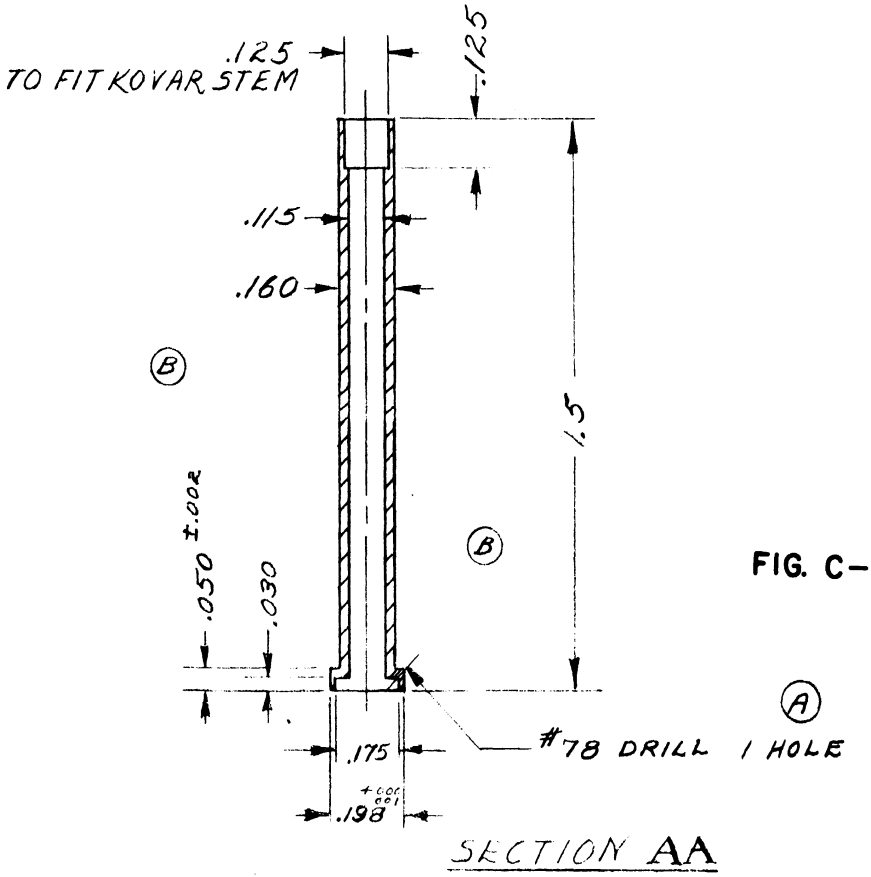

FIG. C-6

MOLY 1 REQ'D.

ALL DIMENSIONS UNLESS OTHERWISE SPECIFIED MUST BE HELD TO A TOLERANCE - FRACTIONAL ± 1/64," DECIMAL ± .005," ANGULAR ± ½°

		ENGINEERING RESEARCH INSTITUTE UNIVERSITY OF MICHIGAN ANN ARBOR MICHIGAN	DESIGNED BY J A R	APPROVED BY J R B
			DRAWN BY P L W	SCALE X 2
			CHECKED BY W P M	DATE 6-6-52
		PROJECT 2009	TITLE LOWER END HAT	
1	7-15-52	CLASSIFICATION	DWG. NO. A-8030-5	
ISSUE	DATE			

	CHANGES	DATE	APPR.
A	ADDED NOTE "#55 DRILL THRU" & DIM 3/4.	11-25-52	

DWG. NO. A-8030-6

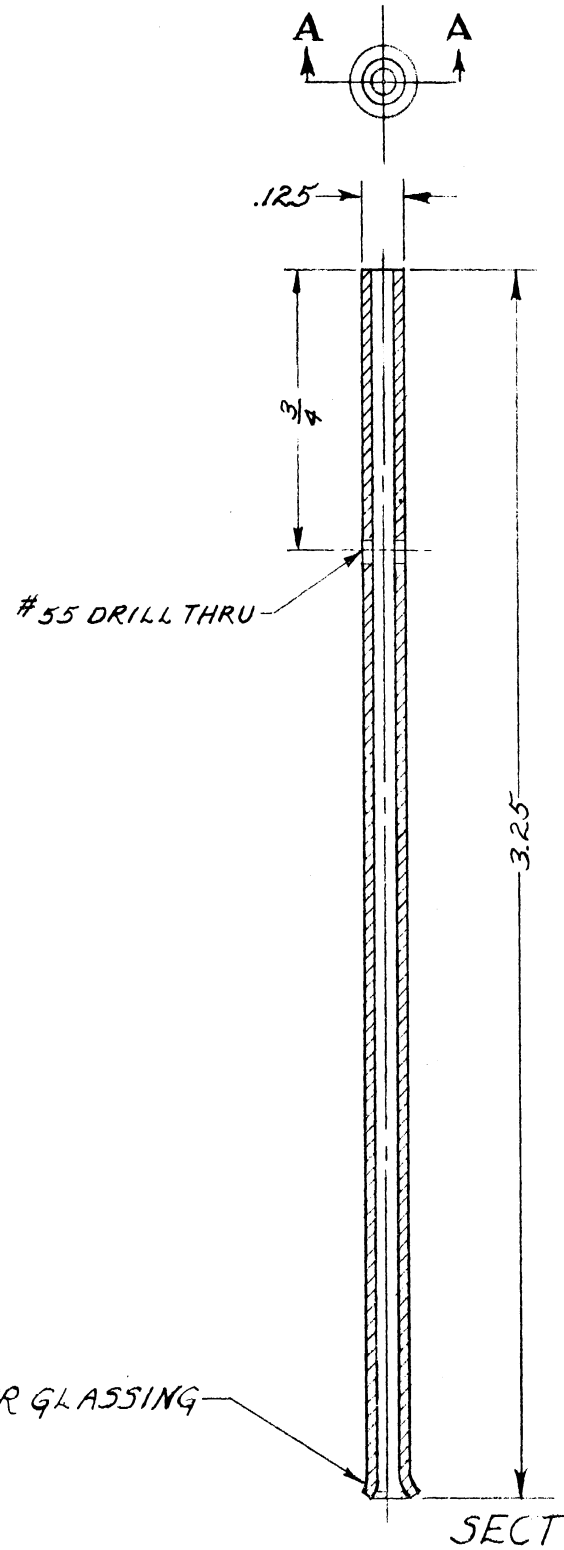

SECTION AA

FIG. C-7

1/8" KOVAR TUBING 1 REQD.

ALL DIMENSIONS UNLESS OTHERWISE SPECIFIED MUST BE HELD TO A TOLERANCE - FRACTIONAL ± 1/64," DECIMAL ± .005," ANGULAR ± ½°

		ENGINEERING RESEARCH INSTITUTE UNIVERSITY OF MICHIGAN ANN ARBOR MICHIGAN	DESIGNED BY JAB	APPROVED BY JKB
			DRAWN BY PLW	SCALE 2X
			CHECKED BY JAB	DATE 7-1-52
		PROJECT 2009	TITLE LOWER STEM	
1	7-1-52	CLASSIFICATION	DWG. NO. A-8030-6	
ISSUE	DATE			

APPENDIX D

ASSEMBLY AND DETAIL DRAWINGS OF DUAL OUTPUT CAVITY FOR MODEL 11 MAGNETRONS

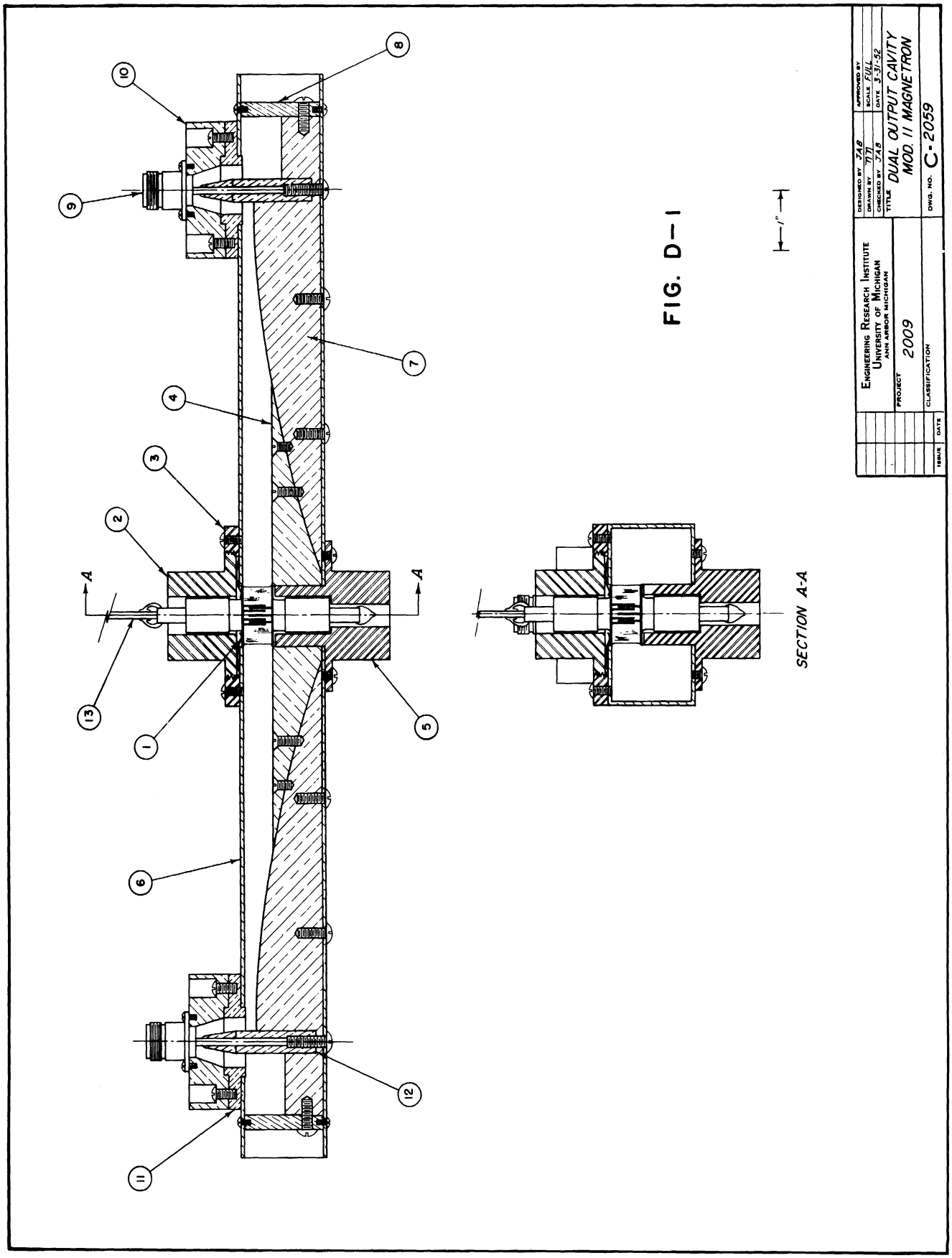
A
A
SECTION A-A
1"
ENGINEERING RESEARCH INSTITUTE
UNIVERSITY OF MICHIGAN
ANN ARBOR MICHIGAN
PROJECT 2009
DESIGNED BY JAB
DRAWN BY TT
CHECKED BY JAB
APPROVED BY
SCALE FULL
DATE 3-31-52
TITLE DUAL OUTPUT CAVITY
MOD. II MAGNETRON
DWG. NO. C-2059
CLASSIFICATION
ISSUE
DATE

FIG. D-1

DWG. NO. A

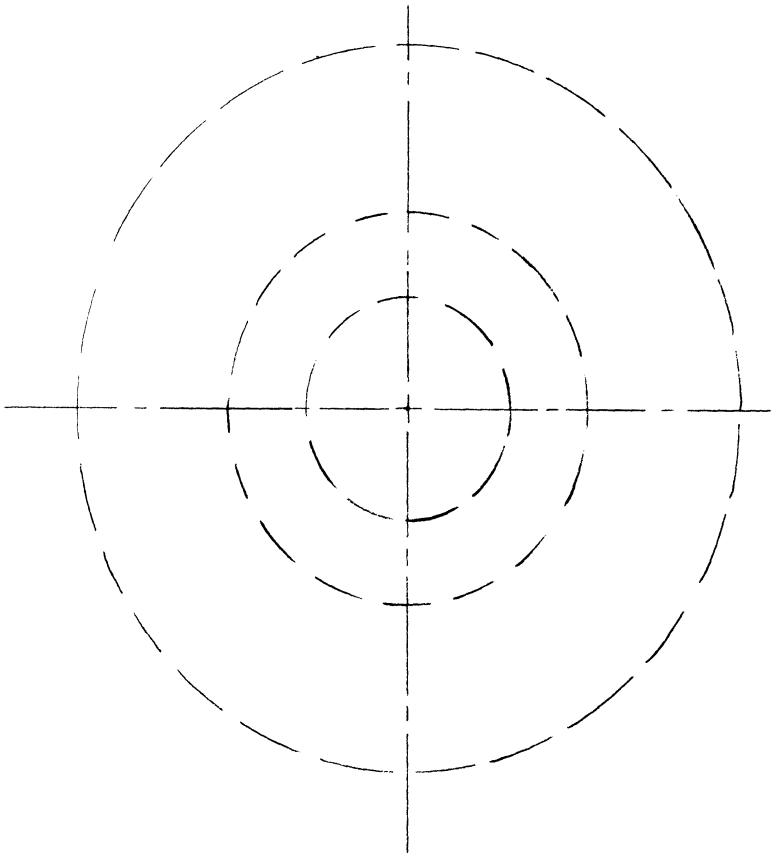

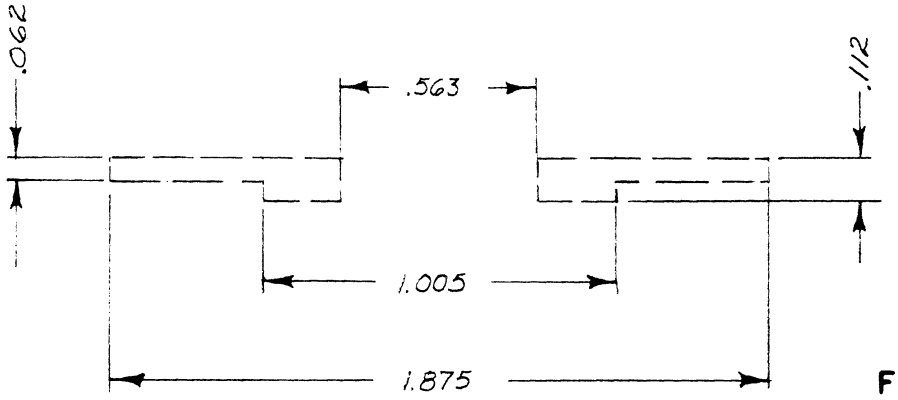

FIG. D-2

NOTE:
MAKE SPRING TO SUIT ABOVE SPACE LIMITATIONS

BERYLLIUM-COPPER

ALL DIMENSIONS UNLESS OTHERWISE SPECIFIED MUST BE HELD TO A TOLERANCE - FRACTIONAL ± 1/64," DECIMAL ± .005," ANGULAR ± ½°

		ENGINEERING RESEARCH INSTITUTE UNIVERSITY OF MICHIGAN ANN ARBOR MICHIGAN	DESIGNED BY [illegible]	APPROVED BY
			DRAWN BY NM	SCALE X2
			CHECKED BY [illegible]	DATE 5-26-52
		PROJECT 2059	TITLE CONTACT SPRING	
		CLASSIFICATION	DWG. NO. A-2059-1	
ISSUE	DATE			

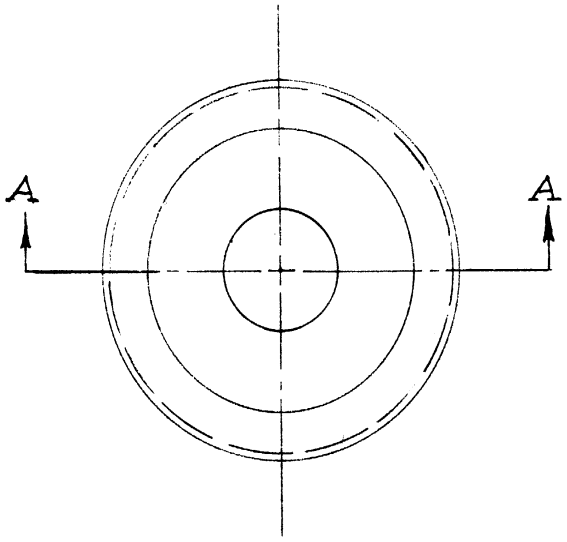

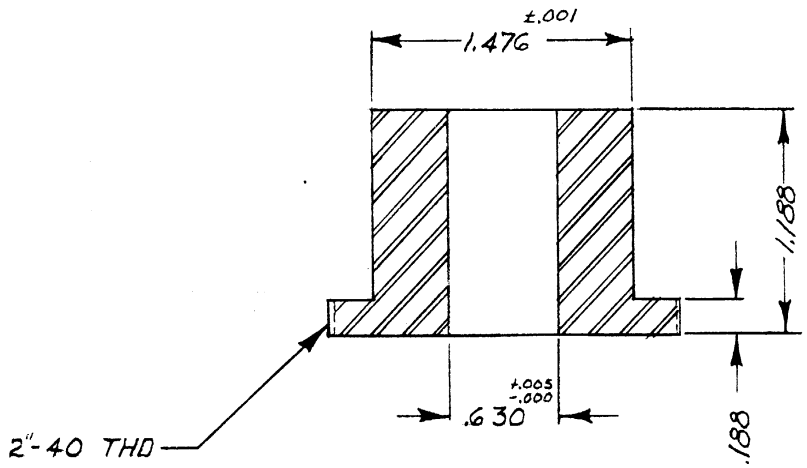

SECTION A-A

FIG. D-3

CRS 1 REQ'D

ALL DIMENSIONS UNLESS OTHERWISE SPECIFIED MUST BE HELD TO A TOLERANCE - FRACTIONAL ± 1/64," DECIMAL ± .005," ANGULAR ± ½°

		ENGINEERING RESEARCH INSTITUTE UNIVERSITY OF MICHIGAN ANN ARBOR MICHIGAN	DESIGNED BY JAB	APPROVED BY
			DRAWN BY BW	SCALE FULL
			CHECKED BY [illegible]	DATE 4-19-52
		PROJECT 2009	TITLE REMOVABLE POLE PIECE	
		CLASSIFICATION	DWG. NO. A-[illegible]	
ISSUE	DATE			

DWG. NO. A

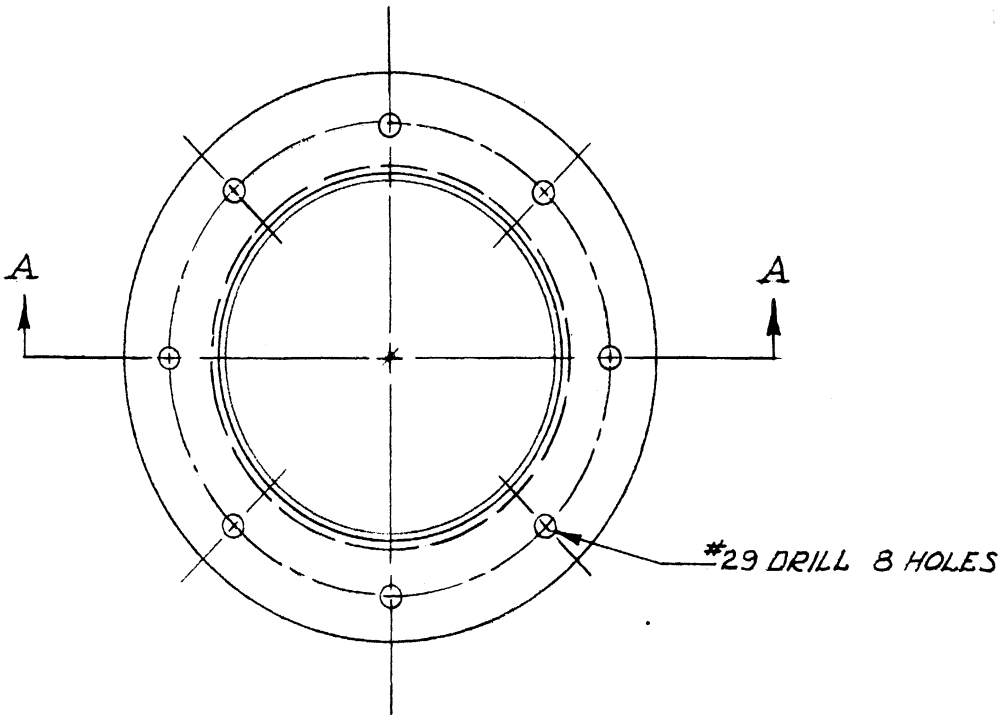

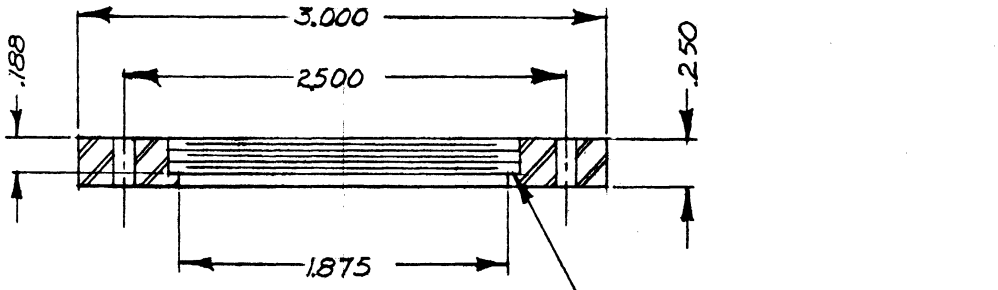

SECTION A-A

FIG. D-4

BRASS OR CRS - 1 REQ'D.

ALL DIMENSIONS UNLESS OTHERWISE SPECIFIED MUST BE HELD TO A TOLERANCE - FRACTIONAL ± 1/64," DECIMAL ± .005," ANGULAR ± ½°

ENGINEERING RESEARCH INSTITUTE UNIVERSITY OF MICHIGAN ANN ARBOR MICHIGAN		DESIGNED BY JAB	APPROVED BY
		DRAWN BY [illegible]	SCALE FULL
		CHECKED BY [illegible]	DATE 1-28-53
PROJECT 2059		TITLE POLE PIECE RING	
CLASSIFICATION		DWG. NO. A-2059-3	

ISSUE | DATE

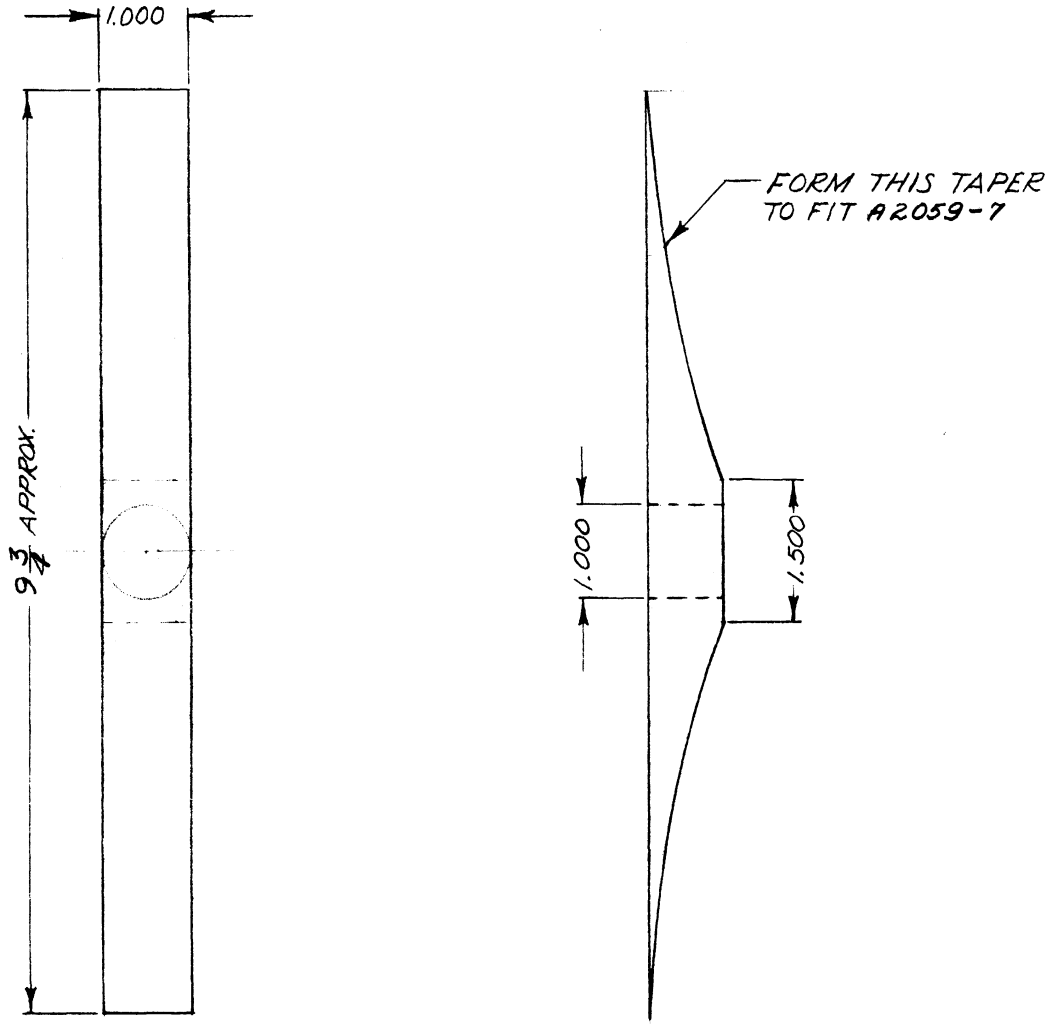

FIG. D-5

BRASS 1 REQ'D

ALL DIMENSIONS UNLESS OTHERWISE SPECIFIED MUST BE HELD TO A TOLERANCE - FRACTIONAL ± 1/64," DECIMAL ± .005," ANGULAR ± 1/2°

ISSUE	DATE			
		ENGINEERING RESEARCH INSTITUTE UNIVERSITY OF MICHIGAN ANN ARBOR MICHIGAN	DESIGNED BY GAB	APPROVED BY
			DRAWN BY [illegible]	SCALE HALF
			CHECKED BY [illegible]	DATE 4-23-52
		PROJECT 2009	TITLE RIDGE	
		CLASSIFICATION	DWG. NO. A-2059-4	

DWG. NO. A

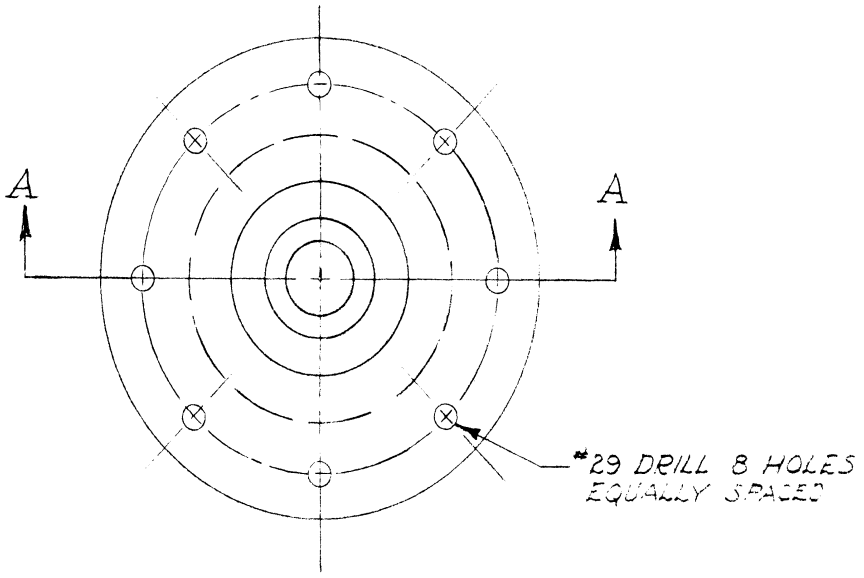

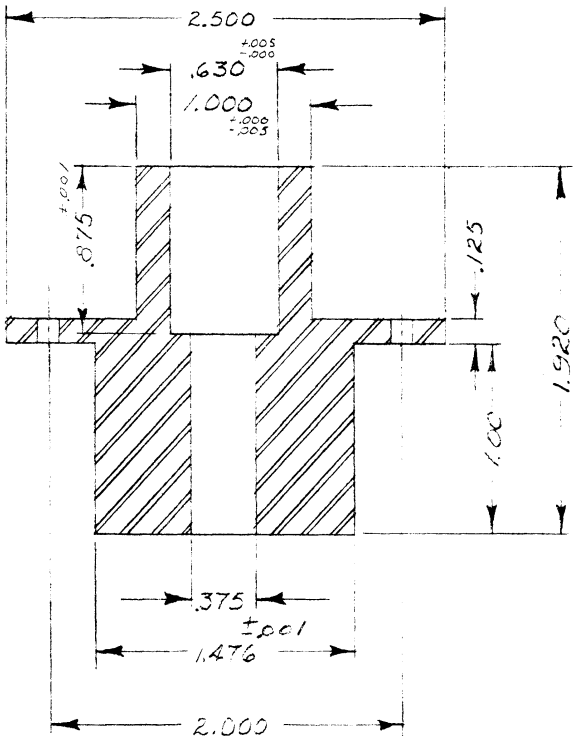

SECTION A-A

FIG. D-6

CRS 1 REQ'D

ALL DIMENSIONS UNLESS OTHERWISE SPECIFIED MUST BE HELD TO A TOLERANCE - FRACTIONAL ± 1/64," DECIMAL ± .005," ANGULAR ± ½°

		ENGINEERING RESEARCH INSTITUTE UNIVERSITY OF MICHIGAN ANN ARBOR MICHIGAN	DESIGNED BY JAB	APPROVED BY
			DRAWN BY [illegible]	SCALE FULL
			CHECKED BY [illegible]	DATE 4-23-52
		PROJECT 2009	TITLE FIXED POLE PIECE	
		CLASSIFICATION	DWG. NO. A-2059-5	
ISSUE	DATE			

DWG. NO. B

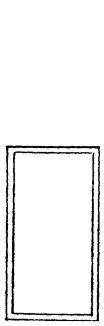

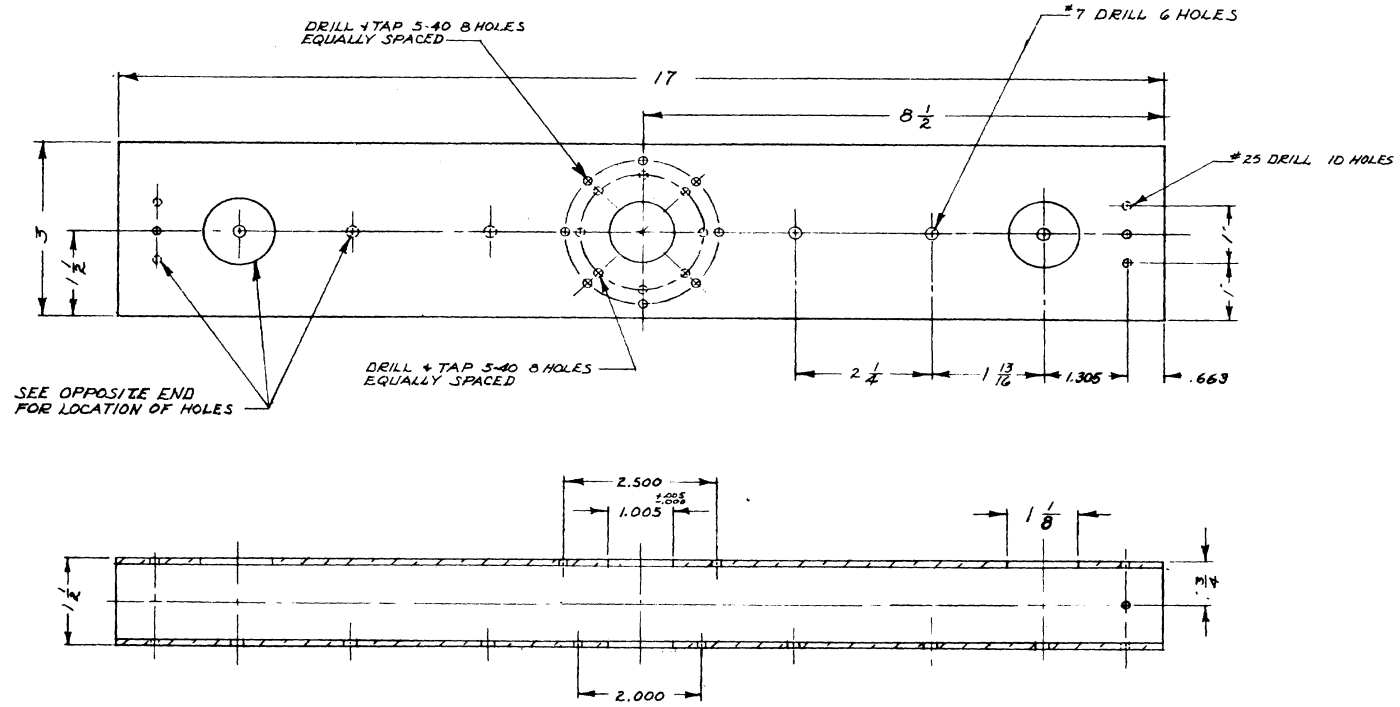

FIG. D – 7

STD. BRASS WAVE GUIDE 1 REQ'D

ALL DIMENSIONS UNLESS OTHERWISE SPECIFIED MUST BE HELD TO A TOLERANCE - FRACTIONAL ± 1/64," DECIMAL ± .005," ANGULAR ± ½°

ISSUE	DATE	ENGINEERING RESEARCH INSTITUTE UNIVERSITY OF MICHIGAN ANN ARBOR MICHIGAN	DESIGNED BY JKB	APPROVED BY
			DRAWN BY MM	SCALE HALF
			CHECKED BY DRA	DATE 4-24-52
		PROJECT 2009	TITLE GUIDE	
		CLASSIFICATION	DWG. NO. B-2059-6	

DWG. NO. A

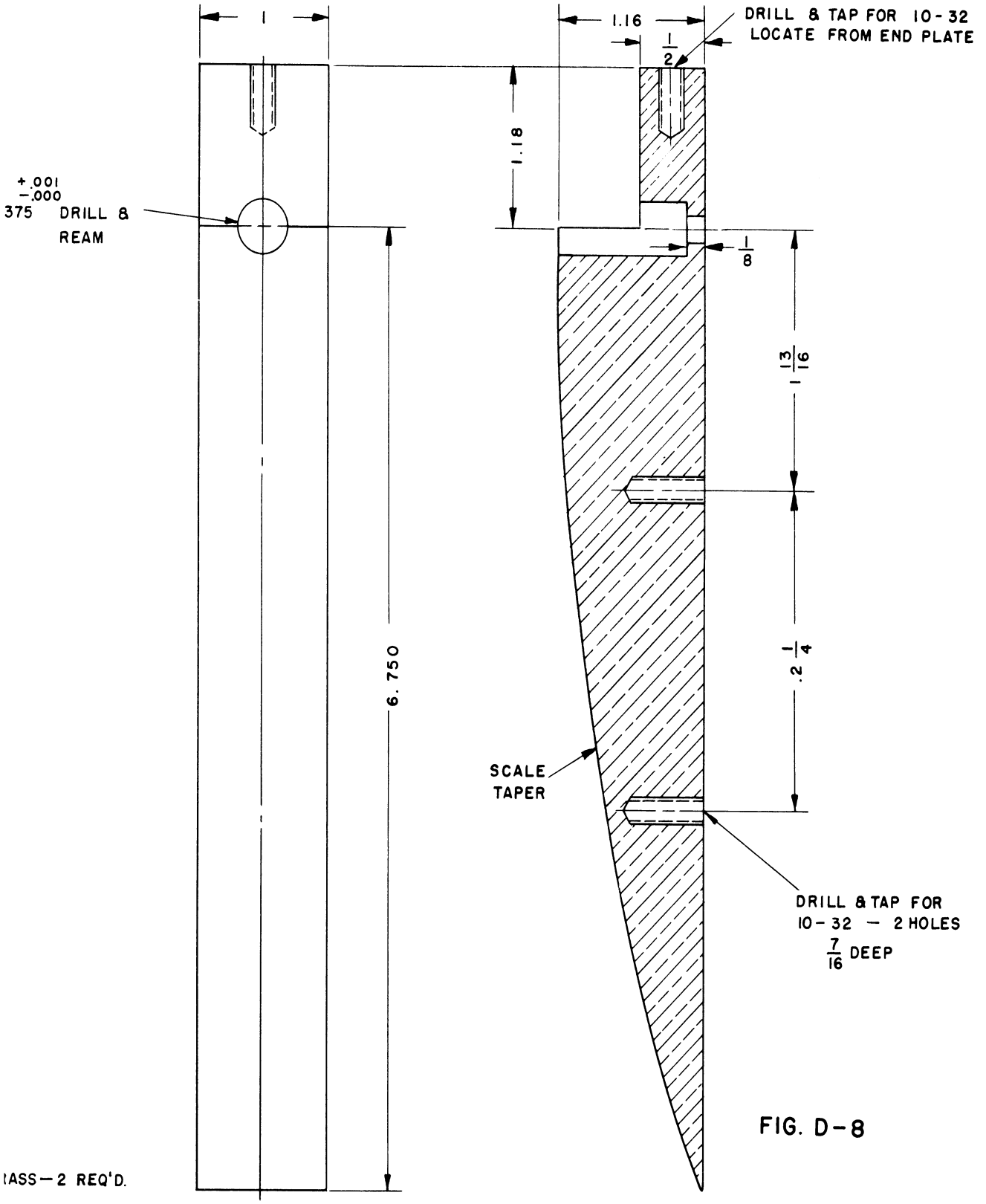

FIG. D-8

ASS — 2 REQ'D.

L DIMENSIONS UNLESS OTHERWISE SPECIFIED MUST BE HELD TO A TOLERANCE - FRACTIONAL ± 1/64," DECIMAL ± .005," ANGULAR ± ½°

		ENGINEERING RESEARCH INSTITUTE UNIVERSITY OF MICHIGAN ANN ARBOR MICHIGAN	DESIGNED BY J.A. BOYD DRAWN BY PLW CHECKED BY [illegible]
		PROJECT 2009	TITLE TAPERED RIDGE
2	4-8-53	CLASSIFICATION	DWG. NO. A-2059-7
SUE	DATE		

APPROVED BY
SCALE FULL
DATE 4-8-53

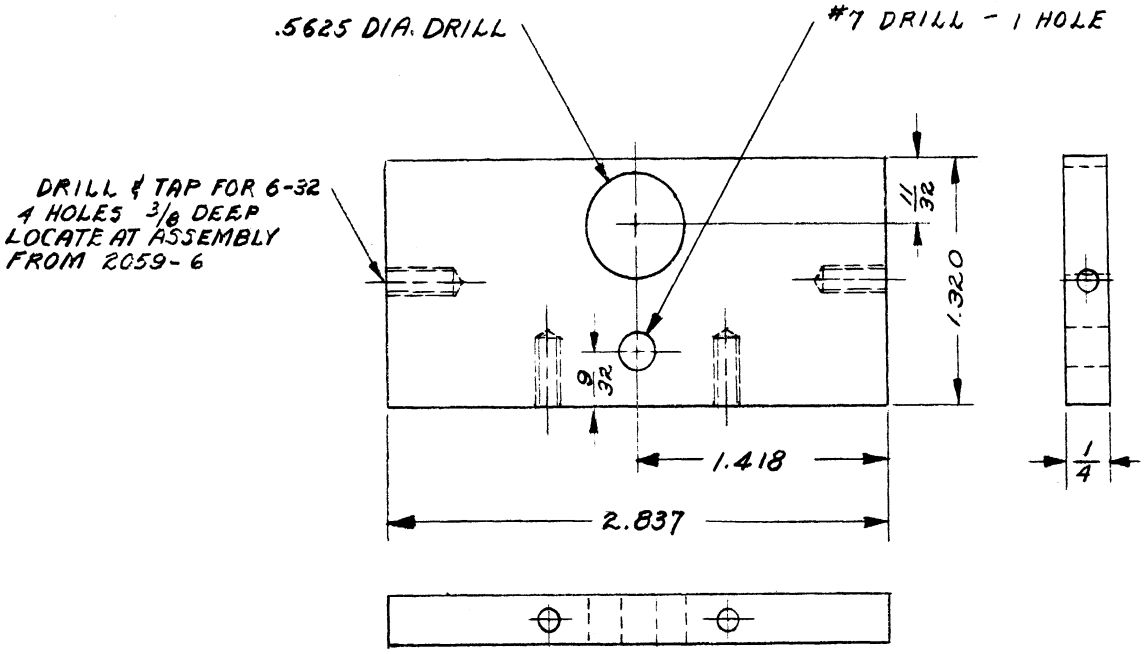

FIG. D-9

BRASS - 2 REQ'D.

ALL DIMENSIONS UNLESS OTHERWISE SPECIFIED MUST BE HELD TO A TOLERANCE - FRACTIONAL ± 1/64," DECIMAL ± .005," ANGULAR ± ½°

ISSUE	DATE			
		ENGINEERING RESEARCH INSTITUTE UNIVERSITY OF MICHIGAN ANN ARBOR MICHIGAN	DESIGNED BY JAB DRAWN BY PLW CHECKED BY [illegible]	APPROVED BY SCALE FULL DATE 2-1-53
		PROJECT 2009	TITLE END PLATE	
		CLASSIFICATION	DWG. NO. A-2059-8	

DWG. NO. A

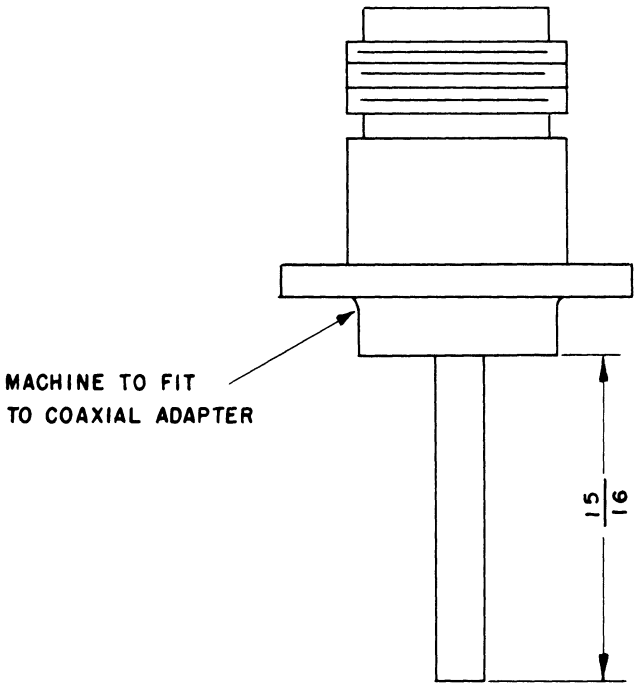

FIG. D-10

CQA 4947 CONNECTOR – 2 REQ'D.

ALL DIMENSIONS UNLESS OTHERWISE SPECIFIED MUST BE HELD TO A TOLERANCE - FRACTIONAL ± 1/64," DECIMAL ± .005," ANGULAR ± ½°

		ENGINEERING RESEARCH INSTITUTE UNIVERSITY OF MICHIGAN ANN ARBOR MICHIGAN	DESIGNED BY J.A. BOYD	APPROVED BY
			DRAWN BY PLW	SCALE 2 X
			CHECKED BY	DATE 4-8-53
		PROJECT 2009	TITLE MODIFIED TYPE "N" CONNECTOR	
2	4-8-53	CLASSIFICATION	DWG. NO. A- 2059-9	
ISSUE	DATE			

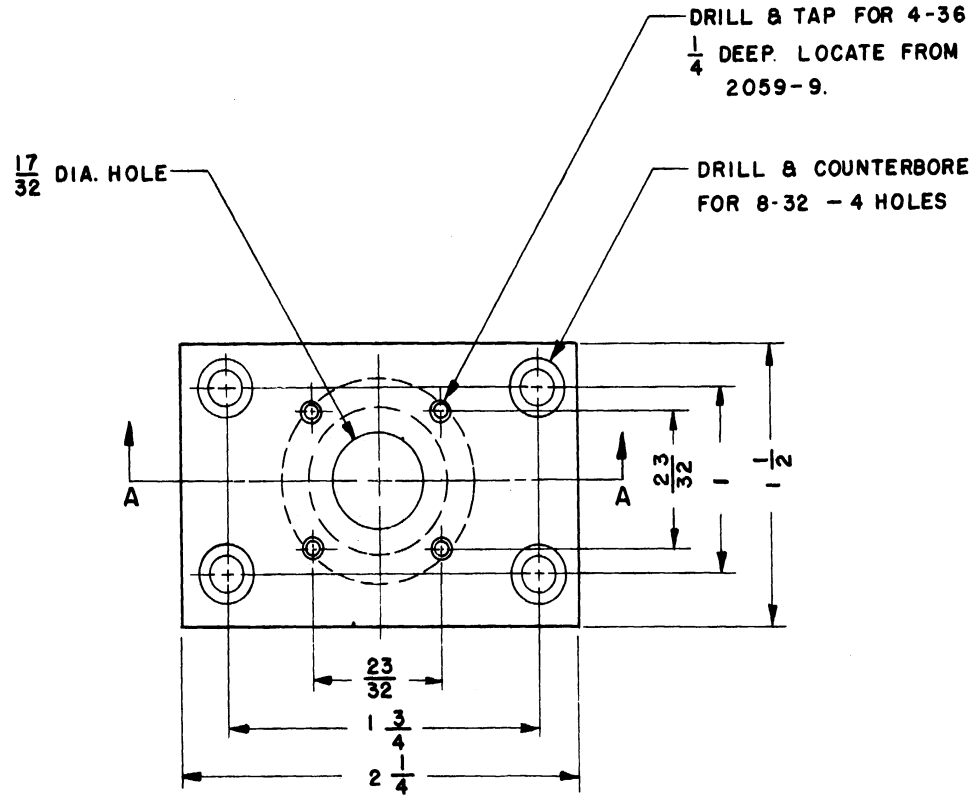

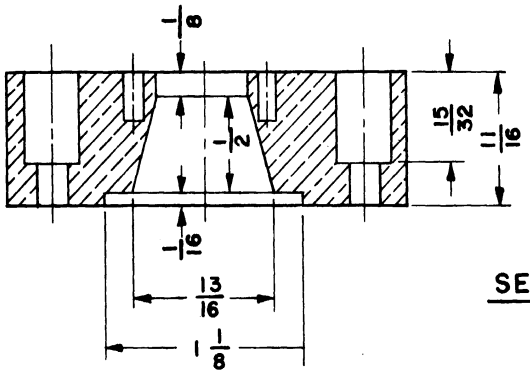

SECTION A-A

FIG. D-11

BRASS — 2 REQ'D.

ALL DIMENSIONS UNLESS OTHERWISE SPECIFIED MUST BE HELD TO A TOLERANCE - FRACTIONAL ± 1/64," DECIMAL ± .005," ANGULAR ± ½°

		ENGINEERING RESEARCH INSTITUTE UNIVERSITY OF MICHIGAN ANN ARBOR MICHIGAN	DESIGNED BY J.A. BOYD	APPROVED BY
			DRAWN BY PLW	SCALE FULL
			CHECKED BY	DATE 4-8-53
		PROJECT 2009	TITLE COAXIAL ADAPTER	
2 ISSUE	4-8-53 DATE	CLASSIFICATION	DWG. NO. A- 2059-10	

DWG. NO. A

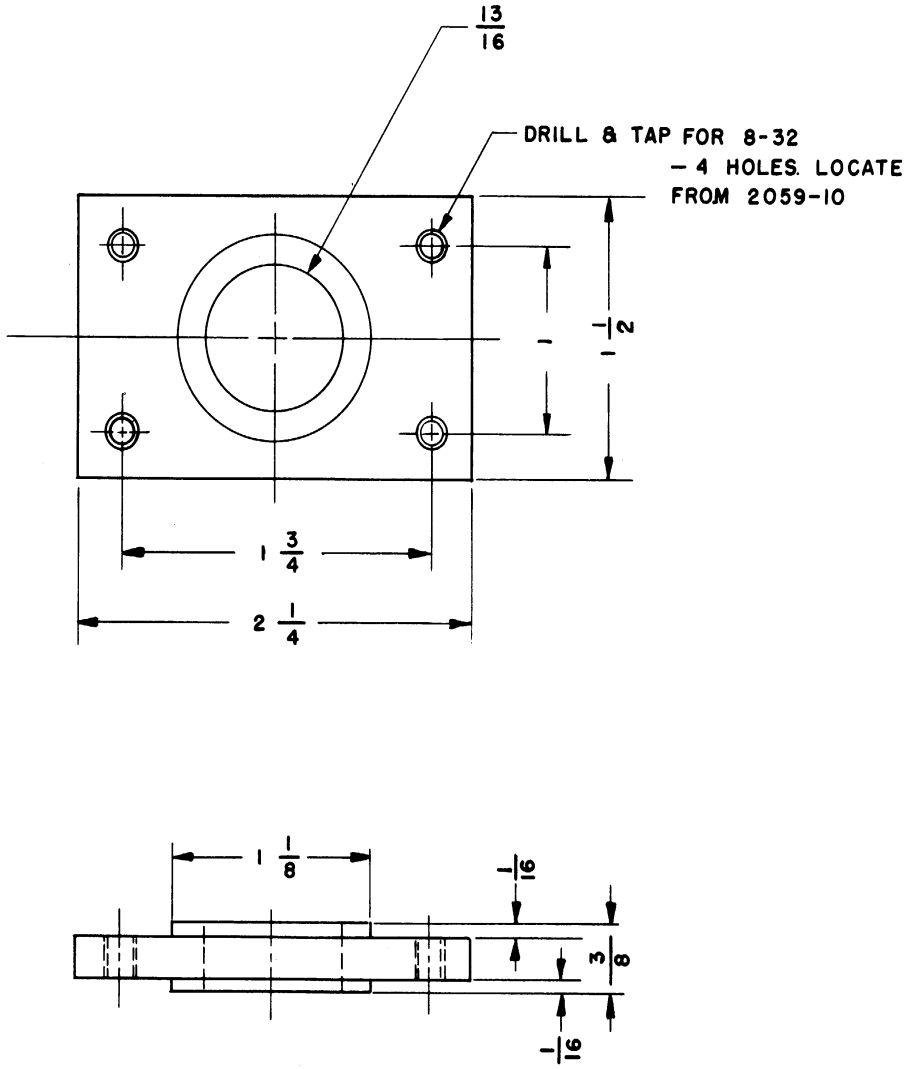

FIG. D-12

BRASS— 2 REQ'D.

L DIMENSIONS UNLESS OTHERWISE SPECIFIED MUST BE HELD TO A TOLERANCE - FRACTIONAL ± 1/64," DECIMAL ± .005," ANGULAR ± ½°

		ENGINEERING RESEARCH INSTITUTE UNIVERSITY OF MICHIGAN ANN ARBOR MICHIGAN	DESIGNED BY J.A. BOYD.	APPROVED BY
			DRAWN BY P.L.W.	SCALE FULL
			CHECKED BY	DATE 4 — 8—53
		PROJECT 2009	TITLE ADAPTER MOUNTING PLATE	
2	4-6-53	CLASSIFICATION	DWG. NO. A-2059—11	
SUE	DATE			

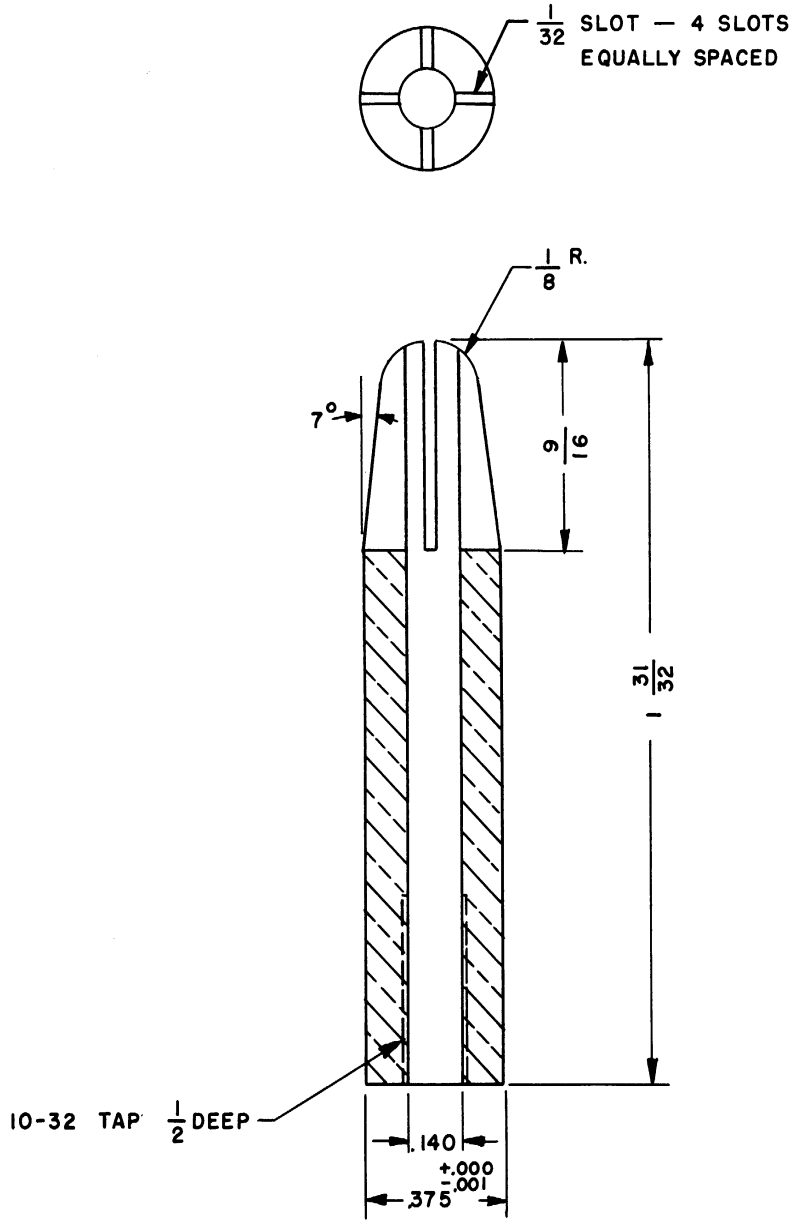

FIG. D-13

BRASS- 1 REQ'D.

ALL DIMENSIONS UNLESS OTHERWISE SPECIFIED MUST BE HELD TO A TOLERANCE - FRACTIONAL ± 1/64," DECIMAL ± .005," ANGULAR ± ½°

		ENGINEERING RESEARCH INSTITUTE UNIVERSITY OF MICHIGAN ANN ARBOR MICHIGAN	DESIGNED BY J.A.B
			DRAWN BY P.L.W.
			CHECKED BY
		PROJECT 2009	TITLE RIDGE TO COAXIAL CONNECTOR
ISSUE	DATE	CLASSIFICATION	DWG. NO. A- 2059-12

APPROVED BY	
SCALE 2X	
DATE 9-1-53	

BIBLIOGRAPHY

1. C. G. Montgomery, "Techniques of Microwave Measurements," Rad. Lab. Series, Vol. 11

2. J. S. Needle, "The Insertion Magnetron," University of Michigan, Electron Tube Laboratory Technical Report No. 11, August 1951

3. Hamilton, Knipp, and Kuper, "Klystrons and Microwave Triodes," Rad. Lab. Series, Vol. 7

4. D. A. Wilbur, A. H. Peters, and H. W. A. Chalberg, "Tunable Miniature Magnetrons," Electronics, January, 1953

5. A. W. Hull, "Effect of a Uniform Magnetic Field on the Motion of Electrons between Coaxial Cylinders," Phys. Rev., Vol. 18, pp. 31-61, July 1921

6. J. Brossart, O. Doehler, "The Travelling-Wave Tube in a Magnetic Field," Annales de Radioélectricité, Vol. 3, No. 14, October 1948

7. E. C. S. Megaw, "An Investigation of the Magnetron Short-Wave Oscillator," Jour. IEE (London), Vol. 72, pp. 326-348, April 1933

8. J. B. Fisk, H. D. Hagstrum, and P. L. Hartman, "The Magnetron as a Generator of Centimeter Waves," Bell System Technical Journal, Vol. 25, No. 2, April 1946

9. G. R. Kilgore, "Magnetron Oscillators for the Generation of Frequencies between 300 and 600 Megacycles," Proc. IRE, Vol. 24, pp. 1140-1146, 1936

10. E. Habann, "A New Vacuum Tube Generator," Zeit. für Hochfrequenz, Vol. 24, pp. 115-135, 1924

11. A. Zacek, "A Method of Generating Short Electromagnetic Waves," Zeit für Hochfrequenz, Vol 32, pp. 172-180, 1928

12. H. Yagi, "Beam Transmission of Ultra Short Waves," Proc. IRE, Vol. 16, pp. 715-722, June 1928

13. K. Okabe, "On the Short-Wave Limit of Magnetron Oscillations," Proc. IRE, Vol. 17, No. 4, pp. 652-661, April 1929

14. K. Posthumus, "Oscillations in a Split-Anode Magnetron, Mechanism of Generations," Wireless Engineer, Vol. 12, pp. 126-132, 1935

15. H. W. Welch, Jr., S. Ruthberg, H. W. Batten, W. Peterson, "Analysis of Dynamic Characteristics of the Magnetron Space Charge, Preliminary Results," University of Michigan, Electron Tube Laboratory Technical Report No. 5, January 1951

16. H. W. Welch, Jr., "Dynamic Frequency Characteristics of the Magnetron Space Charge; Frequency-Pushing and Voltage Tuning," University of Michigan, Electron Tube Laboratory Technical Report No. 12, November 1951

17. D. A. Wilbur, R. B. Nelson, P. H. Peters, A. J. King, and L. R. Koller, C-W Magnetron Research, Final Report, Contract No. 2-36-039 sc-32279, Research Laboratory, General Electric Company, April 1950

18. G. D. O'Neill, "Separate Cavity Tunable Magnetron," Elec. Industries, June 1946

19. F. H. Crawford and M. D. Hare, "A Tunable Squirrel-Cage Magnetron — The Donutron," Proc. IRE, April 1947

20. J. F. Hull and A. W. Randalls, "High-Power Interdigital Magnetrons," Proc. IRE, November 1948

21. S. B. Cohn, "Properties of Ridge Waveguide," Proc. IRE, August 1947

22. Radio Research Laboratory Staff, "Very High Frequency Technique," Vol. II, McGraw-Hill, 1947

23. A. M. Clogston, "Microwave Magnetrons," Vol. 6, Massachusetts Institute of Technology

24. J. C. Slater, "Theory of Magnetron Operation," Rad. Lab. Report 43-28, March 1943

25. J. F. Hull, "Analysis of a Magnetron Interaction Space for Elimination of Hartree Harmonics," Memorandum Report, SCCSCL-RTB2, Proj. 322A, Evans Signal Laboratory, January 1951

26. W. B. Wholey and W. N. Eldred, "A New Type of Slotted Line Section," Proc. IRE, March 1950

27. G. Hok, "Ultra High Frequency Techniques," Vol. 1, Chap. 21, McGraw-Hill, 1947

28. Quarterly Progress Report No. 5, University of Michigan Electron Tube Laboratory, March 1953

29. J. C. Slater, "Microwave Electronics," Bell Laboratory Series, D. Van Nostrand Co., Inc., 1950

DISTRIBUTION LIST

20 copies - Director, Evans Signal Laboratory
Belmar, New Jersey
FOR: Chief, Thermionics Branch

10 copies - Chief, Bureau of Ships
Navy Department
Washington 25, D.C.
ATTENTION: Code 930A

10 copies Chief, Engineering and Technical Service
Office of the Chief Signal Officer
Washington 25, D.C.

10 copies Director, Air Materiel Command
Wright Field
Dayton, Ohio
ATTENTION: Electron Tube Section

2 copies - Mr. John Keto
Director, Aircraft Radiation Laboratory
Air Materiel Command
Wright Field
Dayton, Ohio

2 copies - Document File
Electronic Defense Group
Engineering Research Institute
University of Michigan
Ann Arbor, Michigan

1 copy - H. W. Welch, Jr., Project Supervisor
Electronic Defense Group
Engineering Research Institute
University of Michigan
Ann Arbor, Michigan

Engineering Research Institute File
University of Michigan
Ann Arbor, Michigan

W. E. Quinsey, Assistant to the Director
Engineering Research Institute
University of Michigan
Ann Arbor, Michigan

W. G. Dow, Professor
Department of Electrical Engineering
University of Michigan
Ann Arbor, Michigan

Gunnar Hok, Professor
Department of Electrical Engineering
University of Michigan
Ann Arbor, Michigan

J. R. Black, Research Engineer
Engineering Research Institute
University of Michigan
Ann Arbor, Michigan

J. S. Needle, Assistant Professor
Department of Electrical Engineering
University of Michigan
Ann Arbor, Michigan

Bell Telephone Laboratories
Murray Hill, New Jersey
ATTENTION: S. Millman

Microwave Research Laboratory
University of California
Berkeley, California
ATTENTION: Professor D. Sloan

Air Force Cambridge Research Laboratories
Library of Geophysics Directorate
230 Albany Street
Cambridge, Massachusetts
ATTENTION: Dr. E. W. Beth

Air Force Cambridge Research Laboratories
Library of Radiophysics Directorate
230 Albany Street
Cambridge, Massachusetts

Collins Radio Company
Cedar Rapids, Iowa
ATTENTION: Robert M. Mitchell

Columbia Radiation Laboratory
Columbia University
Department of Physics
New York 27, New York

Department of Physics
Cornell University
Ithaca, New York
ATTENTION: Dr. L. P. Smith

Industry and Science Department
Enoch Pratt Free Library
Baltimore 1, Maryland

Vacuum Tube Department
Federal Telecommunication Laboratories, Inc.
500 Washington Avenue
Nutley 10, New Jersey
ATTENTION: A. K. Wing, Jr.

General Electric Co.
General Engineering Laboratory Library
Building 5, Room 130
1 River Road
Schenectady 5, N. Y.

General Electric Research Laboratory
Schenectady, New York
ATTENTION: Dr. A. W. Hull

General Electric Research Laboratory
Schenectady, New York
ATTENTION: P. H. Peters

Mr. A. C. Gable
Ind. and Trans. Tube Dept.
General Electric Co. (Bldg. 269)
Schenectady, New York

Mrs. Marjorie L. Cox, Librarian
G-16, Littauer Center
Harvard University
Cambridge 38, Massachusetts

Cruft Laboratory
Harvard University
Cambridge, Massachusetts
ATTENTION: Professor E. L. Chaffee

Electron Tube Laboratory
Research and Development Laboratory
Hughes Aircraft Company
Culver City, California
ATTENTION: G. R. Brewer

Electron Tube Laboratory
Department of Electrical Engineering
University of Illinois
Urbana, Illinois

Mr. R. Konigsberg
Radiation Laboratory
Johns Hopkins University
1315 St. Paul's Street
Baltimore, Maryland

Department of Electrical Engineering
University of Kentucky
Lexington, Kentucky
ATTENTION: Professor H. Alexander Romanowit

Gift and Exchange Division
University of Kentucky Libraries
University of Kentucky
Lexington, Kentucky

Mr. R. E. Harrell, Librarian
West Engineering Library
University of Michigan
Ann Arbor, Michigan

Department of Electrical Engineering
University of Minnesota
Minneapolis, Minnesota
ATTENTION: Professor W. G. Shepherd

Document Office - Room 20B-221
Research Laboratory of Electronics
Massachusetts Institute of Technology
Cambridge 39, Massachusetts
ATTENTION: John H. Hewitt

National Bureau of Standards Library
Room 203, Northwest Building
Washington 25, D. C.

Dr. D. L. Marton
Chief, Electron Physics Section
National Bureau of Standards
Washington 25, D. C.

Mr. Stanley Ruthberg
Electron Tube Laboratory
Bldg. 83
National Bureau of Standards
Washington 25, D. C.

National Research Council of Canada
Radio and Electrical Engineering Division
Ottawa, Ontario
Canada

Dr. O. S. Duffendack, Director
Phillips Laboratories, Inc.
Irvington-on-Hudson, New York

Polytechnic Institute of Brooklyn
55 Johnson Street
Brooklyn 1, New York
Attention: Dr. E. Webber

Department of Electrical Engineering
Pennsylvania State College
State College, Pennsylvania
ATTENTION: Professor A. H. Waynick

Radio Corporation of America
RCA Laboratories Division
Princeton, New Jersey
ATTENTION: Fern Cloak, Librarian

Mr. C. L. Cuccia
RCA Laboratories Division
Radio Corporation of America
Princeton, New Jersey

Radio Corporation of America
RCA Laboratories Division
Princeton, New Jersey
ATTENTION: Mr. J. S. Donal, Jr.

Radio Corporation of America
RCA Victor Division
415 South 5th Street
Harrison, New Jersey
ATTENTION: Hans K. Jenny

Raytheon Manufacturing Company
Research Division
Waltham 54, Massachusetts
ATTENTION: W. M. Gottschalk

Magnetron Developement Laboratory
Power Tube Division
Raytheon Manufacturing Company
Waltham 54, Massachusetts
ATTENTION: Edward C. Dench

Magnetron Development Laboratory
Power Tube Division
Raytheon Manufacturing Company
Waltham 54, Massachusetts
ATTENTION: W. C. Brown

Sanders Associates, Inc.
135 Bacon Street
Waltham 54, Massachusetts
ATTENTION: Mr. James D. LeVan

Sperry Gyroscope Company
Library Division
Great Neck, Long Island, New York

Department of Electrical Engineering
Stanford University
Stanford, California
ATTENTION: Dr. S. Kaisel

Sylvania Electric Products, Inc.
70 Forsyth Street
Boston 15, Massachusetts
ATTENTION: Mrs. Mary Timmins, Librarian

Sylvania Electric Products, Inc.
Woburn, Massachusetts
ATTENTION: Mr. Marshall C. Pease

Westinghouse Engineering Laboratories
Bloomfield, New Jersey
ATTENTION: Dr. J. H. Findlay

Department of Electrical Engineering
Yale University
New Haven, Connecticut
ATTENTION: Dr. L. P. Smith